Ethnomedicine-based discovery and characterization of plant-derived $GABA_A$ receptor modulators with new scaffolds.

Inauguraldissertation

zur

Erlangung der Würde eines Doktors der Philosophie
vorgelegt der
Philosophisch-Naturwissenschaftlichen Fakultät
der Universität Basel
von

Diana Carolina Rueda

aus Bogotá

KOLUMBIEN

Basel, 2014

Genehmigt von der Philosophisch-Naturwissenschaften Fakultät
auf Antrag von

Prof. Dr. Matthias Hamburger
Prof. Dr. Anna Rita Bilia

Basel, 22.04.2014

Prof. Dr. Jörg Schibler
Dekan

Namensnennung-Keine kommerzielle Nutzung-Keine Bearbeitung 3.0 Schweiz
(CC BY-NC-ND 3.0 CH)

Sie dürfen: **Teilen** — den Inhalt kopieren, verbreiten und zugänglich machen

Unter den folgenden Bedingungen:

Namensnennung — Sie müssen den Namen des Autors/Rechteinhabers in der von ihm festgelegten Weise nennen.

Keine kommerzielle Nutzung — Sie dürfen diesen Inhalt nicht für kommerzielle Zwecke nutzen.

Keine Bearbeitung erlaubt — Sie dürfen diesen Inhalt nicht bearbeiten, abwandeln oder in anderer Weise verändern.

Wobei gilt:

- **Verzichtserklärung —** Jede der vorgenannten Bedingungen kann **aufgehoben** werden, sofern Sie die ausdrückliche Einwilligung des Rechteinhabers dazu erhalten.
- **Public Domain (gemeinfreie oder nicht-schützbare Inhalte) —** Soweit das Werk, der Inhalt oder irgendein Teil davon zur Public Domain der jeweiligen Rechtsordnung gehört, wird dieser Status von der Lizenz in keiner Weise berührt.
- **Sonstige Rechte —** Die Lizenz hat keinerlei Einfluss auf die folgenden Rechte:
    - Die Rechte, die jedermann wegen der Schranken des Urheberrechts oder aufgrund gesetzlicher Erlaubnisse zustehen (in einigen Ländern als grundsätzliche Doktrin des **fair use** bekannt);
    - Die **Persönlichkeitsrechte** des Urhebers;
    - Rechte anderer Personen, entweder am Lizenzgegenstand selber oder bezüglich seiner Verwendung, zum Beispiel für **Werbung** oder Privatsphärenschutz.
- **Hinweis —** Bei jeder Nutzung oder Verbreitung müssen Sie anderen alle Lizenzbedingungen mitteilen, die für diesen Inhalt gelten. Am einfachsten ist es, an entsprechender Stelle einen Link auf diese Seite einzubinden.

Quelle: http://creativecommons.org/licenses/by-nc-nd/3.0/ch/ Datum: 12.11.2013

To my dearest Chee Seng
and my good friends Yoshie and Inken,
without whose loving support this wouldn't be happening.

TABLE OF CONTENTS

LIST OF ABBREVIATIONS

ADME	Absorption, distribution, metabolism, and excretion
APCI	Atmospheric pressure chemical ionization
BBB	Blood-brain barrier
β-CCM	Methyl β-carboline-carboxylate
BP	British Pharmacopoeia
BZD	Benzodiazepine
CD	Circular dichroism
CHM	Chinese herbal medicine
CID	Collision-induced dissociation
CMM	Chinese Materia Medica
CNS	Central nervous system
COSY	Correlation spectroscopy
DAD	Photodiode array detection
DMSO	Dimethyl sulfoxide
DNP	Dictionary of Natural Products
DORA	Dual orexin receptor antagonist
EP	European Pharmacopoeia
ESI	Electrospray ionization
GABA	Gamma-aminobutyric acid
$GABA_AR$	Gamma-aminobutyric acid type A receptor
$GABA_BR$	Gamma-aminobutyric acid type B receptor
$GABA_CR$	Gamma-aminobutyric acid type C receptor
GP-TCM	Good Practice in Traditional Chinese Medicine Research in the Post-genomic Era
HMBC	Heteronuclear multiple-bond correlation
HMP	Herbal medicinal product
HMQC	Heteronuclear multiple-quantum correlation
HPLC	High-performance liquid chromatography
HSQC	Heteronuclear single-quantum correlation
HTS	High-throughput screening
I_{GABA}	GABA-induced chloride current

INADEQUATE	Incredible natural-abundance double-quantum transfer experiment
LGIC	Ligand-gated ion channel
MS	Mass spectrometry
MS^n	Multi-stage MS/MS
nAChR	Nicotinic acetylcholine receptor
NMR	Nuclear magnetic resonance
NOESY	Nuclear Overhauser effect spectroscopy
NP	Natural product
OR	Optical rotation
ORD	Optical rotatory dispersion
PSA	Polar surface area
QSAR	Quantitative strcuture-activity relationship
ROESY	Rotating-frame Overhauser effect spectroscopy
RO5	Lipinski's *Rule of Five*
SAR	Structure-activity relationship
S/N	Signal-to-noise ratio
TCM	Traditional Chinese medicine
TEVC	Two-microelectrode voltage clamp
TOF	Time-of-flight
TOCSY	Total correlation spectroscopy
USP	United States Pharmacopoeia
UV	Ultraviolet light spectrum
VIS	Visible light spectrum
VTA	Ventral tegmental area
WHO	World Health Organization

SUMMARY

Inhibitory neurotransmission in the central nervous system (CNS) largely relies on the actions of gamma aminobutyric acid (GABA) on $GABA_A$ receptors, heteropentameric ligand-gated chloride channels assembled from 19 possible subunits (α_{1-6}, β_{1-3}, γ_{1-3}, δ, ε, θ, π, ρ_{1-3}). GABA-induced chloride influx through $GABA_A$ receptors causes neuronal hyperpolarization and inhibition of further action potentials. Therefore, impaired GABAergic function results in CNS conditions such as epilepsy, insomnia, anxiety, and mood disorders. A number of clinically important drugs like benzodiazepines, barbiturates, neuroactive steroids, anesthetics, and certain other CNS depressants bind $GABA_A$ receptors. However, these drugs lack of subunit specificity and, therefore, induce serious side effects.

In the search for $GABA_A$ receptor modulators with new scaffolds, a plant extract library was screened at Prof. Hamburger's group by means of an automated two-microelectrode voltage clamp functional assay in *Xenopus laevis* oocytes. Among others, the lipophilic extracts of *Bupleurum chinense* roots, *Pholidota chinensis* stems and roots, *Adenocarpus cincinnatus* roots and tubers, and *Boswellia thurifera* resin positively modulated $GABA_A$ receptors of the subtype $\alpha_1\beta_2\gamma_{2s}$, the most abundant one in the human brain.

In this work, GABAergic activity in the four extracts was tracked using of an HPLC-based activity profiling approach. In total, 22 natural products, eight of them new, were isolated by diverse chromatographic methods and characterized by HR-TOF-MS and microprobe NMR. Absolute configuration of chiral compounds was determined by CD-spectroscopy and polarimetry. Fourteen of the 22 isolates showed $GABA_A$ receptor modulatory activity in the oocyte functional assay. Dihydrostilbenes, *cis*-pterocarpans, and abietane diterpenes were identified as new scaffolds for $GABA_A$ receptor modulators with favorable physicochemical properties for blood-brain barrier permeation.

HPLC-based activity profiling of *P. chinensis* enabled the identification of the dihydrostilbene batatasin III as a very efficient, non-selective $GABA_A$ receptor modulator (maximal potentiation of I_{GABA} 1500%). Two structurally related non-flexible stilbenoids, coelonin and pholidotol D, were also isolated from the extract but they were inactive in the oocyte assay. A preliminary structure-activity relationship study conducted with a series of

commercially available stilbenes and their dihydro derivatives, revealed that conformational flexibility is crucial for $GABA_A$ receptor modulatory activity of stilbenoids.

Fifteen flavonoid and isoflavonoid derivatives, including eight new natural products, were isolated from *A. cincinnatus* and tested in the oocyte assay. At a concentration of 100 μM, 12 of the 15 compounds enhanced the GABA-induced chloride current through $GABA_A$ receptors by more than 190%. Two pterocarpans and one isoflavone showed remarkably higher potency than other natural products previously isolated in this working group (EC_{50} below 10 μM).

B. thurifera and *B. chinense* yielded two more $GABA_A$ receptor modulators, dehydroabietic acid and aristolactone, respectively. However, isolation of aristolactone from a commercial sample of the traditional Chinese herbal drug *Chaihu* (*Bupleurum chinense* roots) led to detection of adulteration of the sample with roots of the nephrotoxic species *Aristolochia manshuriensis*. This case raised concerns about adequate quality control of TCM drugs commercialized in Europe.

ZUSAMMENFASSUNG

Die inhibitorische Neurotransmission im zentralen Nervensystem (ZNS) basiert grössenteils auf der Wechselwirkung zwischen γ-Aminobuttersäure (GABA) und $GABA_A$-Rezeptoren – hetreopentameren, Ligand-gesteuerten Chloridionenkanälen, die aus 19 möglichen Untereinheiten (α_{1-6}, β_{1-3}, γ_{1-3}, δ, ε, θ, π, ρ_{1-3}) aufgebaut sind. Der durch GABA induzierte Einstrom von Chloridionen durch $GABA_A$-Rezeptoren verursacht eine neuronale Hyperpolarisation und hemmt den Aufbau weiterer Aktionspotentiale. Daher führt eine beinträchtigte GABAerge Funktion zu funktionellen Störungen des ZNS wie Epilepsie, Schlafstörungen, Angstzuständen und Gemütsschwankungen. Viele klinisch relevante Arzneimittel wie Benzodiazepine, Barbiturate, neuroaktive Steroide, Anästhetika und andere Substanzen mit ZNS-dämpfendender Wirkung binden an $GABA_A$-Rezeptoren. Da diese jedoch keine Spezifität bezüglich der bestimmten Subtypen aufweisen, rufen diese Arzneimittel ernsthafte unerwünschte Nebenwirkungen hervor.

Im Zuge der Suche nach neuartigen $GABA_A$-Rezeptor Modulatoren wurde in der Arbeitsgruppe von Prof. Hamburger eine Bibliothek von Pflanzenextrakten unter Verwendung eines automatisierten zwei-Mikroelektroden-Spannungsklemmen-Verfahrens an *Xenopus laevis* Oozyten gescreent. Unter anderem zeigten die lipophilen Extrakte von *Bupleurum chinense* Wurzeln, *Pholidota chinensis* Stamm und Wurzeln, *Adenocarpus cincinnatus* Wurzeln und Knollen und *Boswellia thurifera* Harz positive modulatorische Effekte auf $GABA_A$-Rezeptoren des Subtyps $\alpha_1\beta_2\gamma_{2s}$ – den Subtyp, der im menschlichen Gehirn am häufigsten vorkommt.

In dieser Arbeit wurde die GABAerge Aktivität in den vier beschriebenen Extrakten mittels HPLC basiertem Aktivitäts-Profiling charakterisiert. Im Ganzen wurden 22 Naturstoffe, acht davon bisher unbekannt, mittels verschiedener chromatographischer Methoden isoliert und ihre Struktur anhand von HR-TOF-MS und microprobe NMR aufgeklärt. Die absolute Konfiguration von chiralen Strukturen liess sich durch CD-Spektroskopie und Polarimetrie bestimmen. Vierzehn der 22 Substanzen zeigten positive modulatorische Effekte auf $GABA_A$-Rezeptoren im Oozyten-Assay. Dihydrostilbene, *cis*-Pterocarpane und Abietan-Diterpene wurden als neue Grundstrukturen für $GABA_A$-Rezeptor Modulatoren mit für den Bluthirnschranken Übergang günstigen physikochemischen Eigenschaften identifiziert.

Aus dem HPLC basierten Aktivitäts-Profiling von *P. chinensis* ging das Dihydrostilben Batatasin III als sehr effizienter, nicht selektiver $GABA_A$-Rezeptor Modulator hervor (maximale Potenzierung von I_{GABA} 1500%). Zwei strukturell verwandte, nicht flexible Stilbene, Coelonin and Pholidotol D, wurden aus demselben Extrakt isoliert, waren im Oozyten-Assay allerdings nicht aktiv.

Eine erste Untersuchung der Sturktur-Aktivitäts Beziehung anhand einer Serie kommerziell erhältlicher Stilbene und ihrer Dihydro-derivate zeigte, dass die Flexibilität der Konformation für die modulatorische Aktivität von Stilbenen am $GABA_A$-Rezeptor essentiell ist.

Fünfzehn Flavonoid- und Isoflavonoid-Derivate, davon acht neue Naturstoffe, konnten aus *A. cincinnatus* isoliert und im Oozyten-Assay getestet werden. Bei einer Konzentration von 100 µM, erhöhten 12 der 15 Substanzen den GABA induzierten Chloridionen Einstrom durch die $GABA_A$-Rezeptoren um mehr als 190%. Zwei Pterocarpane und ein Isoflavon zeigten eine deutlich höhere Potenz als bisher in der Arbeitsgruppe isolierte Substanzen (EC_{50} < 10 µM).

B. thurifera und *B. chinense* lieferten zwei weitere $GABA_A$-Rezeptor Modulatoren, Dehydroabietis-säure bzw. Aristolacton. Dass Aristolacton aus *Chaihu* (*Bupleurum chinense* Wurzeln), einem kommerziell erhältlichen Produkt der traditionellen Chinesischen Medizin, isoliert wurde, deckte auf, dass das Produkt mit Wurzeln der nephrotoxischen Spezies *Aristolochia manshuriensis* versetzt war. Dieser Fall wirft Fragen auf über die angemessene Qualitätskontrolle von kommerziell erhältlichen TCM Produkten in Europa.

"The journey of a thousand miles begins with a single step"

Laozi (604-531 BC)

1. AIM OF THE WORK

Pharmacological management of CNS conditions such as epilepsy, insomnia, anxiety, and mood disorders involves, for the most part, positive modulation of $GABA_A$ receptors by clinically relevant drugs like benzodiazepines and several other CNS depressants. However, these drugs interact in a non-selective way with several $GABA_AR$ subtypes and thus induce a number of serious side effects like reduced coordination, cognitive impairment, tolerance, and drug dependence. Selective modulators are expected to improve the safety profile of the current treatments. However, despite the availability of experimental subunit-specific GABAergic drugs for more than a decade, no subtype-selective $GABA_A$ receptor modulator has been introduced into clinical practice to this day [1].

Historically, natural products have been a very important source of drugs, providing myriads of biologically relevant compounds of great chemical diversity. At least 50% of the currently marketed drugs including antibiotics and anticancer agents have counted directly or indirectly on natural products for their development [2]. The occurrence of $GABA_A$ receptor modulators has been reported for several plant species and a number of structurally diverse natural products have been identified to interact with this receptor [3]. However, the number of structural templates is still limited, and the search for selective $GABA_AR$ modulators with new scaffolds must be continued.

In our research group, previous works have been carried out on the identification of $GABA_A$ receptor modulators from nature. The starting material for these studies was an extract library assembled on the basis of traditional use of plants as tranquilizers and sleep-inducers in different cultures. These extracts were preliminarily screened in a two-microelectrode voltage clamp (TEVC) assay in *Xenopus* oocytes, using potentiation of GABA-induced chloride current (I_{GABA}) through $\alpha_1\beta_2\gamma_{2s}$ $GABA_A$ receptors as the evaluation parameter. Extracts that potentiated I_{GABA} by more than 30% at 100 µg/mL, were selected for further isolation of potentially active compounds.

The aim of the present work was to trace GABAergic activity in four of those plant extracts in order to find at least one new scaffold for $GABA_A$ receptor modulators with suitable physicochemical properties for further optimization and development. The extracts were chosen based chemotaxonomic considerations and potentiation of I_{GABA}. Using an HPLC-based activity profiling approach in combination with the TEVC functional assay in *Xenopus* oocytes, the major bioactive compounds in each extract were to be isolated by means of

diverse chromatographic methods and identified using spectrometric and spectroscopic techniques. Concomitant isolation and identification of structurally related compounds had to be performed for evaluation of possible structure-activity relationships.

Pharmacological characterization of the isolates as $GABA_A$ receptor modulators had to be carried out in the oocyte assay, by determining potency (EC_{50}) and efficiency (maximal potentiation of I_{GABA}) from concentration-response experiments in receptors of the subtype $\alpha_1\beta_2\gamma_{2s}$. Compounds with outstanding activity at this receptor subtype and favorable physicochemical properties, would be submitted to subunit specificity evaluation in receptors with varying α and β subunit composition.

References

[1] Griebel G, Holmes A. 50 years of hurdles and hope in anxiolytic drug discovery. Nat Rev Drug Discov 2013;12:667–87.

[2] Cragg GM, Newman DJ. Natural products: A continuing source of novel drug leads. Biochim Biophys Acta BBA - Gen Subj 2013;1830:3670–95.

[3] Zaugg J. Discovery of new scaffolds for GABAA receptor modulators from natural origin. Univertität Basel, Basel; 2011.

2. INTRODUCTION

2.1. Natural products in drug discovery

"(...) but nature is always more subtle, more intricate, more elegant than what we are able to imagine"

Carl Sagan in The Demon-Haunted World: Science as a Candle in the Dark (1995)

Natural products: an invaluable source of novel drug leads

The use of plants to alleviate and treat human diseases can be traced to prehistoric times. Plants, in particular, have formed the basis of sophisticated traditional medicine systems [1]. Earliest written documentation of knowledge on medicinal properties of plants is found on Assyrian clay tablets dated about 2000 B.C. Millenary cultures such as Egyptian, Indian, and Chinese hold a well-established tradition on the popular use of medicinal plants [2]. The Greeks and Romans significantly influenced the rational use of herbal drugs in the ancient Western world, with the contributions of Dioscorides (100 A.D) and Galen (130-200 A.D). During the Dark and Middle Ages (5^{th} to 12^{th} centuries), the Greco-Roman knowledge was preserved by the Arabs, who expanded it to include the use of their own sources, together with Chinese and Indian herbs [1]. Centuries later, Paracelsus (1493 – 1541) developed the first idea of active principles in plants (the so-called *Arcanum*, which he considered as an immaterial principle) and the concept of dose dependency of drug action and toxicity (*sola dosis facit venum*) [2].

In 1806, the German pharmacist Friedrich Sertürner reported the first isolation of a pharmacologically active pure natural product (NP), a white crystalline powder from opium (*Papaver somniferum*) which he named morphine after Morpheus, the Greek god of dreams [3]. Thus began an era in which drugs from natural sources could be purified, studied, and administered, eventually leading to pharmaceutical drug development as it stands today [4]. Microorganisms, plants, and more recently marine organisms, became prolific sources of structurally diverse bioactive metabolites that have yielded a number of very important drugs [1,5]. Quinine, isolated from the bark of cinchona tree (1820), salicylic acid from willow bark extract (1838), and penicillin from *Penicillium* fungi (1938), are some of the most popular examples (Figure 2.1) [3].

Pharmaceutical research expanded after the Second World War to include massive screening of microorganisms for new antibiotics after the discovery of penicillin [4]. Research on NPs as source of novel drugs reached its peak in the Western drug industry in the period 1970-1980, which resulted in a pharmaceutical landscape heavily influenced by non-synthetic molecules [6]. By 1990, about 80% of the drugs were either NPs or had a NP-origin. Antibiotics, antiparasitics, antimalarials, lipid lowering agents, immunosuppressants for organ transplants, and anticancer drugs, all of them based on the exquisite structural diversity and biological specificity of NPs, revolutionized medicine [4].

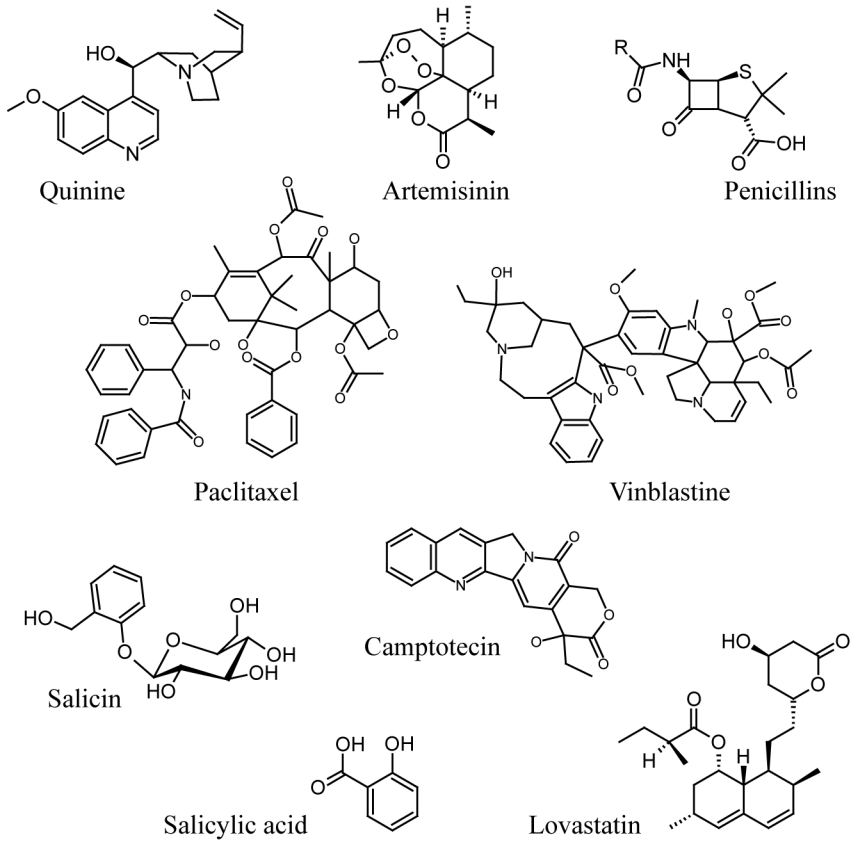

Figure 2.1. Structures of representative natural product-derived drugs (adapted from Wetzel et al. 2010 [3]).

According to Newmann and Cragg in their review of 2012 [7], the NP field was still producing or was involved in ca. 50% of all small molecules approved in the years 2000-2010. In their review of 2013 [1], the authors revealed that of the 1073 small-molecule New Chemical Entities (NCEs) approved between 1981 and 2010, only 36% can be classified as truly synthetic (i.e., devoid of natural inspiration) in origin. The two main disease categories in which NPs have played a crucial role in drug discovery are infectious diseases (caused by

bacteria, fungi, parasites, or viruses) and oncology, with 69% and 75% of the approved drugs being NP-derived or -inspired, respectively.

These data highlight the continuing importance of NPs as a source and inspiration for novel drugs, representing a highly validated strategy in drug discovery. Even more remarkable is the fact that, despite the intensive investigation, this potential remains virtually unexplored. It is estimated that only 6% of the total number of higher plant species have been studied pharmacologically and 15%, phytochemically. The surface of this unique source for bioactive compounds has barely been scratched. Many interesting drugs from natural sources remain to be discovered [1].

Challenges to natural product-based drug discovery

Despite the success of natural product-based drug discovery over the last decades, the search for new drug substances from "Mother Nature's Combinatorial Libraries" has fallen out of favor in recent years [5]. Many pharmaceutical companies have discontinued their NP screening programs [8] and rather embraced the 'biopharma' approach for innovation in drug discovery, relying on biological macromolecules such as monoclonal antibodies. On the other hand, a number of innovative strategies such as combinatorial chemistry, diversity-oriented synthesis, fragment-based drug discovery, chemical biology, and *in silico* screening have, for the most part, replaced NPs in drug discovery process [9].

Drug discovery and development is an extremely competitive and cost-intensive business. Due to the financial pressure, firms involved in drug discovery must hit the target accurately, as quickly and profitably as possible [4]. As a result, major pharmaceutical companies are currently working under an increasingly sophisticated high-throughput screening (HTS) scheme that allows the evaluation of libraries containing hundreds of thousands of compounds a week, using enzyme- or receptor-based assays designed to discover leads with specific mechanisms of action [5]. The classical approach of NP discovery based on bioactivity-guided fractionation does not fit too well in this picture, for it requires multidisciplinary expertise, is more time consuming and costly than most current approaches, and poses a number of technical challenges [9].

When working with NPs, libraries of crude extracts rather than pure compounds are typically screened for activity. Although operatively it is similar to the screening of small-molecule

libraries, results are influenced by the complex chemical composition of crude extracts. Low concentration of active compounds, poor solubility, chemical instability, presence of compounds with opposite activity, fluorescent or colored contaminants, or synergistic action of several constituents, are only few of the factors that can originate unreliable results [9]. Additional complications include insufficient access and supply of natural sources, low reproducibility of the activity or chemical composition of the source (easily affected by environmental or seasonal factors), and intellectual property rights [4].

In the light of the increased demand for compounds generated from the HTS approach, combinatorial chemistry appeared as a perfect fit due to its ability to generate large libraries of chemically diverse small molecule hits. However, only few drug candidates have been discovered with the fusion HTS-combinatorial chemistry [5,10], and only one *de novo* NCE has been approved for drug use in the period 1981-2010 (Bayer's antitumor compound sorafenib) [7]. In recent years, the output of the R&D programs of the pharmaceutical industry has declined considerably from over 60 NCEs/year in the late 1980s to over 23 in 2001-2010 [1], and it seems likely that the decreased emphasis on NPs in drug discovery has contributed to this decline [11].

These unexpected results have pointed out that success in drug discovery depends on the quality, rather than the quantity of the library members, and quality is determined by three factors: chemical diversity, lead-likeness, and biological relevance [11]. NP-based libraries are superior to combinatorial ones in every aspect. NPs offer a source of chemical diversity unmatched by any synthetic combinatorial collection: They are sterically more complex, cover a much larger volume of the chemical space, and display a broader dispersion of structural and physicochemical properties. In addition, many NP exhibit more favorable ADME properties than synthetic products [10,12]. Analyses of the database Dictionary of Natural Products (DNP) have revealed that at least 60% of the entries comply with *Lipinski's Rule of 5* for lead-like properties (see section 2.4), with only about 10% exhibiting two or more violations. Last but not least, most NPs have the imprinted ability to recognize and interact with protein surfaces, as a result of their biosynthetic origin. They constitute thus privileged structures for drug design from both a chemical and a biological point of view [5,9,11].

Besides their potential as lead structures, NPs also provide attractive scaffolds for combinatorial synthesis and remain essential tools for the validation of new drug targets [10,12]. Research on NPs must turn into a multidisciplinary process to remain competitive in drug discovery. Integration with current strategies of drug discovery like combinatorial chemistry for optimization of active NP templates, derivatization of existing NPs, diverted total synthesis, and the high-throughput *de novo* construction of NP-like scaffolds, must be attempted [1,9].

Although pharmaceutical industry has largely abandoned NP research, there are signs that NPs are experiencing a renaissance. In view of the recent achievements and ongoing developments, exploiting nature's diversity will continue to be an invaluable tool in the never-ending quest for new drugs [3]. In a time where the number of NCEs launched by the pharmaceutical industry is in steady decline, natural products appear more than ever to be an indispensable source for novel and structurally new scaffolds [8].

Tracing bioactivity in natural extracts

Challenges posed by modern drug discovery have been, at the same time, the driving force for unprecedented technological advances in NP-based lead discovery. Generation of large libraries of pre-purified extracts or fractions more suitable for HTS, is now possible thanks to laboratory automation, and the use of hyphenated techniques has accelerated the fractionation and structure elucidation processes. However, despite these remarkable achievements, there is still an urgent need for faster and more efficient strategies to track bioactivity of NPs. The greatest challenges remain the generation of high quality sample libraries and the efficient interfacing of biological data with chemo-analytical information [8,9].

The general strategy to discover new leads from plants involves primarily *i*) screening of extracts, *ii*) dereplication of active compounds, *iii*) bioassay-guided purification and isolation, and *iv*) structure elucidation of new bioactive constituents [9]. A brief description of each step is provided here.

i) **Screening of extracts**

After having established a validated target and a suitable bioassay, plant samples must be processed into a form suitable for screening. Common forms, in increasing order of purity, include the following [11]:

- Crude extract libraries
- Pre-fractionated libraries of crude extracts: by chromatographic methods or liquid-liquid partitioning
- Semipurified extract libraries
- Pre-fractionated libraries of semipurified extracts
- Pure NPs

The degree of pre-purification applied to the samples has a direct impact on the reliability of the screening results, reducing the occurrence of false positives/negatives. Additionally, purification increases the chances of detecting minor bioactive compounds in enriched fractions. Companies like Wyeth have reported that for about 80% of the fractions that proved to be active in the screening, the original extract was not found active, implying that the bioactive compounds would have been missed if only crude extracts had been tested. However, these positive results must be weighed against the rising production and screening costs of the process [8,11].

ii) Dereplication

Dereplication is the use of chromatographic and spectroscopic analysis to get information about the composition of active extracts or fractions, with the aim of discriminating previously isolated substances from novel compounds. For this rapid identification of known compounds, HPLC-MS or HLPC-NMR coupled with reference libraries of NPs (e.g. DNP) is most commonly used. Dereplication is also useful to detect the presence of interfering substances such as tannins or saponins in the mixtures. Furthermore, multiple extracts or fractions containing the same active component can also be identified [5,9,11].

iii) Bioassay-guided purification and isolation

The classical process leading from a bioactive extract to bioactive pure compounds was, for many years, a long and tedious procedure consisting of consecutive preparative separation steps guided by activity assessment of each of the resulting fractions. This slow and costly approach led many times to loss of bioactivity in the course of the purification process and left little room for dereplication in early stages, resulting in disappointing outcomes. In recent years, analysis, purification, and structure elucidation of NPs have experienced a

breakthrough, becoming a technology-driven process with new approaches like HPLC-based and affinity-based methods for the correlation of bioactivity with structural information [12].

HPLC-based methods constitute a sensitive miniaturized approach for the identification of active principles in early stages of the purification process, by combining chemoanalytical and biological data. Among the HPLC-based methods, three different approaches have been developed: on-line post-column bioassays, at-line settings, and off-line activity profiling. The latter, commonly referred to as HPLC-based activity profiling, offers the highest versatility and can be implemented in a high-throughput environment. The procedure starts with the fractionation of bioactive extracts by analytical or semipreparative HPLC and on-line recording of spectroscopic data, generally UV-vis and MS spectra. Simultaneous fraction collection for bioassay is carried out via a T-split of the column effluent. Fractions are dried, re-dissolved in a small volume of a suitable solvent, generally DMSO, and submitted to a bioassay. After assessment of each fraction, the activity profile can be matched with the HPLC chromatogram and correlated with the spectroscopic data recorded on-line, to identify active peaks. The general principle is shown in Figure 2.2. A targeted preparative isolation is then performed, if the compounds in the active time window are proven to be of interest after dereplication. This isolation does not require biological testing after each chromatographic step and therefore, consists of a straightforward peak-guided separation. The whole procedure requires only minute amounts of crude extract [13].

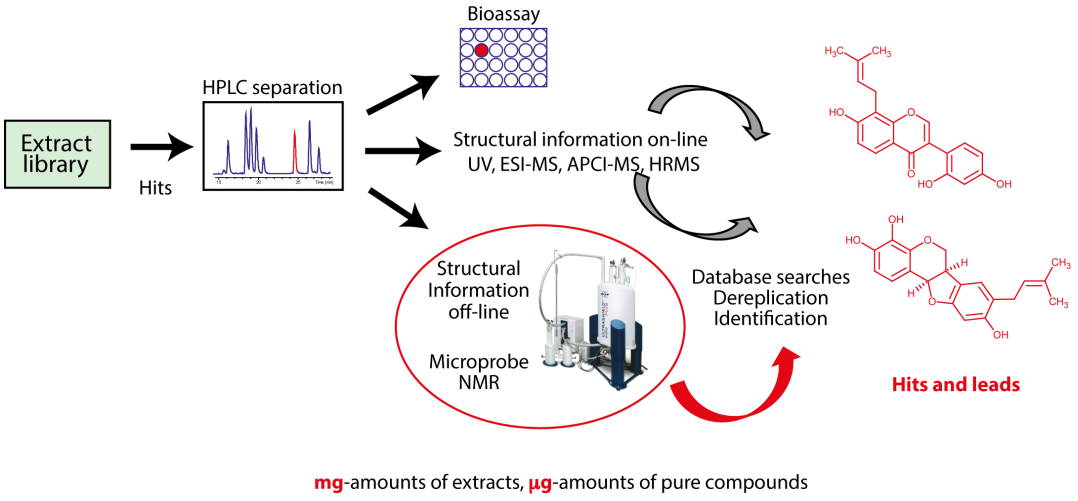

Figure 2.2. Experimental platform for HPLC-based activity profiling of bioactive extracts (adapted from Potterat and Hamburger 2013 [8])

HPLC-based activity profiling is a powerful approach for the rapid identification of bioactive compounds, suitable to be coupled to basically any bioassay that can be performed in a miniaturized format. It can be implemented in any laboratory equipped with the appropriate HPLC instrumentation. A number of research groups have set up platforms for HPLC-based activity profiling [8]. In our group, this approach has been successfully applied to the prioritization and subsequent identification of hits from screening projects using diverse bioassay formats, such as whole organism assays (tropical parasitic diseases) [14–17], cell-based functional assays (e.g. $GABA_A$ receptor modulation) [18–22], and mechanism-based screens (e.g. DYRK1A kinase) [23].

iv) Structure elucidation

Solving the structure of unknown compounds was once considered the bottleneck of the NP discovery process. Fifty years ago, tedious decomposition into fragments or, alternatively, total chemical synthesis were still required to corroborate structure proposals [24]. Modern spectroscopic techniques have revolutionized structure elucidation and quantification. Introduction of novel spectroscopic techniques, and significant advances in sensitivity and resolution have dramatically reduced data acquisition times and required sample amounts, which is key when dealing with NPs [11].

Full structural characterization of compounds eluted in microgram amounts from an HPLC column has become routine thanks to the concerted use of HPLC-DAD, -MS, and -NMR [8]. Among all HPLC detectors, UV is the most common and widely used. A broad range of NPs can be detected provided that they possess UV chromophores. Absorption for most NPs occurs in the range of 200-550 nm. DAD-UV analysis allows the identification of NP classes (terpenoids, alkaloids, polyphenols, etc) based on the absorption patterns of characteristic chromophores [25]. On the other hand, high-resolution MS constitutes a key technique for the identification of NPs. Different ionization sources and mass analyzers are available for the detection of non-volatile NPs. The most common ionization sources are electrospray ionization (ESI) and atmospheric pressure chemical ionization (APCI), since they produce a soft ionization ideal for thermo-labile NPs. Among mass analyzers, single quadrupole, triple quadrupole MS-MS, ion trap, and time-of-flight (TOF) spectrometers are the most used [26,27]. TOF spectrometers are used for routinely accurate mass measurements, which allow the assignment of molecular formulae with high confidence on subnanogram amounts of

compound [11]. Furthermore, HPLC-MS-MS or MS^n experiments provide complementary information through fragmentation of the molecular species by in-source collision-induced dissociation (CID), which can be useful in the case of NPs such as glycosides or prenylated compounds, and the differentiation of isomers [25].

Although MS is a powerful tool in structure elucidation, NMR spectroscopy still provides the most complete information to fingerprint molecules [11]. Technological developments over the past 50 years have significantly improved sensitivity and resolution in NMR, making it suitable for the analysis of small sample quantities. This is mostly enabled by the increase of magnetic field strength and the development of pulse-field gradient experiments. However, big magnets are pricy and may require considerable physical infrastructure and space, making it difficult for most users to acquire, maintain, and operate. A far more practical solution to improve S/N for most NPs is to choose the appropriate NMR probe according to the particular needs. A number of different probes can be chosen based on the available amount of sample, sample solubility, and budget. The most flexible probes are standard 5-mm, operating at room temperature. Smaller diameter (e.g. 1-mm probe) increases mass sensitivity but restricts the analysis of samples with limited solubility. The highest sensitivity can be achieved with small-volume, cryogenically cooled probes, which improve sensitivity by lowering thermal noise. However, costs rise considerably as sensitivity increases [24,28].

The routine strategy for full structure elucidation by NMR begins with a simple ^{1}H-NMR spectrum, which provides an idea of the overall complexity of the structure. At this early stage, it is possible to recognize certain NP classes or characteristic structural features. For known compounds, such tentative structural assignments can be easily confirmed by comparison with reported NMR data. For unknown compounds, the next step usually consists of acquisition of 2D NMR spectra. Four different types of 2D NMR experiments are the most common [28]:

- (^{1}H,^{1}H)-COSY or TOCSY are used for the characterization of proton spin systems. COSY spectra show only directly coupled protons, whereas TOCSY may show crosspeaks for further protons belonging to the same spin system.
- (^{1}H,^{13}C)-HSQC and HMQC serve to identify proton-bearing carbons and to associate these carbon atoms with their attached protons. Multiplicity-edited HSQC versions offer the added benefit of distinguishing CH_3, CH_2, and CH groups.

- (^{1}H,^{13}C)-HMBC provides long-range correlations between protons and carbons – mostly for those being two or three bonds apart from each other. It allows the identification of quaternary carbons and the linkage between separate structural fragments obtained from analysis of COSY/TOCSY and HSQC/HMQC.
- (^{1}H,^{1}H)-NOESY and ROESY provide information about spatial proximity of protons that are separated by up to 5 Å, which can be used to determine relative configuration.

For most organic small molecules, acquisition of 1D ^{13}C-NMR spectrum is not required when well-resolved HSQC and HMBC spectra are available. For NPs that cannot be sufficiently characterized by routine 2D NMR spectroscopy, as in the case of highly unsaturated compounds, (^{13}C,^{13}C)-INADEQUATE experiments are an option. However, due to the low natural abundance of ^{13}C, sensitivity of this method is extremely low and therefore, it requires a large amount of sample [28].

Although NOESY and ROESY experiments provide stereochemical information, only relative configuration can be extracted from these spectra. Thus, the complete spatial arrangement of a chiral molecule, or absolute configuration, needs to be proven by different methods. Determination of the absolute configuration of chiral NPs is essential, for it conditions their stereoselective interaction with biological targets and thus, their biological activity [29].

Although NMR techniques can be used for the determination of absolute configuration, complex experimental procedures are required. Spectroscopic measurement of chiroptical properties such as optical rotation (OR), optical rotatory dispersion (ORD), and circular dichroism (CD), allow the rapid and unambiguous differentiation between stereoisomers without major experimental efforts, using sub-μg amounts of sample [30].

References

[1] Cragg GM, Newman DJ. Natural products: A continuing source of novel drug leads. Biochim Biophys Acta BBA - Gen Subj 2013;1830:3670–95.

[2] Potterat O, Hamburger M. Drug discovery and development with plant-derived compounds. Prog Drug Res 2008;65.

[3] Wetzel S, Lachance H, Waldmann H. 3.02 - Natural Products as Lead Sources for Drug Development. In: Liu H-W (Ben), Mander L, editors. Compr. Nat. Prod. II, Oxford: Elsevier; 2010, p. 5–46.

[4] Li JW-H, Vederas JC. Drug Discovery and Natural Products: End of an Era or an Endless Frontier? Science 2009;325:161–5.

[5] Kingston DGI. Modern Natural Products Drug Discovery and Its Relevance to Biodiversity Conservation. J Nat Prod 2011;74:496–511.

[6] Koehn FE, Carter GT. The evolving role of natural products in drug discovery. Nat Rev Drug Discov 2005;4:206–20.
[7] Newman DJ, Cragg GM. Natural Products As Sources of New Drugs over the 30 Years from 1981 to 2010. J Nat Prod 2012;75:311–35.
[8] Potterat O, Hamburger M. Concepts and technologies for tracking bioactive compounds in natural product extracts: generation of libraries, and hyphenation of analytical processes with bioassays. Nat Prod Rep 2013;30:546.
[9] Appendino G, Fontana G, Pollastro F. 3.08 - Natural Products Drug Discovery. In: Liu H-W (Ben), Mander L, editors. Compr. Nat. Prod. II, Oxford: Elsevier; 2010, p. 205–36.
[10] Lam KS. New aspects of natural products in drug discovery. Trends Microbiol 2007;15:279–89.
[11] Avery VM, Camp D, Carroll AR, Jenkins ID, Quinn RJ. 3.07 - The Identification of Bioactive Natural Products by High Throughput Screening (HTS). In: Liu H-W (Ben), Mander L, editors. Compr. Nat. Prod. II, Oxford: Elsevier; 2010, p. 177–203.
[12] Potterat O, Hamburger M. Natural products in drug discovery - concepts and approaches for tracking bioactvity. Curr Org Chem 2006;10:899–920.
[13] Potterat O. Targeted approaches in natural product lead discovery. Chimia 2006;60:19–22.
[14] Hata Y, Zimmermann S, Quitschau M, Kaiser M, Hamburger M, Adams M. Antiplasmodial and Antitrypanosomal Activity of Pyrethrins and Pyrethroids. J Agric Food Chem 2011;59:9172–6.
[15] Julianti T, Hata Y, Zimmermann S, Kaiser M, Hamburger M, Adams M. Antitrypanosomal sesquiterpene lactones from Saussurea costus. Fitoterapia 2011;82:955–9.
[16] Zimmermann S, Kaiser M, Brun R, Hamburger M, Adams M. Cynaropicrin: The First Plant Natural Product with In Vivo Activity against Trypanosoma brucei. Planta Med 2012;78:553–6.
[17] Zimmermann S. Screening and HPLC-Based Activity Profiling for New Antiprotozoal Leads from European Plants. Sci Pharm 2012;80:205–13.
[18] Zaugg J, Baburin I, Strommer B, Kim H-J, Hering S, Hamburger M. HPLC-Based Activity Profiling: Discovery of Piperine as a Positive GABAA Receptor Modulator Targeting a Benzodiazepine-Independent Binding Site. J Nat Prod 2010;73:185–91.
[19] Yang X, Baburin I, Plitzko I, Hering S, Hamburger M. HPLC-based activity profiling for GABAA receptor modulators from the traditional Chinese herbal drug Kushen (Sophora flavescens root). Mol Divers 2011;15:361–72.
[20] Zaugg J, Eickmeier E, Rueda DC, Hering S, Hamburger M. HPLC-based activity profiling of Angelica pubescens roots for new positive GABAA receptor modulators in Xenopus oocytes. Fitoterapia 2011;82:434–40.
[21] Zaugg J, Ebrahimi SN, Smiesko M, Baburin I, Hering S, Hamburger M. Identification of GABAA receptor modulators in Kadsura longipedunculata and assignment of absolute configurations by quantum-chemical ECD calculations. Phytochemistry 2011;72:2385–95.
[22] Schramm A, Ebrahimi SN, Raith M, Zaugg J, Rueda DC, Hering S, et al. Phytochemical profiling of Curcuma kwangsiensis rhizome extract, and identification of labdane diterpenoids as positive GABAA receptor modulators. Phytochemistry 2013:318–29.
[23] Grabher P, Durieu E, Kouloura E, Halabalaki M, Skaltsounis L A, Meijer L, et al. Library-based Discovery of DYRK1A/CLK1 Inhibitors from Natural Product Extracts. Planta Med 2012;78:951–6.
[24] Bross-Walch N, Kühn T, Moskau D, Zerbe O. Strategies and tools for structure determination of natural products using modern methods of NMR spectroscopy. Chem Biodivers 2005;2:147–77.
[25] Wolfender J-L. HPLC in Natural Product Analysis: The Detection Issue. Planta Med 2009;75:719–34.
[26] Xing J, Xie C, Lou H. Recent applications of liquid chromatography–mass spectrometry in natural products bioanalysis. J Pharm Biomed Anal 2007;44:368–78.
[27] Korfmacher WA. Foundation review: Principles and applications of LC-MS in new drug discovery. Drug Discov Today 2005;10:1357–67.
[28] Edison AS, Schroeder FC. 9.06 - NMR – Small Molecules and Analysis of Complex Mixtures. In: Liu H-W (Ben), Mander L, editors. Compr. Nat. Prod. II, Oxford: Elsevier; 2010, p. 169–96.
[29] Zaugg J. Discovery of new scaffolds for GABAA receptor modulators from natural origin. Universität Basel, Basel; 2011.
[30] Ebrahimi S. Phytochemical profiling of Iranian plants, and ECD calculation as tool for establishing the absolute configuration of new natural products. Universität Basel, Basel; 2013.

2.2. Traditional medicine in drug-discovery: contributions and challenges

"Trees are sanctuaries. Whoever knows how to speak to them,
whoever knows how to listen to them, can learn the truth"

Hermann Hesse in Bäume. Betrachtungen und Gedichte (1984)

The role of ethnopharmacology in drug discovery

When screening for biologically active plant constituents, selection of the plant species to be studied is a crucial factor for the success of the investigation. Focused plant libraries can be assembled on the basis of ethnopharmacological, chemotaxonomic, ecological, or phylogenetic considerations, among others. Although some successful results in drug discovery have been accomplished with random (also known as biodiversity-based) screening, as in the case of taxol, the search based on ethnopharmacology is considered as one of the most effective approaches in the discovery of novel potential drug leads from plants [1–3].

Ethnobotany, also referred to as ethnopharmacology, is defined as the science of people's interaction with plants, including those used with therapeutic purposes [4]. The use of medicinal plants in traditional medicine represents a sort of preexisting clinical testing and a shortcut to biologically active compounds. Analyses of bioactivity databases such as the US National Cancer Institute (NCI) list of active plants, have revealed that species with an ethnopharmacological record are 2-5 times more likely to generate active extracts than those with no traditional use in medicine [3,5]. However, the translation of ethnobotanical knowledge into commercialized products is not easy. Many traditional medicines take holistic approaches and include in their treatments intangible elements that cannot be translated into molecular terms. Further complications can arise from insufficient validation and standardization, sustainability of the source, or intellectual property issues [5].

Ethnobotanical surveys and the study of written records on traditional medicine of cultures around the world have been the basis for the discovery of important therapeutic agents. A famous example is the discovery of the cardiac glycoside digoxin from foxglove (*Digitalis purpurea*), a European plant known as cardiotonic since centuries. Digoxin is nowadays used in the treatment of arrhythmia and congestive hearth failure. Moreover, the study of the

pharmacology of this drug has led to an understanding of the biochemical pathways involved in the development of heart conditions. Galanthamine, a drug currently used in the treatment of Alzheimer's disease, constitutes another example of therapeutic agents isolated from European species (in this case, *Galanthus* spp.) [5–7].

Traditional medicine in other cultures has also guided the discovery of plenty of useful NPs. Ethnopharmacological knowledge on the North American plant *Podophyllum peltatum* led to the discovery of podophyllotoxin, whose derivatives etoposide and teniposide are potent cytotoxic agents used nowadays in the chemotherapy of several types of cancer. *Catharanthus roseus*, a species from Madagascar known for its hypoglycemic properties, yielded the so called *vinca alkaloids* (e.g. vinblastine and vincristine), also used to date in oncology treatments. The study of plants used in traditional Chinese medicine (TCM) such as *Camptotheca acuminata* and *Artemisia annua*, has allowed the discovery of camptothecin and artemisinin, respectively. Semisynthetic derivatives of Camptothecin (i.e. topotecan and irinotecan) and artemisinin (i.e. artesunate and artemether) are nowadays used in clinic as chemotherapeutic agents for the treatment of cancer and malaria [5,6].

These examples above constitute just few of the many contributions of traditional medicine to drug discovery. However, medicinal plants are not only useful as the source of pure, chemically defined active principles. Being an essential component in the healthcare systems of many cultures worldwide[1], medicinal plants are commonly used as complex mixtures containing a broad range of constituents (infusions, tincture, extracts, among other preparations) [8,9]. Due to the rising interest on herbal medicines around the world, a brief description of challenges and perspectives of complex herbal products is provided in the next sections. Owing to the worldwide increasing impact and recognition of TCM as an alternative medicine modality, emphasis has been made on this traditional healthcare system.

Traditional Chinese Medicine

TCM is a holistic medical system for disease prevention, diagnosis, and treatment. It has a long history of development and application in China and, recently, is beginning to play a role in western healthcare as a complementary and alternative medicine modality. The overall

[1] According to the World Health Organization (WHO), traditional medicines represent the primary healthcare system for 60% of the world's population [2].

treatment concept of TCM differs greatly from that of western medicine, for patients are treated in an integral way that combines physical, emotional, and spiritual elements. Based on the Chinese philosophy of *Yin-Yang* balance[2], TCM uses experience-based therapies such as acupuncture and herbal medicine. Preventive approaches such as dietary advice, physical exercises, meditation, and massages, are also common in TCM [10,11].

Medicines prescribed in accordance with the principles and theories of TCM are generally designated as Chinese Materia Medica (CMM). They consist mostly of plants, although animals and minerals can also be used with therapeutic purposes. Prescription and processing of CMM constitute unique and critical aspects in the application of TCM. Prescriptions usually consist of complex mixtures of multiple components, chosen based on differentiation of symptoms and signs including *yin*, *yang*, exterior, interior, cold, heat, deficiency, and excess. In such formulations the balance and interaction of all components are more important than the effect of any individual element [10,11]. Processing is a common practice in TCM, in which CMM are subjected to specific treatments before their use, with the aim of enhancing the efficacy and/or reducing the toxicity of crude drugs. These treatments can go from cleaning and cutting, to boiling, steaming, soaking in vinegar, frying, or roasting, among many others. Fifteen CMM processing methods have been clearly listed in the Chinese Pharmacopoeia (2010 edition), which also comprises the most commonly used TCM drugs, listed as *i*) materia medica and prepared slices of Chinese crude drugs, *ii*) vegetable oils, fats, and extracts, *iii*) patented prescriptions, and *iv*) single preparations. Information on purity standards, testing, dosage, precautions, storage, and strength is provided for each drug [12–14].

Over the past two decades, governmental and non-governmental efforts within and outside China have been made to promote TCM practice, teaching, research, and development. As a result, new international organizations like the International Society for Chinese Medicine, the Modernized Chinese Medicine International Association, and the World Federation of Chinese Medicine Societies have been created. Existing organizations have also taken actions into the matter. In 2009, the International Organization for Standardization (ISO) set up specialized committees dedicated to TCM. In 2010, the WHO set up a program to standardize

[2] *Yin-Yang*: In Chinese philosophy and religion there are two primal, opposite principles. One negative, dark, and feminine (*yin*) and one positive, bright, and masculine (*yang*). From their interaction, all things are produced and dissolved [10].

terms used in TCM and its derivatives (e.g. the Japanese herbal medicine *Kampo*), aiming for the creation of an international platform to harmonize information exchange on traditional medicines. In 2011, the UNESCO inscribed *Ben Cao Gang Mu* (Compendium of Materia Medica) and *Huang Di Nei Jing* (Yellow Emperor's Inner Cannon) in the Memory of the World Register [11].

Herbal medicines: the quality issue

Herbal medicinal products (HMPs) are widely used around the world, increasingly so in western nations. Although HMPs are considered to be safer than synthetic drugs, there has been more recognition of the potential risks associated with this type of products as their use increases. Potential harm can come from diverse sources, most of them involving purity and identity issues. Purity of HMPs may be compromised by the presence of dirt, pesticides, heavy metals, microorganisms or toxins, residual solvents, processing impurities, among others. Identity issues include species substitution, misidentification or adulteration with foreign plant material or synthetic drugs that resemble/mimic the expected action of a given HMP (e.g. addition of benzodiazepines to herbal sleep aids, sildenafil to herbal treatments of erectile dysfunction, etc.) [15,16].

In the case of herbs used in TCM, quality issues can arise from poor authentication of CMM due to similarities in nomenclature. Common Chinese names of CMM are often a source of confusion, since some herbs have more than one name and in occasions, these names are used for more than one herb. Even just similar common names can lead to misidentification and confusions as in the case of *Panax notoginseng* (Sanqi 三七) and *Tupistra chinensis* (Chuansanqi 川三七). These two herbs are commonly confused, although they belong to different families and have different therapeutic effects [13,17]. A well known and tragic case of such confusion is the mistaken use of *Aristolochia* species as a substitute for herbs with similar common name in some slimming preparations, which resulted in the widely reported fatal incidents of "Aristolochic acid nephropathy" [15,18,19].

Morphological similarities between herbal drugs, commonly consisting of dried or processed plant parts, can also be a source of confusion in authentication of CMM. In China, herb authentication in CMM markets is based on the macroscopic evaluation of properties such as shape, size, color, texture, odor, taste, and reaction to water and fire. Being the simplest and fastest method for CMM, authentication by macroscopic inspection relies solely on personal

experience and can be misleading, since organoleptic properties of herbs depend on a number of factors such as growing, harvesting, and processing conditions. Moreover, closely related herbal drugs (e.g. species from the same genus) can be hard to distinguish by the naked senses [20].

An additional complication with quality and safety of Chinese herbs comes from CMM processing. Crude and processed forms of the same herb often have different properties and must be used as such. However, differently processed herbs can be misused as the same drug, resulting in treatment failure or even poisoning. A common example is the misuse of different forms of Semen Strychni, a CMM derived from the seeds of *Strychnos nux-vomica*. In this case, while the processed drug (Zhimaqianzi 制马钱子) is used in the treatment of rheumatic conditions, while the crude seeds (Shengmaqianzi 生马钱子) are highly toxic [12,13].

Authentication and standardization of CMM are urgent tasks to ensure the safety and efficacy of their use. Macroscopic authentication must be confirmed by taxonomic, microscopic, and physicochemical analyses [13,17]. TLC and HPLC fingerprinting are the most widely used techniques in chemical authentication and have been adopted in many pharmacopoeias as identification methods [21–23]. Information obtained from chemical fingerprinting allows reliable confirmation of herb identity and detection of some non-chemically-related contaminants. Furthermore, the quality of different samples of the same herb can be assessed, based on the variable content of active or toxic constituents due to environmental, processing, and storage conditions [13].

Genomic and metabolomic approaches are also being applied in the identification, authentication, and quality control of medicinal herbs. Metabolic fingerprinting allows differentiation between individual species of the same genus and identification of the exact geographic origin of certain species [15,24]. On the other hand, genetic tools provide highly reliable data for the authentication of herbs at the DNA level, which is particularly useful in the case of those herbs that are substituted or adulterated with morphologically and/or chemically similar material. DNA technology provides consistent results that do not depend on the age, tissue origin, physiological conditions, environmental factors, harvest, storage, or processing of the samples. With little amounts of sample, plants can be unequivocally identified up to their species, subspecies, and variety [25].

International regulation and actions on herbal drugs

Increasing discussions on the safety assessment of herbs used in both food and medicines around the world, have resulted in the development of protocols and guidance documents for the assurance of continuing quality of herbal drugs. Examples include the *Dietary Supplement Health and Education Act* (DSHEA) in United States, the *Natural Health Products Regulations* (NHPR) in Canada, and the *Therapeutics Goods Act* in Australia. In the European Union, the Committee on Herbal Medicinal Products (HMPC), part of the European Medicines Agency (EMEA), regulates the use of herbal medicines and publishes herbal monographs for quality control. The WHO has also published guidelines on the quality of HMPs, and specifications for the quality of a number of herbal drugs are set out in pharmacopeias such as the Unites States Pharmacopoeia (USP), the British Pharmacopoeia (BP), and the European Pharmacopoeia (EP) [15].

In the particular case of TCM, due to its globalized use, potential impact on healthcare, and opportunities for new drug development, special international actions have been started up. Two years ago, a new era for modernization of TCM was launched with the successful completion of the *Good Practice in Traditional Chinese Medicine Research in the Post-genomic Era* (GP-TCM) project, under the European Union's 7th Framework Program (FP7). This project brought together a large collaborative network of over 200 Chinese and European scientists, 107 institutions, and 24 countries to work on the analysis of current status, challenges, priorities, and future directions of TCM research. Multiple aspects were covered, i.e. quality control, toxicology, pharmacology, regulatory issues, and acupuncture and moxibustion. As a result of the three-year project, a series of guidelines and technical notes were developed for the harmonization of international TCM research through standard protocols and methodologies [11,26,27].

In April 2012, a consortium called *GP-TCM Research Association* was founded to develop, refine, and disseminate the results generated from the GP-TCM project. One essential point is the application of good practice in authentication, quality control, safety assessment, and sustainable use of TCM drugs. Likewise, agricultural, manufacturing, commercial, and clinical practices must incorporate good practices into their protocols and actions. Beyond quality assessment, efficacy and mechanistic studies have also been defined as priorities on TCM research. In this context, *omics* (genomics, proteomics, metabolomics, etc) and systems

biology technologies are expected to provide a more holistic approach to the study of complex TCM drugs [11,27,28].

References

[1] Cox PA, Balick MJ. The ethnobotanocal aproach to drug discovery. Sci Am 1994;270:82–7.

[2] Brusotti G, Cesari I, Dentamaro A, Caccialanza G, Massolini G. Isolation and characterization of bioactive compounds from plant resources: The role of analysis in the ethnopharmacological approach. J Pharm Biomed Anal 2014;87:218–28.

[3] Gyllenhaal C, Kadushin MR, Southavong B, Sydara K, Bouamanivong S, Xaiveu M, et al. Ethnobotanical approach versus random approach in the search for new bioactive compounds: Support of a hypothesis. Pharm Biol 2011;50:30–41.

[4] McClatchey WC, Mahady GB, Bennett BC, Shiels L, Savo V. Ethnobotany as a pharmacological research tool and recent developments in CNS-active natural products from ethnobotanical sources. Pharmacol Ther 2009;123:239–54.

[5] Appendino G, Fontana G, Pollastro F. 3.08 - Natural Products Drug Discovery. In: Liu H-W (Ben), Mander L, editors. Compr. Nat. Prod. II, Oxford: Elsevier; 2010, p. 205–36.

[6] Heinrich M. 3.12 - Ethnopharmacology and Drug Discovery. In: Liu H-W (Ben), Mander L, editors. Compr. Nat. Prod. II, Oxford: Elsevier; 2010, p. 351–81.

[7] Rishton GM. Natural Products as a Robust Source of New Drugs and Drug Leads: Past Successes and Present Day Issues. Oxidative Stress Heart Dis Oxidative Stress Heart Dis 2008;101:S43–S49.

[8] Cragg GM, Newman DJ. Natural products: A continuing source of novel drug leads. Biochim Biophys Acta BBA - Gen Subj 2013;1830:3670–95.

[9] Cordell GA. Phytochemistry and traditional medicine – A revolution in process. Spec Issue Honour Profr Ayhan Ulubelen 2011;4:391–8.

[10] Yang M, Tao S, Guan S, Wu X, Xu P, Guo D. 3.13 - Chinese Traditional Medicine. In: Liu H-W (Ben), Mander L, editors. Compr. Nat. Prod. II, Oxford: Elsevier; 2010, p. 383–477.

[11] Xu Q, Bauer R, Hendry B, Fan T-P, Zhao Z, Duez P, et al. The quest for modernisation of traditional Chinese medicine. BMC Complement Altern Med 2013;13:132.

[12] Zhao Z, Liang Z, Chan K, Lu G, Lai Mei Lee E, Chen H, et al. A Unique Issue in the Standardization of Chinese Materia Medica: Processing. Planta Med 2010;76:1975–86.

[13] Zhao Z, Hu Y, Liang Z, Yuen J, Jiang Z, Leung K. Authentication is Fundamental for Standardization of Chinese Medicines. Planta Med 2006;72:865–74.

[14] Chinese Pharmacopoeia Commission. Pharmacopoeia of the People's Republic of China, vol. I. vol. Vol. 1. China Medical Science Press, Beijing (English edition); 2010.

[15] Jordan SA, Cunningham DG, Marles RJ. Assessment of herbal medicinal products: Challenges, and opportunities to increase the knowledge base for safety assessment. Saf Assess Saf Assess 2010;243:198–216.

[16] Bilia AR. Herbal drugs, herbal drug preparations and medicinal products: quality standards according to European Pharmacopoeia. Eur J Integr Med 2012;4, Supplement 1:108–9.

[17] Zhao Z, Xiao P, Xiao Y, Yuen JP. Quality assurance of Chinese Herbal Medicines (CHMs). J Food Drug Anal 2007;15:337–46.

[18] Vanhaelen M, Vanhaelen-Fastre R, But P, Vanherweghem J-L. Identification of aristolochic acid in Chinese herbs. The Lancet 1994;343:174.

[19] Vanherweghem J-L, Tielemans C, Abramowicz D, Depierreux M, Vanhaelen-Fastre R, Vanhaelen M, et al. Rapidly progressive interstitial renal fibrosis in young women: association with slimming regimen including Chinese herbs. Orig Publ Vol 1 Issue 8842 1993;341:387–91.

[20] Zhao Z, Liang Z, Ping G. Macroscopic identification of Chinese medicinal materials: Traditional experiences and modern understanding. J Ethnopharmacol 2011;134:556–64.

[21] Bauer R, Franz G. Modern European Monographs for Quality Control of Chinese Herbs. Planta Med 2010;76:2004–11.

[22] Xie P, Chen S, Liang Y, Wang X, Tian R, Upton R. Chromatographic fingerprint analysis—a rational approach for quality assessment of traditional Chinese herbal medicine. Plant Anal 2006;1112:171–80.

[23] Song X-Y, Li Y-D, Shi Y-P, Jin L, Chen J. Quality control of traditional Chinese medicines: a review. Chin J Nat Med 2013;11:596–607.

[24] Sheridan H, Krenn L, Jiang R, Sutherland I, Ignatova S, Marmann A, et al. The potential of metabolic fingerprinting as a tool for the modernisation of TCM preparations. J Ethnopharmacol 2012;140:482–91.

[25] Heubl G. New Aspects of DNA-based Authentication of Chinese Medicinal Plants by Molecular Biological Techniques. Planta Med 2010;76:1963–74.
[26] Chan K, Shaw D, Simmonds MSJ, Leon CJ, Xu Q, Lu A, et al. Good practice in reviewing and publishing studies on herbal medicine, with special emphasis on traditional Chinese medicine and Chinese materia medica. J Ethnopharmacol 2012;140:469–75.
[27] Uzuner H, Bauer R, Fan T-P, Guo D, Dias A, El-Nezami H, et al. Traditional Chinese medicine research in the post-genomic era: Good practice, priorities, challenges and opportunities. J Ethnopharmacol 2012;140:458–68.
[28] Pelkonen O, Pasanen M, Lindon JC, Chan K, Zhao L, Deal G, et al. Omics and its potential impact on R&D and regulation of complex herbal products. J Ethnopharmacol 2012;140:587–93.

2.3. The $GABA_A$ receptor

"(...) and if you take more of those, you will get an overdose.
No more running for the shelter of a mother's little helper.
They just helped you on your way, through your busy dying day"

The Rolling Stones about barbiturates in their song Mother's little helper (1966)

Definition and structural features of $GABA_A$ receptors

Neuronal activity results from the interplay between synaptic excitation and inhibition. In the brain, excitation is mainly generated by the neurotransmitter glutamate, while inhibition is primarily produced by gamma-aminobutyric acid (GABA) [1], synthesized from glutamate by the enzyme glutamic acid decarboxylase [2]. Being the major inhibitory neurotransmitter in the central nervous system (CNS), GABA regulates many physiological and psychological processes through activation of ionotropic $GABA_A$ receptors ($GABA_A$Rs) and metabotropic $GABA_B$ receptors ($GABA_B$Rs), both of which are involved in the modulation of emotions, cognition, pain, and muscle tone. While $GABA_B$Rs are G-protein-coupled receptors mediating slow inhibitory neurotransmission, $GABA_A$Rs are chloride channels that mediate the major form of fast synaptic inhibition in the CNS[3] [5–7]. GABA-induced activation of $GABA_A$Rs triggers a conformational change in the protein and consequent opening of the ion channel [8], which results in increased chloride conductance, hyperpolarization of postsynaptic neurons, and subsequent inhibition of further action potentials. Therefore, impaired GABAergic neurotransmission is often associated with a number of CNS conditions like epilepsy, anxiety, mood disorders, and neurodevelopmental disorders such as autism and schizophrenia [9].

$GABA_A$Rs belong to the gene superfamily of Cys-loop ligand-gated ion channels (LGICs), heteropentameric proteins that work as transducers of chemical messages into electric signals [8]. Receptor activation involves three major stages: agonist binding, transduction of the binding signal down the channel (coupling), and opening of the ion channel (gating) [10]. Five membrane-spanning subunits surround the central chloride-selective pore, each of them consisting of a large N-terminal extracellular hydrophilic domain, four transmembrane regions, and a relatively short extracellular C-terminal domain. The interface between

[3] $GABA_A$Rs are excitatory receptors in embryonic life and inhibitory in the developed nervous system [3]. This switch is essential for structural and functional maturation of neurons [4].

adjacent extracellular domains constitutes the neurotransmitter binding site, whereas the membrane-spanning domains form the ion channel (Figure 2.3) [2,10]. Nineteen different $GABA_AR$ subunit isoforms have been identified so far in mammals, and are divided into eight subunit families on the basis of their sequence homology (Figure 2.4): α_{1-6}, β_{1-3}, γ_{1-3}, δ, ε, θ, π, and ρ_{1-3}, the later of which can form homopentamers previously known as $GABA_C$ receptors[4].

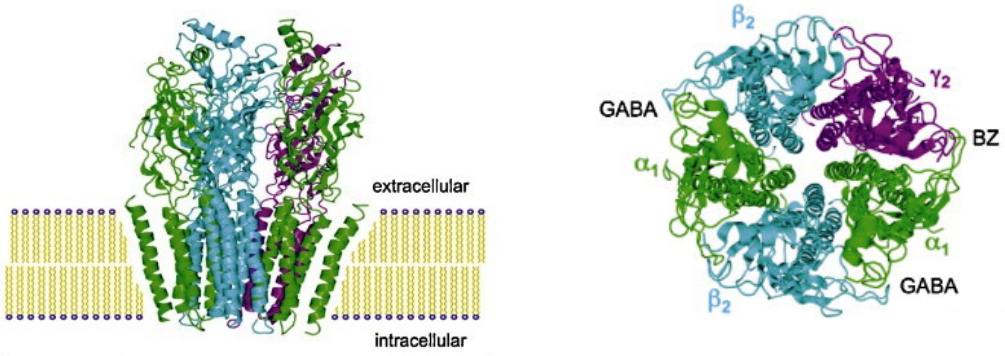

Figure 2.3. Structure of the nicotinic acetylcholine receptor (nAChR) illustrates the general structure of Cys-loop receptors. **Left:** Side view of the receptor embedded in the cell membrane, showing extracellular and membrane-spanning domains. **Right:** View from the top of the receptor. The subunits are labeled according the $GABA_AR$ nomenclature and the most abundant receptor subtype is displayed. The approximate locations of the GABA and benzodiazepine (BZD) binding sites are noted (reproduced from D'Hulst et al., 2009 [2]).

Different subunit combinations result in a large number of structurally and functionally distinct $GABA_AR$ subtypes. Furthermore, structural diversity is increased by the alternative exon splicing of some receptor subunits, primarily γ_2 and β_2. However, despite the vast potential for receptor diversity, only 11 subtypes have been identified as reasonably abundant in the brain and 15 more subtypes are likely to exist although to a much lesser extent [5,11,12]. Explanations include differential gene expression by specific neuronal subtypes, preferential co-assembly of particular subunits [13], and receptor trafficking regulation[5] [4].

The nature, stoichiometry, arrangement, and localization of the subunits involved determine the biophysical and pharmacological profile of the assembled receptor [2,5,9]. $GABA_ARs$

[4] $GABA_CRs$ were originally described based on their distinctive pharmacology. However, they are now designated as part of the $GABA_AR$ family and therefore, the use of this nomenclature is discouraged [5].

[5] $GABA_ARs$ are assembled in the endoplasmic reticulum (ER). Misfolded or in any way immature receptors cannot exit the ER and are subsequently degraded in a proteasome. Only a limited number of the theoretically possible subunit combinations can actually reach the neuronal cell surface. [11].

with stoichiometry 2α:2β:1γ are predominant in the brain [5,14], and show the concatenation pattern α-β-α-γ-β [15]. This arrangement provides two GABA-binding sites at the β-α interfaces, normally containing β_2 or β_3 subunits, and a benzodiazepine (BZD) binding site at the α-γ interface, most commonly comprising γ_2 and α_1, α_2, α_3, or α_5. Approximately 60% of all $GABA_A$Rs have the subunit combination $\alpha_1\beta_2\gamma_2$. Following in abundance are the receptor subtypes $\alpha_2\beta_3\gamma_2$ (15-20% approx), $\alpha_3\beta_n\gamma_2$ (10-15% approx), and $\alpha_4\beta_n\gamma$ or $\alpha_4\beta_n\delta$ (5% approx). Other combinations such as $\alpha_5\beta_2\gamma_2$ and $\alpha_6\beta_{2/3}\gamma_2$ constitute less than 5% of the total $GABA_A$Rs in the CNS [14,15].

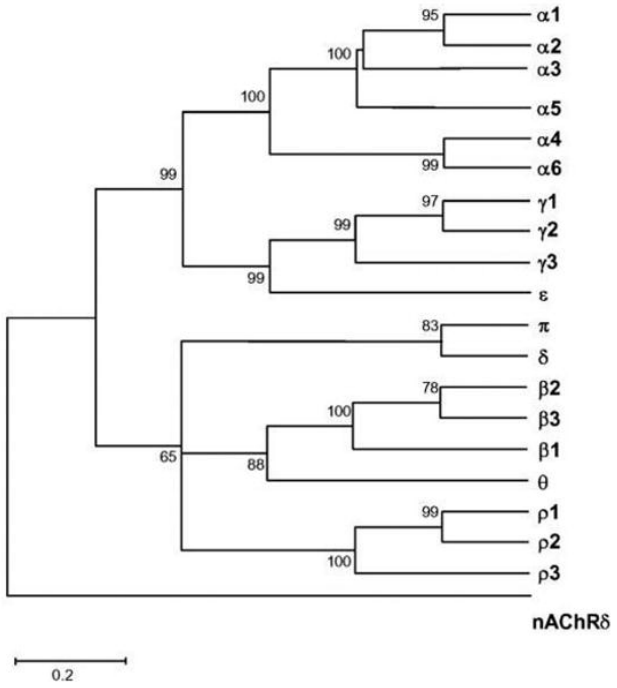

Figure 2.4. Dendrogram of the 19 genes for human $GABA_A$Rs. Distances along each line are proportional to the degree of sequence identity between homologous subunits. Greek letters designate subunit families of high (>70%) identity. The scale bar corresponds to 20% sequence divergence (reproduced from Simon et al., 2004 [16]).

According to the PDB (Protein Data Bank) website, to date there is no available high-resolution structure of the $GABA_A$R [17]. Electron micrographs of nAChRs in the electric ray *Torpedo marmorata*, members of the same gene superfamily, have provided the most complete structure of a Cys-loop receptor so far [10]. Although structural information of $GABA_A$R is much less complete, homology in topography and structure of the functional domain allows comparative modeling of the binding sites of $GABA_A$R based on the nAChR structure [15,18]. However, low sequence identity between target ($GABA_A$R) and template (nAChR) can result in potential inaccuracy and uncertainty of such models, limiting rational drug design of $GABA_A$R ligands [19,20].

Pharmacology of GABA$_A$ receptors

GABA$_A$Rs serve as molecular target for a number of drugs, used both clinically and as research tools. The list of chemically diverse GABA$_A$R ligands includes agonists like muscimol, antagonists like bicuculline, channel blockers like picrotoxin, and receptor modulators such as BZDs, non-benzodiazepines, barbiturates, neurosteroids, ethanol, and some general anesthetics like etomidate and propofol (Figure 2.5) [2,5,18].

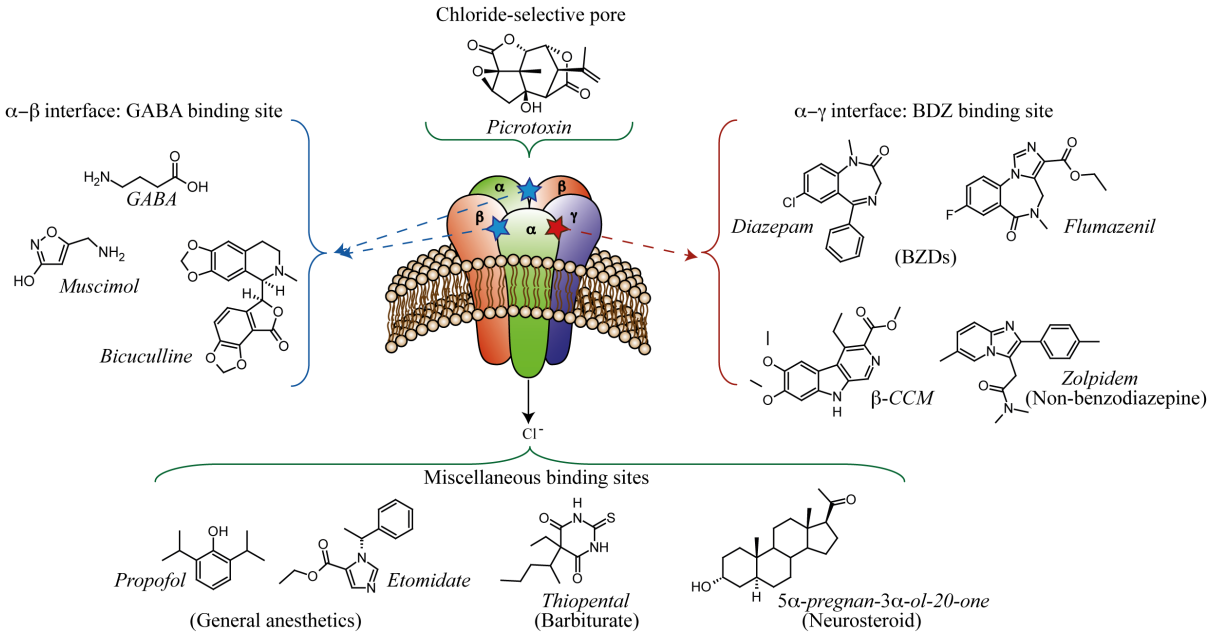

Figure 2.5. Examples of GABA$_A$R ligands. Compounds binding at the α-β interface can be direct agonists (e.g. muscimol) or direct antagonists (e.g. bicuculline). Compounds binding at the α-γ interface are allosteric modulators. This modulation, achieved by stabilizing different conformations of the receptor, can be positive, negative, or neutral. Positive and negative allosteric modulators (also referred as BZD-site agonists and inverse agonists, respectively) enhance or reduce the GABA-induced chloride ion influx. Neutral allosteric modulators (or BZD-site antagonists) do not influence the chloride influx but are able to competitively inhibit the action of positive and negative allosteric modulators. Prototypic examples for positive, negative, and neutral GABA$_A$R allosteric modulators are diazepam, β-CCM (methyl β-carboline-carboxylate), and flumazenil, respectively [5,12,14]. Picrotoxin is a channel blocker. The binding sites for other ligands like barbiturates, general anesthetics, and neurosteroids have not been identified yet [12,21,22].

The interaction of BZDs with GABA$_A$Rs has been most extensively investigated [18]. Unlike barbiturates, BZDs are allosteric modulators of GABA$_A$Rs. They mediate their actions via an alternative binding site also known as BZD binding site. Consequently, they do not activate the receptors in the absence of GABA and thus, modulation is self-limiting: the conductance of the channel in the presence of GABA and BZDs is never higher than the conductance induced by GABA alone [14]. BZDs have been prescribed since 1960, when

chlordiazepoxide (Librium®) was first introduced. Due to their improved therapeutic index over barbiturates, they became the most prescribed drugs in the 1960s and 70s [23]. A number of clinical uses have been approved for BZDs, including the treatment of sleep disturbances, anxiety disorders, epilepsy, and muscular spasms [12]. However, as a consequence of non-selective binding to $GABA_AR$s containing α_1, α_2, α_3, or α_5 subunits, these pharmacological effects are not clearly separated by dosing and thus, BZDs induce a number of side effects including residual sedation, anterograde amnesia, tolerance, physical dependence, and addiction liability [14].

BZDs have been used as research tools to elucidate the functions of individual $GABA_AR$ subtypes in mutated mouse lines, in which specific receptors have been rendered insensitive to diazepam (Figure 2.6). Histidine-to-arginine point mutations at a conserved residue of subunits α_1, α_2, α_3, and α_5 abolish binding of diazepam, whereas the action of the physiological neurotransmitter GABA is preserved [14]. Comparison of diazepam-induced behavioral responses in the mutated and wild-type mice, have revealed that BZD-induced sedation, anterograde amnesia, and anticonvulsant effects are mediated by α_1-containing $GABA_AR$s, while receptors with α_2 mediate the anxiolytic action and to a large degree the myorelaxant effects. Subunits α_3 and α_5 are also involved in myorelaxant action of BZDs [18,21]. The addictive properties of BZDs have been correlated to α_1-containing $GABA_AR$s by a mechanism that involves changes in synaptic plasticity of dopaminergic neurons at the brain's VTA (ventral tegmental area) [12]. The development of tolerance to the sedative properties of diazepam has been associated with α_1 and α_5 subunits, which explains why the partially selective hypnotic Zolpidem (which does not bind to the α_5-containing $GABA_AR$) shows less dependence liability than non-selective BZDs [23].

The identification of physiological and pharmacological functions of $GABA_AR$ subtypes defined by their α subunit composition has renewed the interest in the target for the development of drugs with improved therapeutic profile over BZDs. A number of compounds with receptor subtype selectivity have been identified and evaluated in preclinical and clinical studies. However, further development of such compounds has stopped due to unfavorable pharmacokinetic properties or toxicity issues [14,24]. Non-benzodiazepines (also known as Z-drugs) like zolpidem, zaleplon, and zopiclone, are the only $GABA_AR$ modulators on the market with preferential binding to α_1-containing receptors [25]. However, BZD-like side effects are still being reported for these drugs [26].

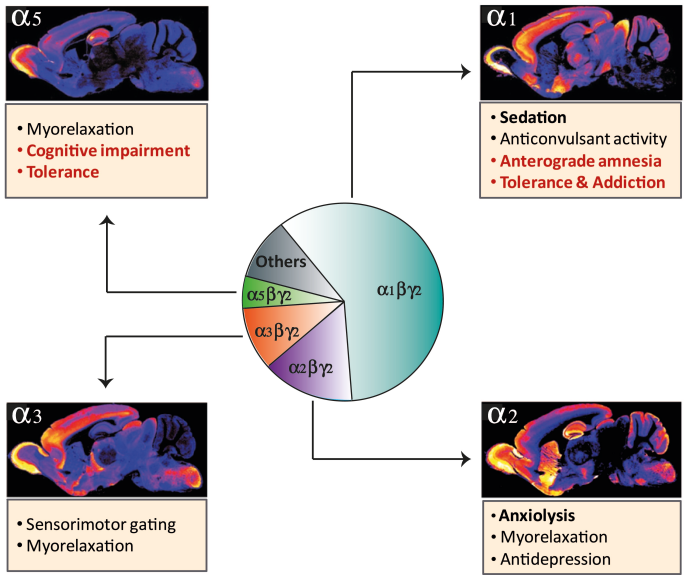

Figure 2.6. Pharmacological effects and distribution of $GABA_AR$ α subunits in the mouse brain. The pie chart represents the approximate abundance of $GABA_AR$ subtypes that are known to exist *in vivo*. α_1 is expressed in cortex, thalamus, pallidum, and hippocampus. α_2 is expressed in hippocampus, cortex, striatum, and nucleus accumbens. α_3 occurs in the cortex and the reticular nucleus of the thalamus, and α_5 in the hippocampus and deep layers of the cortex (adapted from Rudolph and Knoflach, 2011 [14]).

$GABA_A$ receptor modulators: current challenges and perspectives

$GABA_AR$ ligands are well known agents in the history of neuropharmacology. It all began in 1911, when barbiturates hit the market with Bayer's Veronal® (barbital) and Luminal® (phenobarbital). Barbiturates were extensively used as sedative/hypnotic, antiepileptic, and anesthetic drugs until the end of the 1950s [27], when it became evident that high doses of barbiturates lead to pulmonary arrest and death, outcomes that gained further notoriety with the deaths of celebrities like Marilyn Monroe and Jimi Hendrix. The 1960s brought new hope with the introduction of the much safer BZDs, but they too fell out of favor when long-term treatments induced residual sedation, memory impairment, and addiction. Z-drugs came into the picture in the 1990s and have been the hypnotics of choice ever since. However, despite their improved therapeutic profile and partial receptor selectivity, complications such as dependence and "confusional arousals" are still reported [26,28].

Recurrent failure in the development of subtype selective $GABA_AR$ modulators seems to have discouraged pharmaceutical companies from the search of new GABAergic drugs [24]. However, it appears that the problems observed during preclinical and clinical studies are

unrelated to the mechanism of the developed leads and thus, further efforts should be directed towards improving the pharmacokinetics and toxicity of such compounds [12].

In the absence of receptor-selective $GABA_AR$ modulators, new targets are now being explored. Serotonin (5-HT), neuropeptide, glutamate, and endocannabinoid systems stand now as the principal focus of anxiolytic drug discovery research [24]. On the other hand, dual orexin receptor antagonists (DORAs) are rendering promising results in the management of insomnia with a better safety profile [26]. Suvorexant, an orexin receptor-antagonist, was submitted by Merck & Co. for US FDA approval in 2012 [28]. Approval still depends on the results of further safety and manufacturing studies requested by the FDA in 2013. If approved, this would be the first DORA in the market for the treatment of insomnia [29]. Nevertheless, $GABA_ARs$ remain an important target in the development of improved therapeutics for the management of anxiety, epilepsy, insomnia, and cognitive disorders [3,19]. Moreover, the identification of separable key functions of particular $GABA_AR$ subtypes has provided valuable information about novel possible indications of $GABA_AR$ modulators, such as chronic pain, depression, schizophrenia, and stroke [14]. Although the complexity and large structural diversity of $GABA_ARs$ poses a challenge to drug development, it offers plenty of possibilities for fine tuned pharmacological interventions [19]. Further efforts must be directed to the elucidation of the structure of $GABA_ARs$. Together with functional studies, it would provide a clearer picture of the role of these receptors in neurotransmission and the way structural variations between receptor subtypes impart their unique characteristics, facilitating the design of novel and improved therapeutics for the treatment of neurological disorders [10].

In vitro ***assessment of GABAergic activity: two-microelectrode voltage-clamp assay***

Measurement of ion influx across the cell membrane can be achieved using several techniques such as radioactivity-based ion influx assays, fluorescence-based assays, or microphysiometry studies. However, these techniques do not allow the membrane potential to be controlled. As a consequence, the electrochemical gradients that drive the flow through ion channels can get disrupted, leading to false readouts. Further disadvantages of these methods include artifact formation during fluorescence measurements and accumulation of ligands in the cells due to the lack of continuous perfusion systems [30,31].

Electrophysiological techniques offer a better alternative for the study of ion channels. In this case, electrical changes upon receptor activation are measured directly and quantitatively while the membrane potential is controlled (i.e. clamped). Automated patch-clamp systems demand stable cell lines expressing the target of interest and highly specialized consumables, which makes them time-consuming and labor-intensive techniques for electrophysiological measurements. The more flexible two-electrode voltage-clamp (TEVC) technique, a robust electrophysiological technique using *Xenopus* oocytes for expression of the target of interest, in this case $GABA_AR$s, circumvents some of the disadvantages of the automated patch-clamp systems. In this method, cell membrane is clamped at a fixed value and the whole cell currents produced in response to receptor activation are measured in terms of the current required to maintain the voltage clamp. Two electrodes, one controlling membrane potential (VE) and one measuring the current (CE), impale the oocyte during the experiments. By means of a feedback system, the CE provides the current needed to maintain membrane potential. The current flowing though the CE provides a measurement of the current flowing though the ion channels (Figure 2.7) [31,32].

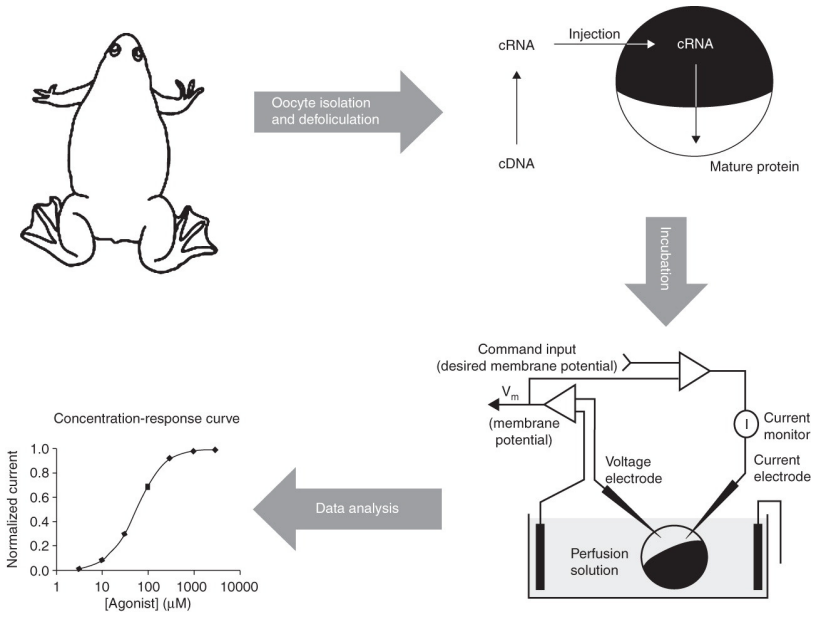

Figure 2.7. Schematic representation of the TVEC recordings workflow using *Xenopus* oocytes, for the study of ion channels. Oocytes are surgically removed from adult female *Xenopus laevis*, defolliculated by enzymatic means, and injected with cRNA (transcripted from cDNA) of the desired receptor subunits. Incubation allows expression of the molecular target. The oocytes with the expressed receptors are used for TEVC recordings (reproduced from Kvist et al. 2011[31])

Xenopus oocytes, the immature egg cells of the South African clawed frog *Xenopus laevis*, are a reliable and powerful system for the transient expression of multi-subunit proteins derived from exogenously introduced RNA or DNA. These cells are easy to handle due to their robustness and large size (1 – 1.2 mm diameter), which make them tolerant to repeated impalement with RNA injection pipettes and microelectrodes used in electrophysiological techniques (Figure 2.8). The relative scarcity of endogenous ion channels in the oocyte membrane makes it a versatile tool for the study of a wide range of ion channel proteins, including members of the LGIC family such as $GABA_A$Rs .

Figure 2.8. Photograph of a *Xenopus* oocyte impaled during TEVC recordings (Picture D. Rueda, Vienna)

Activation and gating of ligand-gated ion channels is characterized by complex kinetics. Fast ("concentration jump") application of neurotransmitter or drug samples during TEVC experiments is crucial for screening on $GABA_A$R. Slow perfusion rates and consequent slow sample application leads to slow channel activation and substantial receptor desensitization during chamber perfusion. As a result, peak current values induced by neurotransmitters or drugs may be underestimated. Therefore, fast perfusion of oocytes is key for the acquisition of reproducible data with the TEVC technique. In order to fulfill these conditions and standardize drug application to the oocytes, a medium-throughput automated system for fast perfusion has been implemented by Professor Hering and coworkers at the University of Vienna. In this optimized system, the oocytes are placed in a small bath chamber and perfused in a vertical direction at a very fast rate (up to 600 µL/s), while compound delivery is controlled by a programmable pipetting workstation. Figure 2.9 provides detailed descriptions of the system [33].

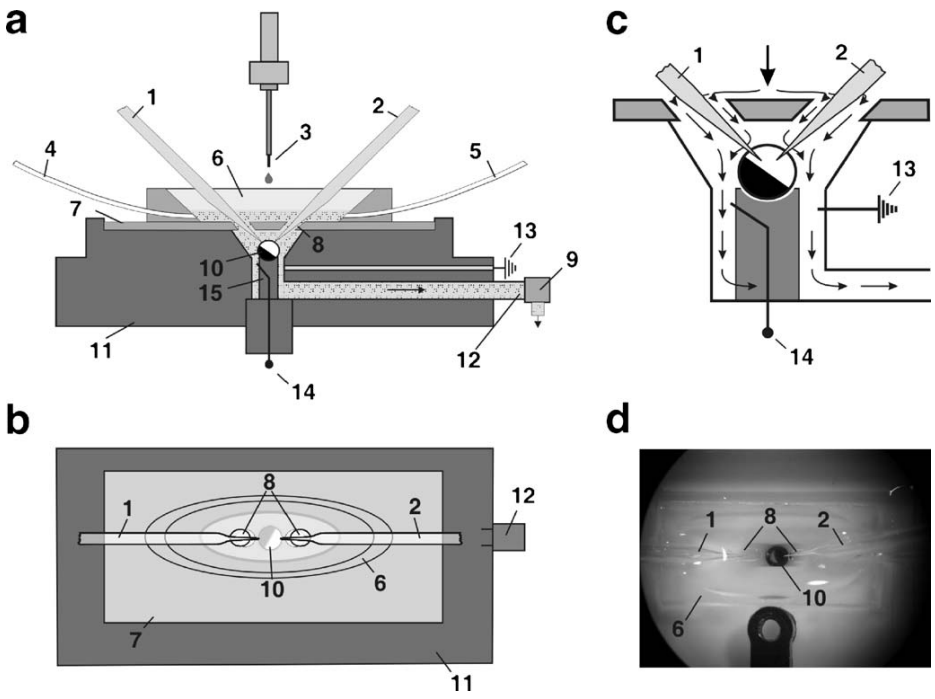

Figure 2.9. Cross-section view (**a**) and top view (**b**) of the oocyte perfusion chamber of the automated two- microelectrode voltage clamp assay as implemented by the Hering group in Vienna [33]. Two microelectrodes (*1* and *2*) are inserted via the sloping access inlets (*8*) through a glass cover plate (*7*) into the small (~ 15 µL) oocyte chamber (c). Samples are applied by the tip of an automated liquid handling arm (*3*) to a funnel reservoir made of quartz (*6*) surrounding the microelectrode access holes. Perfusion of the oocyte (*10*) that is placed on a cylindrical holding device (*15*) is enabled by means of the syringe pump (*9*) connected to the chamber body (*11*) via the outlet (*12*). Residual solution is removed from the funnel before drug application via the funnel outlets (*4* and *5*). In addition to the ground reference electrode (*13*), the cylindrical holder for the oocyte contains a reference electrode (*14*) that serves as an extracellular reference for the potential electrode. Salt bridges can be inserted into the side outlet for the ground electrode (*13*). (**c)** Schematic drawing of the solution flow inside the perfusion chamber and in the annular gap around the cylinder with oocyte. (**d)** Photo of the oocyte perfusion chamber. An oocyte (*10*) is placed on a cylinder and impaled with two microelectrodes (*1,2*) surrounded by the funnel (*6*) (reproduced from Baburin et al. 2006 [33]).

References

[1] Gassmann M, Bettler B. Regulation of neuronal GABAB receptor functions by subunit composition. Nat Rev Neurosci 2012;13:380–94.

[2] D'Hulst C, Atack JR, Kooy RF. The complexity of the GABAA receptor shapes unique pharmacological profiles. Drug Discov Today 2009;14:866–75.

[3] Verkman AS, Galietta LJV. Chloride channels as drug targets. Nat Rev Drug Discov 2009;8:153–71.

[4] Luscher B, Fuchs T, Kilpatrick CL. GABAA Receptor Trafficking-Mediated Plasticity of Inhibitory Synapses. Neuron 2011;70:385–409.

[5] Olsen RW, Sieghart W. International Union of Pharmacology. LXX. Subtypes of γ-Aminobutyric Acid A Receptors: Classification on the Basis of Subunit Composition, Pharmacology, and Function. Update. Pharmacol Rev 2008;60:243–60.

[6] Cryan JF, Kaupmann K. Don't worry "B" happy!: a role for GABAB receptors in anxiety and depression. Trends Pharmacol Sci 2005;26:36–43.

[7] Pin J-P, Prézeau L. Allosteric modulators of GABAB receptors: mechanism of action and therapeutic perspective. Curr Neuropharmacol 2007;5:195.
[8] Kash TL, Jenkins A, Kelley JC, Trudell JR, Harrison NL. Coupling of agonist binding to channel gating in the GABAA receptor. Nature 2003;421:272–5.
[9] Hines RM, Davies PA, Moss SJ, Maguire J. Functional regulation of GABAA receptors in nervous system pathologies. Curr Opin Neurobiol 2012;22:552–8.
[10] Miller PS, Smart TG. Binding, activation and modulation of Cys-loop receptors. Trends Pharmacol Sci 2010;31:161–74.
[11] Jacob TC, Moss SJ, Jurd R. GABAA receptor trafficking and its role in the dynamic modulation of neuronal inhibition. Nat Rev Neurosci 2008;9:331–43.
[12] Tan KR, Rudolph U, Lüscher C. Hooked on benzodiazepines: GABAA receptor subtypes and addiction. Trends Neurosci 2011;34:188–97.
[13] Mortensen M, Patel B, Smart TG. GABA potency at GABAA receptors found in synaptic and extrasynaptic zones. Front Cell Neurosci 2012;6:1–10.
[14] Rudolph U, Knoflach F. Beyond classical benzodiazepines: novel therapeutic potential of GABAA receptor subtypes. Nat Rev Drug Discov 2011;10:685–97.
[15] Barrera NP, Edwardson JM. The subunit arrangement and assembly of ionotropic receptors. Trends Neurosci 2008;31:569–76.
[16] Simon J, Wakimoto H, Fujita N, Lalande M, Barnard EA. Analysis of the Set of GABAA Receptor Genes in the Human Genome. J Biol Chem 2004;279:41422–35.
[17] Protein Data Bank. http://www.rcsb.org/pdb 2014.
[18] Olsen RW, Sieghart W. GABAA receptors: Subtypes provide diversity of function and pharmacology. Neuropharmacology 2009;56:141–8.
[19] Sigel E, Steinmann ME. Structure, function and modulation of GABAA receptors. J Biol Chem 2012;287:40224–31.
[20] Ernst M, Brauchart D, Boresch S, Sieghart W. Comparative modeling of GABAA receptors: limits, insights, future developments. Neuroscience 2003;119:933–43.
[21] Rudolph U, Mohler H. GABA-based therapeutic approaches: GABAA receptor subtype functions. Curr Opin Pharmacol 2006;6:18–23.
[22] Belelli D, Lambert JJ. Neurosteroids: endogenous regulators of the GABAA receptor. Nat Rev Neurosci 2005;6:565–75.
[23] Wafford KA. GABAA receptor subtypes: any clues to the mechanism of benzodiazepine dependence? Curr Opin Pharmacol 2005;5:47–52.
[24] Griebel G, Holmes A. 50 years of hurdles and hope in anxiolytic drug discovery. Nat Rev Drug Discov 2013;12:667–87.
[25] Nutt DJ, Stahl SM. Searching for perfect sleep: the continuing evolution of GABAA receptor modulators as hypnotics. J Psychopharmacol (Oxf) 2010;24:1601–12.
[26] Mignot E. The Perfect Hypnotic? Science 2013;340:36–8.
[27] Löscher W, Rogawski MA. How theories evolved concerning the mechanism of action of barbiturates: *Mechanism of Action of Barbiturates*. Epilepsia 2012;53:12–25.
[28] Crow JM. Insomnia: Chasing the dream. Nature 2013;497:S16–S18.
[29] Merck Newsroom Home: Merck Receives Complete Response Letter for Suvorexant, Merck's Investigational Medicine for Insomnia. 2013.
[30] Zaugg J. Discovery of new scaffolds for GABAA receptor modulators from natural origin. Universität Basel, Basel; 2011.
[31] Kvist T, Hansen KB, Bräuner-Osborne H. The use of *Xenopus* oocytes in drug screening. Expert Opin Drug Discov 2011;6:141–53.
[32] Kapur A, Derry JMC, Hansen RS. Expression and Study of Ligand-Gated Ion Channels in Xenopus laevis Oocytes. Handb. Neurochem. Mol. Neurobiol., Springer; 2007, p. 323–40.
[33] Baburin I, Beyl S, Hering S. Automated fast perfusion of Xenopus oocytes for drug screening. Pflüg Arch - Eur J Physiol 2006;453:117–23.

2.4. $GABA_A$ receptor modulators of natural origin: structural and physicochemical considerations

Structural scaffolds for $GABA_A$ receptor modulators from nature

Plant secondary metabolites are produced as the result of the interaction of plants with their surrounding environment. Some of these compounds are used to attract pollinating insects, provide defense against natural predators or pathogens, or control signaling processes. However, the functions of this sophisticated chemical arsenal are more complex and have not been fully elucidated yet. The biosynthetic pathways for the production of these compounds are often long and involve complex enzymatic reactions. Owing to the interaction with their biosynthetic enzymes, plant secondary metabolites possess the inherent ability to recognize and interact with protein surfaces, which allows them to act on animal targets such as cholinergic, adrenergic, dopaminergic, or GABAergic systems [1,2].

In recent years, a large number of NPs have been identified as $GABA_AR$ ligands. In fact, many of the compounds first used to study $GABA_ARs$ are plant secondary metabolites. The list includes the receptor antagonist **bicuculline** (from *Dicentra cucullaria*), the agonist **muscimol** (from *Amanita muscaria*), and the channel blocker **picrotoxin** (from *Anamirta cocculus*) (Figure 2.10) [3]. NPs with GABAergic activity belong mainly to the flavonoid, terpenoid, and alkaloid families, according to a compilation of plant-derived $GABA_AR$ modulators provided by Zaugg in 2011 [4]. Some new natural scaffolds have been reported in the period 2011-2014, including lignans and piperamides. An overview of the diverse natural scaffolds for $GABA_ARs$ is provided in the next sections.

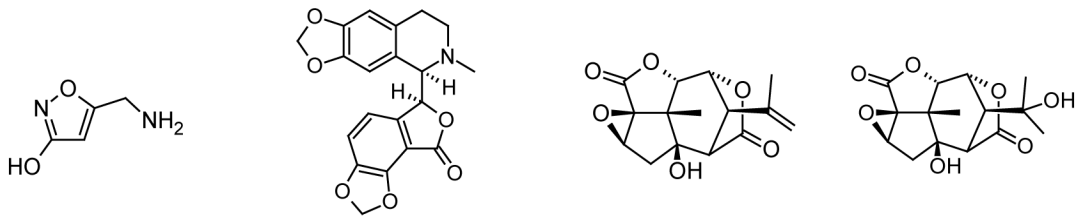

Figure 2.10. Natural products used for the study of $GABA_ARs$, with no clinical application. An equimolar mixture of the sesquiterpene lactones picrotoxinin and picrotin constitutes the convulsant terpenoid picrotoxin [4].

i) Flavonoids

Among all plant-derived $GABA_AR$ modulators, flavonoids have been the most thoroughly studied. A number of flavones (e.g. **chrysin**, **ororylin A**, **quercetin**, and **apigenin**) and biflavones (e.g. **amentoflavone**), have been reported to modulate $GABA_ARs$ via the BZD-binding site [5]. Structure-activity relationship (SAR) studies on the flavonoid scaffold have revealed that substitution at the 6- and/or 3'- positions with electronegative moieties increases affinity towards the BZD-binding site of $GABA_ARs$, which has led to the synthesis of high-affinity derivatives such as **6,3'-dinitroflavone**. The relatively rigid structure of flavonoids makes them valuable scaffolds for medicinal chemistry. Combinatorial libraries have yielded flavones acting as BZD-site agonists (e.g. **6-bromoflavone**) and antagonists (e.g. **6-chloro-3'-nitroflavone**) [6]. Recent studies have identified flavonoids with partially selective $GABA_AR$ modulatory activity (e.g. **6-hydroxyflavone**, **3-hydroxy-2'-methoxy-6-methylflavone**), showing significant preference for α_2 or α_4-containing receptors [7]. *In vitro* and *in vivo* studies on the mechanism for $GABA_AR$ modulation have revealed that certain flavonoids like apigenin and quercetin are able to enhance the actions of other $GABA_AR$ modulators such as diazepam, through an alternative modulatory mechanism called *second order modulation* or *metamodulation*. An alternative low-affinity flumazenil-insensitive binding site has been suggested to be involved in this mechanism [3]. The structures of some representative flavonoids are displayed in Figure 2.11.

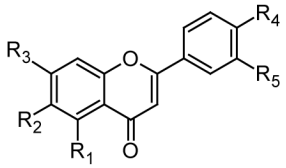

Apigenin: $R_{1,3,4}$ -OH ; $R_{2,5}$ -H
Oroxylin: $R_{1,3}$ -OH ; R_2 -OMe ; $R_{4,5}$ -H
6,3'-dinitroflavone: $R_{1,3,4}$ -H ; $R_{2,5}$ -NO_2

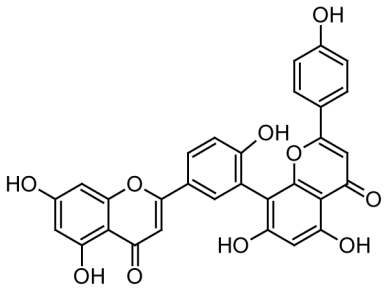

Amentoflavone

Figure 2.11. $GABA_AR$ modulators with flavonoid scaffold.

ii) Isoflavones

Although biogenetically related to flavonoids, isoflavonoids constitute a distinctly separate class of secondary metabolites, differing by the position of the phenolic ring B [8]. Isoflavones, the main subclass among isoflavonoids, had been associated with $GABA_ARs$ ever since some of them were found to displace [^{3}H] diazepam binding in rat brain

membranes [9]. However, it was only until 2011 that they were reported as positive $GABA_AR$ modulators by Gavande et al. [10], as a result of a study on a series of synthetic isoflavone derivatives. The study, conducted in *Xenopus* oocytes expressing receptors of the subtype $\alpha_1\beta_2\gamma_{2L}$, showed that modulation of $GABA_ARs$ by isoflavones is flumazenil-insensitive, suggesting that these compounds might not bind the BZD-site. Figure 2.12 displays the most potent isoflavones of this report, with potencies ranging from 9 to 16 μM and efficiencies between 250 and 1079%.

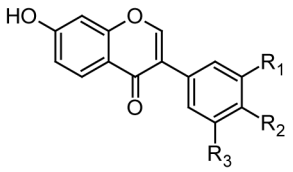

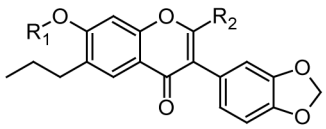

Isoflav. 1: $R_{1,3}$ $-CH_3$; R_2 $-OCH_3$
Isoflav. 2: R_1 $-OCF_3$; $R_{2,3}$ $-H$
Isoflav. 3: R_1 $-H$; R_2 $-CH_3$
Isoflav. 4: R_1 $-CH_2-COOCH_3$; R_2 $-CH_3$
Isoflav. 5: R_1 $-H$; R_2 $-CH_2-CH_3$

Figure 2.12. $GABA_AR$ modulators with isoflavone scaffold.

iii) Terpenoids

Diverse scaffolds for $GABA_AR$ modulators have been identified among terpenoids. Aside from **picrotoxin** (Figure 2.10), the sesquiterpene **valerenic acid** is a well known example. It has been described as a partially specific $GABA_AR$ modulator with preference for $\beta_{2/3}$–containing receptors, able to induce anxiolytic-like effects in mice. Valerenic acid served as a scaffold for medicinal chemistry to develop derivatives with enhanced GABAergic activity [11,12].

Among diterpenes, **miltirone** from the Chinese herb *Salvia miltiorrhiza* has been reported to induce anxiolytic-like behavior in animal models, although the mechanism on $GABA_ARs$ remains unclear [4]. Two new diterpene scaffolds for $GABA_AR$ modulators have been recently identified: pimarane and labdane diterpenes. **Zerumin A**, a labdane diterpene from *Curcuma kwangsiensis*, showed positive $GABA_AR$ modulatory activity in receptors of the subtype $\alpha_1\beta_2\gamma_{2S}$ expressed in *Xenopus* oocytes [13]. Pimarane diterpenes are exemplified by **sandaracopimaric acid** from *Biota orientalis*, which showed non-selective positive $GABA_AR$ modulatory activity in *Xenopus* oocytes expressing different receptors subtypes. The modulatory activity of sandaracopimaric acid was not affected by the absence of γ

subunit in the receptors, which indicates that the compound interacts with a non-BZD binding site. In behavioral experiments using mice, the compound reduced the locomotor activity [14]. The structures of some relevant terpenoids with GABAergic properties are displayed in Figure 2.13.

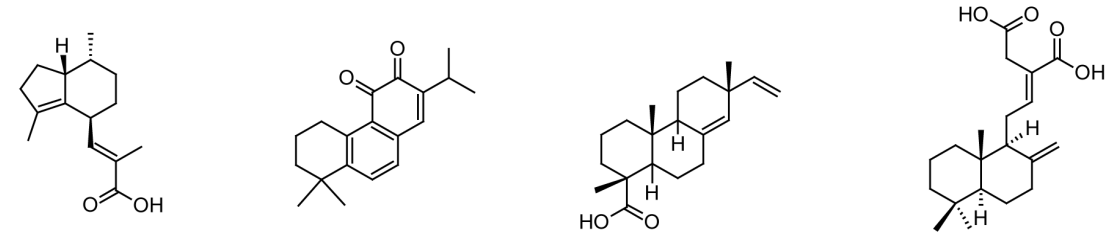

Valerenic acid **Miltiron** **Sandaracopimaric acid** **Zerumin A**

Figure 2.13. $GABA_AR$ modulators with terpenoid scaffold.

iv) Alkaloids

In contrast to the nitrogen-bearing BZDs or nonbenzodiazepines, most natural alkaloids with identified GABAergic activity are direct antagonists of $GABA_ARs$ and therefore, possess convulsant properties. It is the case of **bicuculline** (Figure 2.10), which is devoid of clinical application and used only in basic research on $GABA_ARs$. Alkaloids of the β-carboline type such as **harmane** have been found to act as full, partial or mixed agonists, antagonists, or inverse antagonists at the $GABA_A$ receptor. The β-carboline scaffold has been used for the development of anxiolytic compounds [4].

Recently, a new alkaloid scaffold was reported by Zaugg et al. [15]. By means of an HPLC-based activity profiling approach, **piperine**, isolated from *Piper nigrum*, was identified as a positive allosteric $GABA_AR$ modulator targeting a BZD-independent site. Structurally related piperamides such as trichostachine and piperlonguminine, isolated along with piperine, were inactive in the oocyte assay, suggesting that the piperidine ring is essential for the activity of piperamides. However, Khom et al. [16] reported **SCT-66**, a piperine derivative in which the piperidine ring has been replaced with a *N*,*N*-diisobutyl residue, as a $GABA_AR$ modulator with enhanced *in vitro* and *in vivo* activity over piperine. Both piperine and SCT-66 induce anxiolytic-like effects in rodent models. The structures of some representative piperamides are displayed in figure 2.14.

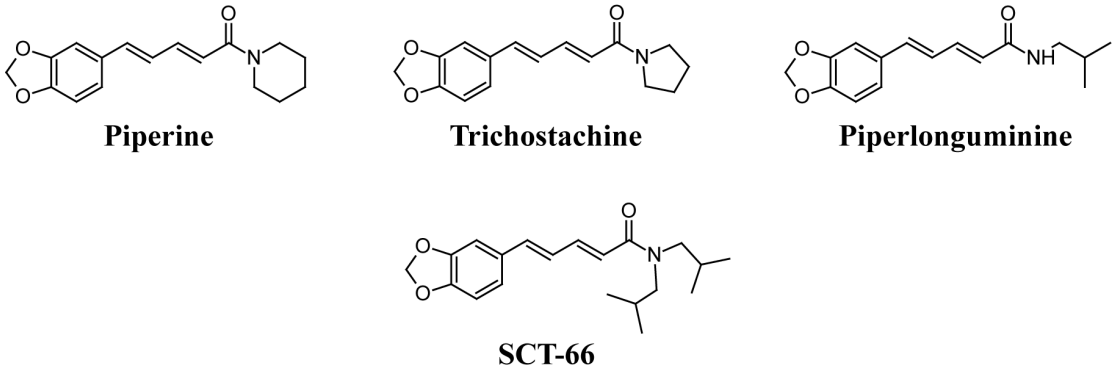

Figure 2.14. $GABA_AR$ modulators with piperamide scaffold.

v) Lignans

The neolignans **honokiol** and **magnolol** from *Magnolia officinalis* have been shown to act as partially selective $GABA_AR$ modulators in binding studies, and have been used in medicinal chemistry to study the potential role of the acetamido group in subunit-dependent receptor modulation. Animal behavior models have revealed that honokiol induces anxiolytic-like effects after oral administration [17]. Lignans such as **arisantetralones A-D** and acyclic lignans like **saururenin** were recently identified as $GABA_AR$ modulators with comparative potency in receptors of the subtype $\alpha_1\beta_2\gamma_{2S}$. Arisantetralones showed a mechanism of action that combines partial agonistic activity, positive modulation, and possibly channel block at high concentrations [18]. Figure 2.15 displays the structures of some lignans with GABAergic properties.

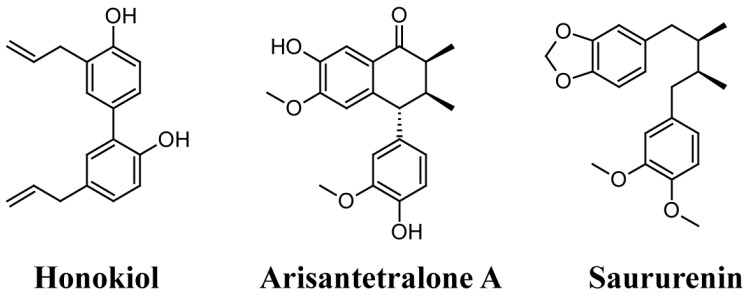

Figure 2.15. $GABA_AR$ modulators with lignan scaffold.

Reaching the target: "drug-likeness" and permeation of blood-brain barrier

In addition to high potency and selectivity towards the biological target, any drug candidate must be able to reach the target tissue in sufficient concentration to achieve therapeutic

efficacy. ADME properties play a pivotal role in defining the availability of a molecule to reach the target *in vivo*. The recognition that poor ADME properties are one of the major reasons for the failure of drug candidates in the pre-clinical or clinical phases of development has driven a revolution in drug discovery research in the last decades. From the mid-1990s, a battery of *in vitro* ADME screens was implemented almost universally in research programs for the screening of intestinal absorption and metabolic stability. In parallel to these *in vitro* technologies, considerable efforts were also invested in the development of computational (or *in silico*) approaches to the prediction of ADME properties [19,20].

Owing to the preference for oral administration, much of the attention of both *in vitro* and *in silico* approaches is focused on the prediction of a compound's intestinal absorption and tissue distribution. However, an additional kinetic process, i.e. blood-brain barrier (BBB) penetration, comes into play when designing CNS drugs [19,20]. A brief description of the general requirements for oral absorption and BBB permeation of drugs is provided here.

i) Oral absorption

The ability of drugs to cross the gastrointestinal epithelium is conditioned by specific physicochemical properties such as molecular size, charge, hydrogen-bonding potential, and lipophilicity [21].

After analyzing the calculated physicochemical properties of several thousands of clinical candidates reaching Phase II trials (or further), in 1997 Lipinski et al. [22] came up with a series of parameters to predict a compound's likelihood of undergoing oral absorption (considering solubility and permeability as the only factors affecting oral bioavailability of drugs). The *Rule of 5* (RO5), as the group of parameters is called, establishes that good absorption or permeability are more likely when

- Number of H-bond donors (expressed as the sum of OHs and NHs) < 5
- cLogP (calculated 1-octanol – water partition coefficient) < 5
- Molecular weight < 500 Da
- Number of H-bond acceptors (expressed as the sum of Ns and Os) < 10

In general, the RO5 properties are interrelated and thus, if two of them are out of the range, poor oral absorption can be expected. Although some orally active drugs lie outside the parameter cutoffs in the rule (i.e. antibiotics, antifungals, vitamins, and cardiac glycosides),

90% of orally active drugs that have achieved phase II clinical status comply with these rules. Thus, compounds with physicochemical properties among the ranges dictated by the RO5 are considered drug-like molecules [22].

However, passing the RO5 does not ensure drug-likeness. On the one hand, the RO5 says nothing about structural features defining drugs or non-drugs. Molecular flexibility for example, has been found to influence oral absorption, with more than 10 rotable bonds decreasing oral bioavailability. On the other hand, the meaning of drug-like is dependent on the administration route and target location. For instance, the number of H-bond acceptors (N + O atoms) for oral drugs intended to act at the CNS must be less than or equal to 5, instead of 10 [23,24].

ii) Blood-brain barrier permeation

The BBB is a dynamic and complex interface that strictly controls the exchanges between bloodstream and brain. It is composed of brain capillary microvascular endothelial cells, supported by other cell types such as pericytes, astrocytes, and neurons (Figure 2.16). Brain microvascular endothelial cells form a tightly sealed monolayer, characterized by the absence of fenestrations, a low number of pinocytic vesicles, high metabolic activity, and complex tight junctions between adjacent endothelial cells. Altogether, the BBB acts as a physical and metabolic barrier that maintains homeostasis in the brain and protects it from xenobiotics, neurotoxic metabolites, and pathogens circulating in the bloodstream [5,25,26].

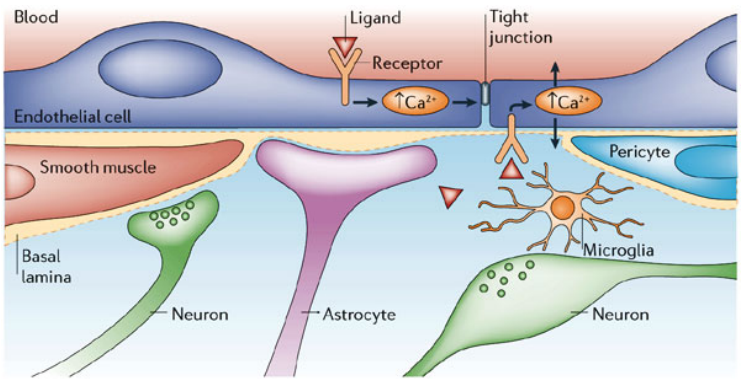

Figure 2.16. Schematic representation the BBB, showing the main cell types. Pericytes are enclosed within the endothelial basal lamina and form the closest associations with the endothelium. The endfeet of astrocytic glial cells are placed in the outer surface of the basal lamina (reproduced from Abbott et al., 2006 [27])

Despite the relative impermeability of the BBB, a number of specific transport processes occur across the barrier, primarily aimed to transport polar nutrients into the brain and to excrete waste products and potential toxicants out of the CNS. Due to the tight junctions between endothelial cells, most molecular traffic across the BBB occurs through transcellular mechanisms, namely *i*) passive diffusion, *ii*) carrier-mediated uptake, *iii*) endocytosis, and *iv*) active efflux (Figure 2.17). Small gaseous molecules such as O_2 and CO_2 can diffuse freely through the lipid membranes of endothelial cells, which is also the route of access for small lipophilic agents including drugs like barbiturates and ethanol. The transcellular traffic of essential polar nutrients is regulated by carrier systems which are specific for small peptides, hexoses, monocarboxylic acids, amino acids, neurotransmitters, and organic ions. Such transporters can be uni- or bidirectional, making it possible for certain molecules to go into or out of the brain depending on the concentration gradient across the BBB. Endocytosis, which occurs via receptor-mediated or adsorptive processes, is the main route of access for high-molecular weight molecules (e.g. peptides and proteins) into the brain. Alternatively, molecules can be pumped back from the brain into the blood by an active transfer process, mainly through p-glycoprotein, using an ATP efflux mechanism [27–29].

It has been estimated that 98% of all small molecules are not able to cross the BBB. Hence, BBB permeation is a major challenge in the development of drugs acting in the CNS, where penetration into the brain is essential to achieve therapeutic effects, except for those drugs intended to be delivered by invasive or intranasal routes [20,25,28]. In early drug discovery and development, NCEs are now screened for their ability to cross the BBB. For this purpose, a wide range of *in silico*, *in vivo* (e.g. *in situ* brain perfusion), and cell-based *in vitro* BBB models for early prediction of brain permeability of compounds have been developed and established [25]. *In silico* prediction methods are typically based on *in vivo* experimental data. The increasing computational possibilities and development of sophisticated modeling algorithms have resulted in accurate prediction of BBB permeability. In general, such predictions seem to correlate well with brain drug penetration *in vivo*. However, computational approaches are only able to predict passive permeation across the BBB [26].

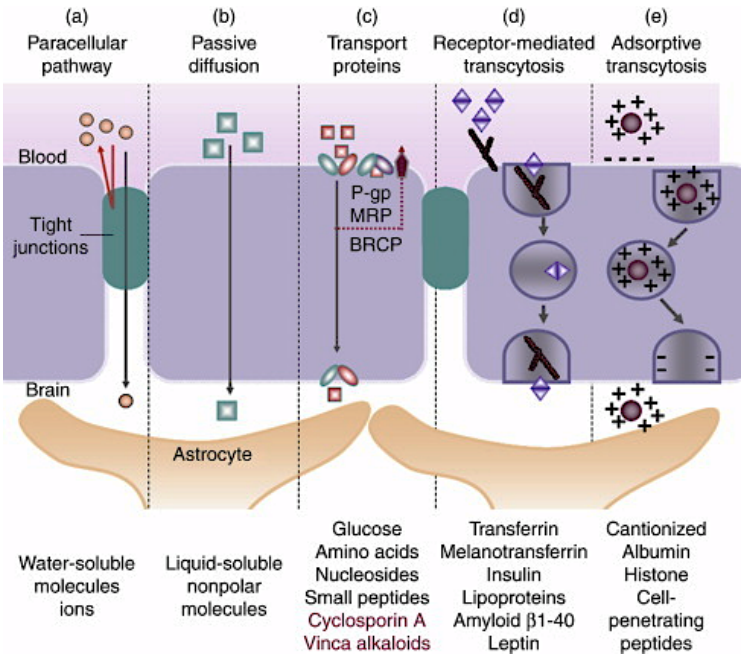

Figure 2.17. Molecular traffic across the BBB. (a) Polar solute transport is severely restricted by tight junctions. (b) Lipophilic or amphiphilic solutes may passively diffuse through the large surface of the lipid cell membrane. (c) Many essential polar molecules (e.g. glucose) can be can be transported into the CNS via carrier-mediated uptake. Active efflux carriers may intercept some of these molecules (e.g. Cyclosporin A and Vinca alkaloids) and pump them out of the endothelial cells. (d) Receptor-mediated transcytosis can transport macromolecules such as proteins and particles across the endothelium (e.g. insulin, cytokines, and viruses such as *Herpes simplex*). (e) Adsorptive transcytosis appears to be nonspecifically induced by positively charged macromolecules. Most CNS active agents enter via route (b) (reproduced from Lalatsa et al., 2011 [28]).

Computational quantitative SAR (QSAR) studies on CNS drugs such as BZDs, barbiturates, and anesthetics, have revealed that lipophilicity, molecular weight, hydrogen bonding, polar surface area (PSA), molecular flexibility, and molecular charge determine diffusion of small molecules across the BBB. In addition to these physicochemical features, some pharmacokinetic properties such as metabolic stability, oral absorption, and protein binding determine the success of BBB permeation, by affecting the concentration at which drugs reach the barrier. In short, for a drug to be able to cross the BBB and hence to elicit therapeutic effects, it should possess the following attributes [19,20,28]:

- Potent activity
- High selectivity
- Molecular weight < 450 Da
- Minimal hydrophobicity (cLogP) < 5
- Number of H-bond donor < 3

- Number of H-bond acceptor < 7
- Number of rotable bonds < 8
- PSA < 90 $Å^2$
- pK_a 7.5-10.5 (neutral or basic nature)
- Metabolic stability, with > 80% remaining after 1 h
- P450 enzyme inhibition > 50% at 30 μM
- Low CYP2D6 metabolism
- Low CYP3A4 inducing properties
- Low affinity for serum albumin (K_d < 10 μM)
- Aqueous solubility > 60 μg/mL
- Intestinal permeability > 1×10^{-6} cm/sec

In general terms, compared to non-CNS drugs, CNS drugs tend to be more lipophilic, less polar (decreased hydrogen bonding and lower PSA), more rigid (reduced number of rotable bonds), and smaller (lower molecular weight).

Pharmacokinetics of $GABA_A$ receptor modulators from nature

Pharmacokinetic studies on most plant-derived scaffolds for $GABA_AR$ modulators are rather limited. Sandaracopimaric acid and piperine have shown CNS effects in rodent models, but their pharmacokinetic behavior has not been studied yet. Recent *in vivo* studies on valerenic acid have revealed that this compound possesses reasonably good oral bioavailability (33.7%), fast tissue distribution (half-life 6-12 min), and slow elimination (half-life 6-46 h) in rats [30]. In the course of *in vitro* studies, valerenic acid has shown BBB permeation [31]. However, BBB penetration of valerenic acid remains to be confirmed in animal models [30].

Numerous *in vitro* and *in vivo* studies have demonstrated that flavonoids are able to cross gastrointestinal and blood-brain barriers [29,32,33]. Most flavonoids are usually present in plants as glycosides. Prior to absorption into systemic circulation, flavonoids undergo deglycosylation in the intestinal lumen, which is mainly mediated by the enzymes lactase, phloridzin hydrolase, and β-glucosidase. After deglycosylation, aglycones can passively diffuse across the intestinal membrane, from the intestinal lumen to the bloodstream. Once absorbed, the flavonoid aglycones are subjected to three main types of conjugation: methylation, sulfation, and glucuronidation. Thus, flavonoids are present in the plasma

almost exclusively in a conjugated form [5,34].

Flavonoids, both as aglycones and in the conjugated form, cross the BBB. During permeation, conjugates may be metabolized back to the parent aglycones, which then enter the CNS. In the brain, flavonoids act on different systems such as $GABA_A$ or 5-HT receptors, thus exerting sedative, anxiolytic, anticonvulsant, antidepressant, or neuroprotective effects, among others [5].

References

[1] Zhong J-J. 3.27 - Plant Secondary Metabolites. In: Moo-Young M, editor. Compr. Biotechnol. Second Ed., Burlington: Academic Press; 2011, p. 299–308.

[2] Appendino G, Fontana G, Pollastro F. 3.08 - Natural Products Drug Discovery. In: Liu H-W (Ben), Mander L, editors. Compr. Nat. Prod. II, Oxford: Elsevier; 2010, p. 205–36.

[3] Johnston GAR, Hanrahan JR, Chebib M, Duke RK, Mewett KN. Modulation of Ionotropic GABA Receptors by Natural Products of Plant Origin. Adv. Pharmacol., vol. 54, Elsevier; 2006, p. 285–316.

[4] Zaugg J. Discovery of new scaffolds for GABAA receptor modulators from natural origin. Universität Basel, Basel; 2011.

[5] Jäger A, Saaby L. Flavonoids and the CNS. Molecules 2011;16:1471–85.

[6] Hanrahan JR, Chebib M, Johnston GAR. Flavonoid modulation of GABAA receptors: Flavonoids and GABAA receptors. Br J Pharmacol 2011;163:234–45.

[7] Karim N, Gavande N, Wellendorph P, Johnston GAR, Hanrahan JR, Chebib M. 3-Hydroxy-2′-methoxy-6-methylflavone: A potent anxiolytic with a unique selectivity profile at GABAA receptor subtypes. Biochem Pharmacol 2011;82:1971–83.

[8] Veitch NC. Isoflavonoids of the Leguminosae. Nat Prod Rep 2007;24:417.

[9] Luk K-C, Stern L, Weigele M, O'Brien RA, Spirt N. Isolation and Identification of "Diazepam-Like" Compounds From Bovine Urine. J Nat Prod 1983;46:852–61.

[10] Gavande N, Karim N, Johnston GAR, Hanrahan JR, Chebib M. Identification of Benzopyran-4-one Derivatives (Isoflavones) as Positive Modulators of GABAA Receptors. ChemMedChem 2011;6:1340–6.

[11] Khom S, Baburin I, Timin E, Hohaus A, Trauner G, Kopp B, et al. Valerenic acid potentiates and inhibits GABAA receptors: Molecular mechanism and subunit specificity. Neuropharmacology 2007;53:178–87.

[12] Khom S, Strommer B, Ramharter J, Schwarz T, Schwarzer C, Erker T, et al. Valerenic acid derivatives as novel subunit-selective GABAA receptor ligands -in vitro and in vivo characterization: GABAA modulation by valerenic acid derivatives. Br J Pharmacol 2010;161:65–78.

[13] Schramm A, Ebrahimi SN, Raith M, Zaugg J, Rueda DC, Hering S, et al. Phytochemical profiling of Curcuma kwangsiensis rhizome extract, and identification of labdane diterpenoids as positive GABAA receptor modulators. Phytochemistry 2013:318–29.

[14] Zaugg J, Khom S, Eigenmann D, Baburin I, Hamburger M, Hering S. Identification and characterization of GABAA receptor modulatory diterpenes from *Biota orientalis* that decrease locomotor activity in mice. J Nat Prod 2011;74:1764–72.

[15] Zaugg J, Baburin I, Strommer B, Kim H-J, Hering S, Hamburger M. HPLC-Based Activity Profiling: Discovery of Piperine as a Positive GABAA Receptor Modulator Targeting a Benzodiazepine-Independent Binding Site. J Nat Prod 2010;73:185–91.

[16] Khom S, Strommer B, Schöffmann A, Hintersteiner J, Baburin I, Erker T, et al. GABAA receptor modulation by piperine and a non-TRPV1 activating derivative. Biochem Pharmacol 2013;85:1827–36.

[17] Woodbury A, Yu SP, Wei L, Garcia P. Neuro-modulating effects of honkiol: a review. Front Neurol 2013;4:1–6.

[18] Zaugg J, Ebrahimi SN, Smiesko M, Baburin I, Hering S, Hamburger M. Identification of GABAA receptor modulators in Kadsura longipedunculata and assignment of absolute configurations by quantum-chemical ECD calculations. Phytochemistry 2011;72:2385–95.

[19] Pajouhesh H, Lenz GR. Medicinal chemical properties of successful central nervous system drugs. NeuroRx 2005;2:541–53.

[20] Clark DE. In silico prediction of blood–brain barrier permeation. Drug Discov Today 2003;8:927–33.

[21] Van de Waterbeemd H, Camenisch G, Folkers G, Chretien JR, Raevsky OA. Estimation of Blood-Brain Barrier Crossing of Drugs Using Molecular Size and Shape, and H-Bonding Descriptors. J Drug Target 1998;6:151–65.
[22] Lipinski CA, Lombardo F, Dominy BW, Feeney PJ. Experimental and computational approaches to estimate solubility and permeability in drug discovery and development settings. Adv Drug Deliv Rev 1997;23:3–25.
[23] Lipinski CA. Lead- and drug-like compounds: the rule-of-five revolution. Drug Discov Today Technol 2004;1:337–41.
[24] Leeson PD, Springthorpe B. The influence of drug-like concepts on decision-making in medicinal chemistry. Nat Rev Drug Discov 2007;6:881–90.
[25] Eigenmann D, Xue G, Kim K, Moses A, Hamburger M, Oufir M. Comparative study of four immortalized human brain capillary endothelial cell lines, hCMEC/D3, hBMEC, TY10, and BB19, and optimization of culture conditions, for an in vitro blood-brain barrier model for drug permeability studies. Fluids Barriers CNS 2013;10:33.
[26] Cardoso FL, Brites D, Brito MA. Looking at the blood–brain barrier: Molecular anatomy and possible investigation approaches. Brain Res Rev 2010;64:328–63.
[27] Abbott NJ, Ronnback L, Hansson E. Astrocyte-endothelial interactions at the blood-brain barrier. Nat Rev Neurosci 2006;7:41 – 53.
[28] Lalatsa A, Schätzlein AG, Uchegbu IF. 5.50 - Drug Delivery Across the Blood–Brain Barrier. In: Moo-Young M, editor. Compr. Biotechnol. Second Ed., Burlington: Academic Press; 2011, p. 657–67.
[29] Faria A, Meireles M, Fernandes I, Santos-Buelga C, Gonzalez-Manzano S, Dueñas M, et al. Flavonoid metabolites transport across a human BBB model. Food Chem 2014;149:190–6.
[30] Sampath C, Haug K, Thanei S, Hamburger M, Derendorf H, Frye R, et al. Pharmacokinetics of Valerenic Acid in Rats after Intravenous and Oral Administrations. Planta Med 2012;78:575–81.
[31] Neuhaus W, Trauner G, Gruber D, Oelzant S, Klepal W, Kopp B, et al. Transport of a GABAA Receptor Modulator and Its Derivatives from Valeriana officinalis L. s.l. Across an in Vitro Cell Culture Model of the Blood-Brain Barrier. Planta Med 2008;74:1338–44.
[32] Grundmann O, Nakajima J-I, Kamata K, Seo S, Butterweck V. Kaempferol from the leaves of Apocynum venetum possesses anxiolytic activities in the elevated plus maze test in mice. Phytomedicine Int J Phytother Phytopharm 2009;16:295–302.
[33] Ader P, Wessmann A, Wolffram S. Bioavailability and metabolism of the flavonol quercetin in the pig. Free Radic Biol Med 2000;28:1056–67.
[34] Wasowski C, Marder M. Flavonoids as GABAA receptor ligands: the whole story? J Exp Pharmacol 2012;4:9–24.

3. RESULTS AND DISCUSSION

3.1. Discovery of $GABA_A$ receptor modulator aristolactone in a commercial sample of the Chinese herbal drug "Chaihu" (*Bupleurum chinense* roots) unravels adulteration by nephrotoxic A*ristolochia manshuriensis* roots

Diana C. Rueda, Janine Zaugg, Melanie Quitschau, Eike Reich, Steffen Hering, and Matthias Hamburger. Planta Med 2012; 78: 207 – 210 (doi: 10.1055/s-0031-1298171)

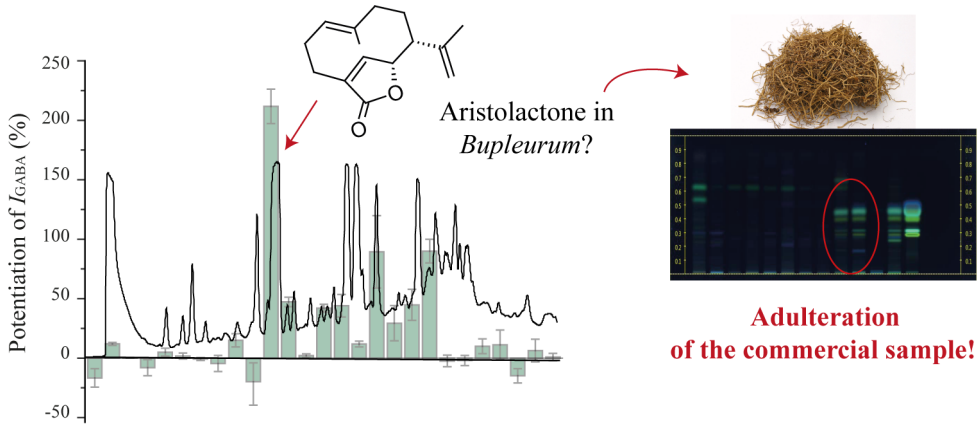

The germacranolide aristolactone, isolated from a commercial sample of the traditional Chinese herbal drug *Chaihu* (*Bupleurum chinense* DC. roots), was identified as a low-potency $GABA_A$ receptor modulator by HPLC-based activity profiling coupled with a functional assay in *Xenopus* oocytes. However, the presence of aristolactone in the sample suggested possible adulteration with *Aristolochia* species. The commercial sample of *Chaihu* was proved to be adulterated with roots of the nephrotoxic herb *Aristolochia manshuriensis,* using a validated HPTLC protocol for detection of aristolochic acids and macroscopic inspection of the drug.

Extraction of the plant material for isolation, HPLC-based activity profiling, isolation of aristolactone, bioactivity assessment of fractions and aristolactone in Xenopus *oocytes, oocyte preparation, recording and interpretation of analytical data for structure elucidation (UV, HRMS, NMR spectra), writing of the manuscript draft, and preparation of the figures (except for Figure 3) were my contributions to this publication. NRM analysis was assisted by M. Quitschau. TLC analyses were performed at CAMAG laboratory, under the supervision of E. Reich.*

Diana C. Rueda

Discovery of $GABA_A$ Receptor Modulator Aristolactone in a Commercial Sample of the Chinese Herbal Drug "*Chaihu*" (*Bupleurum chinense* Roots) Unravels Adulteration by Nephrotoxic *Aristolochia manshuriensis* Roots

Authors **Diana C. Rueda**[1], **Janine Zaugg**[1], **Melanie Quitschau**[1], **Eike Reich**[2], **Steffen Hering**[3], **Matthias Hamburger**[1]

Affiliations
[1] Division of Pharmaceutical Biology, University of Basel, Basel, Switzerland
[2] CAMAG Laboratory, Muttenz, Switzerland
[3] Institute of Pharmacology and Toxicology, University of Vienna, Vienna, Austria

Key words
- *Bupleurum chinense*
- Apiaceae
- *Aristolochia* sp.
- Aristolochiaceae
- aristolactone
- aristolochic acids
- traditional Chinese medicine
- adulteration

Abstract

In a two–microelectrode voltage clamp assay using *Xenopus laevis* oocytes, a petroleum ether extract prepared from a commercial sample of the traditional Chinese herbal drug labelled as "*Chaihu*" (*Bupleurum chinense* DC. roots) enhanced the I_{GABA} by 156% ± 22% when tested at 100 µg/mL. By means of HPLC-based activity profiling combined with high-resolution LC-MS and microprobe NMR, the germacranolide aristolactone (**1**) was identified as one of the main active compounds (EC_{50} 56.02 µM ± 5.09 µM). However, aristolactone has been previously reported only from the genus *Aristolochia* (Aristolochiaceae), suggesting a possible adulteration. With the aid of a validated HPTLC protocol for detection of aristolochic acids and with reference samples, the commercial sample was confirmed to be a mixture of *Aristolochia manshuriensis* root and *Bupleurum chinense* root. This finding was corroborated by macroscopic inspection of the drug. This case of adulteration with a highly nephrotoxic drug raises concerns about adequate quality control of TCM drugs commercialized in Europe.

Supporting information available online at http://www.thieme-connect.de/ejournals/toc/plantamedica

received August 24, 2011
revised Dec. 5, 2011
accepted Dec. 18, 2011

Bibliography
DOI http://dx.doi.org/10.1055/s-0031-1298171
Published online January 23, 2012
Planta Med 2012; 78: 207–210

ISSN 0032-0943

Correspondence
Prof. Dr. Matthias Hamburger
Division of Pharmaceutical Biology
University of Basel
Klingelbergstrasse 50
4056 Basel
Switzerland
Phone: + 41 6 12 67 14 25
Fax: + 41 6 12 67 14 74
Matthias.Hamburger@unibas.ch

Chinese Materia Medica (CMM) is a general term covering medicines, mostly of botanical origin, prescribed in accordance with the principles and theories of traditional Chinese medicine (TCM) [1,2]. In recent years, the use of CMM has enormously increased worldwide, and so has the international attention regarding its safe and effective use [2–4]. Similarities in morphology and nomenclature can lead to misidentification and confusion [2,5], which may result in poisoning incidents. A case in point has been the aristolochic acid (AA) nephropathy caused by a slimming tea which contained *Aristolochia* due to mistaken identity of CMM, and consequent misuse of *Aristolochia* species in some herbal preparations [2, 5–8]. *Aristolochia* species (Aristolochiaceae) have been used in TCM as anti-inflammatory herbs. However, their use is no longer permitted in many countries due to their content of AA shown to be nephrotoxic, carcinogenic, and mutagenic [2,6].

In recent years we have been successfully identifying new structural scaffolds for $GABA_A$ receptor modulators [9–11] by an extract library-based approach and HPLC-based activity profiling [12,13], using an automated functional two–microelectrode voltage clamp assay with *Xenopus laevis* oocytes that transiently express the $GABA_A$ receptor subtype $\alpha_1\beta_2\gamma_{2s}$ [14]. One of the active samples in the library was a petroleum ether extract of a commercial sample labelled as "*Chaihu*" (potentiation of I_{GABA} by 156% ± 22% when tested at 100 µg/mL). The Chinese herbal drug *Chaihu* (Bupleuri Radix) refers to the dried roots of *Bupleurum chinense* DC. (*Bei-chaihu*) or *B. scorzonerifolium* Willd. (*Nan-chaihu*) (Apiaceae) [15,16]. It is a well-known TCM drug claimed to posses, among others, sedative properties [17]. It is widely used in TCM as the principal ingredient of many multi-herb remedies due to its broad spectrum of traditional uses [16,18].

By means of HPLC-based activity profiling [13], a major peak of activity could be located in fraction 11 (potentiation of I_{GABA} by 212% ± 14%) (**Fig. 1**). We isolated the peak contained in this fraction by semipreparative HPLC. A molecular formula $C_{15}H_{20}O_2$ of compound **1** was derived from the accurate mass obtained by LC-TOFMS analysis. A database search with this molecular formula gave no entries for *B. chinense* [19]. For

This is a copy of the author's personal reprint

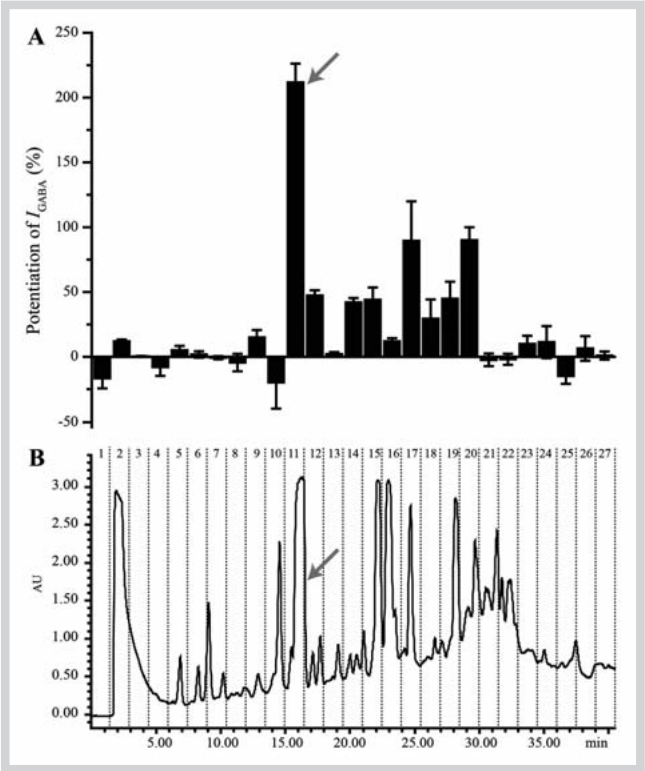

Fig. 1 HPLC-based activity profiling of a petroleum ether extract of a commercial sample labelled as *B. chinense* DC. roots, for $GABA_A$ receptor modulatory activity. **B** HPLC chromatogram (210 nm) of a semipreparative separation of 10 mg of extract. The 27 time-based fractions collected, 90 s each, are indicated with dashed lines. **A** Potentiation of the I_{GABA} by each fraction.

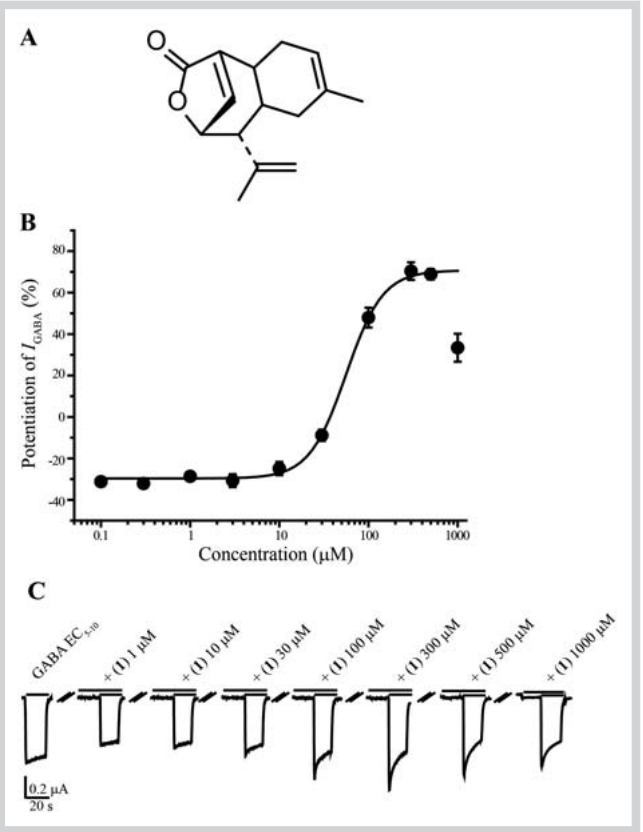

Fig. 2 **A** Chemical structure of compound **1**. **B** Concentration-response curve for **1** on $GABA_A$ receptors of the subunit composition $\alpha_1\beta_2\gamma_{2S}$, using a GABA EC_{5-10}. **C** Typical traces for modulation of I_{GABA} for compound **1**. The flat segments in the currents indicate the absence of direct activation of the receptors.

the entire genus *Bupleurum*, there was only one entry with this molecular formula, corresponding to saikodiyne A. However, the ^{1}H NMR and 2D NMR spectra did not match with this polyacetylenic compound. Detailed analysis of the spectra finally led to identification of **1** as aristolactone (**Fig. 2A**; spectroscopic data in Supporting Information). Concentration dependent $GABA_A$ receptor modulation of **1** was tested in the oocyte assay, at concentrations between 0.1 and 1000 μM. Aristolactone (**1**) potentiated I_{GABA} in a concentration-dependent manner, with an EC_{50} of 56.0 μM ± 5.1 μM and a maximum potentiation of 70.7% ± 2.6% (**Fig. 2B**). No significant direct activation of $GABA_A$ receptors was observed (**Fig. 2C**), but concentrations lower than 100 μM induced inhibition of I_{GABA}. This may indicate a high potency negative modulation binding site interfering with a low potency positive modulation, since concentrations in the range of 100 μM to 1 mM induced moderate enhancement of I_{GABA} (**Fig. 2B** and **2C**).

Aristolactone is a characteristic marker for the genus *Aristolochia*. Due to its unexpected presence in the extract, we suspected adulteration of *B. chinense* roots with an *Aristolochia* species. Therefore, we subjected the commercial herb sample to HPTLC analysis using a validated protocol for detection of AA [20]. The presence of AA was confirmed with the aid of reference solutions, whereas an authentic sample of *Bupleurum chinense* roots was devoid of AA (**Fig. 3**). Further HPTLC fingerprint analyses and macroscopic inspection revealed that the sample was a mixture (approx. 1 : 1) of *B. chinense* roots and *A. manshuriensis* roots (**Fig. 2S**, Supporting Information).

The case described here highlights an apparent gap in appropriate control of TCM herbal drugs imported in Europe. In principle, wholesale distributors importing bulk herbal drugs are legally bound to ensure proper quality control measures using the respective pharmacopoeia monographs. Massive adulteration of a widely used and safe drug, Bupleuri radix (*Chaihu*), with highly toxic AA-containing *Aristolochia* species represents a serious risk for consumer safety [5]. It is worrying to see that almost two decades after the discovery of AA nephropathy [7,8], AA-containing drugs and herbal products are still on the market across the world [21,22], and that certain populations are at a measurable risk of getting AA-related cancer [23]. At this point we can only speculate about the reasons for this case of adulteration. However, root samples often possess few distinctive macroscopic features, especially in their commercial form of cut drugs, and this fact lends to either accidental or intentional adulteration. The rather similar visual appearance of the two drugs in question visibly led to a situation which was only uncovered by chance.

Thus, regulatory bodies should be aware of the specific issues related to TCM herbal drugs, so that proper quality and safety can be ensured. For authentication of TCM herbs, a broad range of methods is available, such as chromatographic and spectroscopic techniques [24,25], as well as DNA fingerprinting and genomic approaches [26,27]. Yet, methods such as HPTLC fingerprinting and macroscopic and microscopic inspection [2,28] remain im-

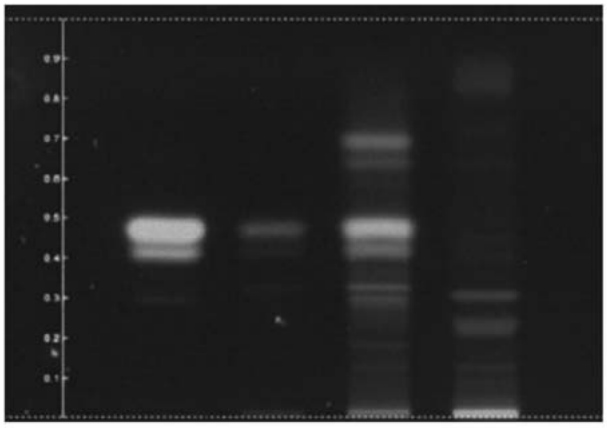

Fig. 3 Detection of AA in the methanol extract of a commercial sample labelled as *B. chinense* DC. roots by HPTLC. Developing system: according to the PhEur *Test for Aristolochic Acids in Herbal Drugs* (2.8.21), *method A*. Derivatization: tin chloride reagent. Visualization: UV 366 nm. Samples: **1**. Reference solution *(a)*, PhEur; **2**. Reference solution *(b)*, PhEur; **3**. Commercial sample of *B, chinense* roots, containing AA; **4**. Authentic *B. chinense*, negative for AA.

portant. The specific case discussed here highlights the high information content of HPTLC fingerprints.

Materials and Methods

Aristolochia reference samples were provided and identified by the European Directorate for the Quality of Medicines & HealthCare (EDQM), and *Bupleurum* reference samples by the American Herbal Pharmacopoeia. The herbal drug labelled as "*Chaihu*" (dried roots of *Bupleurum chinense* DC.) was purchased in 2002 from the Institute of Chinese Medicine, Peter Weinfurth, Ennepetal, Germany. Prior to extraction for the extract library in 2002, the drug was submitted to macroscopic and microscopic analysis in comparison with the respective monograph of the Chinese Pharmacopoeia [29]. A voucher specimen (00 363) is deposited at the herbarium of the Division of Pharmaceutical Biology, University of Basel.

Microfractionation of the extract for activity profiling was performed as previously described [11,13], with minor modifications (see Supporting Information). A total of 27 time-based microfractions of 90 s each were collected for assessment of $GABA_A$ receptor modulatory activity, as previously described [10,11,14]. Details of the bioassay are given in the Supporting Information.

The peak in the active time window was isolated by means of semipreparative HPLC. LC-PDA-ESITOFMS and microprobe NMR were used for structure elucidation. For details, see Supporting Information.

Detection of AA in the commercial sample was performed by HPTLC, according to the PhEur *Test for Aristolochic Acids in Herbal Drugs* (2.8.21), *method A* [30]. HPTLC fingerprint analyses were performed as previously described [20], with minor modifications specified in the Supporting Information. Macroscopic inspection was carried to complement the information about the composition and purity of the sample obtained from HPTLC analysis. By visual comparison to an authentic reference drug, 60% of the sample was found to be different or questionable.

Supporting information

Detailed description of the experimental conditions, NMR spectroscopic data of aristolactone (**1**), and HPTLC evidence of adulteration of the commercial sample of *B. chinense* roots with *A. manshuriensis* roots are available as Supporting Information.

Acknowledgements

Financial support was provided by the Swiss National Science Foundation through project 205320_126888/1 (MH). D.C. Rueda thanks the Swiss Federal Commission for Scholarships for Foreign Students (FCS) for a fellowship. We are grateful to Eliezer Cenivia and Valeria Widmer, both from CAMAG Laboratory, for performing the macroscopic and HPTLC analysis.

Conflict of Interest

The authors have declared no conflict of interest.

References

1 *Zhao Z, Liang Z, Chan K, Lu G, Lee EL, Chen H, Li L.* A unique issue in the standardization of Chinese materia medica: processing. Planta Med 2010; 76: 1975–1986
2 *Zhao Z, Hu Y, Liang Z, Yuen JP, Jiang Z, Leung KS.* Authentication is fundamental for standardization of Chinese medicines. Planta Med 2006; 72: 865–874
3 *Chan K.* Some aspects of toxic contaminants in herbal medicines. Chemosphere 2003; 52: 1361–1371
4 *Zhao Z, Liang Z, Ping G.* Macroscopic identification of Chinese medicinal materials: traditional experiences and modern understanding. J Ethnopharmacol 2011; 134: 556–564
5 *Shaw D.* Toxicological risks of Chinese herbs. Planta Med 2010; 76: 2012–2018
6 *Jordan SA, Cunningham DG, Marles RJ.* Assessment of herbal medicinal products: challenges, and opportunities to increase the knowledge base for safety assessment. Toxicol Appl Pharmacol 2010; 243: 198–216
7 *Vanhaelen M, Vanhaelen-Fastre R, But P, Vanherweghem JL.* Identification of aristolochic acid in Chinese herbs. Lancet 1994; 343: 174
8 *Vanherweghem JL, Tielemans C, Abramowicz D, Depierreux M, Vanhaelen-Fastre R, Vanhaelen M, Dratwa M, Richard C, Vandervelde D, Verbeelen D, Jadoul M.* Rapidly progressive interstitial renal fibrosis in young women: association with slimming regimen including Chinese herbs. Lancet 1993; 341: 387–391
9 *Yang X, Baburin I, Plitzko I, Hering S, Hamburger M.* HPLC-based activity profiling for GABAA receptor modulators from the traditional Chinese herbal drug Kushen (*Sophora flavescens* root). Mol Div 2011; 15: 361–372
10 *Zaugg J, Eickmeier E, Ebrahimi SN, Baburin I, Hering S, Hamburger M.* Positive GABA(A) receptor modulators from *Acorus calamus* and structural analysis of (+)-dioxosarcoguaiacol by 1D and 2D NMR and molecular modeling. J Nat Prod 2011; 74: 1437–1443
11 *Zaugg J, Baburin I, Strommer B, Kim HJ, Hering S, Hamburger M.* HPLC-based activity profiling: discovery of piperine as a positive GABA(A) receptor modulator targeting a benzodiazepine-independent binding site. J Nat Prod 2010; 73: 185–191
12 *Potterat O, Hamburger M.* Natural products in drug discovery – concepts and approaches for tracking bioactivity. Curr Org Chem 2006; 10: 899–920
13 *Kim HJ, Baburin I, Khom S, Hering S, Hamburger M.* HPLC-based activity profiling approach for the discovery of GABAA receptor ligands using an automated two microelectrode voltage clamp assay on *Xenopus* oocytes. Planta Med 2008; 74: 521–526
14 *Baburin I, Beyl S, Hering S.* Automated fast perfusion of *Xenopus* oocytes for drug screening. Pflugers Arch 2006; 453: 117–123

This is a copy of the author's personal reprint

15 *Tian RT, Xie PS, Liu HP.* Evaluation of traditional Chinese herbal medicine: Chaihu (Bupleuri Radix) by both high-performance liquid chromatographic and high-performance thin-layer chromatographic fingerprint and chemometric analysis. J Chromatogr A 2009; 1216: 2150–2155
16 *Tang W, Eisenbrand G.* Handbook of Chinese medicinal plants. Chemistry, pharmacology, toxicology. Weinheim: Wiley-VCH Verlag GmbH & Co. KGaA; 2011
17 *Huang KC.* The pharmacology of Chinese herbs. Boca Raton: CRC Press LLC; 1999
18 *Ashour ML, Wink M.* Genus *Bupleurum*: a review of its phytochemistry, pharmacology and modes of action. J Pharm Pharmacol 2011; 63: 305–321
19 *Chapman J.* Chapman and Hall dictionary of natural products. Boca Raton: CRC Press, Hampden Ltd. Data Services; 2010
20 *Blatter A, Reich E.* High performance thin-layer chromatographic analysis of aristolochic acids in Chinese drugs. J Plan Chromatogr Modern TLC 2004; 17: 355–359
21 *Cheung TP, Xue C, Leung K, Chan K, Li CG.* Aristolochic acids detected in some raw Chinese medicinal herbs and manufactured herbal products – a consequence of inappropriate nomenclature and imprecise labelling? Clin Toxicol (Phila) 2006; 44: 371–378
22 *Debelle FD, Vanherweghem JL, Nortier JL.* Aristolochic acid nephropathy: a worldwide problem. Kidney Int 2008; 74: 158–169
23 *Lai MN, Wang SM, Chen PC, Chen YY, Wang JD.* Population-based case-control study of Chinese herbal products containing aristolochic acid and urinary tract cancer risk. J Natl Cancer Inst 2009; 102: 179–186
24 *Liang YZ, Xie PS, Chan K.* Perspective of chemical fingerprinting of Chinese herbs. Planta Med 2010; 76: 1997–2003
25 *Sun S, Chen J, Zhou Q, Lu G, Chan K.* Application of mid-infrared spectroscopy in the quality control of traditional Chinese medicines. Planta Med 2010; 76: 1987–1996
26 *Heubl G.* New aspects of DNA-based authentication of Chinese medicinal plants by molecular biological techniques. Planta Med 2010; 76: 1963–1974
27 *Youns M, Hoheisel JD, Efferth T.* Toxicogenomics for the prediction of toxicity related to herbs from traditional Chinese medicine. Planta Med 2010; 76: 2019–2025
28 *Bauer R, Franz G.* Modern European monographs for quality control of Chinese herbs. Planta Med 2010; 76: 2004–2011
29 *Stöger EA.* Arzneibuch der Chinesischen Medizin. Stuttgart: Deutscher Apotheker Verlag; 2001
30 *European Directorate for the Quality of Medicines & Health Care.* European Pharmacopoeia 7.0. Strasbourg: European Directorate for the Quality of Medicines & Health Care; 2011

This is a copy of the author's personal reprint

Supporting Information

Discovery of $GABA_A$ receptor modulator aristolactone in a commercial sample of the Chinese herbal drug "Chaihu" (*Bupleurum chinense* roots) unravels adulteration by nephrotoxic *Aristolochia manshuriensis* roots

Diana C. Rueda[1], Janine Zaugg[1], Melanie Quitschau[1], Eike Reich[2], Steffen Hering[3], Matthias Hamburger[1*]

[1] Division of Pharmaceutical Biology, University of Basel, Basel, Switzerland.

[2] CAMAG Laboratory, Muttenz, Switzerland.

[3] Institute of Pharmacology and Toxicology University of Vienna, Vienna, Austria.

*** Address for correspondence**

Prof. Dr. Matthias Hamburger

Division of Pharmaceutical Biology

University of Basel

Klingelbergstrasse 50

CH-4056 Basel

Tel. +41 61 2671425

Fax +41 61 2671474

E-mail: Matthias.Hamburger@unibas.ch

Experimental details

General procedures

High resolution mass spectra were obtained on a microTOF ESI-MS system (Bruker Daltonics) connected via a T-splitter (1:10) to an HP 1100 system (Agilent), consisting of a degasser, a binary mixing pump, autosampler, column oven, and a diode array detector (G1315B). Data acquisition and processing was performed on Hystar 3.0 software (Bruker Daltonics). Semi-preparative HPLC separations for activity profiling and off-line microprobe NMR were performed with an HP 1100 series system (Agilent) consisting of a quaternary pump, column oven, and diode array detector (G1315B). SunFire™ C18 (3.5 μm, 3.0×150 mm) and SunFire™ Prep C18 (5 μm, 10×150 mm) columns (Waters) were used for analytical and semi-preparative HPLC analysis, respectively. Parallel evaporation of semi-preparative HPLC fractions was performed with a Genevac EZ-2 plus vacuum centrifuge (Avantec). 1D and 2D NMR spectra were measured at room temperature on a Bruker Avance III spectrometer operating at 500.13 Mz. A 1mm TXI probe was used. Spectra were analyzed by TopSpin 2.1 software (Bruker). HPLC grade methanol (Scharlau Chemie S.A.) and water were used for HPLC separations. NMR spectra were recorded in d_3-chloroform (Armar Chemicals). Technical grade solvents purified by distillation were used for extraction.

Extraction

For preparation of the extract library, an aliquot of the drug was extracted sequentially with petroleum ether, ethyl acetate and methanol using pressurized liquid extraction (2 cycles of 5 min each for each solvent; pressure 120 bar; temperature 70^{o}C). Extracts were formatted as

DMSO stock solutions (10 mg/mL) and stored at -80°C in 2D-barcoded Matrix^R storage plates. Initial screening and HPLC based activity profiling was carried out with an aliquot from the extract library. For isolation of aristolactone, an aliquot (approximately 50g) of milled drug was extracted by maceration with petroleum ether (4 x 500 mL, 1 h each, rt). The solvent was evaporated at reduced pressure, and the extract was stored at 2-8 ºC until use.

Microfractionation

Microfractionation for $GABA_A$ receptor activity profiling was performed as previously described [10-11, 13], with minor modifications: separation was done on a semipreparative HPLC column with methanol (solvent A) and water (solvent B), using a gradient from 50 to 100% A in 30 min, hold for 15 min. The flow rate was 4 mL/min, and 100 µL of extract (100 mg/mL in DMSO) were injected. A total of 27 time-based microfractions of 90 s each were collected and evaporated in parallel. The dry films were redissolved in1 mL of methanol, and aliquots of 0.5 mL were dispensed in two vials, dried under N_2 gas, and submitted to bioassay.

HPLC-PDA-ESI-TOF-MS

The petroleum ether extract of the commercial sample of *Chaihu* was analyzed with methanol (solvent A) and water (solvent B), both containing 0.1% formic acid, with gradient elution of 50 to 100% A in 30 min, hold for 10 min at a flow rate of 0.4 mL/min. The sample was dissolved in DMSO at a concentration of 10 mg/mL; the injection volume was 5 µL. Spectra were recorded in the range of *m*/*z* 100-800 in positive mode. Nitrogen was used as a nebulizing gas at a pressure of 2.0 bar, and as a drying gas at a flow rate of 9.0 L/min (dry gas temperature 240 °C). Capillary

voltage was set at 4500 V, hexapole at 250.0 Vpp. Instrument calibration was performed using a reference solution of sodium formiate 0.1% in 2-propanol/water (1:1) containing 5 mM NaOH.

Semi-preparative HPLC and Off-Line Microprobe NMR

For isolation of the active peak, the extract was submitted to semi-preparative HPLC using the same solvent system and gradient elution as for HPLC-TOFMS. The flow rate was set at 4 mL/min. The sample was dissolved in DMSO at a concentration of 100 mg/mL, and the injection volume was 100 µL. The peak in fraction 11 was collected, evaporated, and redissolved in d_1-chloroform (10 µL). The following parameters were used for measurements of NMR spectra: 128 scans for ^{1}H spectra; 8 scans for ^{1}H^{1}H-COSY spectra using the *cosygpqf* pulse program; 32 scans and 256 increments to record HSQC experiments using the *hsqcedetgp* pulse program; the HMBC spectrum was recorded with 64 scans and 128 increments, using the *Hmbcgp* pulse program.

HPTLC fingerprint analyses

HPTLC screening test for aristolochic acids on the commercial sample was carried out according PhEur 7 (2.8.81) [30], with minor modifications: the powdered drug (0.5 g) was sonicated with methanol (5 mL) for 10 min.

For detection of *Bupleurum* in the sample, a developing system of ethyl acetate-methanol-water (80:20:10) was used on HPTLC silica gel 60F_{254} (MERCK) in a saturated chamber over a distance of 60 mm. The plate was derivatized with anisaldehyde reagent and evaluated under white light.

Expression of $GABA_A$ Receptors

Stage V-VI oocytes from *Xenopus laevis* were prepared, and cRNA was injected as previously described [13]. Female *Xenopus laevis* (NASCO, Fort Atkinson, WI) were anesthetized by exposing them for 15 min to a 0.2% MS-222 (methanesulfonate salt of 3-aminobenzoic acid ethyl, Sigma) solution before surgically removing parts of the ovaries. Follicle membranes from isolated oocytes were enzymatically digested with 2 mg/mL collagenase from *Clostridium histolyticum* (Type 1A, Sigma). Synthesis of capped runoff poly(A+) cRNA transcripts was obtained from linearized cDNA templates (pCMV vector). Directly after enzymatic isolation, the oocytes were injected with 50 nL of DEPC-treated water (Sigma) containing different cRNAs at a concentration of approximately 300-3000 pg/nL per subunit. The amount of injected cRNA mixture was determined by means of a NanoDrop ND-1000 (Kisker Biotech). To ensure expression of the gamma subunit in $\alpha_1\beta_2\gamma_{2S}$ receptors, rat cRNAs were mixed in a 1:1:10 ratio. Oocytes were then stored at 18 °C in ND96 solution containing 1% of penicillin-streptomycin solution (Sigma-Aldrich). Voltage clamp measurements were performed between days 1 and 5 after cRNA injection.

Positive control

Diazepam (7-chloro-1,3-dihydro-1-methyl-5-phenyl-2H-1,4-benzodiazepin-2-one, Sigma, purity not less than 98%) was used as positive control. At 1 μM diazepam enhanced I_{GABA} up to 231.3 ± 22.6% (n=3). See also Fig S1.

Two-Microelectrode Voltage Clamp Studies

Electrophysiological experiments were performed by the two-microelectrode voltage clamp method making use of a TURBO TEC 03X amplifier (npi electronic GmbH) at a holding potential of -70 mV and pCLAMP 10 data acquisition software (Molecular Devices). Currents were low-pass-filtered at 1 kHz and sampled at 3 kHz. The bath solution contained 90 mM NaCl, 1 mM KCl, 1 mM $MgCl_2$, 1 mM $CaCl_2$, and 5 mM HEPES (pH 7.4). Electrode filling solution contained 2 M KCl. Oocytes with maximal current amplitudes > 3 μA were discarded to exclude voltage clamp errors.

Fast Solution Exchange during I_{GABA} Recordings

Test solutions (100 µL) were applied to the oocytes at a speed of 300 µL/s by means of the ScreeningTool automated fast perfusion system [9]. In order to determine GABA EC_{5-10} (typically between 3 and 10 µM for receptors of subunit composition $\alpha_1\beta_2\gamma_{2s}$), a dose-response experiment with GABA concentrations ranging from 0.1 µM to 1 mM was performed. Stock solution of the petroleum ether extract (10 mg/mL in DMSO) was diluted to a concentration of 100 µg/mL with bath solution containing GABA EC_{5-10} according to a validated protocol [13]. As previously described, microfractions collected from the semipreparative HPLC separations were dissolved in 30 µL of DMSO and subsequently mixed with 2.97 mL of bath solution containing GABA EC_{5-10} [13]. A stock solution of compound **1** (100 mM in DMSO) was diluted to concentrations of 0.1, 0.3, 1.0, 3.0, 10, 30, 100, 300, 500, and 1000 µM with bath solution for measuring direct activation, or with bath solution containing GABA EC_{5-10} for measuring modulation of $GABA_A$ receptors. The final DMSO concentration in all the samples including the GABA control samples was adjusted to 1% to avoid solvent effect at the $GABA_A$ receptor.

Data Analysis

Enhancement of the I_{GABA} was defined as $I_{(GABA+Comp)}/I_{GABA} - 1$, where $I_{(GABA+Comp)}$ is the current response in the presence of a given compound, and I_{GABA} is the control GABA-induced chloride current. Data were analyzed using the ORIGIN 7.0 SR0 software (OriginLab Corporation) and are given as mean ± S.E. of at least two oocytes and ≥2 oocyte batches.

Fig. S1. Diazepam (1 μM) enhanced IGABA through $\alpha_1\beta_2\gamma_{2S}$ $GABA_A$ receptors and was therefore used as positive control for the assay. Currents in the presence of GABA ($EC_{5\text{-}10}$, single bar, control) and during co-application of GABA and diazepam (1 μM, double bar) are shown. At 1 μM diazepam enhanced I_{GABA} up to 231.3 ± 22.6% (n=3).

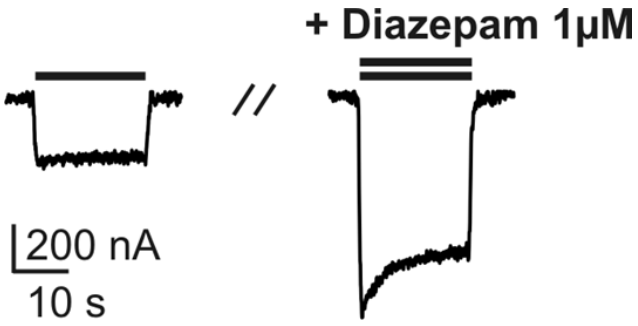

Figure S2: HPTLC fingerprints confirming and identifying the adulteration of a commercial sample labelled as *B*. *chinense* DC. roots.

A: detection of *B*. *chinense* in the commercial sample. Developing system: ethyl acetate-methanol-water (80:20:10). Derivatization: anisaldehyde. Samples: **1**. Authentic *B*. *chinense*; **2**. Commercial sample of *B*. *chinense* roots; **3**. Blank; **4**. *A*. *manshuriensis*; **5**. *A*. *fangii*; **6**. *A*. *serpentaria*; **7**. saikosaponin D; **8**. Saikosaponin A. Bands corresponding to saikosaponins A and D, markers of *Bupleurum* species, are only evident for the authentic sample of *B*. *chinense*, and the commercial sample studied.

B: identification of *A*. *manshuriensis* as the adulterant in the commercial sample. Developing system: water, formic acid, ehtyl acetate, toluene (1:1:10:20). Derivatization: tin chloride reagent. Visualization: UV 366 nm. Samples: **1**. *B*. *bicaule*; **2-8**. Authentic *B*. *chinense*; **9.** Commercial sample of *B*. *chinense* roots; **10**. *A*. *manshuriensis*; **11**. *A*. *serpentaria*; **12**. AA I/II. The analysis of several *B*. *chinense* samples and different *Aristolochia* species confirms the absence of AA in *B*. *chinense* and indicates the presence of *A*. *manshuriensis* in the commercial sample.

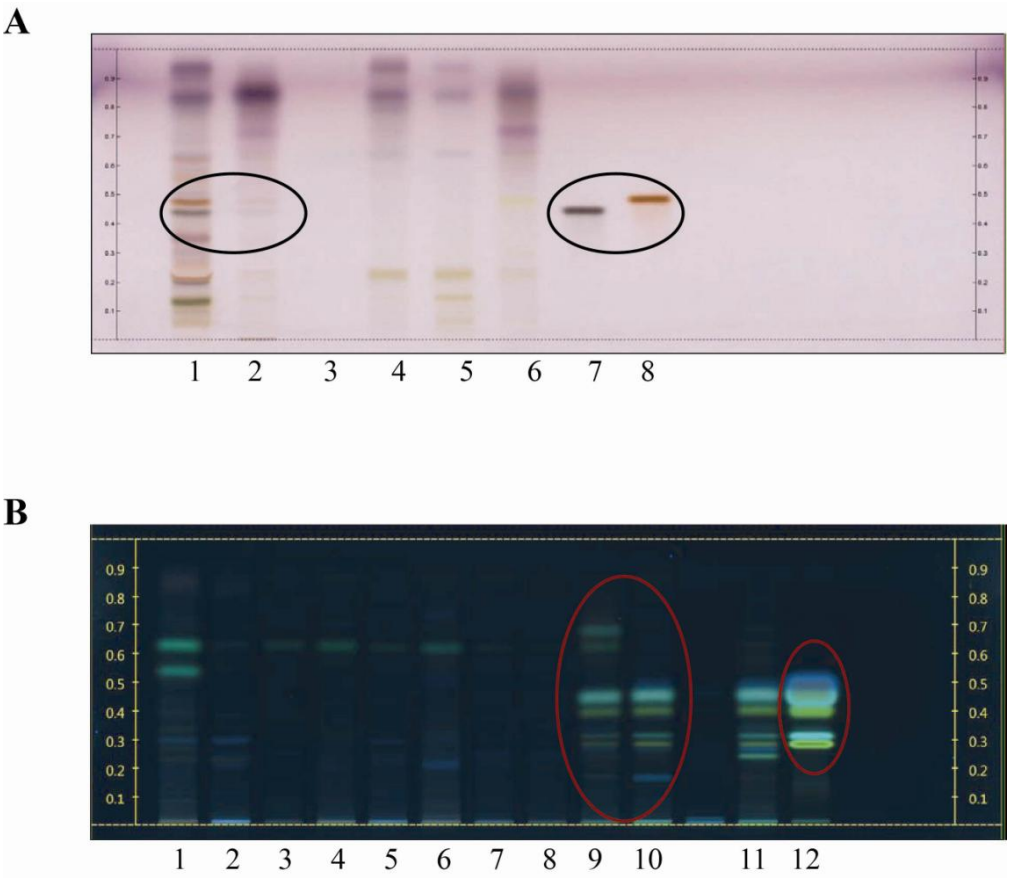

NMR spectroscopic data for compound (1)

Table S1: NMR spectroscopic data (500.13 MHz, $CDCl_3$) for aristolactone (**1**)

CAS Nr. 6790-85-8

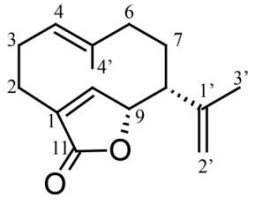

(1)

Position	δ_C [a]	δ_H (I, m, *J* in Hz)
1	132.6	-
2	25.1	2.21 (CH_2, ddd, *13.0*, *10.8*, *7.8*)
3	24.2	2.19 (CH_2, m)
4	128.8	4.57 (CH, $d_{br.}$ *12.5*)
5	136.7	-
6	40.8	1.89 (CH_2, dd, *12.0*, *12.0*)
7	26.3	1.50 (CH_2, dd_{br}, *15.1*, *10.8*)
8	52.5	2.40 (CH, d_{br}, *11.0*)
9	82.3	4.96 (CH, s_{br})
11	173.5	-
12	152.3	6.60 (CH, s_{br})
1’	150.3	-
2’	110.3	4.70 (CH_2, m)
3’	20.2	1.81 (CH_3, s_{br})
4’	15.5	1.47 (CH_3, s_{br})

[a] chemical shifts derived from HMBC spectrum

3.2. Identification of dihydrostilbenes in *Pholidota chinensis* as a new scaffold for $GABA_A$ receptor modulators

Diana C. Rueda, Angela Schöffmann, Maria De Mieri, Melanie Raith, Evelyn A. Jähne, Steffen Hering, and Matthias Hamburger. Bioorg Med Chem 2014; 22(4): 1276 – 84
(doi: 10.1016/j.bmc.2014.01.008)

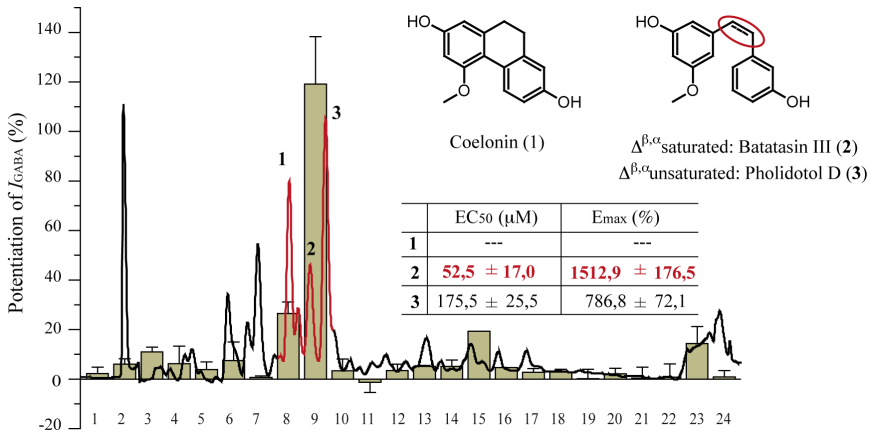

The dihydrostilbene batatasin III was identified as a very efficient, non-selective $GABA_AR$ modulating compound in *P. chinensis* stems and roots by HPLC-based activity profiling. Two structurally related non-flexible stilbenes, coelonin and pholidotol D, were also isolated from the extract but they were inactive in the oocyte assay. Structural flexibility of stilbenes was proved to be crucial for modulation of $GABA_A$ receptors by testing 13 commercially available stilbenes and their corresponding semisynthetic dihydrostilbenes in the oocyte assay.

Extraction of the plant material for isolation, HPLC-based activity profiling, isolation of pure compounds, biological assessment of pure compounds at a single concentration, recording and interpretation of analytical data for structure elucidation (UV, HRMS, NMR spectra), bioactivity assessment of synthetic stilbenes and their semisynthetic dihydro derivatives in Xenopus *oocytes, writing of the manuscript draft, and preparation of the figures (except for Figure 4) were my contributions to this publication. A. Schöffmann performed concentration-response experiments with compounds* ***(1-3)*** *and subunit specificity tests. Semisynthesis of dihydrostilbenes from commercial stilbenes was carried out by M. De Mieri. Structure elucidation of compounds* ***1-3*** *was assisted by M. Raith.*

Diana C. Rueda

Bioorganic & Medicinal Chemistry 22 (2014) 1276–1284

Contents lists available at ScienceDirect

Bioorganic & Medicinal Chemistry

journal homepage: www.elsevier.com/locate/bmc

Identification of dihydrostilbenes in *Pholidota chinensis* as a new scaffold for $GABA_A$ receptor modulators

Diana C. Rueda [a], Angela Schöffmann [b], Maria De Mieri [a], Melanie Raith [a], Evelyn A. Jähne [a], Steffen Hering [b], Matthias Hamburger [a,*]

[a] Division of Pharmaceutical Biology, University of Basel, Klingelbergstrasse 50, CH-4056 Basel, Switzerland
[b] Institute of Pharmacology and Toxicology, University of Vienna, Althanstrasse 14, A-1090 Vienna, Austria

ARTICLE INFO

Article history:
Received 3 October 2013
Revised 20 December 2013
Accepted 3 January 2014
Available online 10 January 2014

Keywords:
Pholidota chinensis
HPLC-based activity profiling
$GABA_A$ receptor modulators
Dihydrostilbenes

ABSTRACT

A dichloromethane extract of stems and roots of *Pholidota chinensis* (Orchidaceae) enhanced GABA-induced chloride currents (I_{GABA}) by 132.75 ± 36.69% when tested at 100 μg/mL in a two-microelectrode voltage clamp assay, on *Xenopus laevis* oocytes expressing recombinant $\alpha_1\beta_2\gamma_{2S}$ $GABA_A$ receptors. By means of an HPLC-based activity profiling approach, the three structurally related stilbenoids coelonin (**1**), batatasin III (**2**), and pholidotol D (**3**) were identified in the active fractions of the extract. Dihydrostilbene **2** enhanced I_{GABA} by 1512.19 ± 176.47% at 300 μM, with an EC_{50} of 52.51 ± 16.96 μM, while compounds **1** and **3** showed much lower activity. The relevance of conformational flexibility for receptor modulation by stilbenoids was confirmed with a series of 13 commercially available stilbenes and their corresponding semisynthetic dihydro derivatives. Dihydrostilbenes showed higher activity in the oocyte assay than their corresponding stilbenes. The dihydro derivatives of tetramethoxy-piceatannol (**12**) and pterostilbene (**20**) were the most active among these derivatives, but they showed lower efficiencies than compound **2**. Batatasin III (**2**) showed high efficiency but no significant subunit specificity when tested on the receptor subtypes $\alpha_1\beta_2\gamma_{2s}$, $\alpha_2\beta_2\gamma_{2s}$, $\alpha_3\beta_2\gamma_{2s}$, $\alpha_4\beta_2\gamma_{2s}$, $\alpha_5\beta_2\gamma_{2s}$, $\alpha_1\beta_1\gamma_{2s}$, and $\alpha_1\beta_3\gamma_{2s}$. Dihydrostilbenes represent a new scaffold for $GABA_A$ receptor modulators.

1. Introduction

$GABA_A$ receptors are ligand-gated chloride channels physiologically activated by GABA, the major inhibitory neurotransmitter in the brain. Structurally, they are heteropentameric assemblies forming a central chloride-selective channel. Up to now 19 different subunits (α1–6, β1–3, γ1–3, δ, ε, θ, π, ρ1–3) have been identified. Depending on the nature, stoichiometry, and arrangement of these subunits, the receptor subtypes exhibit distinct pharmacological profiles providing the potential for rational drug therapy in several disorders related with impaired GABAergic function, such as epilepsy, insomnia, anxiety, and mood disorders.[1–3] $GABA_A$ receptors are the target for many clinically important drugs such as benzodiazepines (BDZs), barbiturates, neuroactive steroids, anesthetics, and certain other CNS depressants. Due to their lack of subunit specificity, these drugs show a number of adverse side effects. Hence, there is a need for subtype-selective drugs devoid of the side effects of the classical BDZs. Despite the availability of experimental subunit-specific GABAergic drugs for more than a decade, no subtype-selective $GABA_A$ receptor modulators have been introduced into clinical practice.[3,4]

In a search for new natural product-derived $GABA_A$ receptor modulators, we screened a library of 880 fungal and plant extracts in an automated functional two-microelectrode voltage clamp assay on *Xenopus* oocytes[5] transiently expressing $GABA_A$ receptors of the $\alpha_1\beta_2\gamma_{2S}$ subtype, the most abundant subunit combination in the human brain.[2] In this screening the dichloromethane extract of stems and roots of *Pholidota chinensis* LINDL (Orchidaceae) showed promising activity.

Orchidaceae is the largest family of flowering plants, with around 25,000 species in over 800 genera. The family shows worldwide distribution, with greatest diversity in tropical and subtropical climate zones. Apart from their ornamental value, many orchids have been used as medicinal plants. In traditional Chinese medicine we find the earliest written records for medicinal uses of orchids.[6–8] In Chinese folk medicine, the whole plant of *P. chinensis* (*shi xian tao*) has long been used in the treatment of diverse conditions, such as hypertension, headache, gastroenteritis, and bronchitis. Previous pharmacological studies on *P. chinensis* reported sedative and anticonvulsant activities.[9–12] The genus *Pholidota* comprises approximately 30 species distributed from tropical Asia to tropical

Abbreviations: BDZs, benzodiazepines; GABA, gamma-aminobutyric acid; $GABA_A$Rs, gamma-aminobutyric acid type A receptors.

* Corresponding author. Tel.: +41 61 2671425; fax: +41 61 2671474.
E-mail address: matthias.hamburger@unibas.ch (M. Hamburger).

0968-0896/$ - see front matter © 2014 Elsevier Ltd. All rights reserved.
http://dx.doi.org/10.1016/j.bmc.2014.01.008

Australia. Phytochemical studies on the genus showed the presence of triterpenes, steroids, lignans, benzoxepines, and stilbenoids.[10] Stilbenoids exhibit a limited but heterogeneous distribution in the plant kingdom, and have been most widely reported from the Orchidaceae family. Dihydrostilbenes and 9,10-dihydrophenanthrenes have been previously identified in the genus *Pholidota*.[13–17]

In this study, batatasin III (**2**) isolated from a DCM extract of *P. chinensis* was identified as a positive $GABA_A$ receptor modulator by means of HPLC-based activity profiling,[18] a miniaturized approach for the rapid identification of new bioactive natural compounds,[19–22] that we have been successfully applying in the discovery of $GABA_A$ receptor ligands of natural origin.[23–27] The subunit selectivity of **2** was assessed at $GABA_A$ receptor subtypes $\alpha_2\beta_2\gamma_{2s}$, $\alpha_3\beta_2\gamma_{2s}$, $\alpha_4\beta_2\gamma_{2s}$, $\alpha_5\beta_2\gamma_{2s}$, $\alpha_1\beta_1\gamma_{2s}$, and $\alpha_1\beta_3\gamma_{2s}$. Furthermore, dihydrostilbenes were established as a new scaffold for $GABA_A$ receptor modulators, by comparison of the performance of a series of commercially available stilbenes and their semisynthetic dihydro derivatives on the oocyte assay.

2. Experimental

2.1. General procedures

1D and 2D NMR spectra were measured at room temperature on a Bruker Avance III 500 MHz spectrometer (Bruker BioSpin, Fällanden, Switzerland) operating at 500.13 MHz. Spectra were recorded at 291.2 K with a 1 mm TXI probe with z-gradient. The following settings were used: 128 scans for ^1H spectra; 8 scans for $^1H^1H$-COSY spectra (*cosygpqf* pulse program); 32 scans and 256 increments for HSQC experiments (*hsqcedetgp* pulse program); 64 scans and 128 increments for HMBC spectra (*hmbcgp* pulse program). Spectra were analyzed by TopSpin 3.0 software (Bruker). High resolution mass spectra (HPLC–ESITOFMS) were recorded in positive mode, *m*/*z* range 100–800, on a Bruker microTOF ESIMS system (Bruker Daltonics, Bremen, Germany) connected via a T-splitter (1:10) to an Agilent HP 1100 system consisting of a degasser, a binary mixing pump, autosampler, column oven, and a diode array detector (G1315B) (Agilent Technologies, Waldbronn, Germany). Nitrogen was used as a nebulizing gas at a pressure of 2.0 bar, and as drying gas at a flow rate of 9.0 L/min (dry gas temperature 240 °C). Capillary voltage was set at 45,000 V; hexapole at 230.0 Vpp. Instrument calibration was done with a reference solution of sodium formate 0.1% in 2-propanol/water (1:1) containing 5 mM NaOH. Data acquisition and processing was performed with Bruker Daltonics Hystar 3.0 software. Semi-preparative HPLC separations for activity profiling and purification were performed with an Agilent HP 1100 series system consisting of a quaternary pump, autosampler, column oven, and diode array detector (G1315B). Waters SunFire™ C18 (3.5 μm, 3.0 × 150 mm) and SunFire™ Prep C18 (5 μm, 10 × 150 mm) columns were used for analytical and semi-preparative HPLC analysis, respectively (Waters, Wexford, Ireland). Parallel evaporation of semi-preparative HPLC fractions was performed with a Genevac EZ-2 plus vacuum centrifuge (Genevac Ltd, Ipswich, United Kingdom). Flash chromatography was performed with pre-packed Buchi Sepacore® silica flash cartridges (40–63 μm, 40 × 150 mm) on a Buchi Sepacore® system consisting of two C-605 pumps, a C-620 control unit, and a C-660 fraction collector (Buchi, Flawil, Switzerland). Sample introduction was carried out with a Buchi Prep Elut adapter filled with the sample adsorbed onto silica gel. The separation was monitored by TLC. Preparative HPLC separations were performed with a Waters SunFire Prep C18 OBD column (5 μM, 30 × 150 mm) connected to a Shimadzu LC-8A preparative HPLC with SPD-M10A VP diode array detector. HPLC-grade MeOH (Scharlau Chemie S.A.), acetonitrile (Scharlau Chemie S.A.) and water were used for HPLC separations. For analytical separations, HPLC solvents contained 0.1% of HCO_2H. NMR spectra were recorded in methanol-d_4 (Armar Chemicals). For extraction and flash chromatography, distilled technical grade solvents were used. Silica gel (63–200 μm, Merck) was used for open column chromatography.

2.2. Plant material

Shi Xian Tao (dried stems/roots of *P. chinensis* Lindl.) was purchased in 2008 from a local herbal market in Kunming and authenticated by Dr. X. Yang (previously Pharmaceutical Biology, University of Basel, now Kunming Institute of Botany, Chinese Academy of Science, Kunming, PR China). A voucher specimen (463) is deposited at the Division of Pharmaceutical Biology, University of Basel.

2.3. Extraction

The plant material was frozen with liquid nitrogen and ground with a ZM1 ultracentrifugal mill (Retsch). The DCM extract for screening and HPLC-based activity profiling was prepared with an ASE 200 extraction system with solvent module (Dionex, Sunnyvale CA). Three extraction cycles (5 min each) were performed, at an extraction pressure of 120 bar and a temperature of 70 °C. For preparative isolation, 293 g of ground plant material was macerated with DCM (4 × 1 L, 3 h each, permanent magnetic stirring). The solvent was evaporated at reduced pressure to yield 10.3 g of extract. The extracts were stored at 2–8 °C until use.

2.4. Microfractionation for activity profiling

Time-based microfractionation for $GABA_A$ receptor activity profiling was performed as previously described,[23,27,28] with minor modifications: separation was done on a semi-preparative HPLC column with MeOH (solvent A) and water (solvent B), using a gradient from 50% A to 80% A in 30 min, followed by 80% A to 100% A in 2 min. The flow rate was 4 mL/min, and 10 mg of extract (in 200 μL of DMSO) were injected. A total of 24 microfractions of 90 s each were collected. After parallel evaporation of solvents, the dry films were redissolved in 1 mL of methanol, and aliquots of 0.5 mL were dispensed in two vials, dried under N_2 gas, and submitted to bioassay.

2.5. Isolation

An aliquot of the DCM extract (450 mg) was dissolved in $CHCl_3$ and adsorbed onto silica gel (3 g), prior to packing into a Buchi Prep Elut adapter. Separation was performed on a Sepacore® silica gel cartridge eluted with an *n*-hexane (solvent A) and EtOAc (solvent B) gradient: 0% B to 30% B in 90 min, followed by 30% B to 50% B in 30 min, and 50% B to 80% B in 30 min. The flow rate was set at 15 mL/min. Fractions of 15 mL were collected and later combined into 18 fractions (1–18) on the basis of a TLC analysis (detection at 254, 366, and at daylight after staining with anisaldehyde–sulfuric acid reagent). Fractions 1–18 were submitted to analytical HPLC–PDA–ESIMS with MeOH (solvent C) and water (solvent D), using a gradient from 50% C to 100% C in 30 min, hold for 15 min. The flow rate was 0.4 mL/min, and 10 μg of each fraction (in 10 μL of DMSO) were injected. Fractions 13 and 14 were found to contain the compounds of interest and were submitted to semi-preparative HPLC using solvents C and D as eluents. A gradient of 50% C to 60% C in 30 min was used for fraction 13, and isocratic conditions (50% C, 30 min) for fraction 14. The flow rate was 4 mL/min. Stock solutions in DMSO (50 mg/mL) were prepared and repeatedly injected in portions of 50–100 μL. A portion

(17 mg) of fraction 13 (25 mg) afforded compounds **1** (2.3 mg) and **2** (6.5 mg). Compound **3** (2 mg) was isolated from 10 mg of fraction 14 (16 mg).

Compounds **1**–**3** were identified by comparison of their physiochemical data (NMR, ESI-TOFMS, and UV–vis) with published values.[14,29–31] The purity was >95% (purity check by ^{1}H NMR).

2.5.1. Coelonin (1)

^{1}H NMR (methanol-d_4, 500.13 MHz) δ_H (ppm): 8.13 (1H, d, J = 8.4 Hz, H-5), 6.62 (1H, dd J = 8.3 and 2.7 Hz, H-6), 6.61 (1H, d, J = 2.6 Hz, H-8), 6.30 (1H, d, J = 2.5 Hz, H-3), 6.26 (1H, d, J = 2.5 Hz, H-1), 3.67 (3H, s, 4-OCH_3), 2.59 (4H, s, H-9 and H-10); ^{13}C shifts (derived from multiplicity-edited HSQC and HMBC spectra), δ_C (ppm): 158.3 (C, C-4), 155.4 (C, C-2), 154.8 (C, C-7), 139.8 (C, C-8a), 138.7 (C, C-10a), 128.6 (CH, C-5), 125.2 (C, C-4b), 114.8 (C, C-4a), 113.8 (CH, C-8), 112.2 (CH, C-6), 104.8 (CH, C-1), 100.1 (CH, C-3), 54.2 (4-OCH_3), 30.8 (CH_2, C-10) 30.1 (CH_2, C-9). HR-ESIMS m/z 243.1016 $[M+H]^+$ (calcd for $C_{15}H_{15}O_3$, 243.1016).

2.5.2. Batatasin III (2)

^{1}H NMR (methanol-d_4, 500.13 MHz) δ_H (ppm): 7.03 (1H, dd, J = 7.9 and 7.5 Hz, H-5′), 6.64 (3H, m, H-2′, H-4′, and H-6′), 6.29 (1H, br s, H-2), 6.23 (2H, m, H-4 and H-6), 3.63 (3H, s, 5-OCH_3), 2.75 (4H, m, H-α and H-β); ^{13}C shifts (derived from multiplicity-edited HSQC and HMBC spectra), δ_C (ppm): 160.9 (C, C-5), 157.6 (C, C-3), 156.7 (C, C-3′), 144.9 (C, C-1), 143.3 (C, C-1′), 129.0 (CH, C-5′), 119.8 (CH, C-6′), 115.3 (CH, C-2′), 112.4 (CH, C-4′), 108.1 (CH, C-2), 105.5 (CH, C-6), 98.7 (CH, C-4), 54.3 (CH_3, 5-OCH_3), 37.6 (CH_2, C-β), 37.0 (CH_2, C-α). HR-ESIMS m/z 245.1176 $[M+H]^+$ (calcd for $C_{15}H_{17}O_3$, 245.1172).

2.5.3. Pholidotol D (3)

^{1}H NMR (methanol-d_4, 500.13 MHz) δ_H (ppm): 7.17 (1H, dd, J = 7.9 and 7.8 Hz, H-5′), 7.00–6.95 (4H, m, H-2′, H-6′, H-α and H-β), 6.69 (1H, dd, J = 8.2 and 2.2 Hz, H-4′), 6.58 (2H, m, H-2 and H-6), 6.31 (1H, t, J = 2 Hz, H-4), 3.76 (3H, s, 5-OCH_3); ^{13}C shifts (derived from multiplicity-edited HSQC and HMBC spectra), δ_C (ppm): 160.8 (C, C-5), 157.7 (C, C-3), 156.0 (C, C-3′), 139.7 (C, C-1), 138.5 (C, C-1′), 129.4 (CH, C-5′), 128.6 (CH, C-β), 128.4 (CH, C-α), 117.8 (CH, C-6′), 114.4 (CH, C-4′), 112.4 (CH, C-2′), 105.8 (CH, C-2), 103.4 (CH, C-6), 100.3 (CH, C-4), 54.4 (CH_3, 5-OCH_3). HR-ESIMS m/z 243.1017 $[M+H]^+$ (calcd for $C_{15}H_{15}O_3$, 243.1016).

Further purification of compound **2** for subunit specificity tests was achieved by separating a portion of the extract (7.3 g) by open column chromatography (6 × 69 cm, 700 g of silica gel), using a step gradient of *n*-hexane–EtOAc (100:0, 95:5, 90:10, 85:15, 80:20, 75:25, 70:30, 65:35, 60:40, 55:45, 50:50, 40:60, 30:70, 20:80, 10:90, 0:100, 1 L each) and washing in the end with MeOH 100% (1.5 L). The flow rate was ca. 50 mL/min. The effluent was combined to 15 fractions (1–15) based on TLC patterns. After HPLC–PDA–MS analysis, fractions 7 and 8 were selected for isolation of compound **2** by preparative HPLC, with acetonitrile (solvent A) and water (solvent B), using a gradient from 40% A to 50% A in 30 min, followed by 50% A to 100% A in 5 min, hold for 10 min. The flow rate was 20 mL/min. Stock solutions in THF (100 mg/mL) were prepared and repeatedly injected in portions of 300–400 μL. The separation of fractions 7 (129 mg) and 8 (132 mg), yielded compound 10.8 mg of **2**.

2.6. Synthesis of dihydrostilbenes

2.6.1. Stilbenes

Compounds **4**–**7**, **9**, **11**, **13**, **15**, **17**, and **19** were purchased from TCI Europe N.V. Compounds **21** and **25** were purchased from Sigma–Aldrich Co. Compound **23** was purchased from Santa Cruz Biotechnology, Inc.

2.6.2. General procedure

Dihydro derivatives of compounds **7**, **9**, **11**, **13**, **15**, **17**, **19**, **21**, and **23** were prepared by hydrogenation of corresponding stilbenes. A standard protocol was followed,[32] with minor modifications. Solutions of each stilbene (10 mg) in absolute EtOH (5 ml) were stirred under H_2 for 3 h in the presence of 10% Pd/C. The reaction mixtures were filtered over Celite to remove the catalyst, and evaporated to dryness. The resulting residues were purified by flash column chromatography, using a hexane/EtOAc gradient, to afford target compounds **8**, **10**, **12**, **14**, **16**, **18**, **20**, **22**, and **24**, respectively, in yields of 85–95%. The spectroscopic data of compounds were in agreement with the literature, except for compound **24**, for which no report was found (^{1}H NMR spectrum is provided as Supporting information).[32–41]

2.6.3. *trans*-2-Fluoro-4′-methoxy-dihydrostilbene (24)

^{1}H NMR (chloroform-d_4, 500.13 MHz) δ_H (ppm): 7.26–7.08 (4H, m), 7.08–7.98 (2H, m), 6.90–6.80 (2H, m), 3.81 (3H, s), 3.05–2.84 (4H, m). HRESI-MS m/z 253.1589 $[M+Na]^+$ (calcd formula weight for $C_{15}H_{15}FO$, 230.2774).

2.7. Expression of $GABA_A$ receptors

Stage V–VI oocytes from *Xenopus laevis* were prepared, and cRNA injected as previously described.[23] Female *Xenopus laevis* (NASCO, Fort Atkinson, WI) were anesthetized by exposing them for 15 min to a 0.2% MS-222 (methanesulfonate salt of 3-aminobenzoic acid ethyl, Sigma) solution before surgically removing parts of the ovaries. Follicle membranes from isolated oocytes were enzymatically digested with 2 mg/mL collagenase from *Clostridium histolyticum* (Type 1A, Sigma). Synthesis of capped runoff poly(A+) cRNA transcripts was obtained from linearized cDNA templates (pCMV vector). Directly after enzymatic isolation, the oocytes were injected with 50 nL of DEPC-treated water (Sigma) containing different cRNAs at a concentration of approximately 300–3000 pg/nL per subunit. The amount of injected cRNA mixture was determined by means of a NanoDrop ND-1000 (Kisker Biotech). To ensure expression of the gamma subunit in $\alpha_1\beta_2\gamma_{2S}$ receptors, rat cRNAs were mixed in a 1:1:10 ratio. Oocytes were then stored at 18 °C in ND96 solution containing 1% of penicillin–streptomycin solution (Sigma–Aldrich). Voltage clamp measurements were performed between days 1 and 5 after cRNA injection.

2.8. Positive control

Diazepam (7-chloro-1,3-dihydro-1-methyl-5-phenyl-2*H*-1,4-benzodiazepin-2-one, Sigma, purity not less than 98%) was used as positive control. At 1 μM diazepam enhanced I_{GABA} up to 231.3 ± 22.6% (n = 3). See also Figure S1, Supporting information.

2.9. Two-microelectrode voltage clamp studies

Electrophysiological experiments were performed by the two-microelectrode voltage clamp method making use of a TURBO TEC 03X amplifier (npi electronic GmbH) at a holding potential of −70 mV and pCLAMP 10 data acquisition software (Molecular Devices). Currents were low-pass-filtered at 1 kHz and sampled at 3 kHz. The bath solution contained 90 mM NaCl, 1 mM KCl, 1 mM $MgCl_2$, 1 mM $CaCl_2$, and 5 mM HEPES (pH 7.4). Electrode filling solution contained 2 M KCl. Oocytes with maximal current amplitudes >3 μA were discarded to exclude voltage clamp errors.

2.10. Fast solution exchange during I_{GABA} recordings

Test solutions (100 μL) were applied to the oocytes at a speed of 300 μL/s by means of the ScreeningTool (npi electronic, Tamm,

Germany) automated fast perfusion system.[5] In order to determine GABA EC_{3-10} (typically between 3 and 10 μM for receptors of subunit composition $\alpha_1\beta_2\gamma_{2s}$), a dose–response experiment with GABA concentrations ranging from 0.1 μM to 1 mM was performed. Stock solution of the DCM extract (10 mg/mL in DMSO) was diluted to a concentration of 100 μg/mL with bath solution containing GABA EC_{3-10} according to a validated protocol.[23] As previously described, microfractions collected from the semi-preparative HPLC separations were dissolved in 30 μL of DMSO and subsequently mixed with 2.97 mL of bath solution containing GABA EC_{3-10}.[23] A stock solution of each pure compound tested (100 mM in DMSO) was diluted to concentrations of 0.1, 1.0, 3.0, 10, 30, 100, 300, and 500 μM with bath solution for measuring direct activation, or with bath solution containing GABA EC_{3-10} for measuring modulation of $GABA_A$ receptors. The final DMSO concentration in all the samples including the GABA control samples was adjusted to 1% to avoid solvent effect at the $GABA_A$ receptor.

2.11. Data analysis

Enhancement of the I_{GABA} was defined as $I_{(GABA+Comp)}/I_{GABA} - 1$, where $I_{(GABA+Comp)}$ is the current response in the presence of a given compound, and I_{GABA} is the control GABA-induced chloride current. Data were analyzed using the ORIGIN 7.0 SR0 software (OriginLab Corporation) and are given as mean ± SE of at least two oocytes and ⩾2 oocyte batches.

3. Results and discussion

3.1. Isolation and structure elucidation of active compounds

Screening for $GABA_A$ modulating activity was performed with *Xenopus laevis* oocytes transiently expressing $GABA_A$ receptors of the subtype $\alpha_1\beta_2\gamma_{2s}$. In an automated fast-perfusion system used for two-microelectrode voltage clamp measurements,[5] a dichloromethane extract (100 μg/mL) of *P. chinensis* roots enhanced the GABA-induced chloride ion current (I_{GABA}) by 132.8 ± 36.7%. To track the activity in the extract, we used HPLC-based activity profiling with a validated protocol.[23] The chromatogram (210–700 nm) of a semipreparative HPLC separation (10 mg of extract) and the corresponding activity profile of the time-based fractionation (24 microfractions of 90 s each) are shown in Figure 1B and A, respectively. The major peak of activity was found in fraction 9, which potentiated I_{GABA} by 119.1 ± 19.1%. Fraction 8 showed marginal activity (enhancement of I_{GABA} by 26.5 ± 4.7%). All the remaining fractions showed minimal activity and were not considered further.

Isolation of the active compounds was achieved by flash chromatography and subsequent purification by semi-preparative HPLC. Compounds were tracked with the aid of TLC and HPLC–ESIMS. The three structurally related stilbenoids coelonin (**1**), batatasin III (**2**), and pholidotol D (**3**) (Fig. 2) were identified by ESI-TOF-MS, 1D and 2D microprobe NMR, and comparison with published data.[14,29–31] The *Z* configuration in compound **3** was corroborated by proton NMR, using the chemical shifts and coupling constant of the two olefinic protons at δ_H 6.95 (2H, d, J = 6.0 Hz, H-β and α), which discards the presence of the *trans*-stereoisomer thunalbene. Detailed spectroscopic data of compounds **1**–**3** are available as Supporting information.

Stilbenoids are the major secondary metabolites in the genus *Pholidota*,[10] and the identification of compounds **1**–**3** in the active fractions of *P. chinensis* DCM extract was not surprising. The three compounds have been previously isolated from the species,[10,12,14] but they have not been reported as $GABA_A$ receptor modulators.

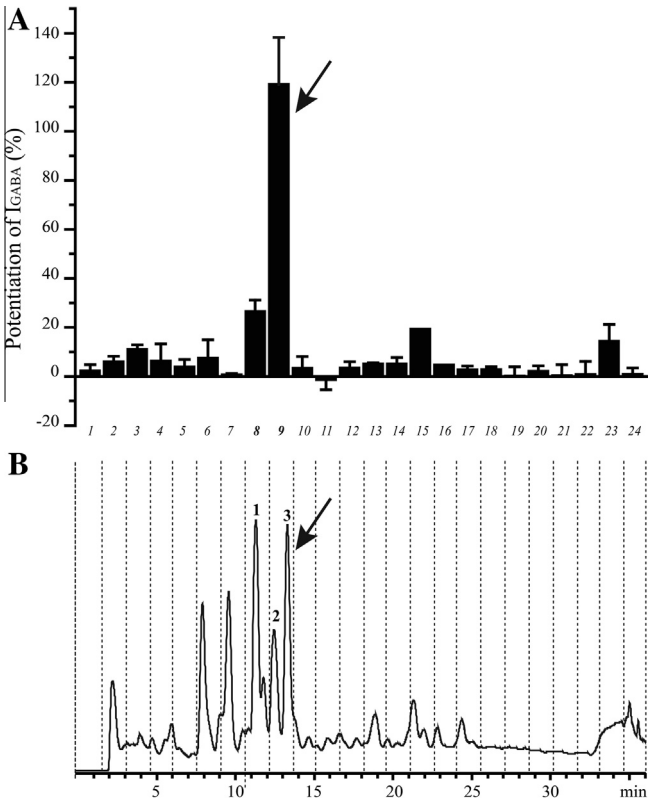

Figure 1. HPLC-based activity profiling of a DCM extract of stems and roots of *P. chinensis*, for $GABA_A$ receptor modulatory activity. (B) HPLC chromatogram (210–700 nm) of a semipreparative separation of 10 mg of extract. The numbers above peaks designate compounds **1**–**3**. The 24 time-based fractions of 90 s each are indicated with dashed lines. (A) Potentiation of the I_{GABA} by each microfraction (error bars correspond to SE).

3.2. Modulation of $GABA_A$ receptors

For a preliminary activity profile at $GABA_A$Rs of the subtype $\alpha_1\beta_2\gamma_{2s}$, **1**–**3** were tested at a concentration of 100 μM in the *Xenopus* oocyte assay. Batatasin III (**2**) was the most efficient among the three compounds. It potentiated I_{GABA} by 628.3 ± 87.1%, while compounds **1** and **3** exhibited weaker enhancements (139.5 ± 14.4% and 192.0 ± 64.1%, respectively) (Fig. 3A). Further concentration–response experiments on $\alpha_1\beta_2\gamma_{2s}$ receptors were performed with compounds **1**–**3**, at concentrations ranging from 1 to 300 μM (500 μM for compound **3**). As shown in Figure 3B, all stilbenoids enhanced I_{GABA} at a GABA EC_{3-10} in a concentration-dependent manner. The bibenzyl batatasin III (**2**) displayed strong $GABA_A$ receptor modulatory activity, with an efficiency (maximal stimulation of I_{GABA}) of 1512.9 ± 176.5% and a potency (higher concentration for half-maximal stimulation of I_{GABA}, or EC_{50}) of 52.5 ± 17.0 μM. The structurally related stilbene pholitodol D (**3**) showed much lower activity, with an efficiency of 786.8 ± 72.1% and potency of 175.5 ± 25.5 μM. The dihydrophenanthrene coelonin (**1**) showed activity similar to compound **2**, but no saturation of the receptors was reached at the highest concentration tested (300 μM). None of the compounds induced direct activation of the receptors when applied prior to GABA, at concentrations lower than 100 μM. This was indicative of an allosteric modulation of the receptor with the subunit composition $\alpha_1\beta_2\gamma_{2s}$, rather than direct agonistic activity (Fig. 3C).

Compared to other natural products tested in the same in vitro model and $GABA_A$ receptor subtype,[24,27,28,33] batatasin III (**2**) exhibited much higher efficiency. The efficiency of **2** in $GABA_A$Rs of the

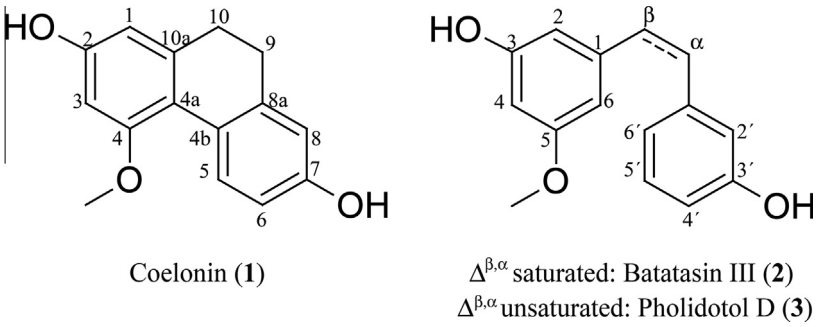

Figure 2. Chemical structures of compounds **1**–**3**.

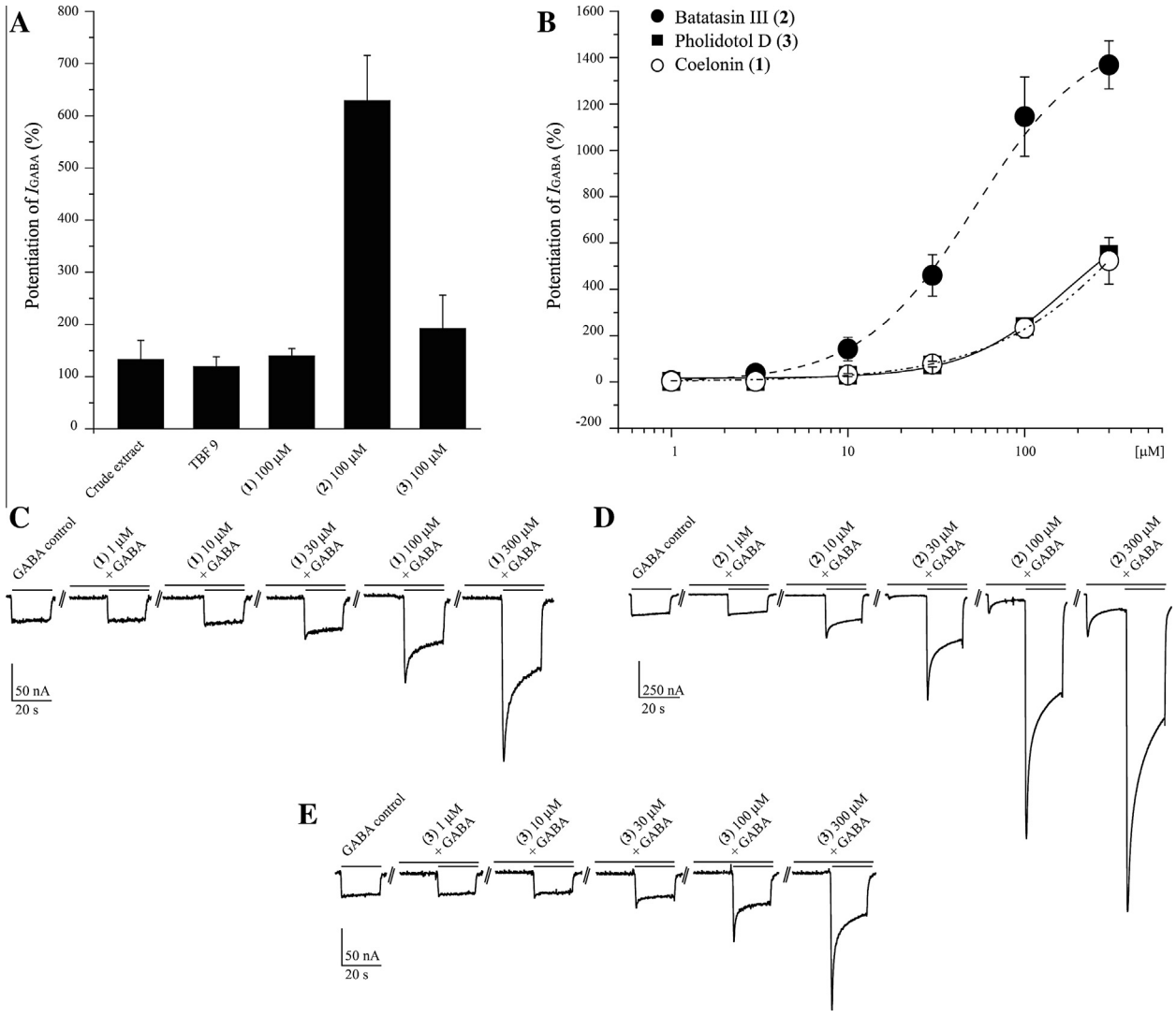

Figure 3. (A) Potentiation of I_{GABA} by the DCM extract of *P. chinensis* stems and roots (100 μg/mL), by microfraction 9, and compounds **1**–**3** (100 μM). (B) Concentration–response curve for compounds **1**–**3** on $GABA_A$ receptors of the subunit composition $\alpha_1\beta_2\gamma_{2S}$. (C–E) Typical traces for modulation of I_{GABA} by compounds **1**–**3**, respectively. The flat segments in the currents indicate the absence of direct activation of the receptors. All experiments in A–E were carried out using a GABA EC_{3-10}.

subtype $\alpha_1\beta_2\gamma_{2s}$ was also significantly higher than that of classical BDZs, with a potentiation of I_{GABA} at least fourfold that of triazolam, clotiazepam, and midazolam.[34] However, its EC_{50} value was significantly higher than that of BDZs and indicated a much lower binding affinity.

Despite the small number of compounds, preliminary structure–activity considerations could be derived. Conformational flexibility as in batatasin III (**2**) appeared to be critical for the modulatory activity of stilbenoids, since introduction of a double bond $\Delta^{\beta,\alpha}$ in pholidotol D (**3**) drastically decreased potency and efficiency. The importance of flexibility was confirmed by the weak activity of coelonin (**1**) in which the dihydrophenanthrene ring conferred additional rigidity to the structure. Although stilbenoids such as resveratrol have been described as neuroprotective

agents,[17,35–38] none of them has been reported as $GABA_A$ receptor ligand so far. Batatasin III (**2**) is thus the first representative of a new scaffold for $GABA_A$ receptor modulators. It is noteworthy that compounds with biosynthetically related scaffolds such as flavonoids,[25,39] coumarins,[24] and lignans[40] have been previously shown to possess $GABA_A$ receptor modulatory properties.

3.3. $GABA_A$ receptor subtype selectivity

Batatasin III (**2**) was tested for potential α subunit specificity, by replacing the α_1 subunit in the receptor subtype $\alpha_1\beta_2\gamma_{2s}$ with α_2, α_3, α_4, and α_5. Likewise, β subunit specificity was evaluated by replacing β_2 with β_1 and β_3. Concentration-dependent I_{GABA} modulation of compound **2** was evaluated on receptor subtypes $\alpha_2\beta_2\gamma_{2s}$, $\alpha_3\beta_2\gamma_{2s}$, $\alpha_4\beta_2\gamma_{2s}$, $\alpha_5\beta_2\gamma_{2s}$, $\alpha_1\beta_1\gamma_{2s}$, and $\alpha_1\beta_3\gamma_{2s}$ (Table 1).

As shown in Figure 4 and summarized in Table 1, compound **2** did not exhibit subtype specificity, as reflected by comparable EC_{50} values with all receptor subtypes studied ($p > 0.05$). The order of potency of batatasin III (**2**) in receptor composed by different α subunits was $\alpha_4\beta_2\gamma_{2s} > \alpha_5\beta_2\gamma_{2s} > \alpha_1\beta_2\gamma_{2s} > \alpha_3\beta_2\gamma_{2s} > \alpha_2\beta_2\gamma_{2s}$. The lower potency on $\alpha_2\beta_2\gamma_{2s}$ receptors compared to $\alpha_4\beta_2\gamma_{2s}$ was statistically significant, while there were no significant differences in efficiency among the other α-containing receptor subtypes. On $GABA_A$ receptors comprising different β subunits, almost no differences in potency and efficiency were observed. Thus, batatasin III (**2**) was a positive allosteric modulator of $GABA_A$Rs, devoid of significant subtype specificity.

Table 1
Potencies and efficiencies of batatasin III (**2**) for $GABA_A$ receptors of different subunit compositions

Subtype	EC_{50} (μM)	Max. potentiation of I_{GABA} (EC_{3-10}) (I_{max}) (%)	Hill coeff. (n_H)	n[a]
$\alpha_1\beta_2\gamma_{2s}$	52.5 ± 17.0	1512.9 ± 176.5	1.4 ± 0.3	5
$\alpha_2\beta_2\gamma_{2s}$	80.8 ± 22.1	1026.5 ± 139.2	1.2 ± 0.1	6
$\alpha_3\beta_2\gamma_{2s}$	67.3 ± 18.6	1694.2 ± 229.0	1.2 ± 0.1	5
$\alpha_4\beta_2\gamma_{2s}$	26.2 ± 3.6	1588.2 ± 97.5	1.5 ± 0.1	6
$\alpha_5\beta_2\gamma_{2s}$	46.7 ± 9.0	1375.7 ± 76.5	1.3 ± 0.1	5
$\alpha_1\beta_1\gamma_{2s}$	66.7 ± 21.0	1251.3 ± 157.0	1.8 ± 0.4	5
$\alpha_1\beta_3\gamma_{2s}$	67.2 ± 10.5	1252.9 ± 79.9	1.4 ± 0.1	5

[a] Number of experiments.

3.4. $GABA_AR$ modulatory activity of dihydrostilbenes

Flexibility appeared to be a critical factor for the $GABA_AR$ modulatory activity of stilbenoids. To confirm the influence of the double bond $\Delta^{\beta,\alpha}$, 13 commercially available stilbenoids and their corresponding dihydro derivatives (compounds **4**–**25**; Fig. 5) were tested in the *Xenopus* oocyte assay. Compounds were initially tested at a concentration of 100 μM on $GABA_A$Rs of the subtype $\alpha_1\beta_2\gamma_{2s}$. As expected, dihydrostilbenes showed higher activity than the corresponding stilbenes (Table 2, Fig. 6A). These differences in the activity of stilbenes and their dihydro derivatives were statistically significant in almost every case, with the exception of the pairs **4** and **5**/**6**, **9**/**10**, **13**/**14**, and **23**/**24** ($p > 0.05$).

Among the stilbenes, tetramethoxy-piceatannol (**11**), resveratrol (**13**), pterostilbene (**19**), and resveratrol triacetate (**21**), displayed the highest activity, potentiating I_{GABA} between 100% and 200%. Their corresponding dihydro derivatives showed the highest activity among dihydrostilbenes, but only compounds **12** and **20** showed efficiencies comparable to that of batatasin III (**2**) (544.5 ± 104.4% and 660.6 ± 100.2% respectively). A comparison of the activity of the dihydrostilbenes at 100 μM revealed that the bibenzyl scaffold alone (**6**) does not possess any $GABA_AR$ modulatory activity. In general, substituents at C-3 and C-5 (**12**, **14**, **16**, **18**, **20**, and **22**) resulted in an enhancement of the activity. Increasing the lipophilicity by replacing the hydroxy groups at C-3 and C-5 with bulkier oxygenated functions (**12**, **20**, and **22**) enhanced the

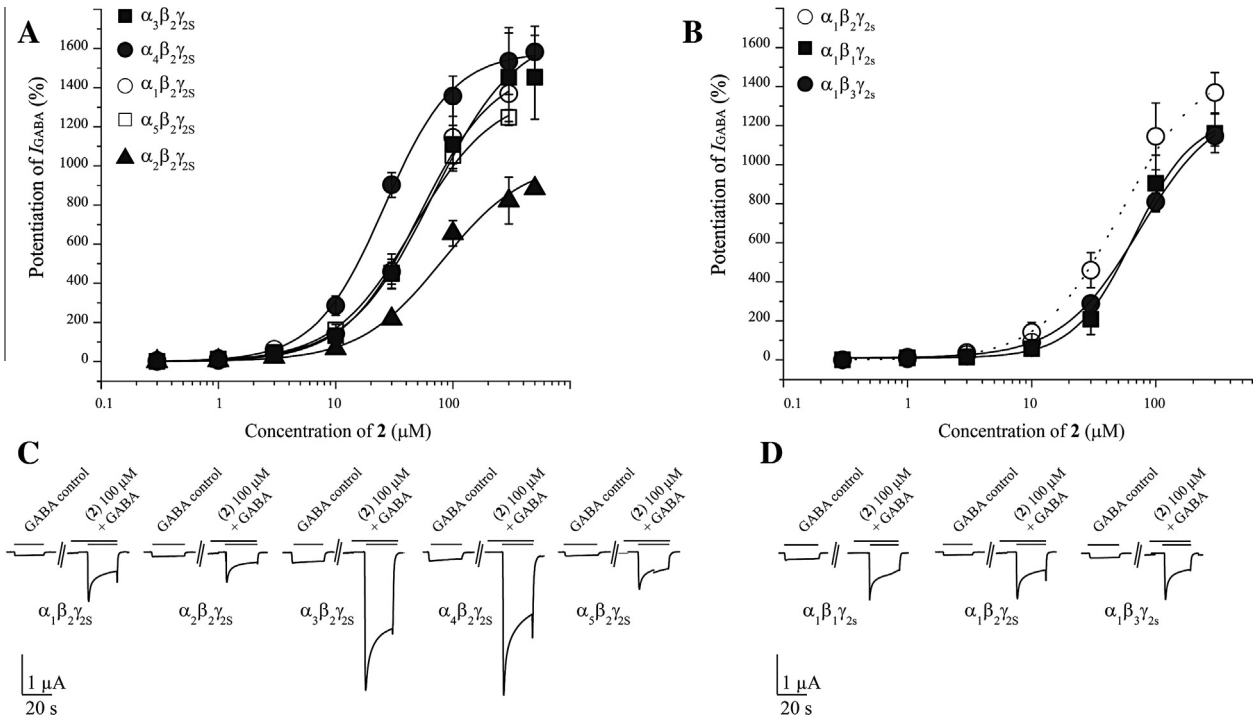

Figure 4. (A) α-Subunit dependency of batatasin III (**2**), depicted as concentration–response curves, with $GABA_A$ receptors of the subunit compositions $\alpha_1\beta_2\gamma_{2s}$, $\alpha_2\beta_2\gamma_{2s}$, $\alpha_3\beta_2\gamma_{2s}$, $\alpha_4\beta_2\gamma_{2s}$, and $\alpha_5\beta_2\gamma_{2s}$. (B) β-Subunit dependency of batatasin III (**2**), depicted as concentration–response curves with $GABA_A$ receptors of the subunit compositions $\alpha_1\beta_1\gamma_{2s}$, $\alpha_1\beta_2\gamma_{2s}$, and $\alpha_1\beta_3\gamma_{2s}$. (C and D) Typical traces for modulation of I_{GABA} by compound **2**, in receptors with different α and β subunit composition, respectively. All experiments were performed using a GABA EC_{3-10}.

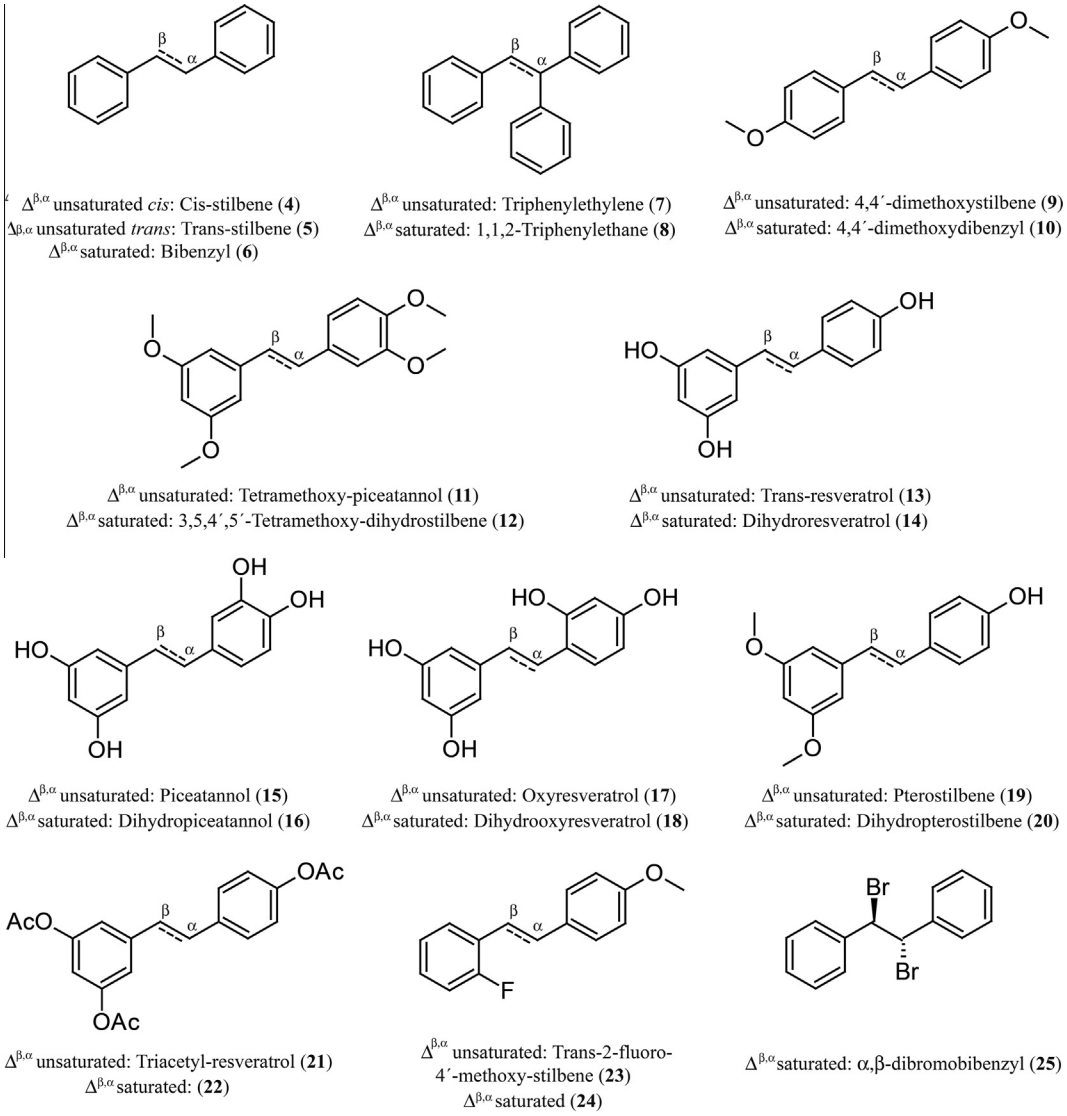

Figure 5. Chemical structures of compounds **4**–**25**.

Table 2
Potentiation of I_{GABA} in $\alpha_1\beta_2\gamma_{2s}$ receptors by compounds **4**–**25**, at a test concentration of 100 μM

Stilbenes			Dihydrostilbenes		
Compound	Max. potentiation of I_{GABA}	n[a]	Compound	Max. potentiation of I_{GABA}	n[a]
4	12.6 ± 9.2	3	**6**	8.3 ± 22.9	3
5	−11.3 ± 12.3	3			
7	−7.3 ± 0.1	3	**8**	51.6 ± 1.1	3
9	−24.8 ± 4.8	3	**10**	−20.9 ± 3.7	3
11	101.3 ± 0.9	3	**12**	544.5 ± 140.4	3
13	121.9 ± 21.8	3	**14**	162.2 ± 17.5	3
15	−35.4 ± 9.8	3	**16**	86.3 ± 9.9	3
17	−19.7 ± 3.9	3	**18**	44.1 ± 19.7	3
19	212.4 ± 10.9	3	**20**	660.6 ± 100.2	3
21	122.8 ± 18.6	3	**22**	227.7 ± 1.3	2
23	−22.9 ± 7.5	3	**24**	−16.8 ± 7.9	3
Diazepam[b] (1 μM)	231.3 ± 22.6	3	**25**	−12.9 ± 0.4	3

[a] Number of experiments.
[b] Positive control.

activity of dihydrostilbenes. The role of substituents in ring B was less clear within this compounds series. In the case of compounds **12** and **20**, different substitution patterns in ring B did not influence the activity. In contrast, when comparing compounds **14**, **16**, and **18**, addition of a hydroxy group in C-4′ or C-6′ led to a significant decrease of activity. Introduction of a halogen atom as in **25** induced slight negative receptor modulation, and substitution at C-4 (compound **10**) decreased activity. Since we had only one pair of *cis* and *trans* isomers (**4** and **5**, both inactive at 100 μM), the role of geometric isomerism could not be assessed in more detail.

The dihydro derivatives of tetramethoxy-piceatannol and pterostilbene (compounds **12** and **20**, respectively) were submitted to further concentration–response experiments on $\alpha_1\beta_2\gamma_{2s}$ receptors. Both compounds enhanced I_{GABA} at a GABA EC_{3-10} in a concentration-dependent manner (Fig. 6B). Compounds **12** and **20** had lower efficiency than the natural dihydrostilbene **2** (Table 3), with maximal stimulations of I_{GABA} of 870.7 ± 106.8% and 694.2 ± 86.0%, respectively. In terms of potency, **20** was comparable to **2** (EC_{50} 54.5 ± 13.4 μM), whereas **12** was twice as potent (EC_{50} 20.2 ±

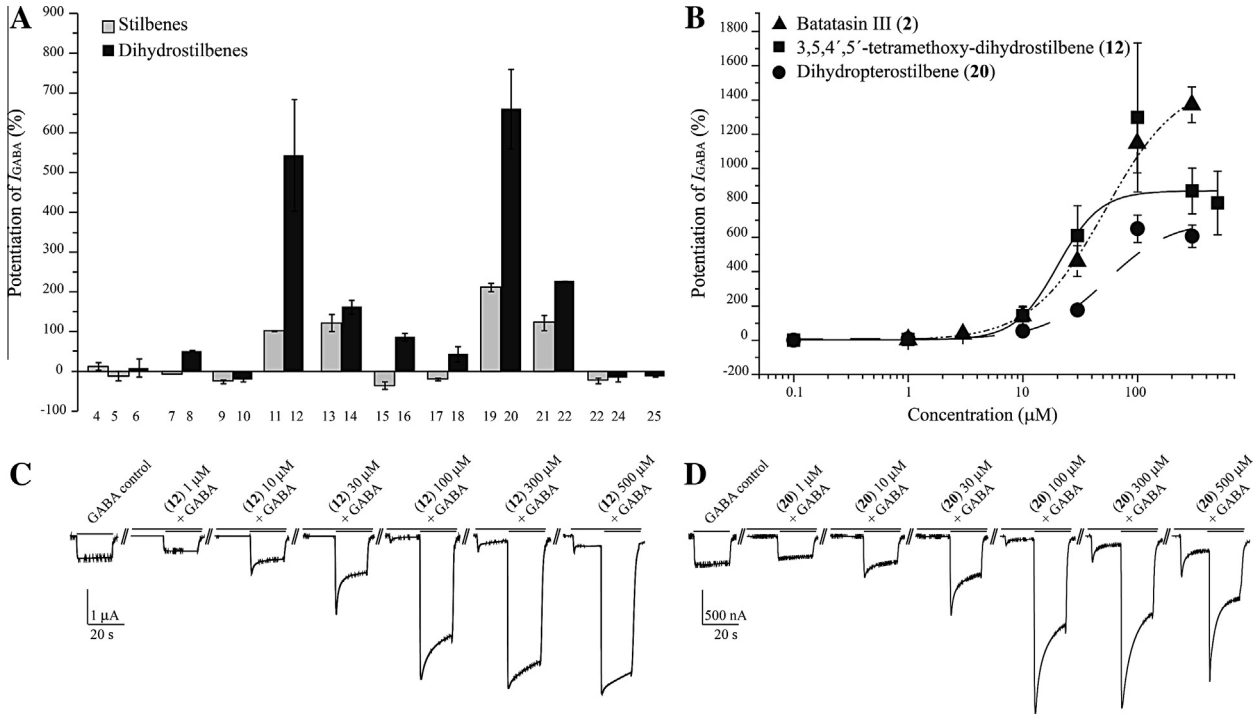

Figure 6. (A) Potentiation of I_{GABA} by compounds **4**–**25** (100 μM). (B) Potentiation of I_{GABA} by compounds **2**, **12** and **20**. Concentration–response curves are shown for $GABA_A$ receptors of the subunit composition $\alpha_1\beta_2\gamma_{2s}$. (C and D) Typical traces for modulation of I_{GABA} by compounds **12** and **20**, respectively. The inward currents induced in the absence of GABA (C and D) indicate direct activation of the receptors. All experiments shown in A–D were performed using a GABA EC_{3-10}.

Table 3
Potencies and efficiencies of compounds **2**, **3**, **12** and **20** for $\alpha_1\beta_2\gamma_{2s}$ $GABA_A$ receptors

Compound	EC_{50} (μM)	Max. potentiation of I_{GABA} (EC_{3-10}) (I_{max}) (%)	Hill coeff. (n_H)	n[a]
2	52.5 ± 17.0	1512.9 ± 176.5	1.2 ± 0.1	5
3	175.5 ± 25.5	786.8 ± 72.1	1.5 ± 0.2	5
12	20.2 ± 6.4	870.7 ± 106.8	2.3 ± 1.0	4
20	54.5 ± 13.4	694.2 ± 86.0	1.6 ± 0.2	4

[a] Number of experiments.

6.4 μM). This suggests that increased lipophilicity of ring B may have a positive effect on the potency of dihydrostilbenes. However, further studies with a larger series of compounds are needed for confirmation. None of the compounds induced direct activation of the receptors when applied prior to GABA, at concentrations lower than 100 μM (Fig. 6C).

Stilbenoids have attracted significant attention in recent years due to their wide range of useful properties, including applications in optics, biochemistry, and chemotherapy.[13,41] The stilbenoid scaffold can be considered as a priviledged structure.[42,43] However, there have been no reports on $GABA_A$ receptor modulatory activity of stilbenoids up to now, despite a significant number of publications on biological activities of natural stilbenoids, and in particular, on resveratrol. Dihydrostilbenes such as **2** may thus be an interesting starting point for the synthesis of new $GABA_A$ receptor modulators.

4. Conclusions

With the aid of an HPLC-based profiling approach, we identified batatasin III (**2**) as the major compound responsible for $GABA_AR$ modulatory activity of the dichloromethane extract of *P. chinensis*. This dihydrostilbene showed allosteric modulation in $\alpha_1\beta_2\gamma_{2s}$ $GABA_A$ receptors with a higher efficiency than any other natural products tested up to now, but its EC_{50} value was significantly higher than that of BDZs. Dihydrostilbenes represent a new scaffold for $GABA_A$ receptor modulators.

The conformational flexibility of dihydrostilbenoids appeared critical for $GABA_AR$ modulatory properties. For a further exploration of this scaffold, conformationally restricted derivatives should be synthesized in order to explore in more detail the optimal orientation of the aromatic rings and substituents.

Acknowledgements

Financial support was provided by the Swiss National Science Foundation through project 205320_126888 (M.H.). D.C.R. thanks the Swiss Federal Commission for Scholarships for Foreign Students (FCS) and the Department of Education of Canton Basel (Erziehungsdepartement des Kantons Basel-Stadt) for fellowships granted in 2011 and 2012, respectively.

Supplementary data

Supplementary data associated with this article can be found, in the online version, at http://dx.doi.org/10.1016/j.bmc.2014.01.008.

References and notes

1. Olsen, R. W.; Sieghart, W. *Pharmacol. Rev.* **2008**, *60*, 243.
2. Rudolph, U.; Knoflach, F. *Nat. Rev. Drug Disc.* **2011**, *10*, 685.
3. D'Hulst, C.; Atack, J. R.; Kooy, R. F. *Drug Discovery Today* **2009**, *14*, 866.
4. Tan, K. R.; Rudolph, U.; Lüscher, C. *Trends Neurosci.* **2011**, *34*, 188.
5. Baburin, I.; Beyl, S.; Hering, S. *Pflug. Arch. Eur. J. Physiol.* **2006**, *453*, 117.
6. Pérez Gutiérrez, R. M. *J. Med. Plants Res.* **2010**, *4*, 592.
7. Williams, R.; Martin, S.; Hu, J.-F.; Garo, E.; Rice, S.; Norman, V.; Lawrence, J.; Hough, G.; Goering, M.; O'Neil-Johnson, M.; Eldridge, G.; Starks, C. *Planta Med.* **2011**, *78*, 160.
8. Bulpitt, C. J.; Li, Y.; Bulpitt, P. F.; Wang, J. *J. R. Soc. Med.* **2007**, *100*, 558.
9. Wang, J.; Matsuzaki, K.; Kitanaka, S. *Chem. Pharm. Bull. (Tokyo)* **2006**, *54*, 1216.
10. Bandi, A. K. R.; Lee, D.-U. *Chem. Biodiversity* **2011**, *8*, 1400.
11. Wu, B.; Qu, H.; Cheng, Y. *Chem. Biodiversity* **1803**, *2008*, 5.

12. Yao, S.; Tang, C.-P.; Li, X.-Q.; Ye, Y. *Helv. Chim. Acta* **2008**, *91*, 2122.
13. Rivière, C.; Pawlus, A. D.; Mérillon, J.-M. *Nat. Prod. Rep.* **2012**, *29*, 1317.
14. Majumder, P. L.; Roychowdhury, M.; Chakraborty, S. *Phytochemistry* **1998**, *49*, 2375.
15. Kovacs, A.; Vasas, A.; Hohmann, J. *Phytochemistry* **2008**, *69*, 1084.
16. Shen, T.; Wang, X.-N.; Lou, H.-X. *Nat. Prod. Rep.* **2009**, *26*, 916.
17. Greger, H. *J. Nat. Prod.* **2012**, *75*, 2261.
18. Potterat, O.; Hamburger, M. *Curr. Org. Chem.* **2006**, *10*, 899.
19. Danz, H.; Stoyanova, S.; Wippich, P.; Brattstrom, A.; Hamburger, M. *Planta Med.* **2001**, *67*, 411.
20. Dittmann, K.; Gerhauser, C.; Klimo, K.; Hamburger, M. *Planta Med.* **2004**, *70*, 909.
21. Adams, M.; Christen, M.; Plitzko, I.; Zimmermann, S.; Brun, R.; Kaiser, M.; Hamburger, M. *J. Nat. Prod.* **2010**, *73*, 897.
22. Adams, M.; Zimmermann, S.; Kaiser, M.; Brun, R.; Hamburger, M. *Nat. Prod. Commun.* **2009**, *4*, 1377.
23. Kim, H. J.; Baburin, I.; Khom, S.; Hering, S.; Hamburger, M. *Planta Med.* **2008**, *74*, 521.
24. Li, Y.; Plitzko, I.; Zaugg, J.; Hering, S.; Hamburger, M. *J. Nat. Prod.* **2010**, *73*, 768.
25. Yang, X.; Baburin, I.; Plitzko, I.; Hering, S.; Hamburger, M. *Mol. Diversity* **2011**, *15*, 361.
26. Zaugg, J.; Khom, S.; Eigenmann, D.; Baburin, I.; Hamburger, M.; Hering, S. *J. Nat. Prod.* **2011**, *74*, 1764.
27. Zaugg, J.; Eickmeier, E.; Rueda, D. C.; Hering, S.; Hamburger, M. *Fitoterapia* **2011**, *82*, 434.
28. Zaugg, J.; Baburin, I.; Strommer, B.; Kim, H. J.; Hering, S.; Hamburger, M. *J. Nat. Prod.* **2010**, *73*, 185.
29. Wang, J.; Wang, L.; Kitanaka, S. *J. Nat. Med.* **2007**, *61*, 381.
30. Majumder, P.; Laha, S.; Datta, N. *Phytochemistry* **1982**, *21*, 478.
31. Hashimoto, T.; Hasegawa, K.; Yamaguchi, H.; Saito, M.; Ishimoto, S. *Phytochemistry* **1974**, *13*, 2849.
32. Oh, K. B.; Kim, S. H.; Lee, J.; Cho, W. J.; Lee, T.; Kim, S. *J. Med. Chem.* **2004**, *47*, 2418.
33. Zaugg, J.; Eickmeier, E.; Ebrahimi, S. N.; Baburin, I.; Hering, S.; Hamburger, M. *J. Nat. Prod.* **2011**, *74*, 1437.
34. Khom, S.; Baburin, I.; Timin, E. N.; Hohaus, A.; Sieghart, W.; Hering, S. *Mol. Pharmacol.* **2006**, *69*, 640.
35. Richard, T.; Pawlus, A. D.; Iglésias, M.-L.; Pedrot, E.; Waffo-Teguo, P.; Mérillon, J.-M.; Monti, J.-P. *Ann. N.Y. Acad. Sci.* **2011**, *1215*, 103.
36. Vingtdeux, V.; Dreses-Werringloer, U.; Zhao, H.; Davies, P.; Marambaud, P. *BMC Neurosci.* **2008**, *9*, S6.
37. Sun, A. Y.; Wang, Q.; Simonyi, A.; Sun, G. Y. *Mol. Neurobiol.* **2010**, *41*, 375.
38. Zhang, F.; Liu, J.; Shi, J. S. *Eur. J. Pharmacol.* **2010**, *636*, 1.
39. Hanrahan, J. R.; Chebib, M.; Johnston, G. A. *Br. J. Pharmacol.* **2011**, *163*, 234.
40. Zaugg, J.; Ebrahimi, S. N.; Smiesko, M.; Baburin, I.; Hering, S.; Hamburger, M. *Phytochemistry* **2011**, *72*, 2385.
41. Gray, E. E.; Rabenold, L. E.; Goess, B. C. *Tetrahedron Lett.* **2011**, *52*, 6177.
42. Welsch, M. E.; Snyder, S. A.; Stockwell, B. R. *Curr. Opin. Chem. Biol.* **2010**, *14*, 1.
43. Breinbauer, R.; Vetter, I. R.; Waldmann, H. *Angew. Chem., Int. Ed.* **2002**, *41*, 2878.

Supporting Information

Identification of dihydrostilbenes in *Pholidota chinensis* as a new scaffold for $GABA_A$ receptor modulators

Diana C. Rueda[a], Angela Schöffmann[b], Maria De Mieri[a], Melanie Raith[a], Evelyn Jähne[a], Steffen Hering[b], and Matthias Hamburger[a,*]

[a] *Division of Pharmaceutical Biology, University of Basel, Klingelbergstrasse 50, CH-4056 Basel, Switzerland*
[b] *Institute of Pharmacology and Toxicology, University of Vienna, Althanstrasse 14, A-1090 Vienna, Austria*

* Corresponding author. Tel.: +41-61-2671425; fax: +41-61-2671474.
E-mail: matthias.hamburger@unibas.ch

Fig. S1. Diazepam (1 µM) enhanced IGABA through $\alpha_1\beta_2\gamma_{2S}$ $GABA_A$ receptors and was therefore used as positive control for the assay. Currents in the presence of GABA ($EC_{5\text{-}10}$, single bar, control) and during co-application of GABA and diazepam (1 µM, double bar) are shown. At 1 µM diazepam enhanced I_{GABA} up to 231.3 ± 22.6% (n=3).

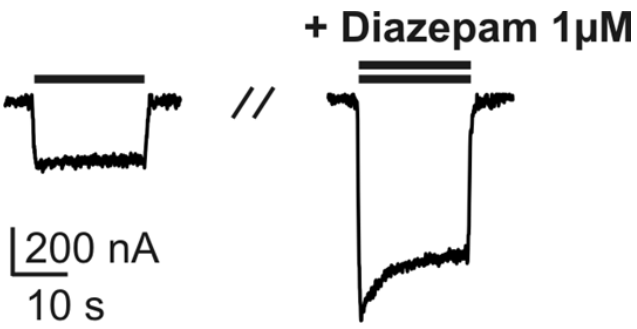

Fig. S2. Analytical HPLC chromatogram of a dichloromethane extract of *P. chinensis*. **A**. UV trace (210-700 nm). **B**. ELSD trace (45°C, N_2 2.8 L/min). Compounds **1**-**3** appear as the major constituents of the extract. Separation was performed with MeOH (solvent A) and water (solvent B), using a gradient from 50% A to 80% A in 40 min, followed by 80% A to 100% A in 5 min. The flow rate was 0.4 mL/min, and 50 μg of extract (in 10 μL of DMSO) were injected.

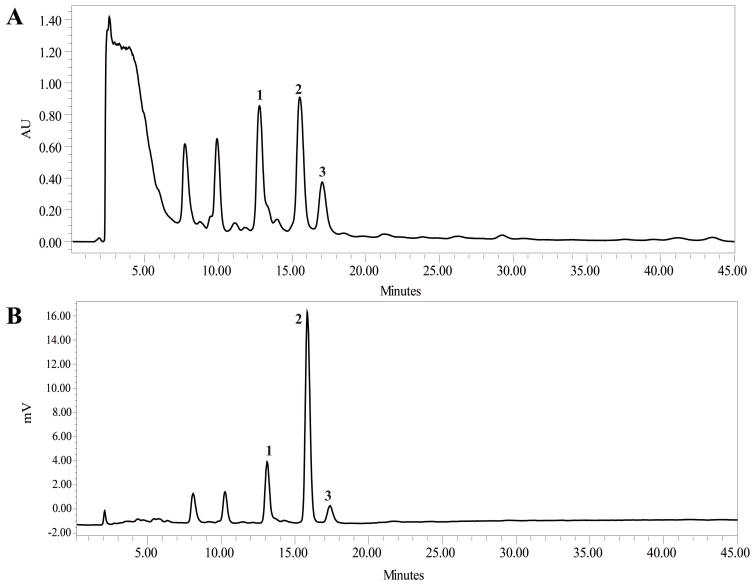

Fig. S3. ^{1}H NMR spectrum of compound **24**

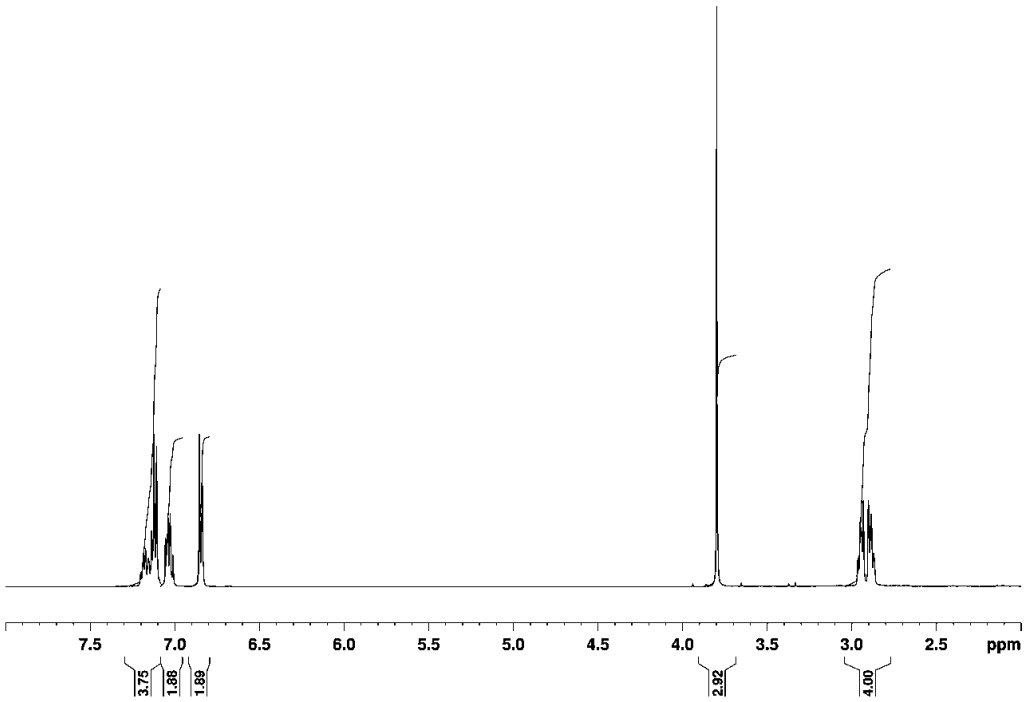

Table S1: NMR spectroscopic data (500.13 MHz, methanol-d_3) for coelonin (**1**)

Molecular formula: $C_{15}H_{14}O_3$; Formula weight: 242.26986; CAS Nr. 82344-82-9

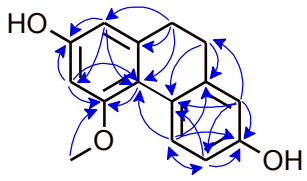

Position	δ_C[a]	δ_H (I, m, *J* in Hz)
1	104.8	6.26 (CH, d, *2.5*)
2	155.4	-
3	100.1	6.30 (CH, d, *2.5*)
4	158.3	-
4a	114.8	-
4b	125.2	-
5	128.6	8.13 (CH, d, *8.4*)
6	112.2	6.62 (CH, dd, *8.3*, *2.7*)
7	154.8	-
8	113.8	6.61 (CH, d, *2.6*)
8a	139.8	-
9	30.1	2.59 (CH_2, s)
10	30.8	2.59 (CH_2, s)
10a	138.7	-
4-OCH_3	54.2	3.67 (CH_3, s)

[a] chemical shifts derived from multiplicity-edited HSQC and HMBC spectra. Blue arrows in structural formula indicate observed HMBC correlations.

Table S2: NMR spectroscopic data (500.13 MHz, methanol-d_3) for batatasin III (**2**)

Molecular formula: $C_{15}H_{16}O_3$; Formula weight: 244.28574; CAS Nr. 56684-87-8

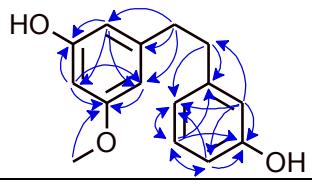

Position	δ_C [a]	δ_H (I, m, *J* in Hz)
1	144.9	-
2	108.1	6.29 (CH, br s)
3	157.6	-
4	98.7	6.23 (CH, m)
5	160.9	-
6	105.5	6.23 (CH, m)
1´	143.3	-
2´	115.3	6.64 (CH, m)
3´	156.7	-
4´	112.4	6.64 (CH, m)
5´	129.0	7.03 (CH, dd, *7.9*, *7.5*)
6´	119.8	6.64 (CH, m)
α	37.0	2.75 (CH_2, m)
β	37.6	2.75 (CH_2, m)
5-OCH_3	54.3	3.63 (CH_3, s)

[a] chemical shifts derived from multiplicity-edited HSQC and HMBC spectra. Blue arrows in structural formula indicate observed HMBC correlations.

Table S3: NMR spectroscopic data (500.13 MHz, methanol-d_3) for pholidotol D (**3**)

Molecular formula: $C_{15}H_{14}O_3$; Formula weight: 242.26986; CAS Nr. 1006380-82-0

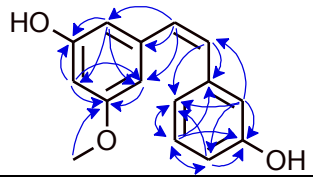

Position	δ_C[a]	δ_H (I, m, *J* in Hz)
1	139.7	-
2	105.8	6.58 (CH, m)
3	157.7	-
4	100.3	6.31 (CH, t, *2.0*)
5	160.8	-
6	103.4	6.58 (CH, m)
1´	138.5	-
2´	112.4	7.00-6.65 (CH, m)
3´	156.0	-
4´	114.4	7.00-6.65 (CH, m)
5´	129.4	7.17 (CH, dd, *7.9*, *7.8*)
6´	117.8	6.69 (CH, dd, *8.2*, *2.2*)
α	128.4	7.00-6.65 (CH, m)
β	128.6	7.00-6.65 (CH, m)
5-OCH_3	54.4	3.76 (CH_3, s)

[a] chemical shifts derived from multiplicity-edited HSQC and HMBC spectra. Blue arrows in structural formula indicate observed HMBC correlations.

3.3. HPLC-based activity profiling for $GABA_A$ receptor modulators in *Adenocarpus cincinnatus*

Diana C. Rueda, Maria De Mieri, Steffen Hering, and Matthias Hamburger. J Nat Prod 2014. Published online (doi: 10.1021/np500016z)

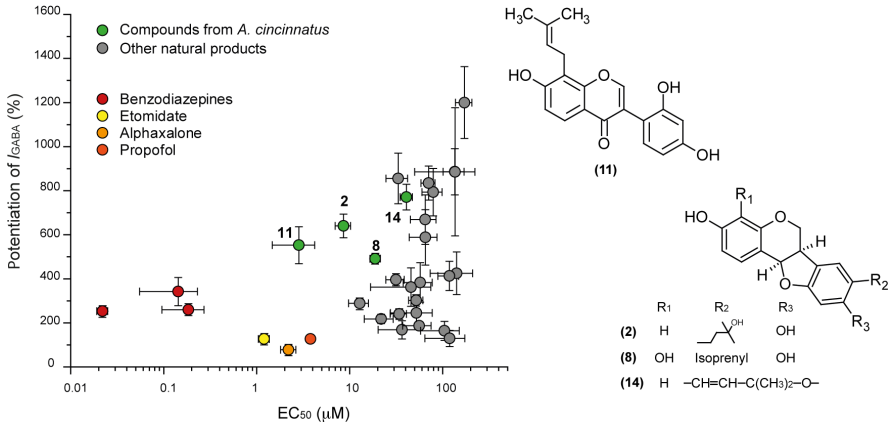

HPLC-based activity profiling enabled the isolation of 15 flavonoid and isoflavonoid derivatives, including 8 new natural products, from *A. cincinnatus* roots and tubers. Structure elucidation was achieved by high-resolution mass spectroscopy, microprobe NMR, ECD, and polarimetry. All compounds were tested at 100 μM in the oocyte assay and the most active one were submitted to concentration-response experiments. Two pterocarpans and one isoflavone showed remarkably higher potency than other natural products previously isolated in our group (EC_{50} below 10 μM).

Extraction of the plant material for isolation, HPLC-based activity profiling, isolation of pure compounds, bioactivity assessment of fractions and pure compounds in Xenopus *oocytes, oocyte preparation, recording and interpretation of analytical data for structure elucidation (UV, HRMS, NMR and CD spectra, optical rotation), writing of the manuscript draft, and preparation of the figures were my contributions to this publication. Structure elucidation and discussion writing were supported by M. De Mieri.*

Diana C. Rueda

JOURNAL OF NATURAL PRODUCTS

Article

pubs.acs.org/jnp

HPLC-Based Activity Profiling for $GABA_A$ Receptor Modulators in *Adenocarpus cincinnatus*

Diana C. Rueda,[†] Maria De Mieri,[†] Steffen Hering,[‡] and Matthias Hamburger*[,†]

[†]Division of Pharmaceutical Biology, University of Basel, Klingelbergstrasse 50, 4056 Basel, Switzerland

[‡]Department of Pharmacology and Toxicology, University of Vienna, Althanstrasse 14, 1090 Vienna, Austria

Supporting Information

ABSTRACT: In a two-microelectrode voltage clamp assay with *Xenopus laevis* oocytes, a dichloromethane extract of *Adenocarpus cincinnatus* roots and tubers (Leguminosae) enhanced the GABA-induced chloride current (I_{GABA}) through receptors of the subtype $\alpha_1\beta_2\gamma_{2s}$ by 126.5 ± 25.1% when tested at 100 μg/mL. By means of HPLC-based activity profiling, 15 flavonoid and isoflavonoid derivatives, including eight new compounds, were identified in the active fractions of the extract. Isoflavone **11** and pterocarpans **2** and **8** showed promising activity in the oocyte assay, with EC_{50} values between 2.8 ± 1.4 and 18.8 ± 2.3 μM. Maximal potentiation of I_{GABA} ranged between 490% and 640%. This is the first report of pterocarpans as $GABA_A$ receptor modulators.

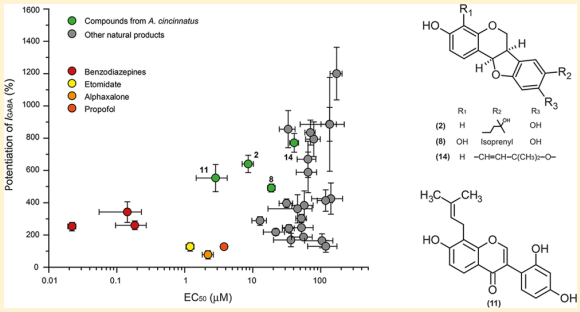

$GABA_A$ receptors ($GABA_A$Rs) are ligand-gated chloride channels that mediate the major form of fast inhibitory neurotransmission in the CNS. They are heteropentamers assembled from 19 known subunits (α_{1-6}, β_{1-3}, γ_{1-3}, δ, ε, θ, π, ρ_{1-3}), forming an integral chloride-selective channel. GABA-induced chloride influx hyperpolarizes the postsynaptic neurons, inhibiting further action potentials, and thus, impaired GABAergic function results in CNS disorders such as epilepsy, insomnia, anxiety, and mood disorders.[1−3] A number of clinically important drugs such as benzodiazepines (BDZs), barbiturates, neuroactive steroids, anesthetics, and certain other CNS depressants bind $GABA_A$Rs. However, these drugs lack subunit specificity and, therefore, exhibit a number of unwanted side effects.[4] Hence, there is a need for $GABA_A$R modulators with new structural scaffolds.

In recent years, a large number of natural products have been identified as $GABA_A$R ligands. Among these, flavonoids have been extensively studied as first- and second-order $GABA_A$R modulators interacting with the BDZ binding site and with alternative BDZ-insensitive sites of the receptor.[5−7] Recently, isoflavones have also been identified as $GABA_A$ receptor modulators.[8] Although biogenetically related to flavonoids, isoflavonoids represent a structurally distinct scaffold.

In the search for new $GABA_A$ receptor modulators, we screened a library of 880 fungal and plant extracts in an automated two-microelectrode voltage clamp assay in *Xenopus* oocytes[9] expressing $GABA_A$Rs of the subtype $\alpha_1\beta_2\gamma_{2s}$, the most abundant one in the human brain.[1] The dichloromethane extract of the roots and tubers of *Adenocarpus cincinnatus* (Ball) Maire (Fabaceae) potentiated the GABA-induced chloride current by 126.5 ± 25.1% when tested at 100 μM. *A. cincinnatus*, native to Morocco,[10,11] is one of the ca. 25 species of the genus *Adenocarpus*, subfamily Papilionoideae. Quinolizidine, pyrrolizidine, and bipiperidyl alkaloids, flavonoids, and isoflavonoids have been described as chemosystematic markers for the genus.[11,12] However, information available on the species is very limited.

We here describe the identification of 15 flavonoid and isoflavonoid derivatives from the active extract of *A. cincinnatus* by means of HPLC-based activity profiling[13] and report pterocarpans as a new scaffold for $GABA_A$ receptor modulators. Eight new natural products were identified in the extract, while the remaining seven are reported for the species for the first time.

RESULTS AND DISCUSSION

Isolation and Structure Elucidation of Active Compounds. The activity in the extract was tracked by means of HPLC-based activity profiling using a previously validated protocol.[14] The chromatogram (210−700 nm) of a semi-preparative HPLC separation (10 mg of extract) and the corresponding activity profile of the time-based fractionation (24 microfractions of 90 s each) are shown in Figure 1B and A, respectively. The $GABA_A$ receptor modulatory activity of the extract was localized in microfractions 7 to 13. Fractions 9 and 10 potentiated I_{GABA} by 334.15 ± 113.12% and 245.43 ± 141.70%, while fractions 7, 8, and 13 potentiated I_{GABA} between

Special Issue: Special Issue in Honor of Otto Sticher

Received: January 9, 2014
Published: February 26, 2014

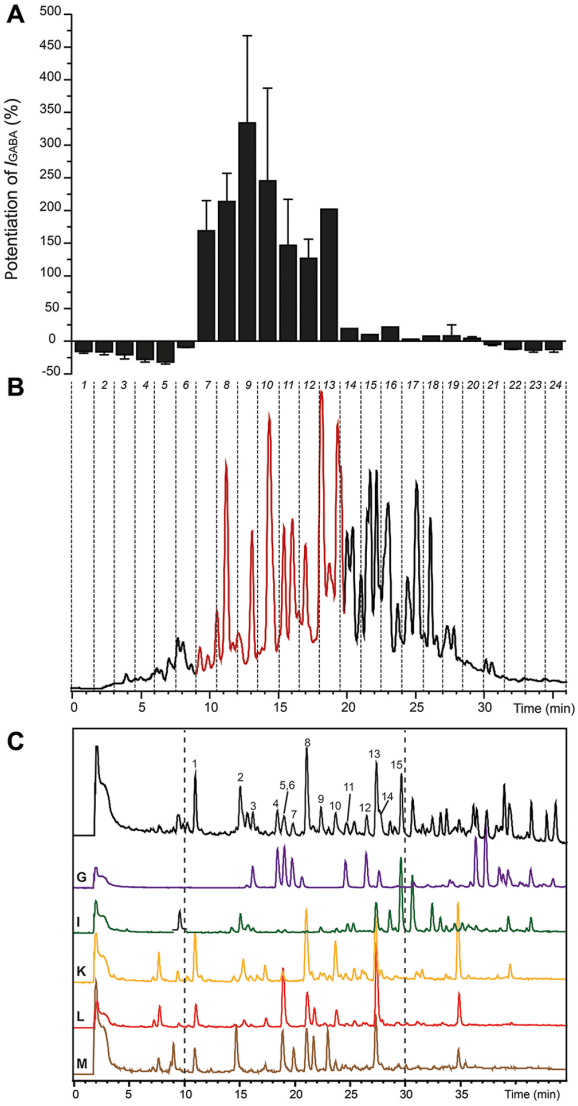

Figure 1. HPLC-based activity profiling of a dichloromethane extract of roots and tubers of *Adenocarpus cincinnatus*, for $GABA_A$ receptor modulatory activity. (B) HPLC chromatogram (210−700 nm) of a semipreparative separation of 10 mg of extract. The 24 time-based fractions of 90 s each are indicated with dashed lines. (A) Potentiation of the I_{GABA} by each microfraction (error bars correspond to SE). (C) Optimized analytical HPLC traces (210−700 nm) of open column fractions G, I, and K−M. The first trace at the top corresponds to the crude extract. The numbers above peaks designate compounds **1**−**15**. The active time window from the HPLC-based activity profile (time-based fractions 7−13) is indicated between dashed lines.

170% and 213%. Fractions 11 and 12 enhanced I_{GABA} by 146.51 ± 70.60% and 126.76 ± 29.40%, respectively. Owing to the occurrence of unresolved peaks in the active time window of the chromatogram, a single-step purification of active compounds by means of semipreparative or preparative HPLC was not possible.

Preparative isolation was started with open column chromatography on silica gel, and 19 fractions (A−S) were collected on the basis of TLC patterns. HPLC-ESIMS analysis under optimized separation conditions (Figure 1C) revealed that the extract was significantly more complex than suggested by the time-based fractionation (Figure 1B). Peaks with retention times fitting active microfractions 7−13 were detected in fractions G−M. Active compounds were isolated from fractions G, I, and K−M (Figure 1C) with the aid of preparative and semipreparative HPLC. A total of 15 flavonoid and isoflavonoid derivatives (**1**−**15**) were isolated from the active time window of the extract, including eight new natural products: **2**, **4**, **6**, **7**, **8**, **9**, **11**, and **12** (Figure 2). Structure

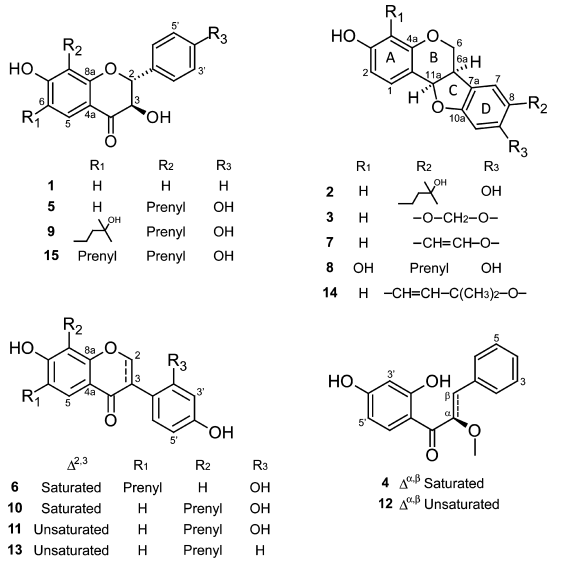

Figure 2. Flavonoid and isoflavonoid derivatives isolated from *A. cincinnatus*.

elucidation was achieved by means of ESITOFMS and 1D and 2D microprobe NMR spectroscopy, and absolute configuration was established by electronic circular dichroism (ECD) spectroscopy.

The NMR data of compounds **1**, **5**, **9**, and **15** showed resonances of two vicinal oxygenated methines (H-2 and H-3), a carbonyl function (C-4), and a set of aromatic protons suggesting a 7-hydroxydihydroflavonol scaffold. Compound **1** had a molecular formula of $C_{15}H_{12}O_4$ based on HRESIMS (*m*/*z* 279.0626 $[M + Na]^+$) and ^{13}C NMR data. Its structure was established by NMR spectroscopic data as 7-hydroxydihydroflavonol. The compound had been previously isolated from *Virgilia oroboides* (Fabaceae), but was identified only as its 3,7-diacetate.[15] Compounds **5** and **15** were identified as lespecyrtin A_1[16] and lespeflorin B_2,[17] respectively. The large $^3J_{H,H}$ coupling constant (~11.8 Hz) between H-2 and H-3 indicated *trans* configurations for **1**, **5**, and **15** (S5, Supporting Information). In agreement with previous reports,[15−17] the three compounds showed a 2*R*,3*R* absolute configuration. Their ECD spectra (Figure 3A) exhibited the typical pattern of (2*R*,3*R*)-dihydroflavonols, with a positive CE at 320−303 nm and negative CE at 270−290 nm, due to n→π^* and $\pi\rightarrow\pi^*$ transitions, respectively.[18,19] It is noteworthy that the original report of the (2*R*,3*R*)-lespecyrtin (**5**)[16] describes a CD spectrum with positive CEs for both transitions. However, such data would contradict the expected behavior, and we

dx.doi.org/10.1021/np500016z | *J. Nat. Prod.* 2014, 77, 640−649

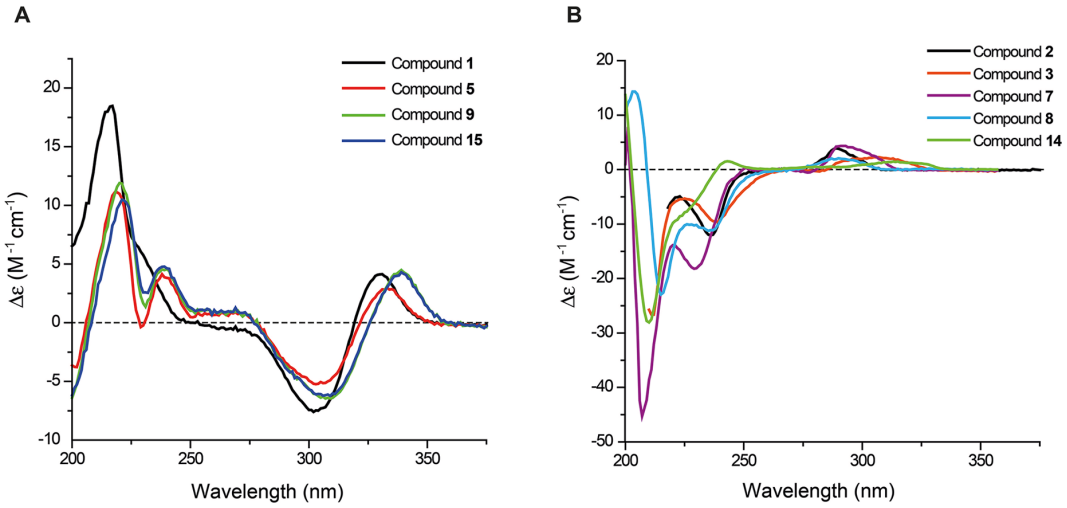

Figure 3. (A) ECD spectra of dihydroflavonols **1**, **5**, **9**, and **15**. (B) ECD spectra of pterocarpans **2**, **3**, **7**, **8**, and **14**.

assume our experimental data are proper indicators of the 2*R*,3*R* absolute configuration of this compound.

Compound **9** has a molecular formula of $C_{25}H_{30}O_6$ based on HRESIMS (*m*/*z* 449.2087 [M + Na]$^+$) and ^{13}C NMR data. Strong similarities with the NMR data of **15** indicated that **9** was also a 7,4′-dihydroxydihydroflavonol. The only major difference in the ^{1}H NMR spectrum of **9** (Table 1) was seen with resonances at δ_H 2.67 (2H, m, H-α), δ_H 1.73 (2H, m, H-β), and δ_H 1.26 (6H, s, H-δ and -ε). These data were indicative of a 3-hydroxy-3-methylbutyl moiety, which was corroborated by the corresponding ^{13}C NMR resonances of C-α–C-ε (δ_C 25.9, 44.6, 71.6, 29.43, and 29.41, respectively). The attachment of the side chain at C-6 (δ_C 117.5) was established via the NOESY (H-5/H-α, H-β) and HMBC (H-α/C-5, C-7) correlations. The absolute configuration was established as 2*R*,3*R* based on the ECD spectrum (Figure 3A). Hence, the structure of compound **9** was established as (2*R*,3*R*)-7,4′-dihydroxy-6-(3-hydroxy-3-methylbutyl)-8-(3-methylbut-2-en-1-yl)dihydroflavonol.

The UV and NMR spectra of compounds **2**, **3**, **7**, **8**, and **14** showed distinctive features of the pterocarpan scaffold.[19,20] The absolute configuration of the five pterocarpans was confirmed as 6a*R*,11a*R* by ECD spectra (Figure 3B) and specific rotation values.[19] Compounds **3** and **14** were identified as (−)-(6a*R*,11a*R*)-maackiain[21] and (−)-(6a*R*,11a*R*)-isoneorautenol,[22,23] by comparison with published NMR spectroscopic data (S6, Supporting Information).

Compound **2** had a molecular formula of $C_{20}H_{22}O_5$ based on HRESIMS (*m*/*z* 365.1324 [M + Na]$^+$) and ^{13}C NMR data. A set of ^{1}H NMR aliphatic resonances at δ_H 4.20 (dd, *J* = 10.9 and 5.0 Hz), δ_H 3.57 (dd, *J* = 10.7 and 10.7 Hz), δ_H 3.45 (ddd, *J* = 10.5, 7.0, and 5.0 Hz), and δ_H 5.40 (d, *J* = 7.0 Hz) was assigned to protons of the heterocyclic B and C rings (Table 2).[19,20] The coupling constant between H-6a and H-11a (7.0 Hz) indicated a *cis*-junction of the fused B/C ring system. Likewise, the ^{13}C NMR shifts of C-6, C-6a, and C-11a of **2** (Table 2) were in agreement with values reported for the *cis*-pterocarpan scaffold.[20] With the aid of COSY, HMBC (H-1/C-11a), and NOESY (H-1/H11a) correlations the three aromatic protons at δ_H 7.31 (d, *J* = 8.5 Hz), δ_H 6.54 (dd, *J* = 8.5 and 2.5 Hz), and δ_H 6.36 (d, *J* = 2.5 Hz) were assigned to the A-ring

Table 1. ^{1}H and ^{13}C NMR Spectroscopic Data for Compound 9 (Methanol-d_4, 500 MHz for ^{1}H and 125 MHz for ^{13}C NMR, δ in ppm)

position	δ_H (*J* in Hz)	δ_C, type
2	4.93 (d, 11.9)	85.6, CH
3	4.46 (d, 11.9)	74.8, CH
4		195.4, C
4a		113.5, C
5	7.49 (s)	126.2, CH
6		117.5, C
7		161.1, C
8		115.7, C
8a		161.9, C
1′		130.0, C
2′	7.37 (d, 8.4)	130.5, CH
3′	6.83 (d, 8.4)	116.2, CH
4′	-	159.2, C
5′	6.83 (d, 8.4)	116.2, CH
6′	7.37 (d, 8.4)	130.5, CH
R_1 at C-6		
α	2.67 (m)	25.9, CH_2
β	1.73 (m)	44.6, CH_2
γ		71.6, C
δ	1.26 (s)	29.43, CH_3[a]
ε	1.26 (s)	29.41, CH_3[a]
R_2 at C-8		
α'	3.28 (m)	23.3, CH_2
β'	5.13 (tsp, 7.3, 1.3)	123.2, CH
γ'		132.7, C
δ'	1.61 (s)	26.1, CH_3
ε'	1.52 (s)	18.1, CH_3

[a]Interchangeable within the same column.

spin system. ^{1}H and ^{13}C NMR data indicated the presence of two hydroxy groups, which were located at C-3 (δ_C 160.1) and C-9 (δ_C 157.1) through HMBC correlations (H-1, H-2, H-4/C-3; H-7, H-10, H-α/C-9) and comparison of ^{13}C NMR data for other 3,9-dihydroxy-*cis*-pterocarpans such as erylysin C.[24] A 3-hydroxy-3-methylbutyl group was indicated by the aliphatic resonances at δ_H 1.24 (6H, s), δ_H 2.64 (2H, m), and δ_H 1.70

Table 2. ^{1}H and ^{13}C NMR Spectroscopic Data for Compounds 2, 7, and 8 (Methanol-d_4, 500 MHz for ^{1}H and 125 MHz for ^{13}C NMR, δ in ppm)

	2		7		8	
position	δ_H (J in Hz)	δ_C, type	δ_H (J in Hz)	δ_C, type	δ_H (J in Hz)	δ_C, type
1	7.31 (d, 8.5)	133.4, CH	7.28 (d, 8.3)	133.5, CH	6.87 (d, 8.4)	124.7, CH
1a		113.3, C		113.0, C		114.2, C
2	6.54 (dd, 8.5, 2.5)	110.9, CH	6.51 (dd, 8.3, 2.3)	111.0, CH	6.59 (d, 8.4)	110.6, CH
3		160.1, C		160.5, C		147.2, C
4	6.36 (d, 2.5)	104.3, CH	6.33 (d, 2.1)	104.4, CH		134.5, C
4a		158.1, C		158.3, C		145.9, C
6	4.20 (dd, 10.9, 5.0)	68.0, CH_2	4.23 (dd, 10.0, 4.0)	67.7, CH_2	4.33 (dd, 10.8, 4.8)	68.2, CH_2
	3.57 (dd, 10.7, 10.7)		3.58 (dd, 10.0, 10.0)		3.64 (dd, 10.6, 10.6)	
6a	3.45 (ddd, 10.5, 7.0, 5.0)	41.4, CH	3.60 (ddd, 10.0, 6.0, 4.0)	41.3, CH	3.50 (m)	41.3, CH
7a		119.4, C		125.8, C		119.1, C
7	7.01 (s)	126.6, CH	7.42 (s)	117.9, CH	7.01 (s)	126.3, CH
8		124.5, C		122.9, C		121.9, C
9		157.1, C		157.4, C		157.0, C
10	6.33 (s)	98.5, CH	6.87 (s)	94.6, CH	6.35 (s)	98.6, CH
10a		159.8, C		159.2, C		159.9, C
11a	5.40 (d, 7.0)	80.0, CH	5.49 (d, 6.0)	80.5, CH	5.46 (d, 7.0)	80.1, CH
α	2.64 (m)	26.1, CH_2			3.26 (d, 7.1)	29.1, CH_2
β	1.70 (dd, 9.6, 7.3)	45.5 CH_2			5.35 (tsp 7.3, 1.3)	122.3, CH
γ		71.8, C				132.5, C
δ	1.24 (s)	29.1, CH_3[a]			1.76 (s)	26.1, CH_3
ε	1.24 (s)	29.2, CH_3[a]			1.77 (s)	18.1, CH_3
O-CH_2-O						
1′			7.56 (d, 2.3)	145.6, CH		
2′			6.70 (d, 2.1)	107.8, CH		

[a]Interchangeable within the same column.

(2H, dd, J = 9.6 and 7.3 Hz) and was attached at C-8 (δ_C 124.5) based on HMBC (H-α/C-7, C-8, and C-9; H-β/C-8) and NOESY (H-7/H-β) correlations. Thus, the structure of compound **2** was established as (−)-(6a*R*,11a*R*)-3,9-dihydroxy-8-(3-hydroxy-3-methylbutyl)pterocarpan.

Compound **7** had a molecular formula of $C_{17}H_{12}O_4$ based on its HRESIMS (m/z 303. 1141 $[M + Na]^+$) and ^{13}C NMR data. Its NMR data (Table 2) were similar to those of compound **3**, the only difference being the substituents at C-8 and C-9. An AX system (δ_H 7.56, CH, d, J = 2.3 Hz; δ_H 6.70, CH, d, J = 2.1 Hz) indicated the presence of a furan ring fused at C-8 and C-9. The structure of **7** was thus established as (−)-(6a*R*,11a*R*)-3-hydroxyfuro[3′,2′:8,9]pterocarpan.

For compound **8**, a molecular formula of $C_{20}H_{20}O_5$ was deduced from HRESITOFMS (m/z 363.1187 $[M + Na]^+$) and ^{13}C NMR data. The UV spectrum was similar to that of **2** (λ_{max} 290 nm), and analysis of the ^{1}H NMR data (Table 2) revealed that compounds **2** and **8** were closely related. An upfield shift of H-1 in **8** (δ_H 6.87, d, J = 8.4 Hz) was attributed to the positive mesomeric effect induced by a second hydroxy moiety located at C-4. The substitution pattern was corroborated by diagnostic changes in the ^{13}C NMR chemical shifts (Table 2) of C-1 (δ_C 124.7 in **8**; 133.4 in **2**), C-3 (δ_C 147.2 in **8**; 160.1 in **2**), C-4 (δ_C 134.5 in **8**; 104.3 in **2**), and C-4a (δ_C 145.9 in **8**; 158.1 in **2**). An isoprenyl residue (δ_H 3.26, 2H, d, J = 7.1 Hz; 5.35, 1H, tsp, J = 7.3 and 1.3 Hz; 1.76, 3H, s; 1.77, 3H, s) was attached at C-8 (δ_C 121.9) based on HMBC correlations (H-α/C-7, C-8, and C-9; H-β/C-8). Compound **8** was thus characterized as (−)-(6a*R*,11a*R*)-3,4,9-trihydroxy-8-(3-methylbut-2-en-1-yl)-pterocarpan.

Compound **4** had a molecular formula of $C_{16}H_{16}O_4$ based on HRESIMS (m/z 295.0941 $[M + Na]^+$) and ^{13}C NMR data, and the UV spectrum showed absorption maxima at 210, 284, and 319 nm. 1D and 2D NMR data (Table 3) displayed resonances attributable to a monosubstituted (δ_H 7.10−7.21, 5H, m) and a 1,2,4-trisubstituted aromatic ring, based on the ABX system at δ_H 6.32, d, J = 2.2 Hz; 6.36, dd, J = 8.7 and 2.2 Hz; and 7.78, d, J = 8.7 Hz. Two hydroxy functions were evidenced by two quaternary ^{13}C NMR resonances at δ_C 167.6 and 167.2. The remaining resonances in the ^{1}H and ^{13}C NMR spectra indicated the presence of a 2-methoxypropan-1-one moiety (δ_H 3.26, 3H, s; 3.00, 2H, m; 4.75, 1H, dd, J = 7.5 and 5.4 Hz; δ_C 40.3, 58.2, 85.2, and 204.2). HMBC correlations from H-3′ and H-6′ to the carbonyl carbon and from the CH_2-β to H-2/6 were indicative of a dihydrochalcone.[25,26] C-α (*R*) absolute configuration was determined by comparison of the specific rotation of **4** ($[\alpha]^{25}_D$ +47; c 0.1, MeOH) with reported values[26,27] and was confirmed by a positive Cotton effect (CE) around 300 nm in the ECD spectrum.[27] Thus, compound **4** was identified as (+)-(α*R*)-α-methoxy-2′,4′-dihydroxydihydrochalcone.

The molecular formula of compound **12** ($C_{16}H_{14}O_4$; m/z 293.0798 $[M + Na]^+$) differed from that of **4** by 2 mass units. ^{1}H and ^{13}C NMR spectra of compound **12** closely resembled those of **4** (Table 3), except for the absence of the aliphatic resonances. An additional olefinic proton resonance at δ_H 6.18 (1H, s) in **12** was assigned to H-β and permitted definition of the structure of **12** as α-methoxy-2′,4′-dihydroxychalcone.

Compound **6** had a molecular formula of $C_{20}H_{20}O_5$ based on the HRESIMS (m/z 363.1311 $[M + Na]^+$) and ^{13}C NMR data. The NMR spectroscopic data showed strong similarities to those of 5-deoxykievitone (**10**),[28] which indicated an isoflavanone scaffold. This was confirmed by the ^{1}H NMR resonances for H-2a (δ_H 4.39, dd, J = 11.0 and 5.4 Hz), H-2b

Table 3. ^{1}H and ^{13}C NMR Spectroscopic Data for Compounds 4 and 12 (Methanol-d_4, 500 MHz for ^{1}H and 125 MHz for ^{13}C NMR, δ in ppm)

	4		12	
position	δ_H (J in Hz)	δ_C, type	δ_C, type	δ_H (J in Hz)
1		138.5, C	135.5, C	
2	7.10−7.21 (m)	130.5, CH	131.0, CH	7.76 (dd, 7.3, 1.2)
3	7.10−7.21 (m)	129.4, CH	129.6, CH	7.37 (dd, 7.5, 7.3)
4	7.10−7.21 (m)	127.7, CH	129.4, CH	7.30 (tt, 7.3, 1.3)
5	7.10−7.21 (m)	129.4, CH	129.6, CH	7.37 (dd, 7.5, 7.3)
6	7.10−7.21 (m)	130.5, CH	131.0, CH	7.76 (dd, 7.3, 1.2)
α	4.75 (dd, 7.5, 5.4)	85.2, CH	154.2, C	
β	3.00 (m)	40.3, CH_2	120.4. CH	6.18 (s)
C═O		204.2, C	195.8, C	
1′		113.0, C	113.7, C	
2′		167.6, C	168.3, C	
3′	6.32 (d, 2.2)	104.0, CH	104.2, CH	6.33 (d, 1.5)
4′		167.2, C	167.5, C	
5′	6.36 (dd, 8.7, 2.2)	109.9, CH	110.0, CH	6.37 (dd, 8.6, 1.5)
6′	7.78 (d, 8.7)	133.6, CH	135.8, CH	7.84 (d, 8.6)
β-OCH_3	3.26 (s)	58.2, CH_3	58.7, CH_3	3.66 (s)

(δ_H 4.54, dd, J = 10.9 and 10.9 Hz), and H-3 (δ_H 4.09, dd, J = 11.0 and 5.4 Hz), typical for ring C of isoflavanones (Table 4).[29] The presence of a 3-methylbut-2-en-1-yl (isoprenyl) group in **6** at C-6 (δ_C 125.0) was established via the HMBC correlation between H-α (δ_H 3.23, d, J = 7.3 Hz) and C-5 and C-7 (δ_C 129.1 and 164.4, respectively). Compound **6** was therefore identified as 7,2′,4′-trihydroxy-6-(3-methylbut-2-en-1-yl)isoflavanone. The ECD spectra of compounds **6** and **10** were devoid of CEs in the 200−450 nm region. This is reminiscent of racemates, since it is known that racemization occurs in isoflavanones even under mild conditions.[19] The absolute configuration of 5-deoxykievitone (**10**) and structurally similar isoflavanones has not been established. However, the absolute configuration of other prenylated isoflavanones has been determined by ECD.[30]

Table 4. ^{1}H and ^{13}C NMR Spectroscopic Data for Compounds 6 and 11 (Methanol-d_4, 500 MHz for ^{1}H and 125 MHz for ^{13}C NMR, δ in ppm)

	6		11	
position	δ_H (J in Hz)	δ_C, type	δ_C, type	δ_H (J in Hz)
2	4.39 (dd, 11.0, 5.4) 4.54 (dd, 10.9, 10.9)	72.2, CH_2	156.9, CH	8.17 (s)
3	4.09 (dd, 11.0, 5.4)	48.8, CH	123.9, C	
4		195.2, C	179.9, C	
4a		115.3, C	118.0, C	
5	7.60 (s)	129.1, CH	125.7, CH	7.92 (d, 8.8)
6		125.0, C	116.0, CH	6.96 (d, 8.8)
7		164.4, C	162.3,C	
8	6.35 (s)	103.0, CH	117.0, C	
8a		164.2, C	157.7, C	
1′		114.7, C	112.4, C	
2′		157.8, C	158.2, C	
3′	6.36 (d, 2.3)	103.8, CH	105.0, CH	6.42 (d, 2.2)
4′		159.0, C	160.4, C	
5′	6.26 (dd, 8.3, 2.3)	107.9, CH	108.7, CH	6.38 (d, 8.2, 2.2)
6′	6.81 (d, 8.3)	131.8, CH	133.2, CH	7.05 (d, 8.2)
α	3.23 (d, 7.3)	28.5, CH_2	23.0, CH_2	3.55 (d, 7.0)
β	5.29 (tsp, 7.3, 1.3)	123.4, CH	123.0, CH	5.25 (tsp, 7.3, 1,3)
γ		133.6, C	133.4, C	
δ	1.72 (s)	25.9, CH_3	26.3, CH_3	1.68 (s)
ε	1.68 (s)	17.8, CH_3	18.2, CH_3	1.82 (s)

Compound **11** had a molecular formula of $C_{20}H_{18}O_5$ based on its HRESIMS (m/z 361.1067 $[M + Na]^+$) and ^{13}C NMR data. Its UV and NMR data (Table 4) were similar to those of 8-prenyldaidzein (**13**)[31] (S7, Supporting Information). Differences in the NMR data of **11** and **13** were observed for resonances attributable to ring B. The ^{1}H NMR spectrum of **11** displayed an ABX system due to a hydroxy group attached to C-2′. The assignment was supported by the HMBC correlation of H-3′/C-2′, C-4′ and ^{13}C NMR data (Table 4). The structure of compound **11** was thus established as 2′,4′,7-trihydroxy-8-(3-methylbut-2-en-1-yl)isoflavone.

Modulation of $GABA_A$ Receptors. Compounds **1**−**15** were tested at an initial concentration of 100 μM in the *Xenopus* oocyte assay (Figure 4A, Table 5). In $\alpha_1\beta_2\gamma_{2s}$ receptors, isoflavone **11** enhanced I_{GABA} by 560.34 ± 387.06%, while 8-prenyldaidzein (**13**), differing only by the substituent at C-2′, modulated I_{GABA} to a lower extent (192.35 ± 47.30%). Pterocarpans **2** and **8** enhanced I_{GABA} by 488.57 ± 268.62% and 453.87 ± 141.03%, respectively, while **3** and **7** exhibited lower efficiency. This suggested that an additional five-membered ring attached to C-8 and C-9 had a negative influence in the $GABA_AR$ modulatory activity of pterocarpans. In contrast, a six-membered ring fused at the same position as in isoneorautenol (**14**) (I_{GABA} potentiation by 388.50 ± 47.30%) did not negatively affect activity. Among dihydroflavonols, lespecyrtin A_1 (**5**) and lespeflorin B_2 (**15**) significantly enhanced I_{GABA} (272.42 ± 132.19% and 287.35 ± 60.59%, respectively), whereas **1** was essentially inactive. In the case of chalcone derivatives **4** and **12**, which potentiated I_{GABA} by 88.82 ± 28.94% and 227.81 ± 48.14%, respectively, increased conformational flexibility appeared to have a negative effect on potency.

Concentration−response curves were recorded for compounds **2**, **8**, **11**, and **14**, which potentiated I_{GABA} by more than 380% at the initial concentration of 100 μM (Figure 4B). Isoflavone **11** displayed the highest potency (EC_{50} of 2.84 ± 1.37 μM), followed by pterocarpans **2** (8.60 ± 1.64 μM) and **8** (18.83 ± 2.34 μM). Isoneorautenol (**14**) displayed a much lower potency (EC_{50} of 40.74 ± 4.08 μM), although it showed the highest efficiency (E_{max}), enhancing I_{GABA} by 771.09 ± 57.94% (Table 6).

No direct receptor activation was observed at concentrations lower than 100 μM (Figure 4C−F). This suggested allosteric modulation rather than direct agonistic activity on the receptors. A strong decrease in I_{GABA} enhancement was observed with pterocarpans **2**, **8**, and **14** at 300 μM (Figure 4B, C, D, and F). This reduced modulation at high concentrations suggests that the mechanism of action of pterocarpans may combine modulation of $GABA_ARs$ and low-affinity open channel block, as in the case of valerenic acid, a $\beta_{2/3}$ subunit-specific modulator of the receptor.[32] In the case of

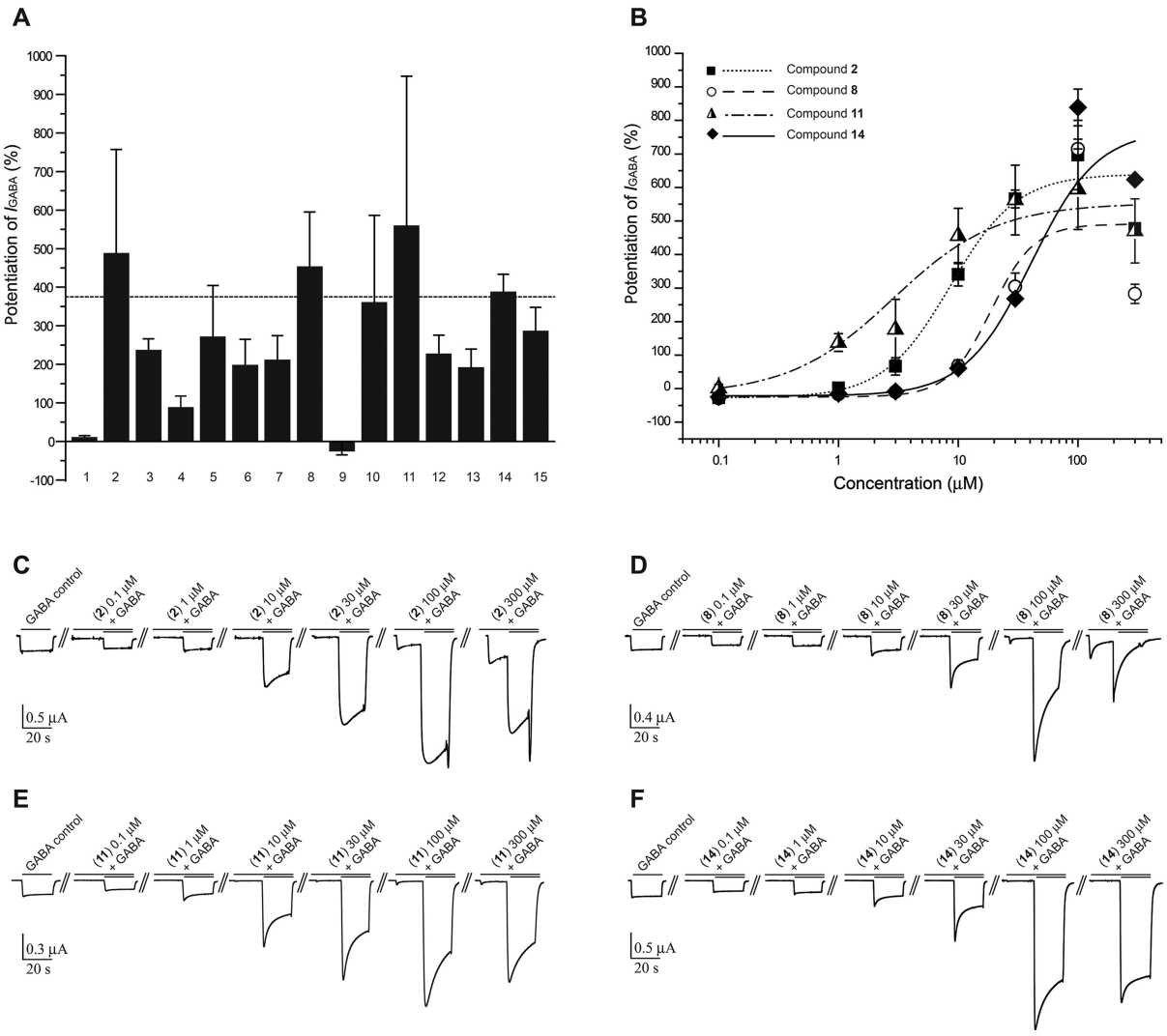

Figure 4. (A) Potentiation of I_{GABA} by compounds **1**–**15** (100 μM). Data obtained from three oocytes (two different batches). (B) Concentration–response curves for compounds **2**, **8**, **11**, and **14** recorded with $GABA_A$ receptors of the subunit composition $\alpha_1\beta_2\gamma_{2s}$. Data points represent means ± SE from four oocytes (three different batches). (C–F) Typical traces for modulation of I_{GABA} by compounds **2**, **8**, **11**, and **14**, respectively. The flat segments in the currents indicate the absence of direct activation of the receptors. All experiments in **A**–**F** were carried out using a GABA EC_{5-10}.

isoflavone **11**, potentiation of I_{GABA} did not drop significantly at high test concentrations, in agreement with the simple modulation mechanism recently proposed for isoflavones acting at this biological target.[8]

We compared the potency and efficiency of **2**, **8**, **11**, and **14** to other natural products identified as $GABA_A$ receptor modulators[33−36] (Figure 5). Compounds **11** and **2** exhibited remarkably higher potency, with EC_{50} values below 10 μM, indicating higher binding affinity toward the receptor. The efficiencies of the compounds on $\alpha_1\beta_2\gamma_{2s}$ $GABA_A$Rs were higher than that of BDZs such as triazolam, clotiazepam, and midazolam.[37]

Pterocarpans are the second largest subclass of isoflavonoids after isoflavones. They are known as phytoalexins, and a range of other biological activities,[20,38,39] but no GABAergic properties, have been reported for these compounds. Compounds **2**, **8**, and **14** thus represent a new scaffold for $GABA_A$ receptor modulators. In vivo studies show that certain flavonoids are absorbed after oral administration, cross the blood–brain barrier (BBB), and bind to $GABA_A$ receptors, resulting in sedation, anxiolytic, or anticonvulsant effects.[40,41] Being biosynthetically and structurally related, a similar behavior could be expected from pterocarpans. Their physicochemical properties are favorable for a possible BBB permeation (Table 6) (cLogP ≤ 5, MW ≤ 450, and topological polar surface area (tPSA) ≤ 90 Å^2).[42,43] Hence, they expand the spectrum of known $GABA_A$ receptor modulators among flavonoids beyond flavones and isoflavones.[8,44] Behavioral studies in rodents are needed to evaluate the in vivo activity of these pterocarpans.

Using an HPLC-based activity profiling approach, we identified 15 dihydroflavonols, isoflavones, isoflavanones, chalcones, and pterocarpans from a lipophilic extract of *A. cincinnatus*. Among these were eight new natural products (**2**, **4**, **6**, **7**, **8**, **9**, **11**, and **12**); known compounds **1**, **3**, **5**, **10**, **13**, and

Table 5. Potentiation of I_{GABA} in $\alpha_1\beta_2\gamma_{2s}$ Receptors by Compounds 1−15, at a Test Concentration of 100 μM

compound	max. potentiation of I_{GABA} (%)[a]
1	11.73 ± 2.97
2	488.57 ± 268.62
3	237.75 ± 28.56
4	88.82 ± 28.94
5	272.42 ± 132.19
6	198.60 ± 66.39
7	212.56 ± 61.40
8	453.87 ± 141.03
9	−26.01 ± 9.03
10	361.45 ± 224.48
11	560.34 ± 387.06
12	227.81 ± 48.14
13	192.35 ± 47.30
14	388.50 ± 47.30
15	287.35 ± 60.59

[a]Modulation measured in three oocytes from two different batches.

14 have not been previously isolated from *A. cincinnatus*. We identified pterocarpans as a new scaffold for $GABA_A$ receptor modulators. Further pharmacological studies on subunit specificity, binding properties, and in vivo activity are needed to further explore the potential of this scaffold.

EXPERIMENTAL SECTION

General Experimental Procedures. Optical rotations were measured with a Perkin-Elmer 341 polarimeter using a 10 cm microcell and MeOH (1 mg/mL) as solvent. UV and ECD spectra were recorded in MeOH (120 μg/mL) on a Chirascan CD spectrometer and analyzed with Pro-Data V2.4 software. NMR spectra were recorded on a Bruker Avance III spectrometer operating at 500.13 for ^{1}H and 125.77 MHz for ^{13}C. ^{1}H NMR, COSY, HSQC, HMBC, and NOESY spectra were measured at 18 °C in a 1 mm TXI probe with a *z*-gradient, using standard Bruker pulse sequences. ^{13}C NMR/DEPT spectra were recorded at 23 °C in a 5 mm BBO probe with a *z*-gradient. Spectra were analyzed by Bruker TopSpin 3.0 software. ESITOFMS spectra were recorded in positive mode on a Bruker microTOF ESIMS system. Nitrogen was used as a nebulizing gas at a pressure of 2.0 bar and as drying gas at a flow rate of 9.0 L/min (dry gas temperature 240 °C). Capillary voltage was set at 45 000 V, and hexapole at 230.0 Vpp. Instrument calibration was done with a reference solution of 0.1% sodium formate in 2-propanol/water (1:1) containing 5 mM NaOH.

HPLC-PDA-ESIMS spectra were obtained in positive mode on a Bruker Daltonics Esquire 3000 Plus ion trap MS system, connected via T-splitter (1:10) to an Agilent HP 1100 system consisting of a degasser, binary mixing pump, autosampler, column oven, and diode array detector (G1315B). Data acquisition and processing was performed with Bruker Daltonics Hystar 3.0 software. Semipreparative HPLC separations were carried out with an Agilent HP 1100 series system consisting of a quaternary pump, autosampler, column oven, and diode array detector (G1315B). Preparative HPLC separations were performed on a Shimadzu LC-8A preparative HPLC system with an SPD-M10A VP diode array detector. Waters SunFire C18 (3.5 μm, 3.0 × 150 mm i.d.), SunFire Prep C18 (5 μm, 10 × 150 mm i.d.), and SunFire Prep C18 OBD (5 μM, 30 × 150 mm i.d.) columns were used for analytical, semipreparative, and preparative separations, respectively. HPLC-grade MeOH (Scharlau Chemie S.A.) and water were used for HPLC separations. HPLC solvents contained 0.1% of HCO_2H for analytical and semipreparative separations. NMR spectra were recorded in methanol-d_4 (Armar Chemicals). Technical grade solvents purified by distillation were used for extraction and open column chromatography. Silica gel (63−200 μm, Merck) was used for open column chromatography.

Plant Material. Dried roots and tubers of *A. cincinnatus* were collected in 2005 in Beni Tajjite, Morocco, by Thomas Friedrich. The identity of the plant material was confirmed at the Division of Pharmaceutical Biology, University of Basel, where a voucher specimen (092) is deposited.

Extraction. The plant material was frozen with liquid N_2 and ground with a ZM1 ultracentrifugal mill (Retsch). The DCM extract for screening and HPLC-based activity profiling was prepared with an ASE 200 extraction system with solvent module (Dionex Sunnyvale, CA, USA). In total, three extraction cycles (5 min each) were performed, at a pressure of 120 bar and a temperature of 70 °C. For preparative isolation, 304 g of ground plant material was macerated with DCM (4 × 1 L, 3 h each, permanent magnetic stirring). The solvent was evaporated at reduced pressure to yield 8.5 g of extract. The extracts were stored at 2−8 °C until use.

Microfractionation for Activity Profiling. Time-based microfractionation of the extract for $GABA_A$ receptor activity profiling was performed as previously described,[14] with minor modifications: separation was done on a semipreparative HPLC column with MeOH (solvent A) and H_2O (solvent B), using a gradient from 50% A to 100% A in 30 min, hold for 15 min. The flow rate was 4 mL/min, and 10 mg of extract (in 100 μL of DMSO) was injected. A total of 24 time-based microfractions of 90 s each were collected and evaporated in parallel. The dry films were redissolved in 1 mL of MeOH, and aliquots of 0.5 mL were dispensed in two vials, dried under N_2 gas, and submitted to bioassay.

Isolation. A portion of the extract (7 g) was separated by open column chromatography (6 × 69 cm, 700 g of silica gel), using a step gradient of *n*-hexane/EtOAc (100:0, 95:5, 90:10, 85:15, 80:20, 75:25, 70:30, 65:35, 60:40, 55:45, 50:50, 30:70, 0:100, 1 L each), and washing in the end with MeOH 100% (1.5 L). The flow rate was ca. 50 mL/min. The effluent was combined to 19 fractions (A−S) based on TLC patterns (detection at 254 nm and at daylight after staining with vanillin−sulfuric acid reagent). Fractions A−S were subjected to analytical HPLC-PDA-ESIMS with MeOH (solvent A) and H_2O (solvent B), using an optimized gradient of 50% A to 100% A in 50 min, hold for 10 min. The flow rate was 0.4 mL/min, and 50 μg of each fraction (in 5 μL of DMSO) was injected. Fractions G−M were found to contain the compounds of interest. Therefore, fractions G, I, and K−M were submitted to preparative HPLC using solvents A and B as eluents, with a flow rate of 20 mL/min. Stock solutions in THF (100 mg/mL) were prepared and repeatedly injected in portions of 300−400 μL. Fraction G (314 mg) was separated into 12 fractions (G1−G12), using a gradient of 50% A to 60% A in 30 min, followed

Table 6. Potency and Efficiency of Compounds 2, 8, 11, and 14 as Positive Modulators of $GABA_A$ Receptors of $\alpha_1\beta_2\gamma_{2s}$ Subunit Composition, Calculated log P, and Topological Polar Surface Area

compound	E_{max} (%)[a]	EC_{50} (μM)[a]	n_H[b]	ClogP[c]	tPSA (Å²)[c]
2	640.02 ± 53.56	8.6 ± 1.6	1.56 ± 0.22	2.58	79.15
8	490.97 ± 22.34	18.8 ± 2.3	2.42 ± 0.43	3.76	79.15
11	552.73 ± 84.07	2.8 ± 1.4	1.00 ± 0.46	3.07	86.99
14	771.09 ± 57.94	40.7 ± 4.08	1.57 ± 0.10	4.41	47.92

[a]Modulation measured in four oocytes from three different batches. [b]Hill coefficient. Indicates the slope of the concentration−response curve at the EC_{50} point. [c]ClogP and topological polar surface area (tPSA) calculated with ChemBioDraw Ultra 12.0 software (CambridgeSoft).

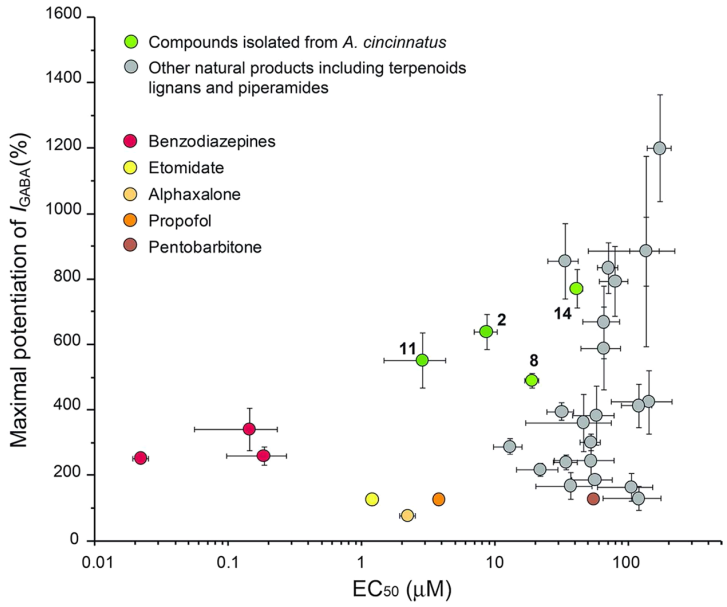

Figure 5. Overview of $GABA_A$ receptor modulatory efficiency and potency of selected plant-derived natural products, at the $\alpha_1\beta_2\gamma_{2s}$ $GABA_A$ receptor. Compounds in gray correspond to compounds previously isolated from *Piper nigrum* fruits,[33] *Acorus calamus* roots,[35] *Biota orientalis* leaves and twigs,[36] and *Kadsura longipedunculata* fruits.[34] Reference data of benzodiazepines (triazolam, midazolam, clotiazepam) are taken from Khom et al., 2006.[37] Etomidate and alphaxalone values were measured by Pau et al., 2003.[45] Pentobarbitone was investigated by Thompson et al., 1996,[46] using a GABA EC_{20}, meaning that its efficiency is underestimated compared to the rest. (Adapted from Zaugg, 2011.[47])

by 60% A to 100% A in 20 min, hold for 10 min. Fraction I (889 mg) was separated into 14 fractions (I1−I14), with a gradient of 50% A to 80% A and 80% A to 100% A in 50 and 5 min, respectively (hold for 10 min). Separation of fraction K (376 mg) yielded 14 fractions (K1−K14) with a gradient of 50% A to 70% A in 50 min, followed by 70% A to 100% A in 5 min, hold for 10 min. The same gradient was used for the separation of fractions L (185 mg) and M (270 mg), which were separated into 16 fractions each (L1−L16 and M1−M16, respectively). Owing to the complexity of the fractions, separation by preparative HPLC did not yield any pure compounds. Thus, preparative HPLC fractions selected on the basis of their LC-MS profiles were submitted to further purification by semipreparative HPLC, using solvents A and B as eluents. The flow rate was 4 mL/min. Stock solutions in DMSO (100 mg/mL) were prepared and repeatedly injected in portions of 40 to 70 μL. Fraction G1 (11 mg) was separated under isocratic conditions of 55% A for 25 min to yield 5.8 mg of (−)-6a*R*,11a*R*-maackiain (**3**). Separation of fraction G2 (32.4 mg) under the same conditions yielded compounds **4** (10 mg) and **7** (2.5 mg). Fractions G4 (4.4 mg) and G5 (4.9 mg) were separated with a gradient of 60% A to 75% A in 35 min to obtain compounds **12** (2.7 mg) and **14** (2.1), respectively. A gradient of 50% A to 80% A in 50 min was used to obtain compound **1** (3.2 mg) from fraction I1 (5.1 mg). Fraction I11 (28.6 mg) was separated with a gradient of 65% A to 80% A in 40 min, to yield 11.5 mg of lespeflorin B_2 (**15**). Compound **11** (2.3 mg) was obtained from separation of fraction K10 (5.6 mg) with a gradient of 65% A to 75% A in 40 min. Fractions L6 (3.2 mg) and L7 (12.7) were separated with a gradient of 60% A to 80% A in 40 min to obtain 1.4 mg of compound **5** and 6.5 mg of compound **6**, respectively. The same conditions were used for the separation of fractions M4 (17.8 mg), M8 (10.1 mg), M9 (6.2 mg), and M10 (5.3 mg), which yielded compounds **2** (9.5 mg), **8** (7.2 mg), **9** (2.7 mg), and **10** (3.4 mg), respectively. Separation of fraction L13 (12.8 mg) with a gradient of 65% A to 80% A in 40 min resulted in 7.9 mg of 8-prenyldaidzein (**13**). The purity of all compounds was >95% (purity check by ^{1}H NMR).

*(−)-(2R,3R)-7-Hydroxydihydroflavonol (**1**):* $[\alpha]^{25}_D$ −4 (*c* 0.1, MeOH); UV (MeOH) λ_{max} (log ε) 211 (4.43), 276 (4.04), 312 (3.88) nm; ECD (MeOH, $c = 4.9 \times 10^{-4}$ M, 1 cm path length) λ_{max} ($\Delta\varepsilon$) 217 (+18.47), 302 (−7.60), 331 (+4.13) nm; ^{1}H and ^{13}C NMR data, see S5 (Supporting Information); HRESIMS *m*/*z* 279.0626 [M + Na]$^+$ (calcd for $C_{15}H_{12}NaO_4$, 279.0628). NMR spectra of **1** are available as Supporting Information.

*(−)-(6aR,11aR)-3,9-Dihydroxy-8-(3-hydroxy-3-methylbutyl)-pterocarpan (**2**):* $[\alpha]^{25}_D$ −135 (*c* 0.1, MeOH); UV (MeOH) λ_{max} (log ε) 288 (3.78) nm; ECD (MeOH, $c = 3.6 \times 10^{-4}$ M, 1 cm path length) λ_{max} ($\Delta\varepsilon$) 236 (−12.04), 289 (+3.90) nm; ^{1}H and ^{13}C NMR data, see Table 2; HRESIMS *m*/*z* 365.1324 [M + Na]$^+$ (calcd for $C_{20}H_{22}NaO_5$, 365.1359). NMR spectra of **2** are available as Supporting Information.

*(+)-(αR)-α-Methoxy-2′,4′-dihydroxydihydrochalcone (**4**):* $[\alpha]^{25}_D$ +47 (*c* 0.1, MeOH); UV (MeOH); λ_{max} (log ε) 210 (4.23), 233 (sh) (3.82), 284 (4.03), 319 (3.84) nm; ECD (MeOH, $c = 9.2 \times 10^{-4}$ M, 1 cm path length) λ_{max} ($\Delta\varepsilon$) 283 (+1.91) nm; ^{1}H and ^{13}C NMR data, see Table 3; HRESIMS *m*/*z* 295.0941 [M + Na]$^+$ (calcd for $C_{16}H_{16}NaO_4$, 295.0941). NMR spectra of **4** are available as Supporting Information.

*7,2′,4′-Trihydroxy-6-(3-methylbut-2-en-1-yl)isoflavanone (**6**):* UV (MeOH) λ_{max} (log ε) 279 (4.10), 319 (3.80) nm; ^{1}H and ^{13}C NMR data, see Table 4; HRESIMS *m*/*z* 363.1311 [M + Na]$^+$ (calcd for $C_{20}H_{20}NaO_5$, 363.1203). NMR spectra of **6** are available as Supporting Information.

*(−)-(6aR,11aR)-3-Hydroxyfuro[3′,2′:8,9]pterocarpan (**7**):* $[\alpha]^{25}_D$ −211 (*c* 0.1, MeOH); UV (MeOH) λ_{max} (log ε) 206 (4.83), 245 (4.10), 253 (4.09), 295 (3.92) nm; ECD (MeOH, $c = 4.5 \times 10^{-4}$ M, 1 cm path length) λ_{max} ($\Delta\varepsilon$) 207 (−45.28), 229 (−18.19), 290 (+4.27) nm; ^{1}H and ^{13}C NMR data, see Table 2; HRESIMS *m*/*z* 303.1141 [M + Na]$^+$ (calcd for $C_{17}H_{12}NaO_4$, 303.1137). NMR spectra of **7** are available as Supporting Information.

*(−)-(6aR,11aR)-3,4,9-Trihydroxy-8-(3-methylbut-2-en-1-yl)-pterocarpan (**8**):* $[\alpha]^{25}_D$ −132 (*c* 0.1, MeOH); UV (MeOH) λ_{max} (log ε) 207 (4.67), 290 (3.71) nm; ECD (MeOH, $c = 3.7 \times 10^{-4}$ M, 1 cm path length) λ_{max} ($\Delta\varepsilon$) 204 (+14.32), 215 (−22.93), 237 (−11.14), 290 (+2.05) nm; ^{1}H and ^{13}C NMR data, see Table 2; HRESIMS *m*/*z* 363.1187 [M + Na]$^+$ (calcd for $C_{20}H_{20}NaO_5$, 363.1203). NMR spectra of **8** are available as Supporting Information.

dx.doi.org/10.1021/np500016z | *J. Nat. Prod.* 2014, 77, 640−649

*(−)-(2R,3R)-7,4′-Dihydroxy-6-(3-hydroxy-3-methylbutyl)-8-(3,3-dimethylallyl)dihydroflavonol (**9**):* $[\alpha]^{25}_{D}$ −2 (*c* 0.1, MeOH); UV (MeOH) λ_{max} (log ε) 224 (4.38), 284 (4.01), 323 (sh) (3.68) nm; ECD (MeOH, $c = 2.9 \times 10^{-4}$ M, 1 cm path length) λ_{max} ($\Delta\varepsilon$) 220 (+11.91), 238 (+4.54), 307 (−6.46), 339 (+4.48) nm; ^{1}H and ^{13}C NMR data, see Table 1; HRESIMS *m*/*z* 449.2087 $[M + Na]^+$ (calcd for $C_{25}H_{30}NaO_6$, 449.2087). NMR spectra of **9** are available as Supporting Information.

*7,2′,4′-Trihydroxy-8-(3-methylbut-2-en-1-yl)isoflavone (**11**):* UV (MeOH) λ_{max} (log ε) 251 (4.17), 291 (3.85) nm; ^{1}H and ^{13}C NMR data, see Table 4; HRESIMS *m*/*z* 361.1067 $[M + Na]^+$ (calcd for $C_{20}H_{18}NaO_5$, 361.1046). NMR spectra of **11** are available as Supporting Information.

*α-Methoxy-2′,4′-dihydroxychalcone (**12**):* UV (MeOH) λ_{max} (log ε) 244 (4.06), 297 (sh) (4.07), 347 (4.18) nm; ^{1}H and ^{13}C NMR data, see Table 3; HRESIMS *m*/*z* 293.0798 $[M + Na]^+$ (calcd for $C_{16}H_{14}NaO_4$, 293.0784). NMR spectra of **12** are available as Supporting Information.

Expression of $GABA_A$ Receptors. Stage V−VI oocytes from *Xenopus laevis* were prepared, and cRNA was injected as previously described.[14] Female *Xenopus laevis* (NASCO, Fort Atkinson, WI, USA) were anesthetized by exposing them for 15 min to a 0.2% MS-222 (methanesulfonate salt of 3-aminobenzoic acid ethyl, Sigma) solution before surgically removing parts of the ovaries. Follicle membranes from isolated oocytes were enzymatically digested with 2 mg/mL collagenase from *Clostridium histolyticum* (Type 1A, Sigma). Synthesis of capped runoff poly(A+) cRNA transcripts was obtained from linearized cDNA templates (pCMV vector). Directly after enzymatic isolation, the oocytes were injected with 50 nL of DEPC-treated water (Sigma) containing different cRNAs at a concentration of approximately 300−3000 pg/nL per subunit. The amount of injected cRNA mixture was determined by means of a NanoDrop ND-1000 (Kisker Biotech). To ensure expression of the gamma subunit in $\alpha_1\beta_2\gamma_{2s}$ receptors, rat cRNAs were mixed in a 1:1:10 ratio. Oocytes were then stored at 18 °C in ND96 solution containing 1% of penicillin−streptomycin solution (Sigma-Aldrich). Voltage clamp measurements were performed between days 1 and 5 after cRNA injection.

Positive Control. Diazepam (7-chloro-1,3-dihydro-1-methyl-5-phenyl-2*H*-1,4-benzodiazepin-2-one, Sigma, purity ≥98%) was used as positive control. At 1 μM, diazepam enhanced I_{GABA} up to 231.3 ± 22.6% (n = 3). See also S1, Supporting Information.

Two-Microelectrode Voltage Clamp Studies. Electrophysiological experiments were performed by the two-microelectrode voltage clamp method making use of a TURBO TEC 03X amplifier (npi Electronic GmbH) at a holding potential of −70 mV and pCLAMP 10 data acquisition software (Molecular Devices). Currents were low-pass-filtered at 1 kHz and sampled at 3 kHz. The bath solution contained 90 mM NaCl, 1 mM KCl, 1 mM $MgCl_2$, 1 mM $CaCl_2$, and 5 mM HEPES (pH 7.4). Electrode filling solution contained 2 M KCl.

Fast Solution Exchange during I_{GABA} Recordings. Test solutions (100 μL) were applied to the oocytes at a speed of 300 μL/s by means of the ScreeningTool automated fast perfusion system.[9] In order to determine GABA EC_{5-10} (typically between 3 and 10 μM for receptors of subunit composition $\alpha_1\beta_2\gamma_{2s}$), a dose−response experiment with GABA concentrations ranging from 0.1 μM to 1 mM was performed. Stock solution of the DCM extract (10 mg/mL in DMSO) was diluted to a concentration of 100 μg/mL with bath solution containing GABA EC_{5-10} according to a validated protocol.[14] As previously described, microfractions collected from the semi-preparative HPLC separations were dissolved in 30 μL of DMSO and subsequently mixed with 2.97 mL of bath solution containing GABA EC_{5-10}.[14] A stock solution of each pure compound tested (100 mM in DMSO) was diluted to concentrations of 0.1, 1.0, 3.0, 10, 30, 100, and 300 μM with bath solution for measuring direct activation or with bath solution containing GABA EC_{5-10} for measuring modulation of $GABA_A$ receptors. The final DMSO concentration in all the samples and the GABA control samples was adjusted to 1% to avoid solvent effect at the $GABA_A$ receptor.

Data Analysis. Enhancement of the I_{GABA} was defined as $I_{(GABA+Comp)}/I_{GABA} - 1$, where $I_{(GABA+Comp)}$ is the current response in the presence of a given compound, and I_{GABA} is the control GABA-induced chloride current. Data were analyzed using Origin 7.0 SR0 software (OriginLab Corporation) and are given as mean ± SE of at least two oocytes from ≥2 oocyte batches.

■ ASSOCIATED CONTENT

Ⓢ Supporting Information

Positive control (diazepam) currents used in the oocyte assay, detailed information of known compounds, ^{1}H and ^{13}C NMR data of known compounds **1**, **3**, **5**, **10**, **13**, **14**, and **15**, as well as ^{1}H and ^{13}C NMR spectra of new compounds **2**, **4**, **6**, **7**, **8**, **9**, **11**, and **12**. This material is available free of charge via the Internet at http://pubs.acs.org.

■ AUTHOR INFORMATION

Corresponding Author

*Tel: +41-61-2671425. Fax: +41-61-2671474. E-mail: matthias.hamburger@unibas.ch.

Notes

The authors declare no competing financial interest.

■ ACKNOWLEDGMENTS

ECD spectra were measured at the Biophysics Facility, Biozentrum, University of Basel. Financial support was provided by the Swiss National Science Foundation through project 205320_126888/1 (M.H.). D.C.R. thanks the Department of Education of Canton Basel (Erziehungsdepartement des Kantons Basel-Stadt) for a fellowship granted in 2012.

■ DEDICATION

Dedicated to Prof. Dr. Otto Sticher, of ETH-Zürich, Zürich, Switzerland, for his pioneering work in pharmacognosy and phytochemistry.

■ REFERENCES

(1) Olsen, R. W.; Sieghart, W. *Pharmacol. Rev.* **2008**, *60*, 243−60.
(2) Rudolph, U.; Knoflach, F. *Nat. Rev. Drug Discovery* **2011**, *10*, 685−697.
(3) D'Hulst, C.; Atack, J. R.; Kooy, R. F. *Drug Discovery Today* **2009**, *14*, 866−875.
(4) Tan, K. R.; Rudolph, U.; Lüscher, C. *Trends Neurosci.* **2011**, *34*, 188−197.
(5) Yang, X.; Baburin, I.; Plitzko, I.; Hering, S.; Hamburger, M. *Mol. Diversity* **2011**, *15*, 361−372.
(6) Karim, N.; Gavande, N.; Wellendorph, P.; Johnston, G. A. R.; Hanrahan, J. R.; Chebib, M. *Biochem. Pharmacol.* **2011**, *82*, 1971−1983.
(7) Johnston, G. A. R.; Hanrahan, J. R.; Chebib, M.; Duke, R. K.; Mewett, K. N. *Adv. Pharmacol.* **2006**, *54*, 285−316.
(8) Gavande, N.; Karim, N.; Johnston, G. A. R.; Hanrahan, J. R.; Chebib, M. *ChemMedChem* **2011**, *6*, 1340−1346.
(9) Baburin, I.; Beyl, S.; Hering, S. *Pflueg. Arch. Eur. J. Physiol.* **2006**, *453*, 117−123.
(10) (ILDIS) International Legume Database & Information service. Adenocarpus cincinnatus. http://www.ildis.org/LegumeWeb?version~10.01&LegumeWeb&tno~5579&genus~Adenocarpus&species~cincinnatus.
(11) Essokne, R. S.; Grayer, R. J.; Porter, E.; Kite, G. C.; Simmonds, M. S. J.; Jury, S. L. *Biochem. Syst. Ecol.* **2012**, *42*, 49−58.
(12) Greinwald, R.; Bachmann, P.; Witte, L.; Acebes-Grinoves, J. R.; Cyzgan, F.-C. *Biochem. Syst. Ecol.* **1992**, *20*, 69−73.
(13) Potterat, O.; Hamburger, M. *Nat. Prod. Rep.* **2013**, *30*, 546−64.
(14) Kim, H. J.; Baburin, I.; Khom, S.; Hering, S.; Hamburger, M. *Planta Med.* **2008**, *74*, 521−526.

(15) Malan, E.; Swinny, E. *Phytochemistry* **1990**, *29*, 3307−3309.
(16) Mori-Hongo, M.; Yamaguchi, H.; Warashina, T.; Miyase, T. *J. Nat. Prod.* **2009**, *72*, 63−71.
(17) Mori-Hongo, M.; Takimoto, H.; Katagiri, T.; Kimura, M.; Ikeda, Y.; Miyase, T. *J. Nat. Prod.* **2009**, *72*, 194−203.
(18) Gaffield, W. *Tetrahedron* **1970**, *26*, 4093−4108.
(19) Slade, D.; Ferreira, D.; Marais, J. P. *Phytochemistry* **2005**, *66*, 2177−2215.
(20) Goel, A.; Kumar, A.; Raghuvanshi, A. *Chem. Rev.* **2013**, *113*, 1614−1640.
(21) Tőkés, A. L.; Litkei, G.; Gulácsi, K.; Antus, S.; Baitz-Gács, E.; Szántay, C.; Darkó, L. *Tetrahedron* **1999**, *55*, 9283−9296.
(22) Mitscher, L. A.; Okwute, S. K.; Gollapudi, S. R.; Drake, S.; Avona, E. *Phytochemistry* **1988**, *27*, 3449−3452.
(23) Nkengfack, A. E.; Vardamides, J. C.; Fomum, Z. T.; Meyer, M. *Phytochemistry* **1995**, *40*, 1803−1808.
(24) Dao, T. T.; Nguyen, P. H.; Thuong, P. T.; Kang, K. W.; Na, M.; Ndinteh, D. T.; Mbafor, J. T.; Oh, W. K. *Phytochemistry* **2009**, *70*, 2053−2057.
(25) Li, W.; Koike, K.; Asada, Y.; Hirotani, M.; Rui, H.; Yoshikawa, T.; Nikaido, T. *Phytochemistry* **2002**, *60*, 351−355.
(26) Ferrari, F.; Botta, B.; Alves De Lima, R. *Phytochemistry* **1983**, *22*, 1663−1664.
(27) Augustys, J. A. N.; Bezuidenhoudt, B. C. B.; Swanepoel, A.; Ferreira, D. *Tetrahedron* **1990**, *46*, 4429−4442.
(28) Woodward, M. D. *Phytochemistry* **1979**, *18*, 2007−2010.
(29) O'Neill, M. J.; Adesanya, S. A.; Roberts, M. F.; Pantry, I. R. *Phytochemistry* **1986**, *25*, 1315−1322.
(30) Galeffi, C.; Rasoanaivo, P.; Federici, E.; Palazzino, G.; Nicoletti, M.; Rasolondratovo, B. *Phytochemistry* **1997**, *45*, 189−192.
(31) Hakamatsuka, T.; Ebizuka, Y.; Sankawa, U. *Phytochemistry* **1991**, *30*, 1481−1482.
(32) Khom, S.; Baburin, I.; Timin, E.; Hohaus, A.; Trauner, G.; Kopp, B.; Hering, S. *Neuropharmacology* **2007**, *53*, 178−187.
(33) Zaugg, J.; Baburin, I.; Strommer, B.; Kim, H. J.; Hering, S.; Hamburger, M. *J. Nat. Prod.* **2010**, *73*, 185−191.
(34) Zaugg, J.; Ebrahimi, S. N.; Smiesko, M.; Baburin, I.; Hering, S.; Hamburger, M. *Phytochemistry* **2011**, *72*, 2385−2395.
(35) Zaugg, J.; Eickmeier, E.; Ebrahimi, S. N.; Baburin, I.; Hering, S.; Hamburger, M. *J. Nat. Prod.* **2011**, *74*, 1437−1443.
(36) Zaugg, J.; Khom, S.; Eigenmann, D.; Baburin, I.; Hamburger, M.; Hering, S. *J. Nat. Prod.* **2011**, *74*, 1764−1772.
(37) Khom, S.; Baburin, I.; Timin, E. N.; Hohaus, A.; Sieghart, W.; Hering, S. *Mol. Pharmacol.* **2006**, *69*, 640−649.
(38) Veitch, N. C. *Nat. Prod. Rep.* **2007**, *24*, 417.
(39) Goel, A.; Kumar, A.; Hemberger, Y.; Raghuvanshi, A.; Jeet, R.; Tiwari, G.; Knauer, M.; Kureel, J.; Singh, A. K.; Gautam, A.; Trivedi, R.; Singh, D.; Bringmann, G. *Org. Biomol. Chem.* **2012**, *10*, 9583.
(40) Wasowski, C.; Marder, M. *J. Exp. Pharm.* **2012**, *4*, 9−24.
(41) Jäger, A.; Saaby, L. *Molecules* **2011**, *16*, 1471−1485.
(42) Clark, D. E. *Drug Discovery Today* **2003**, *8*, 927−933.
(43) Pajouhesh, H.; Lenz, G. R. *Neurorx* **2005**, *2*, 541−553.
(44) Hanrahan, J. R.; Chebib, M.; Johnston, G. A. R. *Br. J. Pharmacol.* **2011**, *163*, 234−245.
(45) Pau, D.; Belelli, D.; Callachan, H.; Peden, D. R.; Dunlop, J. I.; Peters, J. A.; Guitart, X.; Gutierrez, B.; Lambert, J. J. *Neuropharmacology* **2003**, *45*, 1029−1040.
(46) Thompson, S. A.; Whiting, P. J.; Wafford, K. A. *Br. J. Pharmacol.* **1996**, *117*, 521−527.
(47) Zaugg, J. Ph.D. Thesis, Universität Basel, Basel, 2011.

SUPPORTING INFORMATION

HPLC-based Activity Profiling for $GABA_A$ Receptor Modulators in *Adenocarpus cincinnatus*

Diana C. Rueda,[†] Maria De Mieri,[†] Steffen Hering,[‡] and Matthias Hamburger[*,†]

[†] Division of Pharmaceutical Biology, University of Basel, Klingelbergstrasse 50, 4056 Basel, Switzerland.

[‡] Department of Pharmacology and Toxicology, University of Vienna, Althanstrasse 14, 1090 Vienna, Austria.

* Corresponding author. Tel.: +41-61-2671425; fax: +41-61-2671474.

E-mail: matthias.hamburger@unibas.ch

S1. Diazepam (1 μM) enhances I_{GABA} through $\alpha_1\beta_2\gamma_{2S}$ $GABA_A$ receptors and was therefore used as positive control for the assay. Currents in the presence of GABA ($EC_{5\text{-}10}$, single bar, control) and during co-application of GABA and diazepam (1 µM, double bar) are shown. At 1 µM diazepam enhanced I_{GABA} up to 231.3 ± 22.6% (n=3).

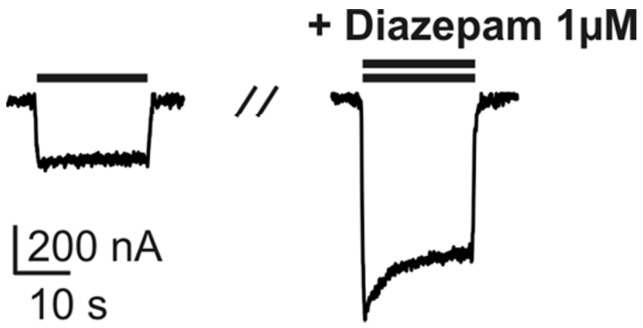

S2. Optimized analytical HPLC traces (210-700 nm) of open column fractions G, I, and K-M. The first trace at the top corresponds to the crude extract. The numbers above peaks designate compounds **1-15.** The active time window from the HPLC-based activity profile (time-based fractions 7-13) is indicated between dashed lines.

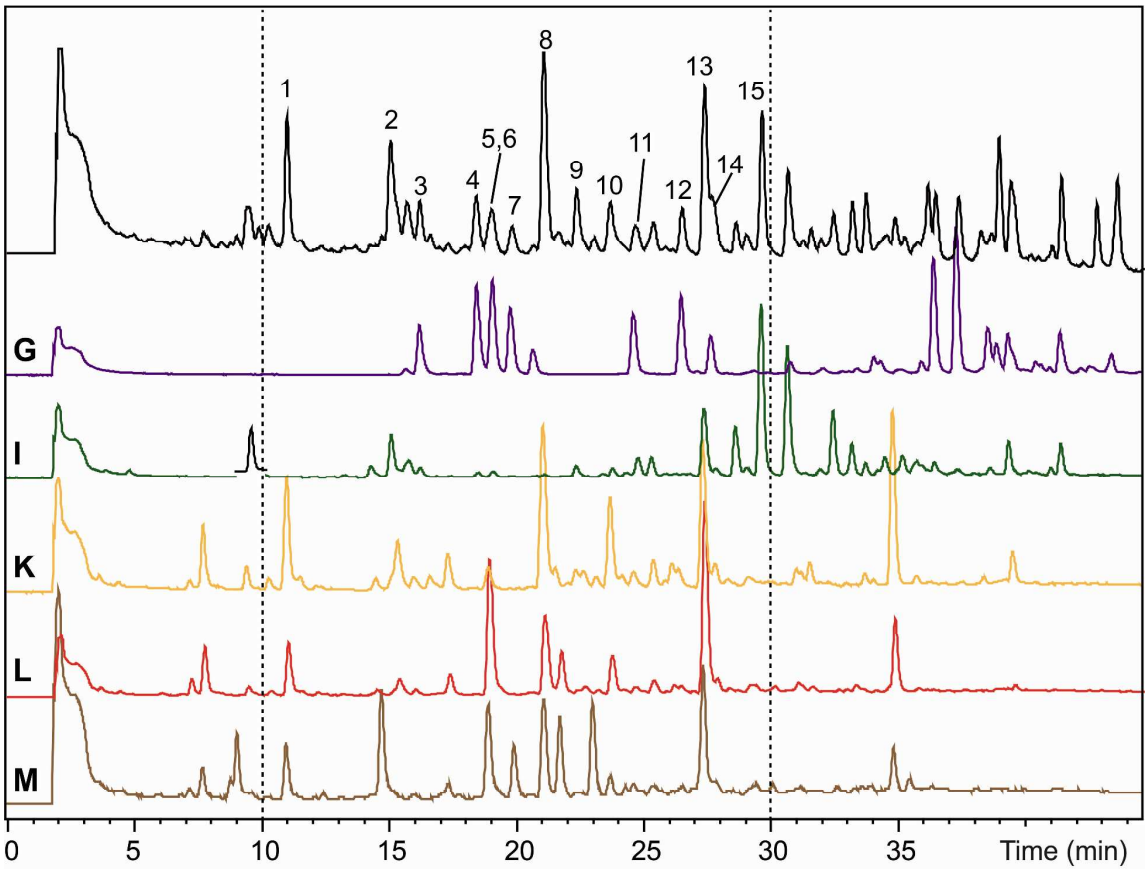

S3. Compounds isolated from *A. cincinnatus* roots and tubers, DCM extract.

	Trivial Name	CAS number	Sum formula	MW	Structure	Ref
1	---	34198-87-3	$C_{15}H_{12}O_4$	256	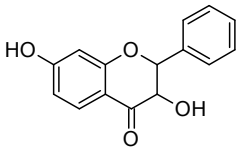	15
2	---	1177129-77-9	$C_{20}H_{22}O_5$	342	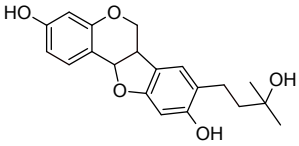	---
3	*6aR,11aR*-Maackiain	2035-15-6	$C_{16}H_{12}O_5$	284	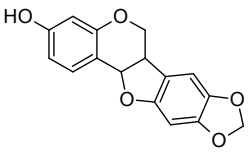	21
4	---	---	$C_{16}H_{16}O_4$	272	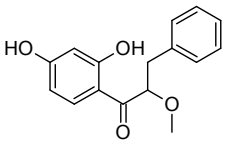	---
5	*2R,3R*-Lespecyrtin A1	1103683-88-0	$C_{20}H_{20}O_5$	340	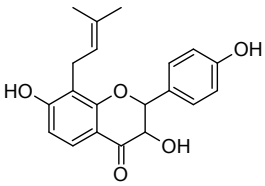	16

6	---	---	$C_{20}H_{20}O_5$	340	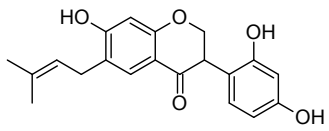	---
7	---	---	$C_{17}H_{12}O_4$	280	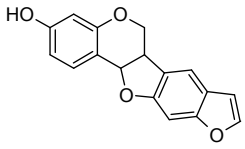	---
8	---	1177965-92-2	$C_{20}H_{20}O_5$	340	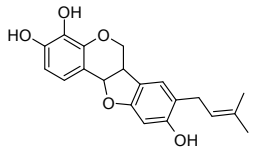	---
9	---	---	$C_{25}H_{30}O_6$	426	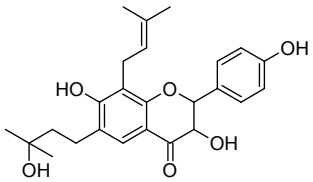	---
10	5-Deoxykievitone	74161-24-3	$C_{20}H_{20}O_5$	340	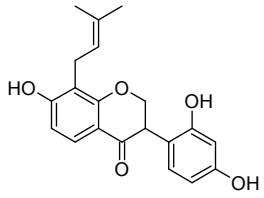	28

5

11	---	---	$C_{20}H_{18}O_5$	338	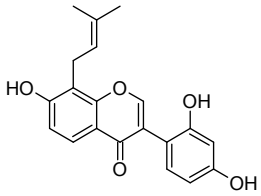	---
12	---	---	$C_{16}H_{14}O_4$	270	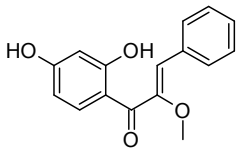	---
13	8-Prenyldaidzein	135384-00-8	$C_{20}H_{18}O_4$	322	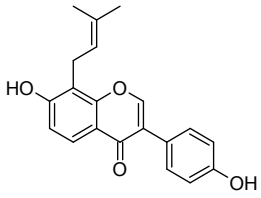	31
14	*6aR,11aR*-Isoneorautenol	98755-24-9	$C_{20}H_{18}O_4$	322	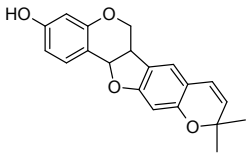	22, 23
15	*2R,3R*-Lespeflorin B2	1108717-54-9	$C_{25}H_{28}O_5$	408	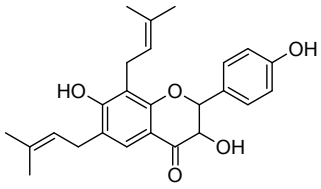	17

6

S4. Analytical data of known compounds **3**, **5**, **10**, **13**, **14**, and **15**.

*(–)-(6aR,11aR)-Maackiain (**3**):* $[\alpha]_D^{25}$ −196 (*c* 0.1, MeOH); UV (MeOH) λ_{max} (log ε) 203 (4.09), 311 (3.81) nm; ECD (MeOH, $c = 4.4 \times 10^{-4}$ M, 1 cm pathlength): λ_{max} ($\Delta\varepsilon$) 212 (–26.64), 239 (–9.59), 307 (+2.27) nm; HRESIMS *m/z* 307.0579 $[M+Na]^+$ (calcd for $C_{16}H_{12}NaO_5$, 307.0577).

*(–)-(2R,3R)-Lespecyrtin A1 (**5**)*: $[\alpha]_D^{25}$ −10 (*c* 0.0577, MeOH); UV (MeOH) λ_{max} (log ε) 219 (4.32), 284 (4.00) nm; ECD (MeOH, $c = 3.7 \times 10^{-4}$ M, 1 cm pathlength): λ_{max} ($\Delta\varepsilon$) 218 (+11.11), 238 (+4.13), 303 (–5.23), 333 (+3.00) nm; HRESIMS *m/z* 363.1294 $[M+Na]^+$ (calcd for $C_{20}H_{20}NaO_5$, 363.1203).

*5-Deoxykievitone (**10**)*: UV (MeOH) λ_{max} (log ε) 217 (4.37), 286 (4.07) nm; HRESIMS *m/z* 363.1266 $[M+Na]^+$ (calcd for $C_{20}H_{20}NaO_5$, 363.1203).

*8-Prenyldaidzein (**13**)*: UV (MeOH) λ_{max} (log ε) 253 (4.53), 306 (4.00) nm; HRESIMS *m/z* 345.1204 $[M+Na]^+$ (calcd for $C_{20}H_{18}NaO_4$, 345.1097).

*(–)-(6aR,11aR)-Isoneorautenol (**14**)*: $[\alpha]_D^{25}$ −139 (*c* 0.089, MeOH); UV (MeOH) λ_{max} (log ε) 220 (4.50), 286 (3.85), 313 (3.85) nm; ECD (MeOH, $c = 7.8 \times 10^{-4}$ M, 1 cm pathlength): λ_{max} ($\Delta\varepsilon$) 210 (–28.06), 315 (+1.46) nm; HRESIMS *m/z* 345.1138 $[M+Na]^+$ (calcd for $C_{20}H_{18}NaO_4$, 345.1097)

*(–)-(2R,3R)-Lespeflorin B2 (**15**)*: $[\alpha]_D^{25}$ –2 (*c* 0.1, MeOH); UV (MeOH) λ_{max} (log ε) 223 (4.44), 268 (4.23), 329 (sh) (3.68) nm; ECD (MeOH, *c* = 3.1 x 10^{-4} M, 1 cm pathlength): λ_{max} ($\Delta\varepsilon$) 221 (+10.48), 239 (+4.74), 309 (–6.23), 339 (+4.30) nm; HRESIMS *m/z* 431.1809 $[M+Na]^+$ (calcd for $C_{25}H_{28}NaO_5$, 431.1829)

8

S5. ^{1}H and ^{13}C NMR spectroscopic data for known pterocarpans **1**, **5** and **15** (CD_3OD, 500 MHz for ^{1}H, 125 MHz for ^{13}C, δ in ppm)

	1		**5**		**15**	
Position	δ_H (J in Hz)	δ_C, type	δ_H (J in Hz)	δ_C, type	δ_H (J in Hz)	δ_C, type
2	5.07 (d, 11.8)	85.8, CH	4.94 (d, 11.7)	83.9, CH	4.93 (d, 11.8)	83.8, CH
3	4.49 (d, 11.8)	74.8, CH	4.46 (d, 11.7)	73.1, CH	4.46 (d, 11.8)	73.2, CH
4	-	194.4, C	-	193.6, C	-	193.6, C
4a	-	113.5, C	-	112.4, C	-	112.8, C
5	7.72 (d, 8.6)	130.3, CH	7.56 (d, 8.6)	125.5, CH	7.41 (s)	124.3, CH
6	6.54 (dd, 8.6, 2.3)	112.4, CH	6.53 (d, 8.6)	110.0, CH	-	121.7, C
7	-	167.2, C	-	162.6, C	-	160.6, C
8	6.35 (d, 2.3)	103.9, CH	-	116.2, C	-	115.6, C
8a		165.1, C	-	161.4, C	-	159.1, C
1’	-	138.9, C	-	128.7, C	-	129.9, C
2’	7.53 (dd, 8.3, 1.6)	129.1, CH	7.36 (d, 8.0)	128.7, CH	7.38 (d, 8.4)	130.4, CH
3’	7.42-7.33 (m)*	129.5, CH	6.83 (d, 8.0)	114.7, CH	6.87 (d, 8.4)	114.4, CH
4’	7.42-7.33 (m)*	130.0, CH	-	157.2, C	-	157.0, C

5’	7.42-7.33 (m)*	129.5, CH	6.83 (d, 8.0)	114.7, CH	6.87 (d, 8.4)	114.4, CH
6’	7.53 (dd, 8.3, 1.6)	129.1, CH	7.36 (d, 8.0)	128.7, CH	7.38 (d, 8.4)	130.4, CH
R_1 at C-6						
α					3.26 (m)	29.0, CH_2
β					5. 32 (tsp, 7.0, 1.0)	122.8, CH
γ					-	134.4, C
δ					1.76 (s)	26.0, CH_3
ε					1.69 (s)	17.9, CH_3
R_2 at C-8						
α’			3.23 (m)	21.3, CH_2	3.29 (m)	23.0, CH_2
β’			5.14 (tsp, 7.3, 1.3)	121.7, CH	5.15 (tsp, 7.0, 1.0)	123.0, CH
γ’			-	131.2, C	-	132.6, C
δ’			1.58(s)	24.5, CH_3	1.62 (s)	26.0, CH_3
ε’			1.51 (s)	16.7, CH_3	1.54 (s)	18.1, CH_3

*: overlapped signals

S6. ^{1}H and ^{13}C NMR spectroscopic data for known pterocarpans **3** and **14** (CD_3OD, 500 MHz for ^{1}H, 125 MHz for ^{13}C, δ in ppm)

Position	**3**		**14**	
	δ_H (J in Hz)	δ_C, type	δ_C, type	δ_H (J in Hz)
1	7.24 (d, 8.5)	131.5, CH	133.4, CH	7.27 (d, 8.4)
1a	-	111.5, C	113.0, C	-
2	6.48 (dd, 8.5, 2.3)	109.2, CH	111.0, CH	6.49 (dd, 8,5, 2.5)
3	-	158.5, C	160.3, C	-
4	6.31 (d, 2.3)	102.8, CH	104.3, CH	6.32 (d, 2.5)
4a	-	156.5,C	158.2, C	-
6	4.17 (dd, 10.6, 4.8)	65.9, CH_2	67.8, CH_2	4.18 (dd, 10.6, 4.8)
	3.55 (dd, 10.7, 10.7)			3.53 (dd, 10.7, 10.7)
6a	3.42 (m)	40.1, CH	41.0, CH	3.45 (ddd, 10.5, 6.9, 4.8)
7a	-	118.4, C	121.2, C	-
7	6.74 (s)	104.8, CH	123.4, CH	6.89 (s)
8	-	141.7, C	116.4, C	-
9	-	148.2, C	156.0, C	-
10	6.34 (s)	92.9, CH	100.0, CH	6.19 (s)
10a	-	154.2, C	161.8, C	-
11a	5.40 (d, 7.1)	78.6, CH	80.3, CH	5.42 (d, 6.9)
α			123.4, CH	6.28 (d, 10.0)
β			128.6, CH	5.47 (d, 10.0)
γ			77.5, C	-
δ			28.2, CH_3	1.35* (s)
ε			28.2, CH_3	1.36* (s)
O-CH_2-O	5.83 (dd, 12.3, 1.0)	100.8, CH_2		

* = interchangeable within the same column

S7. ^{1}H and ^{13}C NMR spectroscopic data for known isoflavonoids **10** and **13** (CD_3OD, 500 MHz for ^{1}H, 125 MHz for ^{13}C, δ in ppm)

	10		**13**	
Position	δ_H (*J* in Hz)	δ_C, type	δ_C, type	δ_H (*J* in Hz)
2	4.50 (dd, *10.7*, *5.4*)	69.9, CH_2	154.8, CH	8.07 (s)
	4.62 (*10.7*)			
3	4.13 (dd, *10.7*, *5.4*)	47.0, CH	125.5, C	-
4	-	193.7, C	178.9, C	-
4a	-	112.1, C	118.4, C	-
5	7.66 (d, *8.7*)	125.4, CH	125.4, CH	7.87 (d, *8.7*)
6	6.56 (d, *8.9*)	109.3, CH	115.7, CH	6.91 (d, *8.7*)
7	-	162.0, C	161.7, C	-
8	-	115.3, C	117.1, C	-
8a	-	161.5, C	157.6, C	-
1′	-	113.3, C	124.5, C	-
2′	-	156.0, C	131.6, CH	7.34 (dd, *8.6*)
3′	6.38 (d, *2.0*)	102.5, CH	116.3, CH	6.83 (dd, *8.6*)
4′	-	157.0, C	158.8, C	-
5′	6.29 (dd, *8.5*, *2.5*)	106.4, CH	116.3, CH	6.83 (dd, *8.6*)
6′	6.86 (d, *8.5*)	130.2, CH	131.6, CH	7.34 (dd, *8.6*)
α	3.34 (d, *7.0*)	21.1, CH_2	23.1, CH_2	3.50 (d, *7.1*)
β	5.23 (tsp, *7.3*, *1.3*)	122.0, CH	122.9, CH	5.23 (tsp, *7.3*, *1.3*)
γ	-	130.8, C	133.2, C	-
δ	1.67 (s)	24.4, CH_3	26.1, CH_3	1.64 (s)
ε	1.75 (s)	16.6, CH_3	18.2, CH_3	1.79 (s)

S8. ^{1}H-NMR spectrum (500 MHz in CD_3OD) of compound **2**

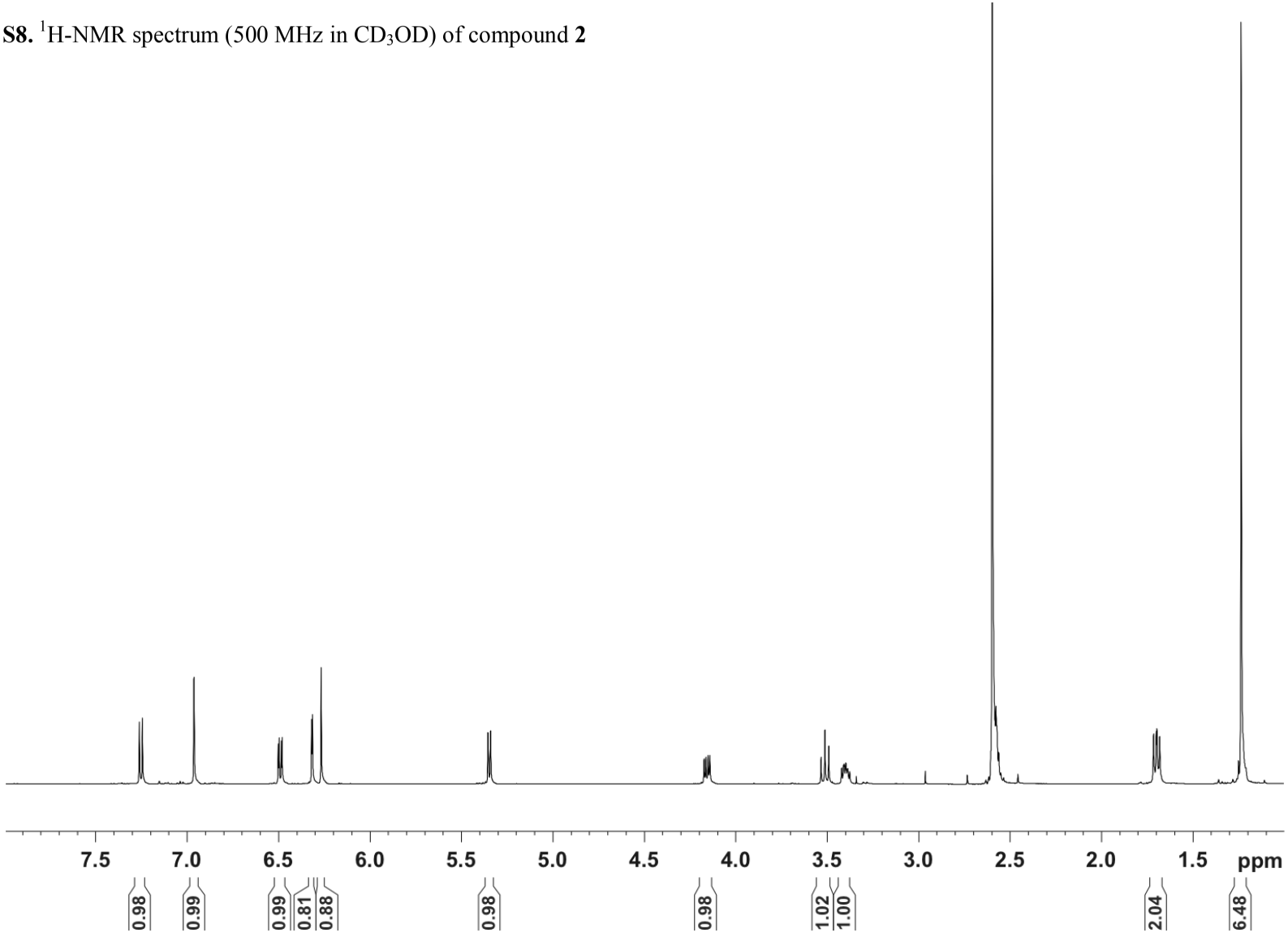

S9. DEPT spectrum (125 MHz in CD_3OD) of compound **2**

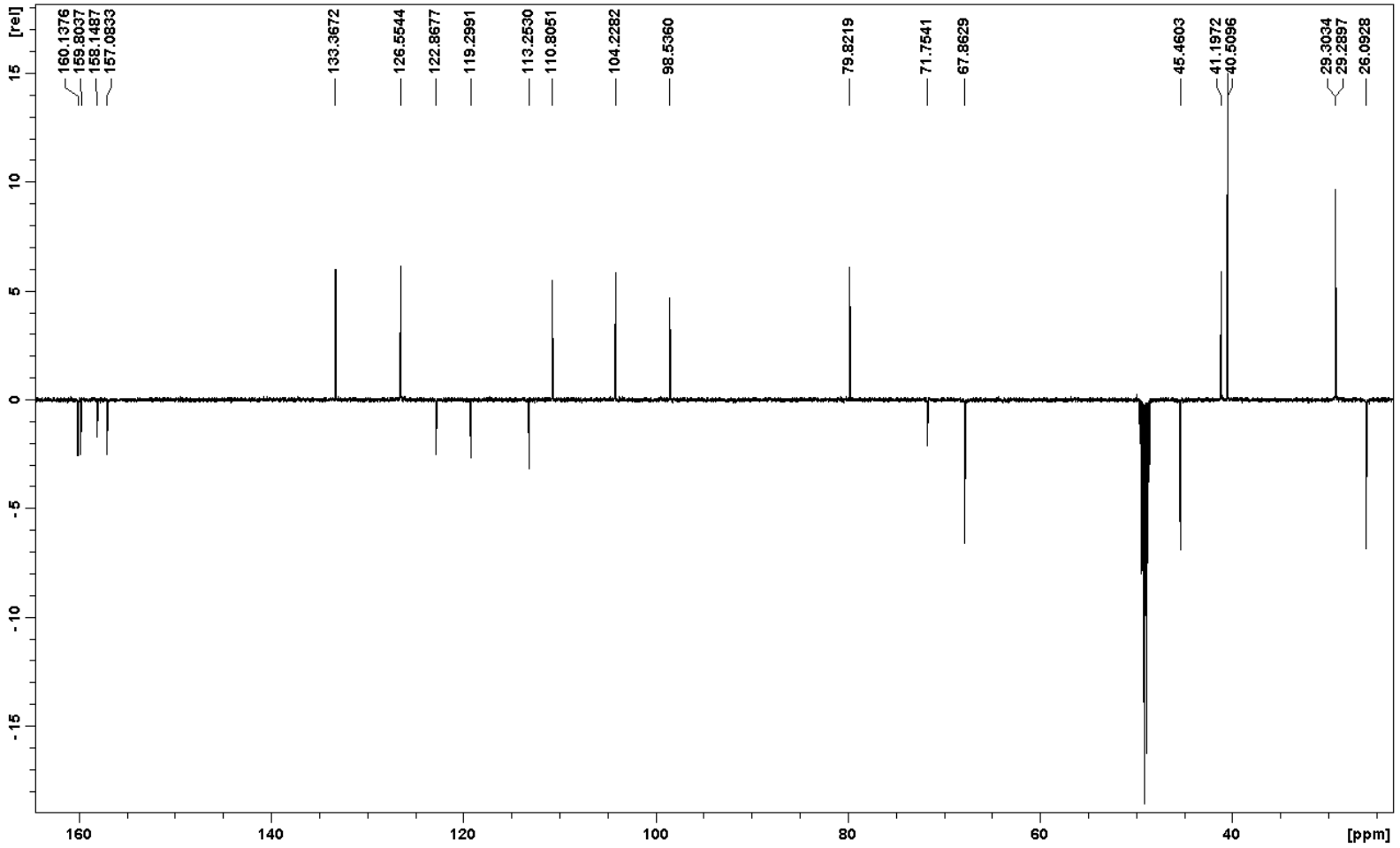

S10. HSQC (light green/dark green) and HMBC (red) spectra of compound **2**, overlaid.

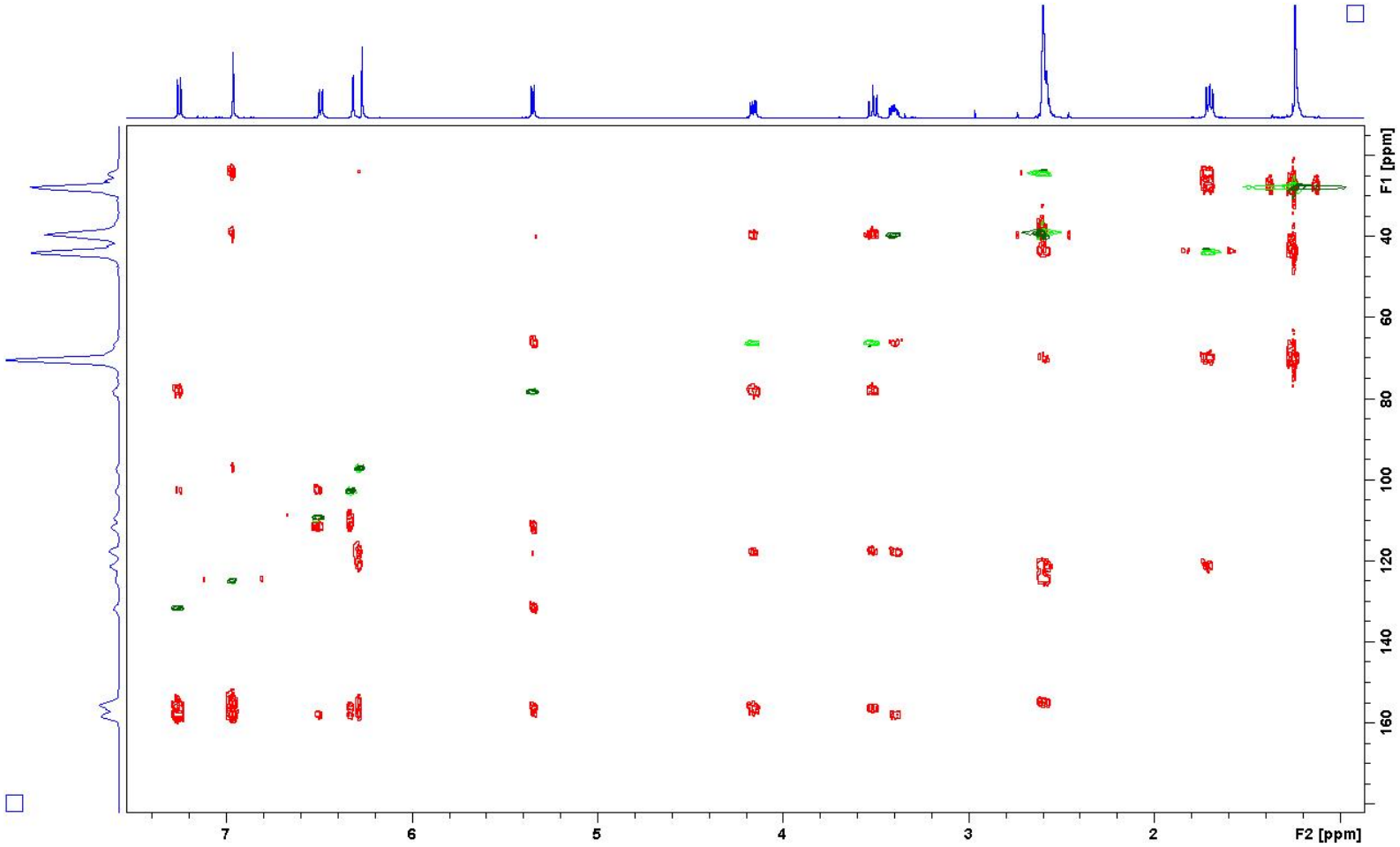

S11. ^{1}H-NMR spectrum (500 MHz in CD_3OD) of compound **4**

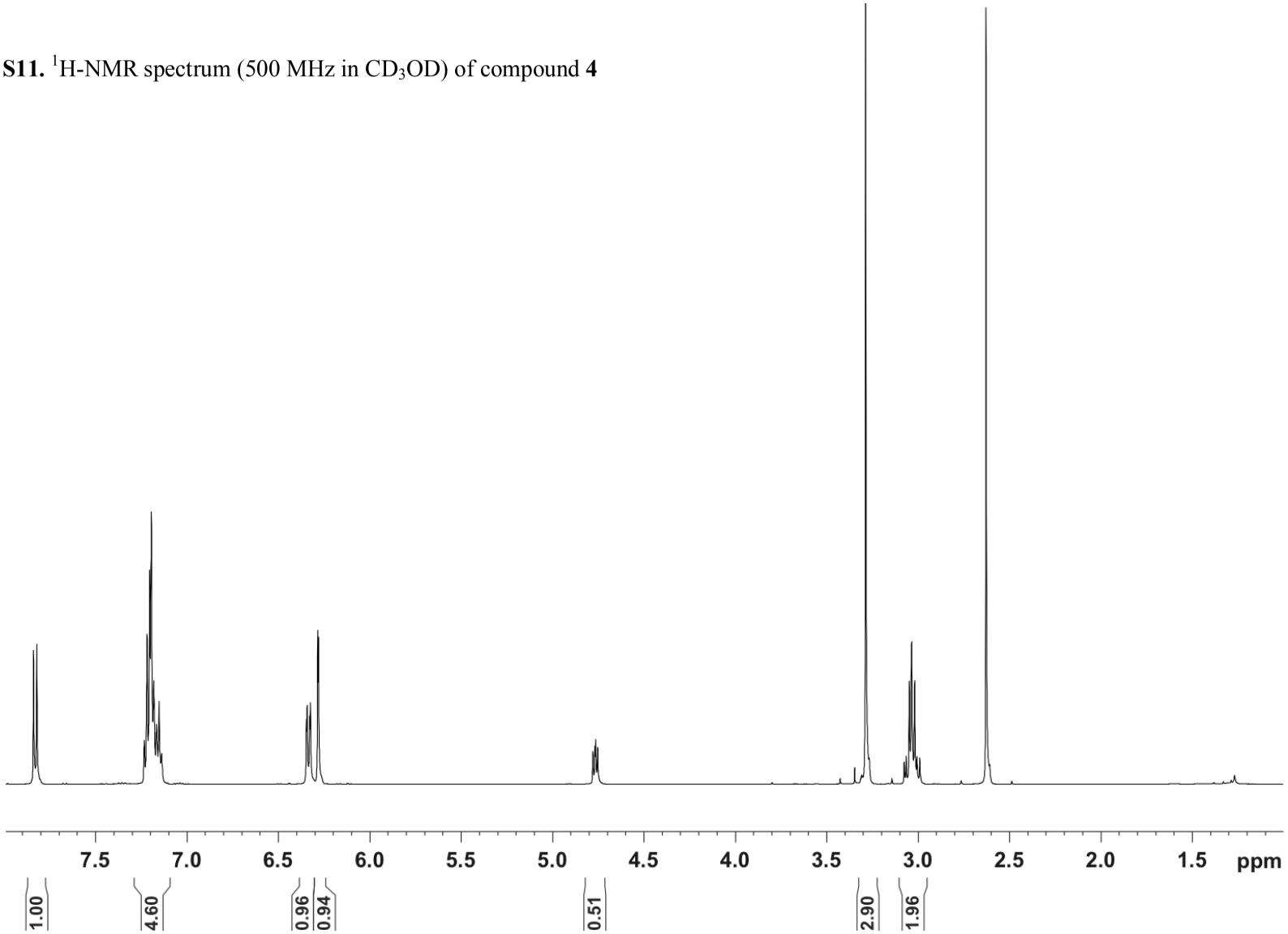

S12. DEPT spectrum (125 MHz in CD_3OD) of compound **4**

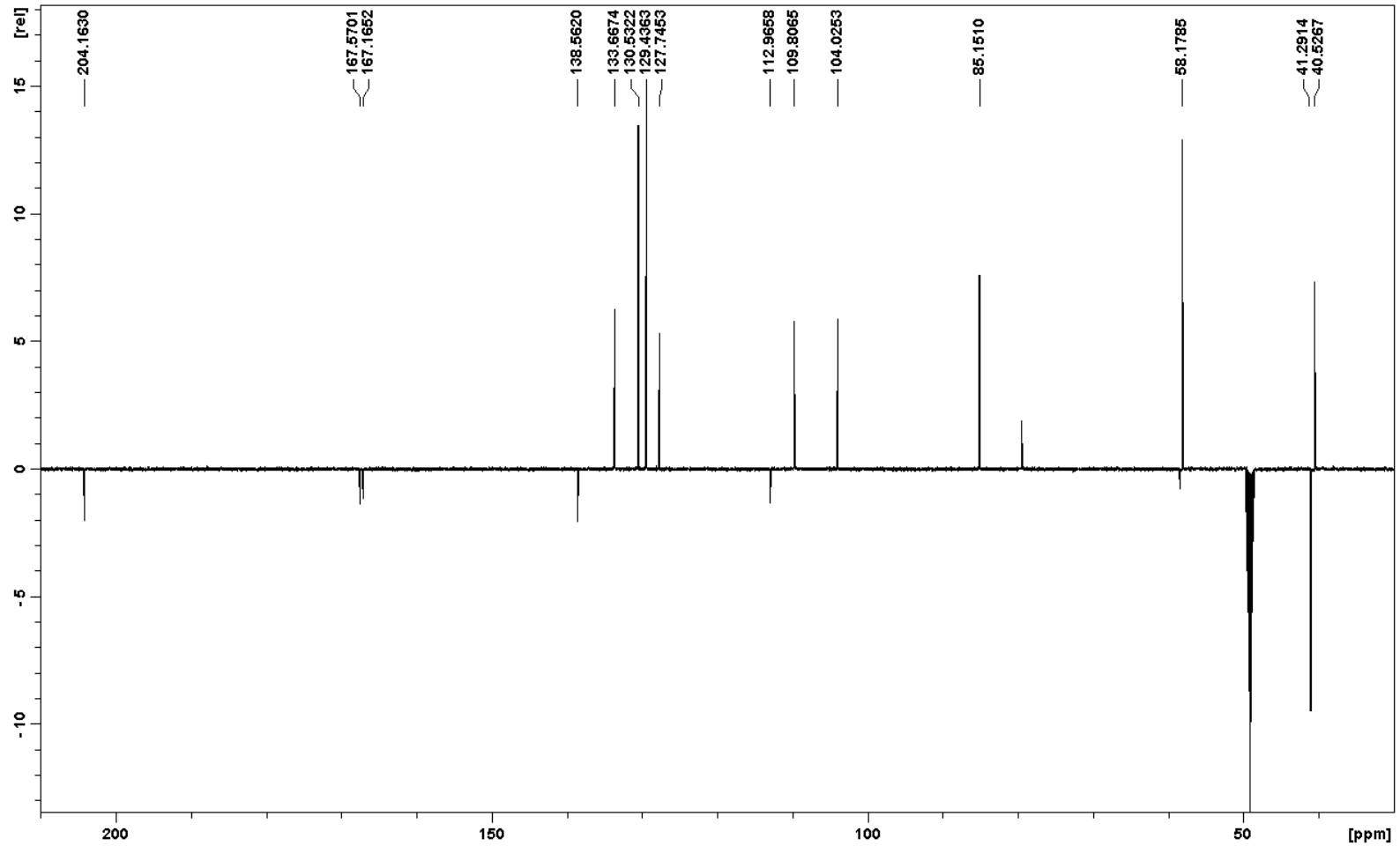

S13. HSQC (light green/dark green) and HMBC (red) spectra of compound **4**, overlaid.

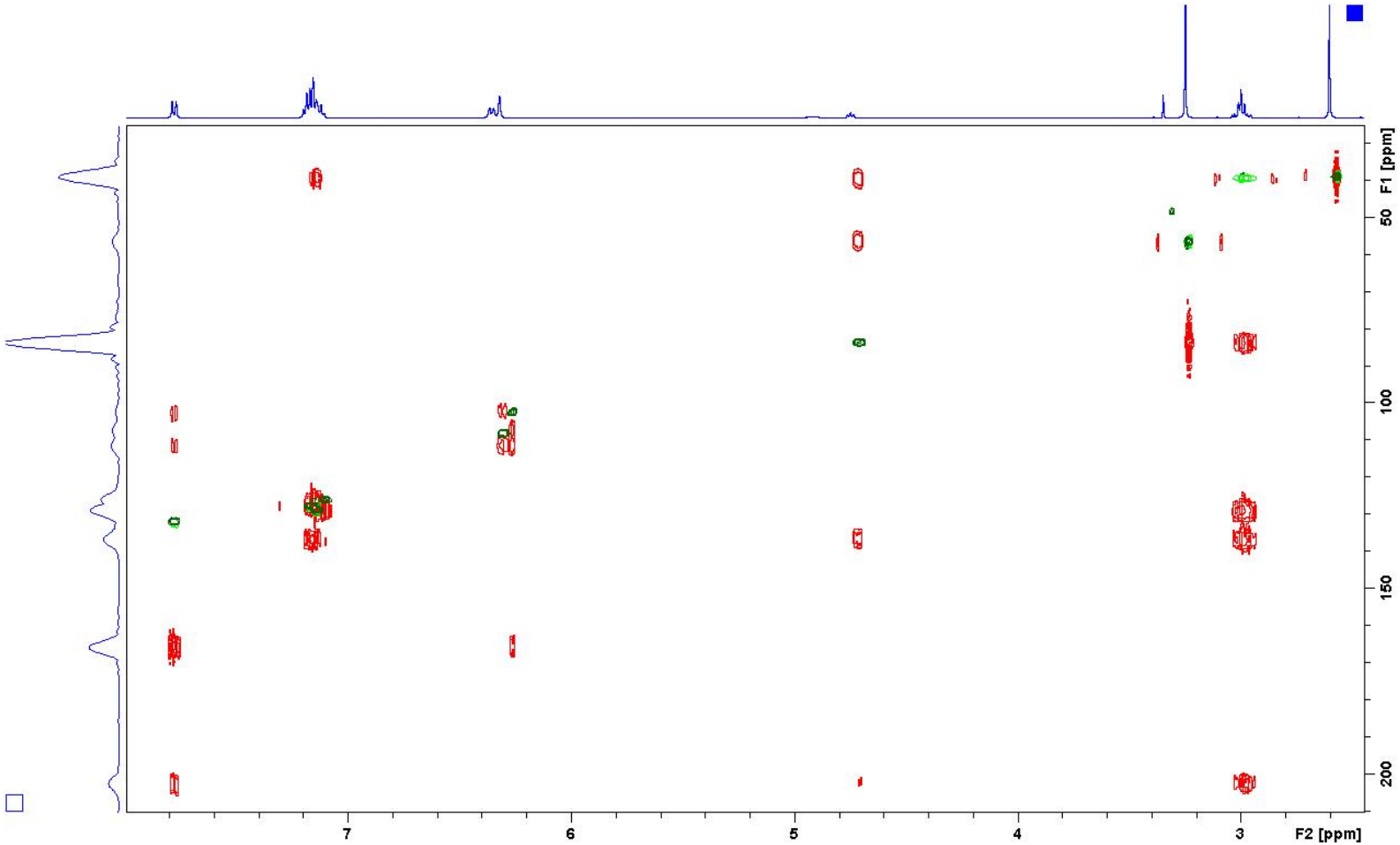

S14. ^{1}H-NMR spectrum (500 MHz in CD_3OD) of compound **6**

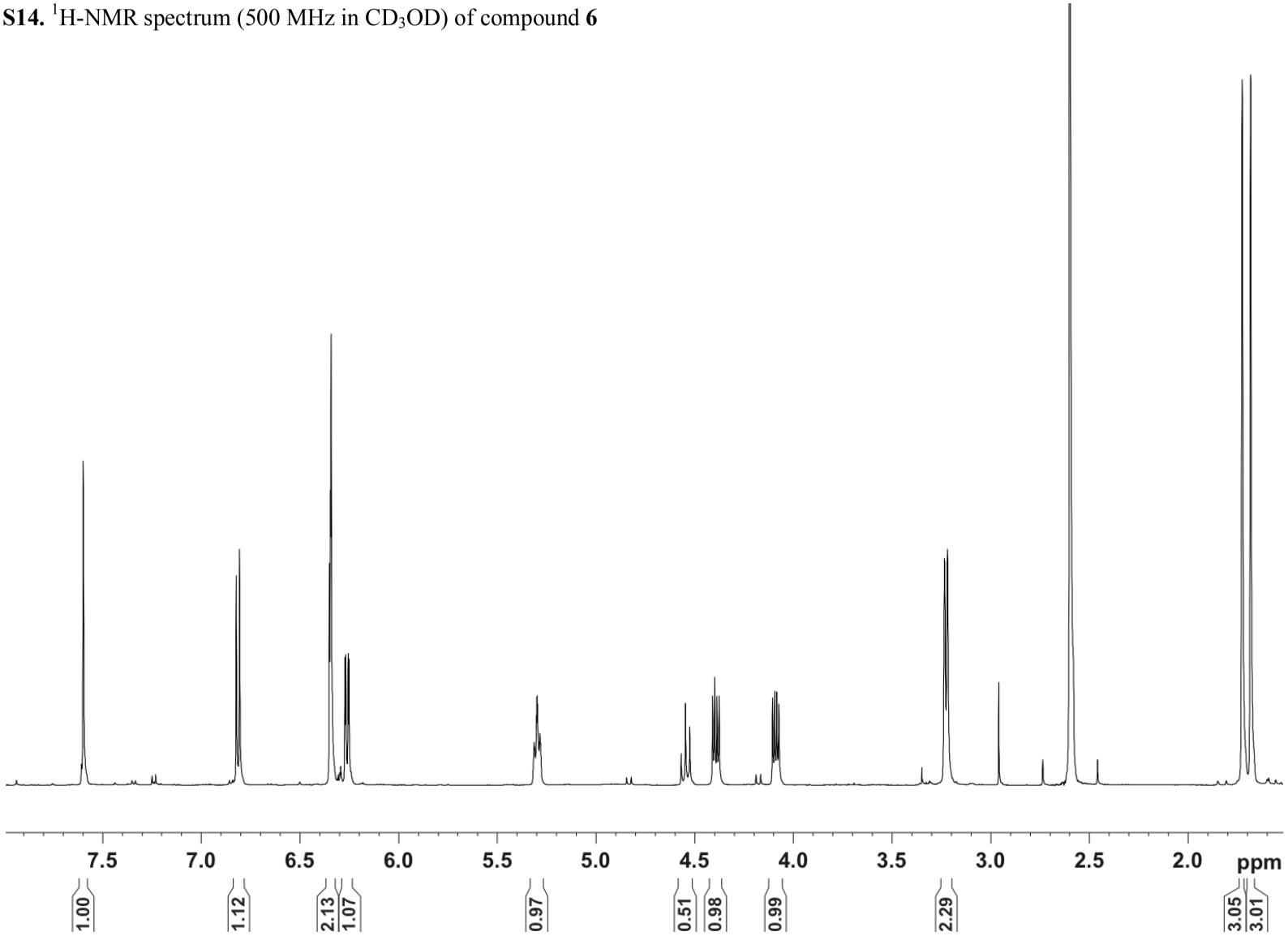

S15. DEPT spectrum (125 MHz in CD_3OD) of compound **6**

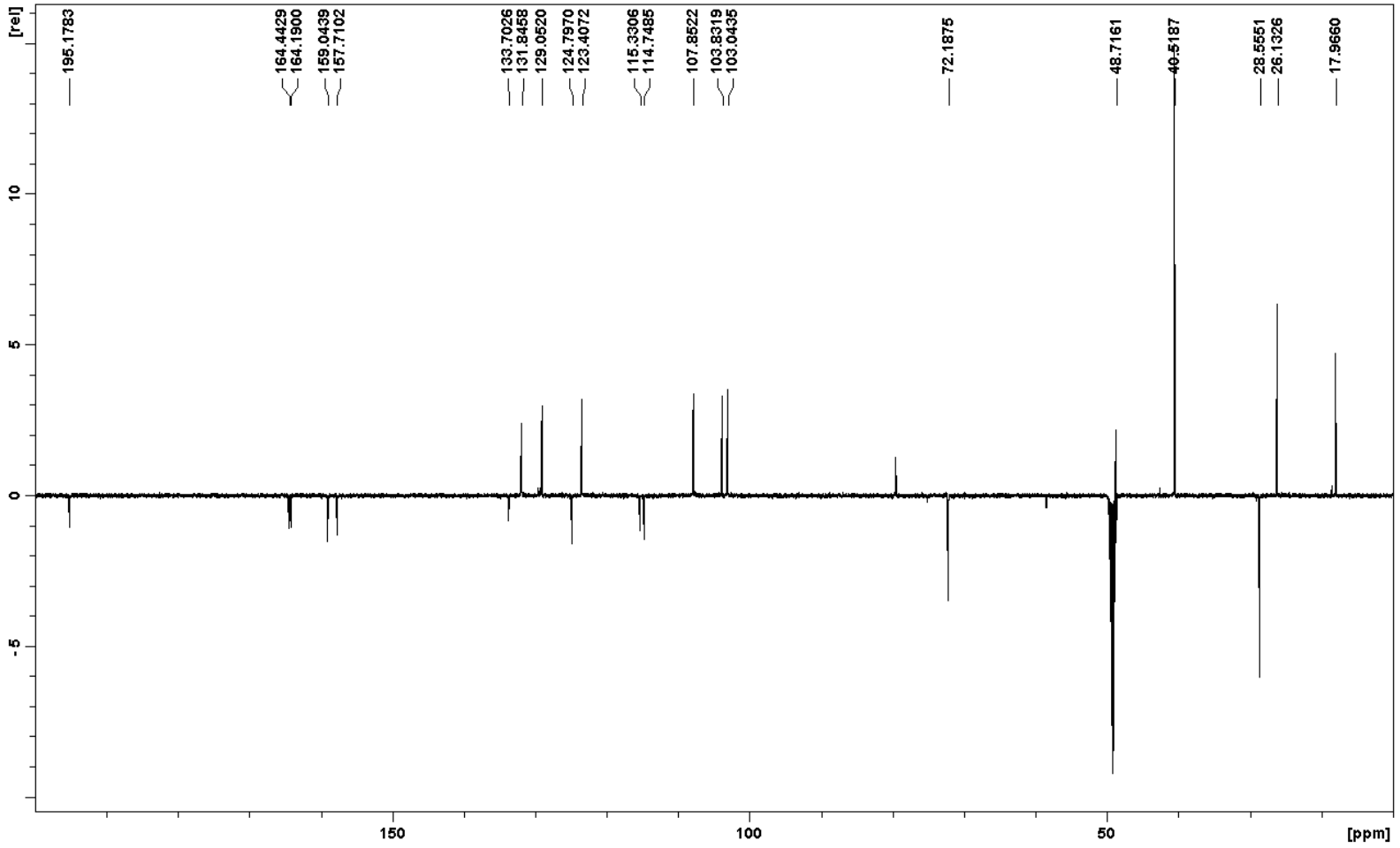

S16. HSQC (light green/dark green) and HMBC (red) spectra of compound **6**, overlaid.

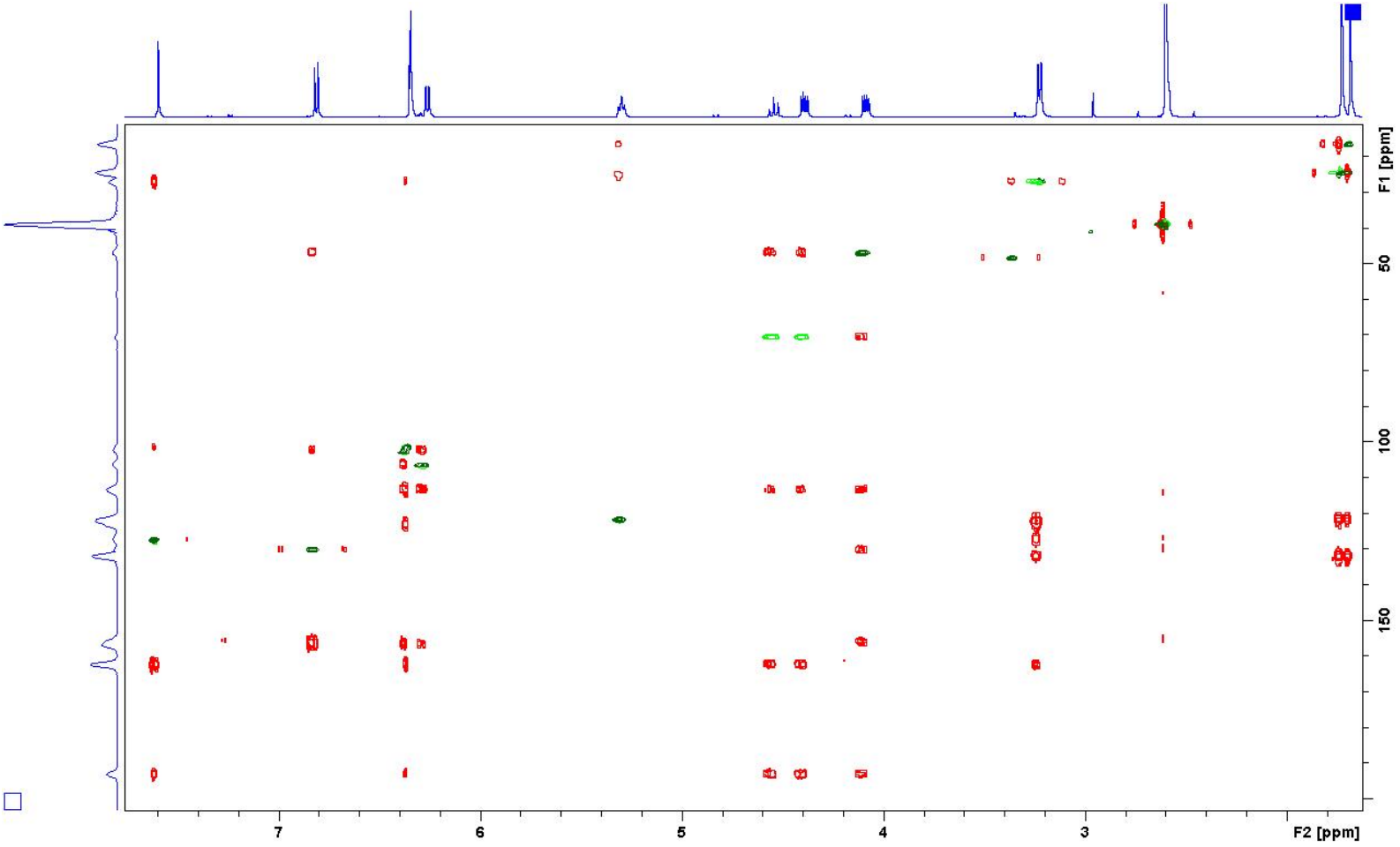

S17. ^{1}H-NMR spectrum (500 MHz in CD_3OD) of compound **7**

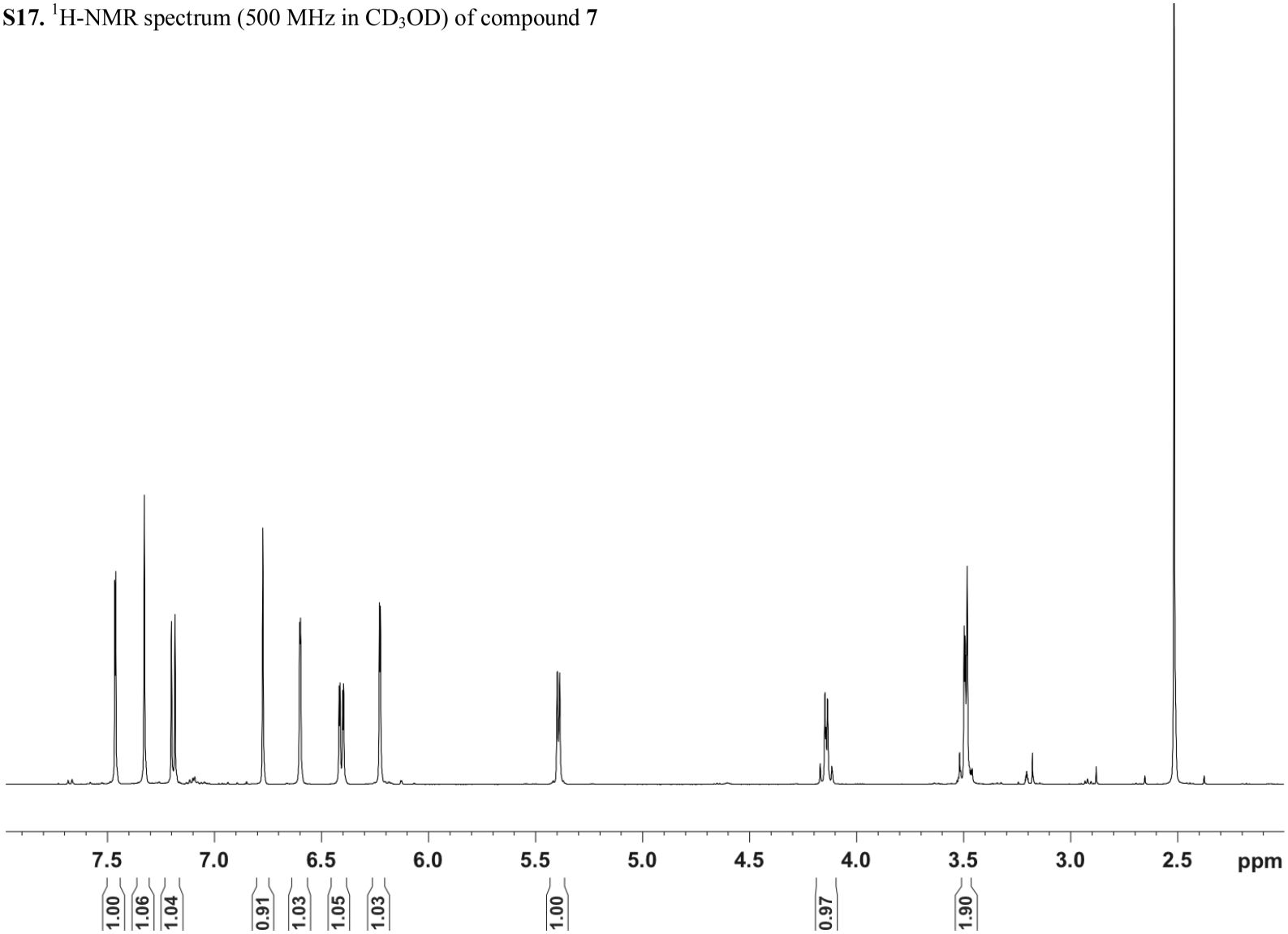

S18. DEPT spectrum (125 MHz in CD_3OD) of compound **7**

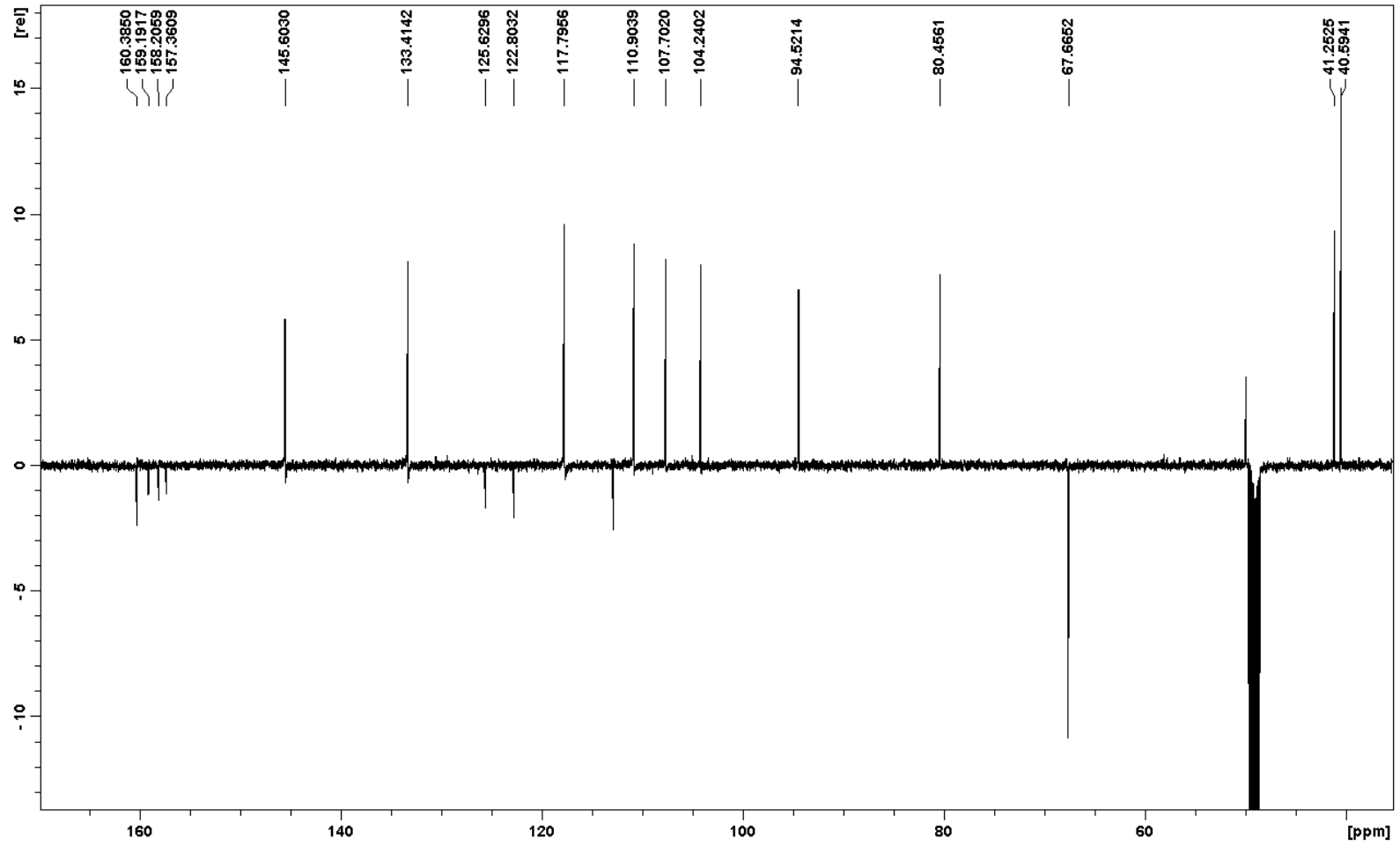

S19. HSQC (light green/dark green) and HMBC (red) spectra of compound **7**, overlaid.

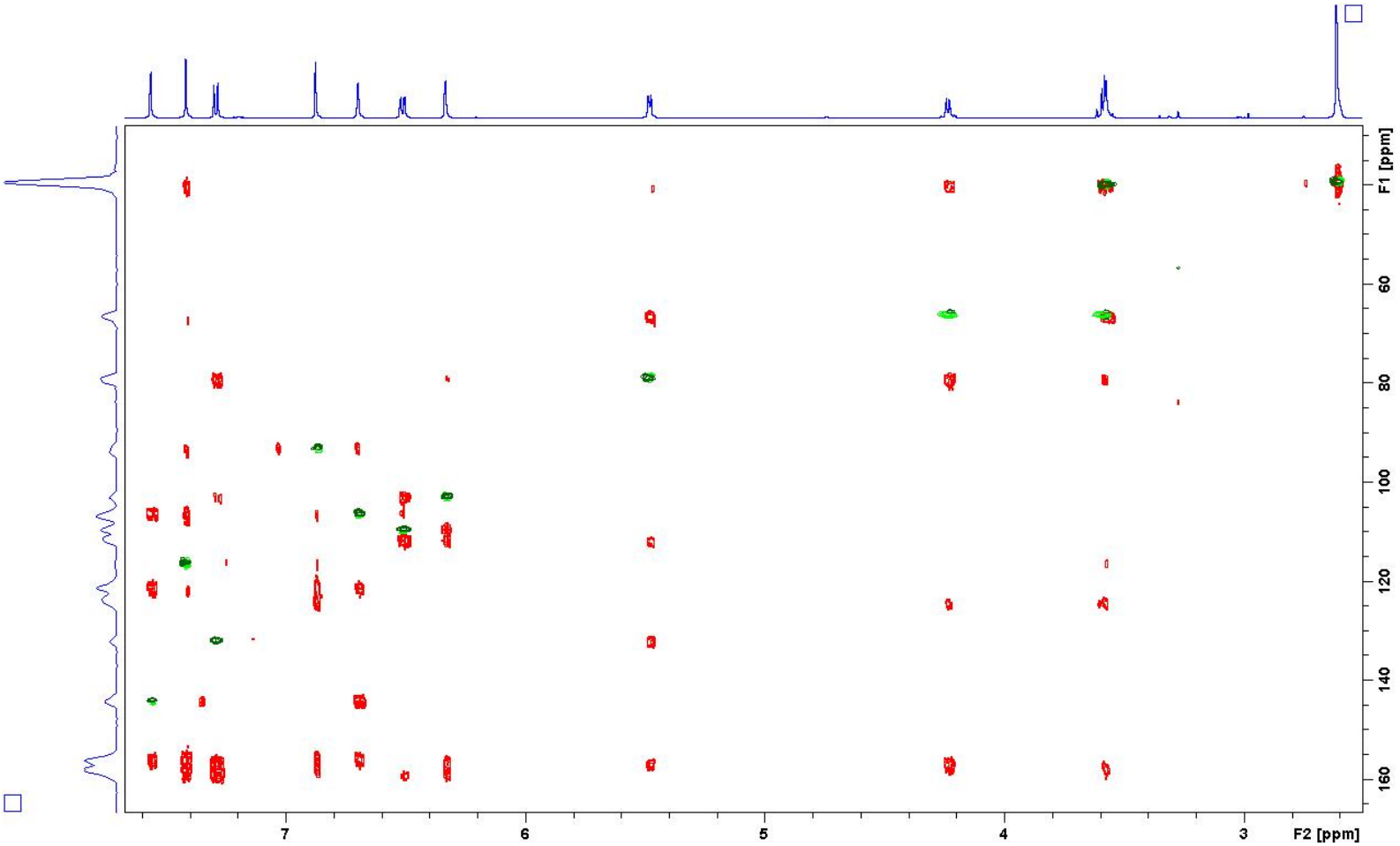

S20. ^{1}H-NMR spectrum (500 MHz in CD_3OD) of compound **8**

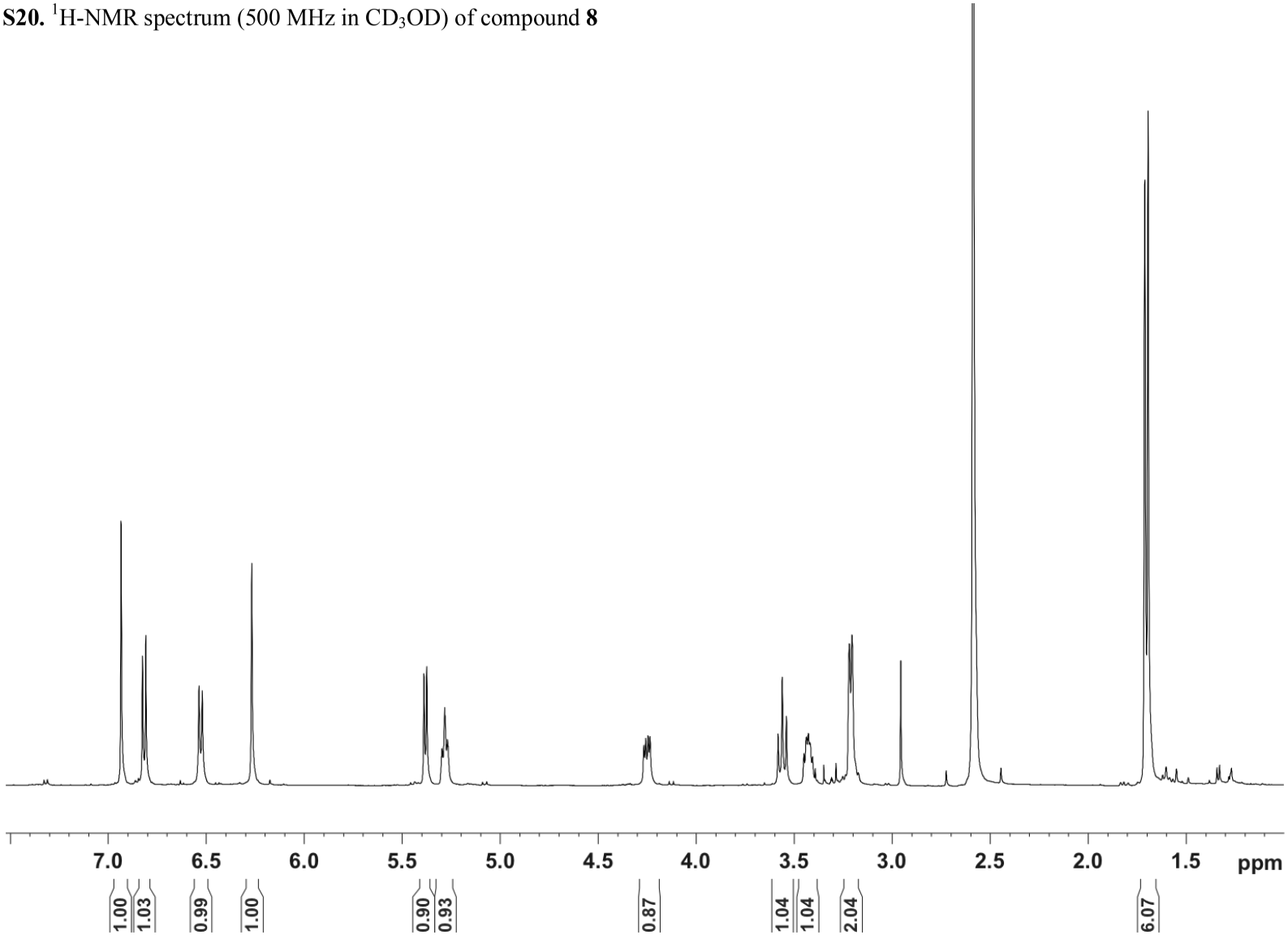

S21. DEPT spectrum (125 MHz in CD_3OD) of compound **8**

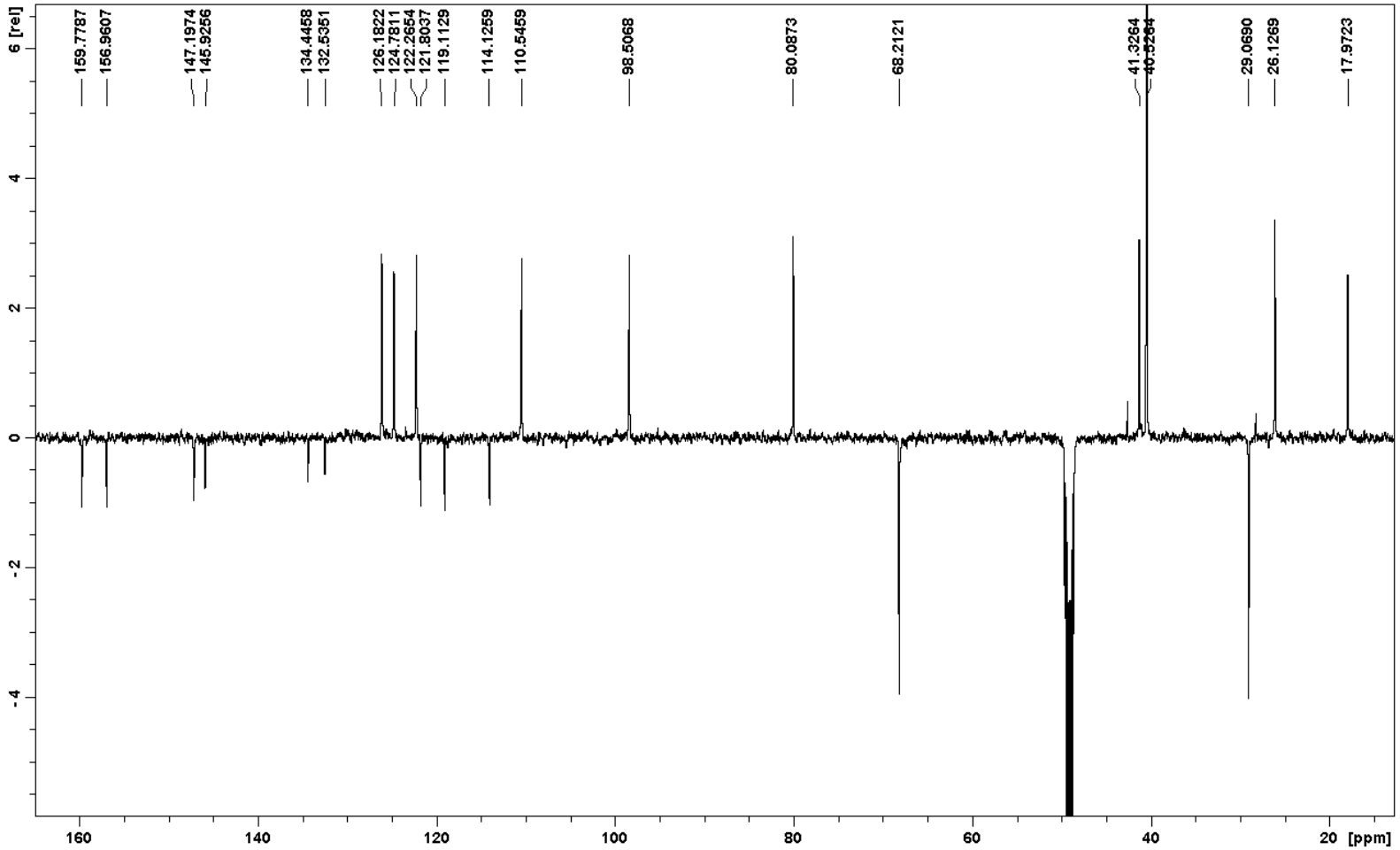

S22. HSQC (light green/dark green) and HMBC (red) spectra of compound **8**, overlaid.

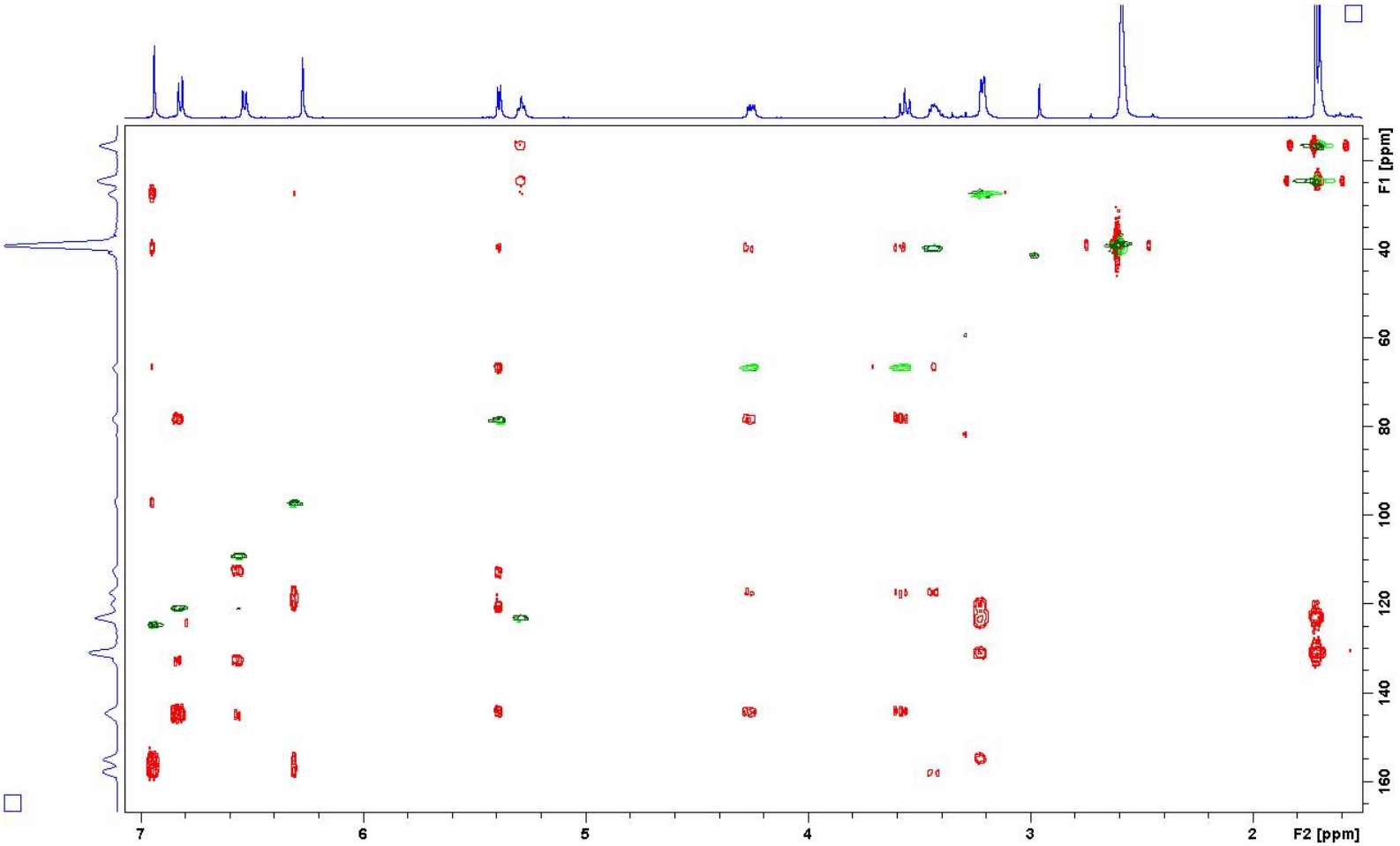

S23. ^{1}H-NMR spectrum (500 MHz in CD_3OD) of compound **9**

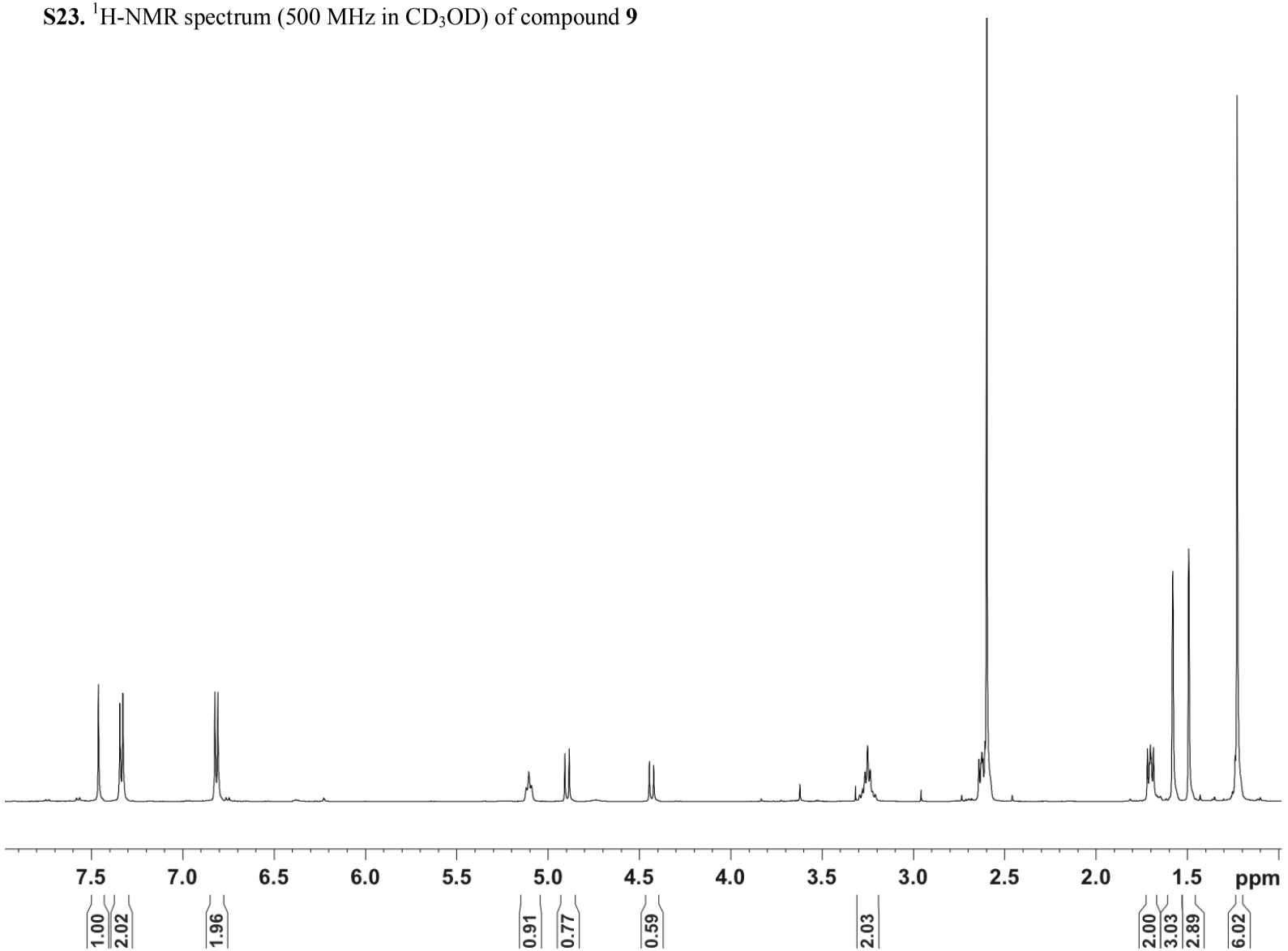

S24. DEPT spectrum (125 MHz in CD_3OD) of compound **9**

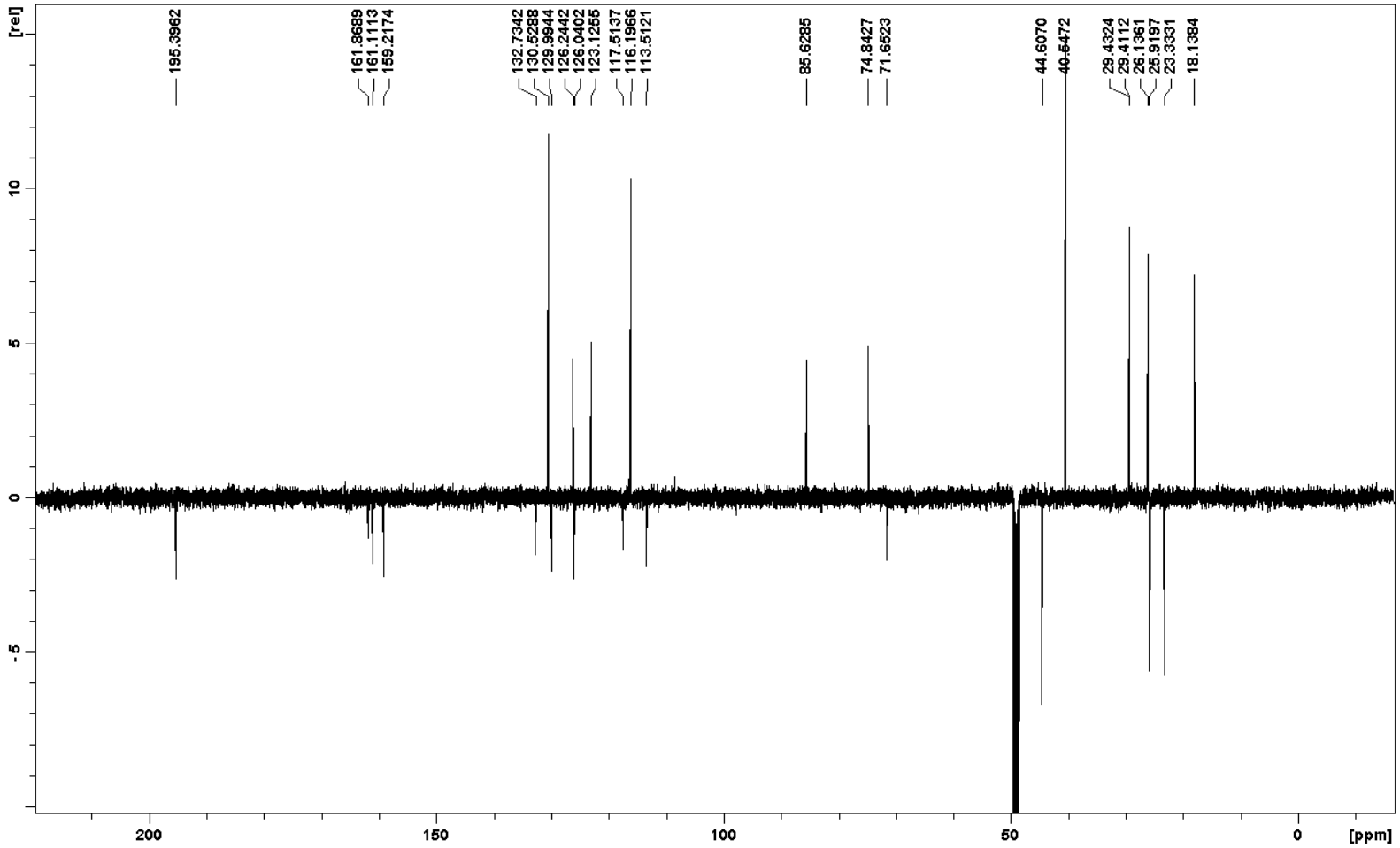

S25. HSQC (light green/dark green) and HMBC (red) spectra of compound **9**, overlaid.

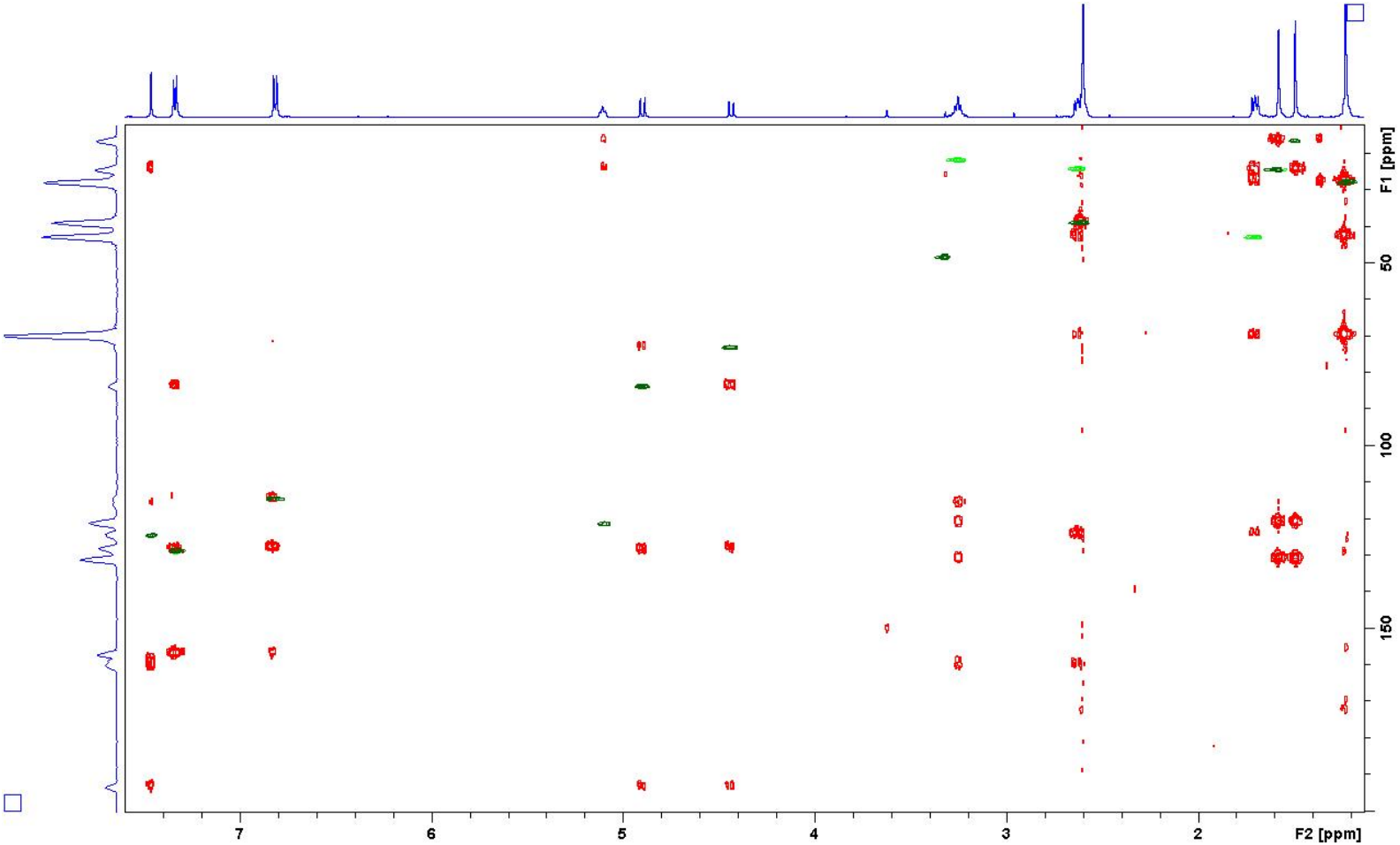

S26. ^{1}H-NMR spectrum (500 MHz in CD_3OD) of compound **11**

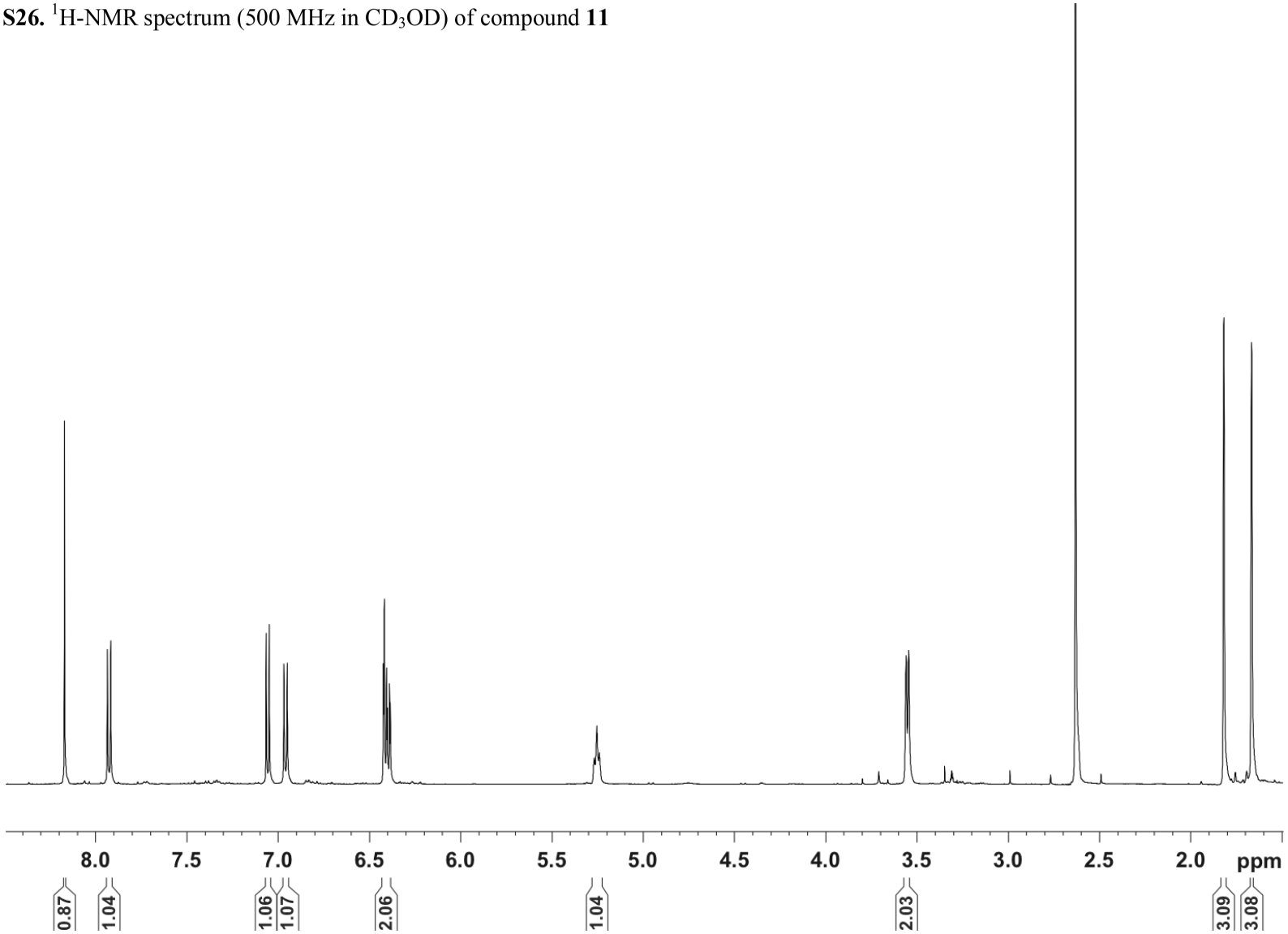

S27. DEPT spectrum (125 MHz in CD_3OD) of compound **11**

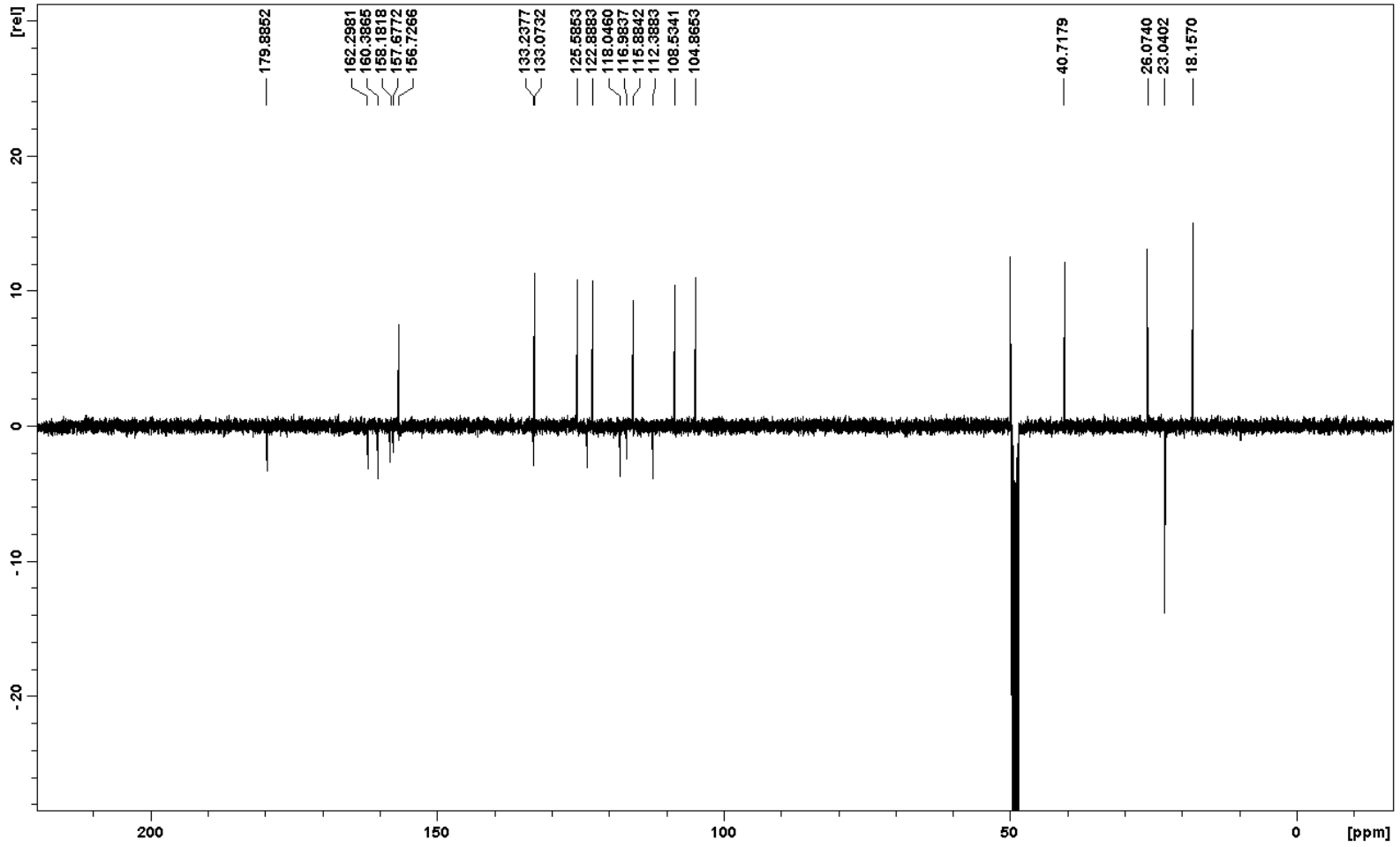

S28. HSQC (light green/dark green) and HMBC (red) spectra of compound **11**, overlaid.

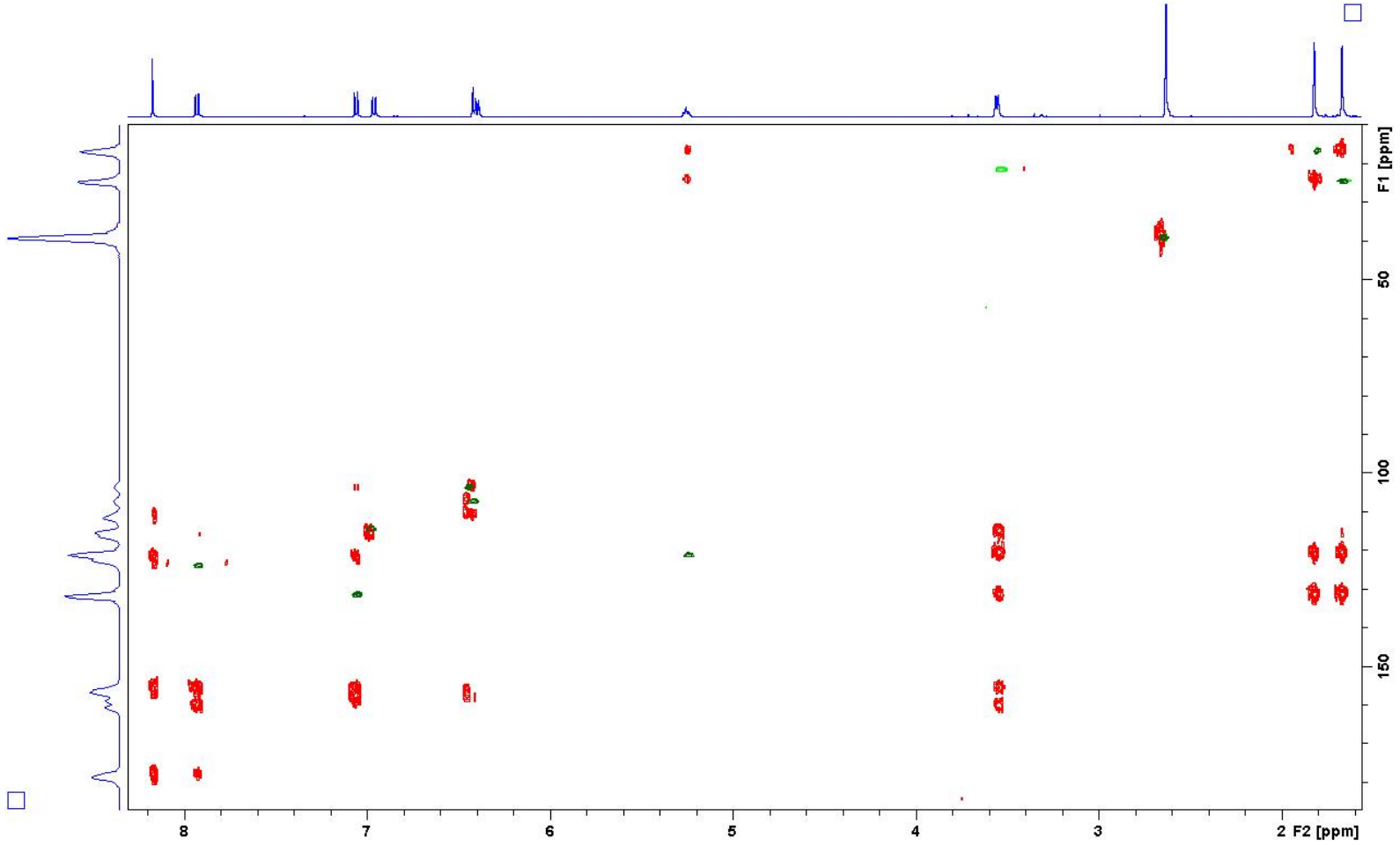

S29. ^{1}H-NMR spectrum (500 MHz in CD_3OD) of compound **12**

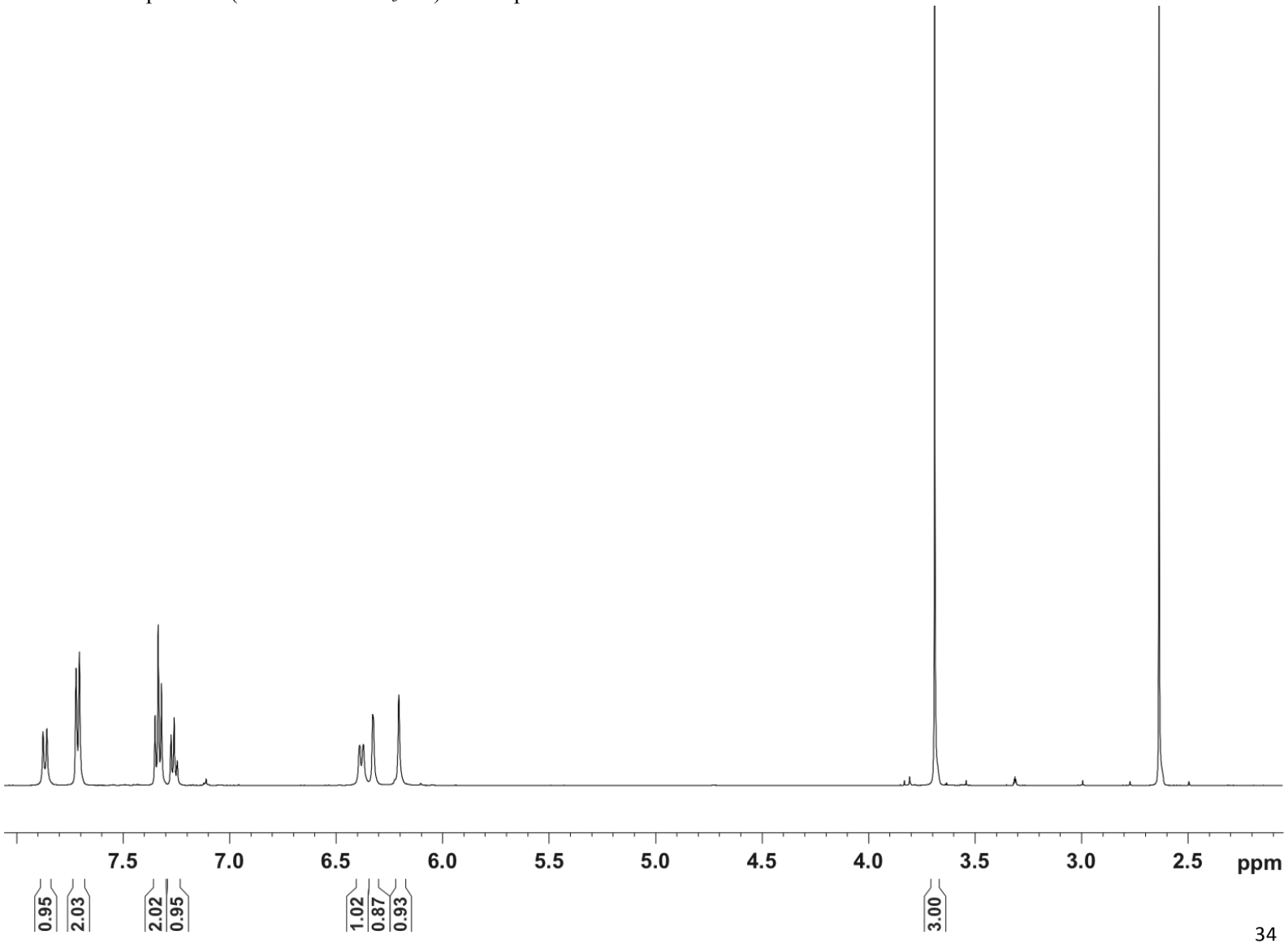

S30. DEPT spectrum (125 MHz in CD_3OD) of compound **12**

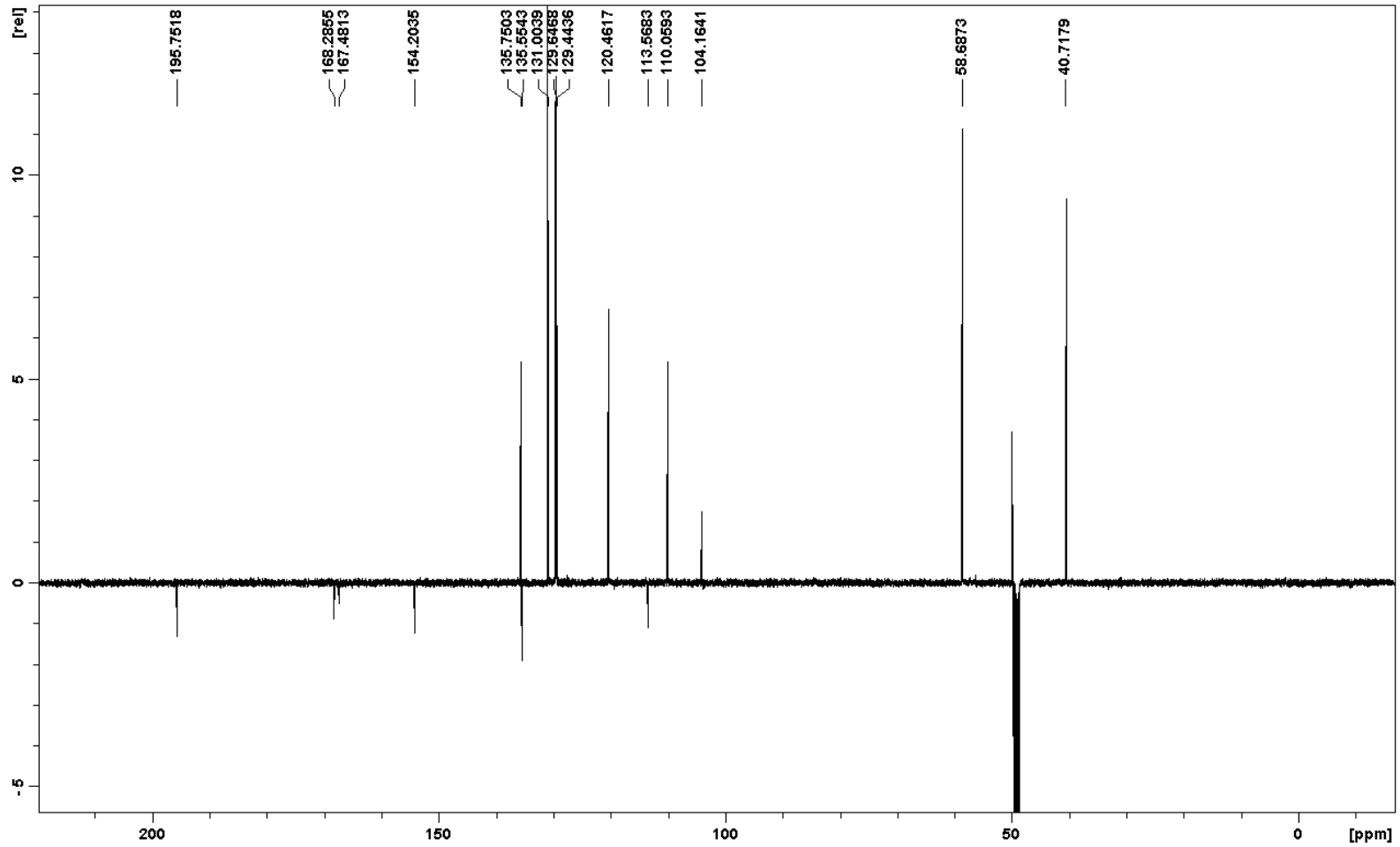

S31. HSQC (light green/dark green) and HMBC (red) spectra of compound **12**, overlaid.

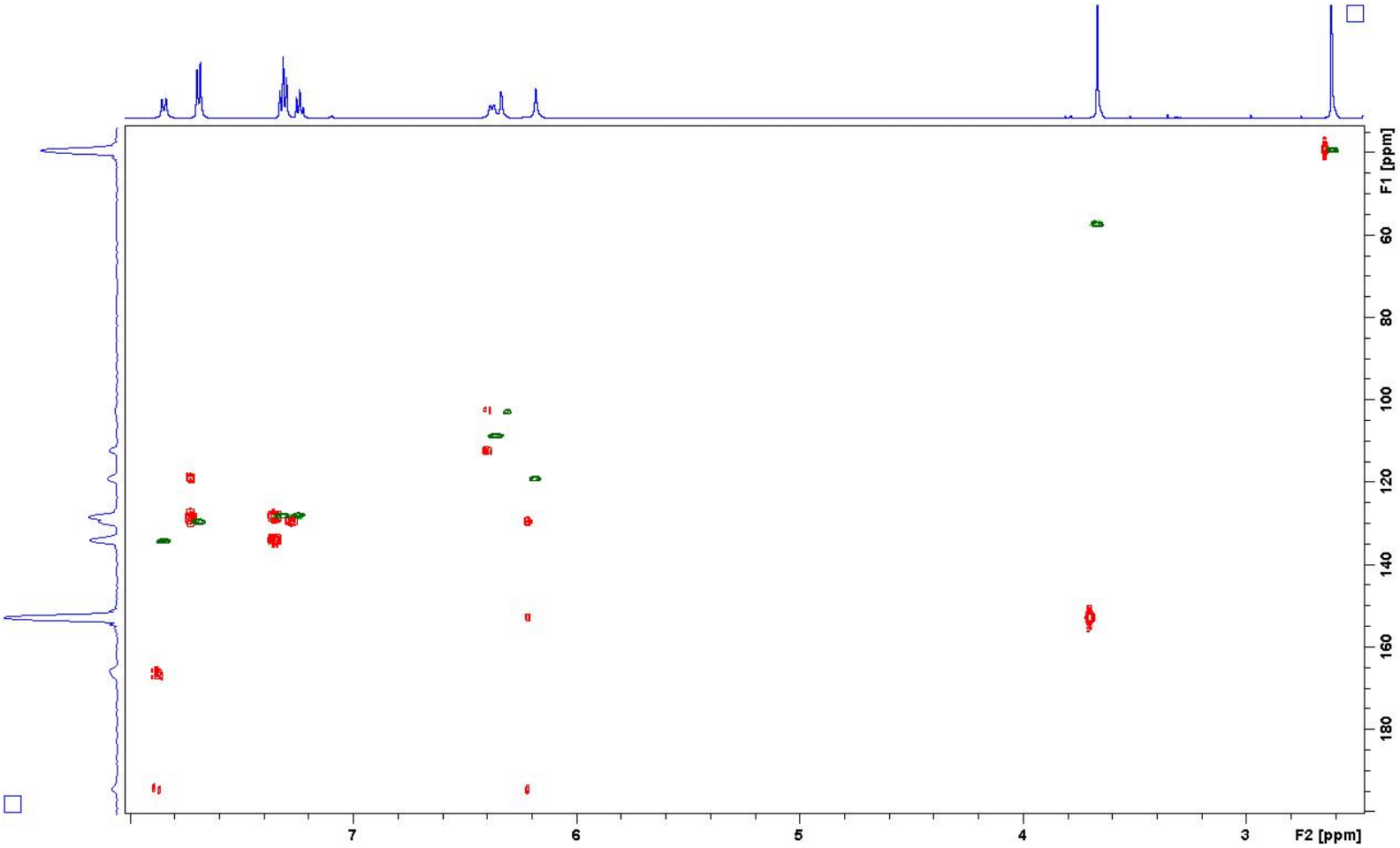

3.4. Identification of dehydroabietc acid from *Boswellia thurifera* resin as a positive $GABA_A$ receptor modulator

Diana C. Rueda, Melanie Raith, Maria De Mieri, Steffen Hering, and Matthias Hamburger.
Manuscript ready for submission

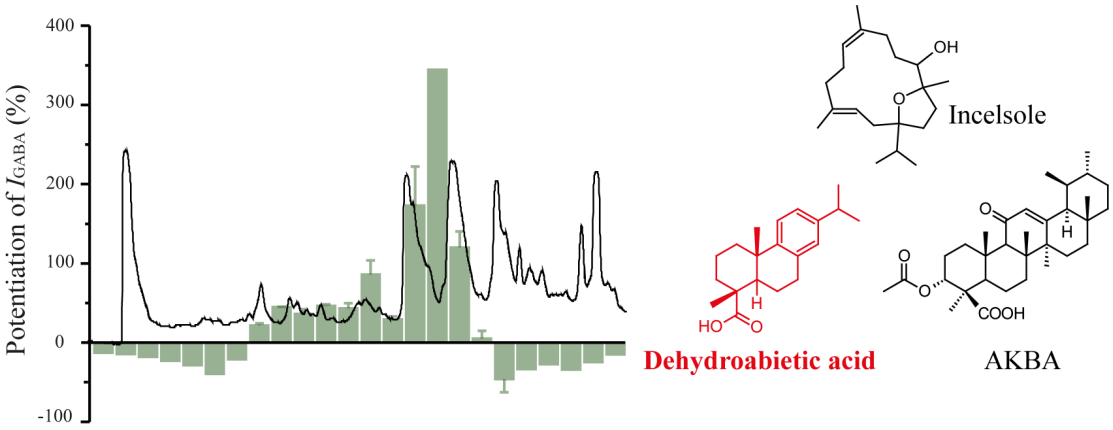

The abietane diterpene dehydroabietic acid, isolated from a petroleum ether extract of *Boswellia thurifera* resin, was identified as a positive $GABA_A$ receptor modulator by means of HPLC-based activity profiling and a functional *in vitro* assay in *Xenopus* oocytes. Incensole and AKBA were also isolated from the active time window, but they showed no activity in the oocyte assay. Structure elucidation was achieved by high-resolution mass spectroscopy and microprobe NMR. Abietane diterpenes constitute a new scaffold for $GABA_A$ receptor modulators.

Extraction of the plant material for isolation, HPLC-based activity profiling, isolation of pure compounds, bioactivity assessment of fractions and pure compounds in Xenopus *oocytes, oocyte preparation, recording and interpretation of analytical data for structure elucidation (UV, HRMS, NMR spectra), writing of the manuscript draft, and preparation of the figures were my contributions to this publication. Structure elucidation was supported by M. Raith. Writing of the experimental section was supported by M. De. Mieri.*

Diana C. Rueda

Identification of dehydroabietc acid from *Boswellia thurifera* resin as a positive $GABA_A$ receptor modulator

Diana C. Rueda[a], Melanie Raith[a], Maria De Mieri[a], Angela Schöffmann[b], Steffen Hering[b], and Matthias Hamburger[a,*]

[a] *Division of Pharmaceutical Biology, University of Basel, Klingelbergstrasse 50, CH-4056 Basel, Switzerland*

[b] *Institute of Pharmacology and Toxicology, University of Vienna, Althanstrasse 14, A-1090 Vienna, Austria*

* Corresponding author. Tel.: +41-61-2671425; fax: +41-61-2671474.

E-mail: matthias.hamburger@unibas.ch

ABSTRACT

In a two-microelectrode voltage clamp assay with *Xenopus laevis* oocytes, a petroleum ether extract (100 μg/mL) of the resin of *Boswellia thurifera* (Burseraceae) potentiated GABA-induced chloride currents (I_{GABA}) through receptors of the subtype $\alpha_1\beta_2\gamma_{2s}$ by 319.8% ± 79.8%. With the aid of HPLC-based activity profiling three known terpenoids, dehydroabietic acid (**1**), incensole (**2**), and AKBA (**3**), were identified in the active fractions of the extract. Structure elucidation was achieved by means of HR-MS and microprobe 1D/2D NMR spectroscopy. Compound **1** induced significant receptor modulation in the oocyte assay, with a maximal potentiation of I_{GABA} of 397.5% ± 34.0%, and EC_{50} of 8.7 μM ± 1.3 μM. This is the first report of dehydroabietic acid as a positive $GABA_A$ receptor modulator.

Keywords: *Boswellia thurifera*, olibanum, HPLC-based activity profiling, $GABA_A$ receptor modulators, abietane diterpenes, dehydroabietic acid.

Abbreviations

AKBA: 3α-acetoxy-11-keto-β-boswellic acid

BBB: Blood-brain barrier

BDZs: benzodiazepines

CNS: central nervous system

DHA: Dehydroabietic acid

GABA: gamma-aminobutyric acid

$GABA_A$Rs: gamma-aminobutyric acid type A receptors

I_{GABA}: GABA-induced chloride current

1. Introduction

A number of plants belonging to the Burseraceae family are the source of strongly aromatic resins of considerable commercial value. The resin obtained by incision of *Boswellia* spp. (Burseraceae), also called *frankincense* or *olibanum*, has been used as incense in religious and cultural ceremonies since the beginning of written history and, in ancient times, was ranked along with gold and ivory as a precious trading good [1,2].

Olibanum is known in Chinese and other traditional medicines for its anti-inflammatory, antiseptic, wound-healing, and sedative properties [1,3,4]. It is a complex mixture composed of polysaccharides, monoterpenes, sesquiterpenes, diterpenes like incensole, isoincensole, and their oxide or acetate derivatives, and triterpenoids such as boswellic acids [1,5,6]. Boswellic acids are considered as marker compounds of the resin, and they have been found responsible for the anti-inflammatory properties. Incensole acetate and its derivatives have been reported as inhibitors of NF-κB and potent activators of TRPV3 channels in the brain, which confers them antidepressant and anxiolytic properties [1,7]. Monographs on olibanum can be found in the Chinese Pharmacopoeia [8] and ESCOP monographs [9], where it is referred as the dried resin from the bark of *B. carterii* Birdw. and *B. bhawdajiana* Birdw., or from stems and branches of *Boswellia serrata* Roxb. ex Colebr., respectively. Indications include the treatment of painful or inflammatory conditions. *B. carterii*, *B. frereana*, and *B. serrata*, are the three main olibanum-producing species [10,11].

$GABA_A$ receptors ($GABA_ARs$) are ligand-gated chloride channels physiologically activated by GABA, the major inhibitory neurotransmitter in the brain. They are heteropentameric assemblies with a central chloride-selective channel. Up to now 19 subunits (α_{1-6}, β_{1-3}, γ_{1-3}, δ, ε, θ, π, ρ_{1-3}) have been identified in $GABA_ARs$. GABA-induced chloride influx generates a

negative potential in the postsynaptic neurons, thereby inhibiting further action potentials. Impaired GABAergic function results in CNS disorders such as epilepsy, insomnia, anxiety, and mood disorders [12,13]. A number of clinically important drugs like benzodiazepines (BDZs), barbiturates, neuroactive steroids, anesthetics, and certain other CNS depressants bind $GABA_A$Rs.

In a search for natural products acting as $GABA_A$ receptor modulators, we tested a petroleum ether extract of the resin of *Boswellia thurifera* Roxb. ex Fleming in an automated two-microelectrode voltage clamp assay with *Xenopus* oocytes [15]. At a concentration of 100 μM, the extract enhanced I_{GABA} by 319.8% ± 79.8%, in receptors of the subtype $\alpha_1\beta_2\gamma_{2S}$. GABAergic activity of the active extract was traced using an HPLC-based activity profiling approach [16], which has been previously validated and used for the discovery of $GABA_A$ receptor ligands from plant sources [17–23]. Pure compounds isolated from the active time window of the extract were tested in the oocyte functional assay to assess their $GABA_A$ receptor modulatory activity.

2. Experimental

2.1. General procedures

1D and 2D NMR spectra were recorded on a Bruker Avance III spectrometer operating at 500.13 MHz. ^{1}H NMR, COSY, HSQC, HMBC, and NOESY spectra were measured at 18 °C in a 1 mm TXI probe with a z-gradient, using standard Bruker pulse sequences. Spectra were analyzed by Bruker TopSpin 3.0 software. ESI-TOF-MS spectra were recorded in positive mode, *m*/*z* range 100-800, on a Bruker microTOF ESIMS system. Nitrogen was used as a nebulizing gas at a pressure of 2.0 bar, and as drying gas at a flow rate of 9.0 L/min (dry gas temperature 240°C). Capillary voltage was set at 45000 V; hexapole at 230.0 Vpp. Instrument calibration was done with a reference solution of sodium formiate 0.1% in 2-propanol/water (1:1) containing 5 mM NaOH.

HPLC-PDA-ESIMS spectra were obtained in positive ion mode on a Bruker Daltonics Esquire 3000 Plus ion trap MS system, connected via T-splitter (1:10) to an Agilent HP 1100 system consisting of a degasser, a binary mixing pump, autosampler, column oven, and a diode array detector (G1315B). Data acquisition and processing was performed on Bruker Daltonics Hystar 3.0 software. Semipreparative HPLC separations were performed with an Agilent HP 1100 series system consisting of a quaternary pump, autosampler, column oven, and diode array detector (G1315B). Preparative HPLC separations were performed on a Shimadzu LC-8A preparative HPLC system with an SPD-M10A VP diode array detector. Flash chromatography was performed with pre-packed Sepacore ® silica flash cartridges (40-63 μm, 40×150 mm) on a Sepacore ® system consisting of two C-605 pumps, a C-620 control unit, and a C-660 fraction collector (all Buchi, Flawil, Switzerland). The separation was monitored by TLC. Waters SunFire™ C18 (3.5 μm, 3.0×150 mm i.d.), SunFire™ Prep

C18 (5 μm, 10×150 mm i.d.), and SunFire™ Prep C18 OBD (5 μM, 30×150 mm i.d.) columns were used for analytical, semipreparative, and preparative separations, respectively. HPLC-grade MeOH (Scharlau Chemie) and water, both containing 0.1% of formic acid, were used for HPLC separations. NMR spectra were recorded in methanol-d_4 and DMSO-d_6 (Armar Chemicals). For extraction and flash chromatography technical grade solvents purified by distillation were used.

2.2. Plant material

Resin of *Boswellia thurifera* Roxb. ex Fleming were purchased by Dan Yang in 2008 from Juhuayuan Herbal Market, Kunming, Yunnan, province, China. Identity of the material was confirmed at Yunnan Baiyao group Co.LTD, Kunming, China. A voucher specimen (433) is deposited at the Division of Pharmaceutical Biology, University of Basel.

2.3. Extraction

The petroleum ether extract for screening and HPLC-based activity profiling was prepared with an ASE 200 extraction system with solvent module (Dionex, Sunnyvale, CA). In total, 3 extraction cycles (5 min each) were performed, at an extraction pressure of 120 bar and a temperature of 70°C. Extracts were combined, and the solvent was evaporated at reduced pressure to yield 4.6 g of extract. The extract was stored at 2-8°C until use.

2.4. Microfractionation for activity profiling

Time-based microfractionation of the extract for $GABA_A$ receptor activity profiling was performed as previously described [24], with minor modifications: separation was done on a semi-preparative HPLC column with MeOH (solvent A) and water (solvent B), using a gradient from 70% A to 100% A in 30 min, hold for 15 min. The flow rate was 4 mL/min, and 10mg of extract (in 100 μL of DMSO) were injected. A total of 24 time-based

microfractions of 90 s each were collected and evaporated in parallel. The dry films were redissolved in 1 mL of methanol, and aliquots of 0.5 mL were dispensed in two vials, dried under N_2 gas, and submitted to bioassay.

2.5. Isolation

An aliquot of the petroleum ether extract (1 g) was dissolved in *n*-hexane and submitted to purification by flash chromatography. Separation was performed on a Sepacore ® silica gel cartridge eluted with an *n*-hexane (solvent A) and EtOAc (solvent B) gradient: 0% B to 20% B in 60 min, followed by 30% B to 50% B in 30 min, and 50% B to 100% B in 30 min. The flow rate was set at 15 mL/min. Fractions of 15 mL were collected and later combined to 13 fractions (A-M) on the basis of TLC analysis (detection at 254 nm, 366 nm, and at daylight after staining with anisaldehyde-sulphuric acid reagent). Fractions A-M were submitted to analytical HPLC-PDA-ESIMS with MeOH (solvent C) and water (solvent D), using an optimized gradient from 85% C to 100% C in 30 min, hold for 15 min. The flow rate was 0.4 mL/min, and 5 μg of each fraction (in 5 μL of DMSO) were injected. Fractions F, G, and J were found to contain the compounds of interest and were submitted to purification by semi-preparative HPLC using solvents C and D as eluents. Samples were separated under isocratic conditions (87% C, 20 min). The flow rate was 4 mL/min. Stock solutions in DMSO (100 mg/mL) were prepared and repeatedly injected in portions of 20-50 μL. Compound **1** (1 mg) was isolated from 10 mg of fraction G (63 mg). A portion (10 mg) of fraction F (259 mg) afforded compound **2** (0.6 mg). Compound **3** (0.5 mg) was isolated from 5 mg of fraction J (72 mg). Structure elucidation was achieved by analysis of ESI-TOF-MS and 1D/2D NMR data, and by comparison with published values [25–27]. The purity was > 95% (purity check by ^{1}H NMR).

*2.5.1. Dehydroabietic acid (**1**)*: ^{1}H NMR (DMSO-d_6, 500.13 MHz) δ_H (ppm): 7.14 (1H, d, *J*= 8.2 Hz, H-11), 6.96 (1H,br d, *J*= 8.2 Hz, H-12), 6.84 (1H, br s, H-14), 2.81-2.77 (3H, m, CH_2-7, H-15), 2.28 (1H, br d, *J*= 12.8 Hz, H-1a), 2.03 (1H, br d, *J*= 12.4 and 1.3 Hz, H-5), 1.74-1.70 (3H, m, H-6a, H-2a, H-3a), 1.65 (1H, m, H-2b), 1.56 (1H, br d, *J*= 9.9Hz, H-3b), 1.44 (1H, br dd, *J*=12.0 and 7.0 Hz, H-6b), 1.30 (1H, m, H-1b),1.17 (6H, d, *J*= 6.9 Hz, CH_3-16, CH_3-17), 1.16 (3H, m, CH_3-19), 1.13 (3H, s, CH_3-20); ^{13}C NMR (DMSO-d_6, derived from multiplicity-edited HSQC and HMBC spectra) δ_C (ppm): 180.1 (C, C-18), 147.3 (C, C-9), 145.5 (C, C-13), 134.4 (C, C-8), 126.9 (CH, C-14), 124.2 (CH, C-11), 124.0 (CH, C-12), 47.1 (C, C-4), 45.2 (CH, C-5), 38.3 (CH_2, C-1), 37.7 (C, C-10), 36.8 (CH_2, C-3), 33.2 (CH, C-15), 29.9 (CH_2, C-7), 25.1 (CH_3, C-20), 24.3 (CH_3, C-16/C-17), 21.4 (CH_2, C-6), 18.6 (CH_2, C-2), 17.0 (CH_3, C-19). HR-ESIMS *m/z* 301.2161 $[M+H]^+$ (calcd for $C_{20}H_{29}O_2$, 301.2162).

*2.5.2. Incensole (**2**)*: ^{1}H NMR (DMSO-d_6, 500.13 MHz) δ_H (ppm): 5.05 (1H, t, *J*= 7.0 Hz, H-3), 5.00 (1H, t, *J*= 6.8 Hz, H-7), 3.10 (1H, d, *J*= 9.9 Hz, H-11), 2.12-1.96 (9H, m, CH_2-6, H-2a, H-13a, CH_2-5, H-2b, CH_2-9), 1.83 (1H, sept, *J*= 6.7 Hz, H-15), 1.76 (1H, m, H-14a), 1.64 (1H, dd, *J*= 13.0 and 3.0 Hz, H-10a), 1.60-1.50 (5H, m, H-13b, CH_3-19, H-14b), 1.47 (3H, s, CH_3-18), 1.25 (1H, m, H-10b), 0.98 (3H, s, CH_3-20), 0.87 and 0.86 (6H, each d, *J*= 6.8 Hz, CH_3-16, CH_3-17); ^{13}C NMR (DMSO-d_6, derived from multiplicity-edited HSQC and HMBC spectra) δ_C (ppm): 134 (C, C-8), 133.5 C-4, 124.7 (CH, C-7), 122.2 (CH, C-3), 87.8 (C, C-1), 85.0 (C, C-12), 73.7 (CH, C-11), 38.6 (CH_2, C-5), 36.3 (CH_2, C-13), 35.1 (CH, C-15), 33.8 (CH_2, C-9), 32.2 (CH_2, C-2), 30.7 (CH_2, C-14), 30.1 (CH_2, C-10), 24.7 (CH_2, C-6), 21.4 (CH_3, C-20), 18.4 ($3CH_3$, C-16, C-17, C-19), 16.3 (CH_3, C-18). HR-ESIMS *m/z* 307.2663 $[M+H]^+$ (calcd for $C_{20}H_{35}O_2$, 307.2632)

*2.5.3. 3α-acetoxy-11-keto-β-boswellic acid (AKBA) (**3**)*: ^{1}H NMR (methanol-d_4, 500.13 MHz) δ_H (ppm): 5.52 (1H, s, H-12), 5.27 (1H, t, *J*= 2.7 Hz, H-3), 2.49 (1H, br s,H-9), 2.46 (1H, m, H-1a), 2.27 (1H, tt, *J*= 14.8, 3.4 Hz, H-2a), 2.17 (1H, td, *J*= 13.7, 5.4 Hz, H-16a), 2.07 (3H, s, CH_3-2'), 2.00-1.90 (2H, m, H-6a, H-15a), 1.78 (1H, m, H-6b), 1.72 (1H, m, H-7a), 1. 60-1.32 (12H, m, H-18, H-2b, H-22a, H-19, H-7b, H-21a, H-5, H-22b, CH_3-27, H-21b), 1. 32-1.23 (2H, m, H-15b and H-1b), 1.20 (3H, s, CH_3-26), 1.18 (3H, s, H-23), 1.17 (3H, s, CH_3-25), 1.05 (1H, m, H-16b), 0.97 (4H, br s, H-20, CH_3-30), 0.86 (3H, s, CH_3-28), 0.83 (3H, d, *J*= 6.4 Hz, CH_3-29); ^{13}C NMR (DMSO-d_6, derived from multiplicity-edited HSQC and HMBC spectra) δ_C (ppm): 200.6 (C, C-11), 179.0 (C, C-24), 171.0 (C, C-1'), 166.2 (C, C-13), 129.9 (CH, C-12), 73.3 (CH, C-3), 60.2 (CH, C-9), 59.8 (CH, C-18), 50.3 (CH, C-5), 46.3 (C, C-4), 44.8 (C, C-8), 43.8 (C, C-14), 40.4 (CH_2, C-22), 39.2 (CH, C-19), 39.1 (CH, C-20), 37.3 (C, C-10), 34.7 (CH_2, C-1), 33.6 (C, C-17), 32.2 (CH_2, C-7), 30.6 (CH_2, C-21), 28.0 (CH_3, C-28), 27.1 (CH_2, C-16), 26.8 (CH_2, C-15), 23.2 (CH_2, C-2), 23.1 (CH_3, C-23), 19.9 (CH_3, C-30), 19.8 (CH_3, C-2'), 19.5 (CH_3, C-27), 18.4 (CH_2, C-6), 17.7 (CH_3, C-26), 16.4 (CH_3, C-29),12.6 (CH_3, C-25). HR-ESIMS *m/z* 535.3412 $[M+Na]^+$ (calcd for $C_{32}H_{48}NaO_5$, 535.3394)

Further purification of compounds **1-3** for activity assessment was achieved by submitting fractions F, G, and J to preparative HPLC separation, using solvents C and D as eluents. Samples were run under isocratic conditions (87% C, 20 min). The flow rate was 20 mL/min. Stock solutions in DMSO (150 mg/mL) were prepared and repeatedly injected in portions of 200-400 μL. Compounds **1** (3.13 mg), **2** (10 mg), and **3** (4 mg) were obtained from fractions G (35 mg), F (200 mg), and J (50 mg), respectively.

2.6. Expression of $GABA_A$ Receptors

Stage V-VI oocytes from *Xenopus laevis* were prepared, and cRNA was injected as previously described [24]. Female *Xenopus laevis* (NASCO, Fort Atkinson, WI) were anesthetized by exposing them for 15 min to a 0.2% MS-222 (methane sulfonate salt of 3-aminobenzoic acid ethyl ester, Sigma) solution before surgically removing parts of the ovaries. Follicle membranes from isolated oocytes were enzymatically digested with 2 mg/mL collagenase from *Clostridium histolyticum* (Type 1A, Sigma). Synthesis of capped runoff poly(A+) cRNA transcripts was obtained from linearized cDNA templates (pCMV vector). Directly after enzymatic isolation, the oocytes were injected with 50 nL of DEPC-treated water (Sigma) containing different cRNAs at a concentration of approximately 300-3000 pg/nL per subunit. The amount of injected cRNA mixture was determined by means of a NanoDrop ND-1000 (Kisker Biotech). To ensure expression of the gamma subunit in $\alpha_1\beta_2\gamma_{2S}$ receptors, rat cRNAs were mixed in a 1:1:10 ratio. Oocytes were then stored at 18 °C in ND96 solution containing 1% of penicillin-streptomycin solution (Sigma-Aldrich). Voltage clamp measurements were performed between days 1 and 5 after cRNA injection.

2.7 Positive control

Diazepam (7-chloro-1,3-dihydro-1-methyl-5-phenyl-2H-1,4-benzodiazepin-2-one, Sigma, purity not less than 98%) was used as positive control. At 1 μM diazepam enhanced I_{GABA} up to 231.3 ± 22.6% (n=3). See also S1, supporting information.

2.8. Two-Microelectrode Voltage Clamp Studies

Electrophysiological experiments were performed by the two-microelectrode voltage clamp method making use of a TURBO TEC 03X amplifier (npi electronic GmbH) at a holding potential of -70 mV and pCLAMP 10 data acquisition software (Molecular Devices). Currents were low-pass-filtered at 1 kHz and sampled at 3 kHz. The bath solution contained

90 mM NaCl, 1 mM KCl, 1 mM $MgCl_2$, 1 mM $CaCl_2$, and 5 mM HEPES (pH 7.4). Electrode filling solution contained 2 M KCl. Oocytes with maximal current amplitudes > 3 μA were discarded to exclude voltage clamp errors.

2.9. Fast Solution Exchange during I_{GABA} Recordings

Test solutions (100 μL) were applied to the oocytes at a speed of 300 μL/s by means of the ScreeningTool automated fast perfusion system [15]. In order to determine GABA EC_{5-10} (typically between 3 and 10 μM for receptors of subunit composition $\alpha_1\beta_2\gamma_{2s}$), a dose-response experiment with GABA concentrations ranging from 0.1 μM to 1 mM was performed. Stock solution of the petroleum ether extract (10 mg/mL in DMSO) was diluted to a concentration of 100 μg/mL with bath solution containing GABA EC_{5-10} according to a validated protocol [24]. As previously described, microfractions collected from the semi-preparative HPLC separations were dissolved in 30 μL of DMSO and subsequently mixed with 2.97 mL of bath solution containing GABA EC_{5-10} [24]. Stock solutions of compounds **1-3** (100 mM in DMSO) were diluted to a concentration of 100 μM with bath solution containing GABA EC_{5-10} for measuring modulation of $GABA_A$Rs. For concentration-response experiments, the stock solution of DHA (**1**) was diluted to concentrations of 0.1, 1.0, 3.0, 10, 30, 100, and 300 μM with bath solution for measuring direct activation, or with bath solution containing GABA EC_{5-10} for measuring receptor modulation. The final DMSO concentration in all the samples including the GABA control samples was adjusted to 1% to avoid solvent effect at the receptors.

2.10. Data Analysis

Enhancement of the I_{GABA} was defined as $I_{(GABA+Comp)}/I_{GABA} - 1$, where $I_{(GABA+Comp)}$ is the current response in the presence of a given compound, and I_{GABA} is the control GABA-

induced chloride current. Data were analyzed using the ORIGIN 7.0 SR0 software (OriginLab Corporation) and are given as mean ± S.E. of at least two oocytes and ≥ 2 oocyte batches.

3. Results and Discussion

At a test concentration of 100 μg/mL, the petroleum ether extract of *B. thurifera* resin enhanced I_{GABA} by 319.8% ± 79.8% through $GABA_ARs$ with $\alpha_1\beta_2\gamma_{2s}$ subunit composition. Active compounds were tracked with the aid of a validated protocol for HPLC-based activity profiling [24]. The chromatogram (210 - 700 nm) of a semipreparative HPLC separation (10 mg of extract) and the corresponding activity profile (24 microfractions of 90 s each) are shown in Figure 1. Fractions 15, 16, and 17 potentiated I_{GABA} by 172.8% ± 49.5%, 344.3% ± 78.5%, and 119.7% ± 20.7%, respectively. Optimization of separation conditions enabled resolution of peaks in the active time window (indicated with roman numbers in Fig. 1). Therefore, peak I was resolved into compounds **1** and **2**, and compound **3** was the main constituent of peak II.

To obtain the active compounds in sufficient amounts for structure elucidation and pharmacological testing, a targeted preparative isolation was carried out, combining flash chromatography on silica gel with subsequent purification by semipreparative and preparative HPLC. Two diterpenes, dehydroabietic acid (**1**) and incensole (**2**), and the triterpene AKBA (**3**) (Fig. 2) were identified with the aid of ESI-TOF-MS, 1D and 2D microprobe NMR, and by comparison with published data [25–27]. Spectroscopic data of **1-3** are available as supporting information. The three compounds have been previously reported from olibanum, although not specifically from the resin of *Boswellia thurifera*.

Compounds **1-3** were tested at a concentration of 100 μM in the oocyte assay, for a preliminary assessment of their activity in $\alpha_1\beta_2\gamma_{2s}$ $GABA_ARs$ (Table 1). Only DHA (**1**) modulated the receptors (potentiation of I_{GABA} of 682.3% ± 44.7%), while incensole and AKBA were inactive (enhancements of −13.9% ± 3.2% and −19.8% ± 4.5%, respectively)

(Fig. 3A). Thus, further concentration-response experiments were performed only with DHA at concentrations ranging from 0.1 to 300 μM. In $GABA_A$Rs of $\alpha_1\beta_2\gamma_{2s}$ subunit composition DHA enhanced I_{GABA} in a concentration-dependent manner (Figure 3B). At a GABA EC_{5-10}, maximal potentiation of I_{GABA} (397.5% ± 34.0%) was observed at ~100 μM, with an EC_{50} of 8.7 μM ± 1.3 μM. Direct activation of the receptor was observed at DHE concentrations higher than 30 μM suggesting partial agonism. This suggests that the mechanism of action involves allosteric receptor modulation rather than direct agonistic activity (Fig. 3C).

Due to their toxicity to fish, DHA and other abietane monocarboxylic acids (resin acids) have been studied for their potential effect on the CNS. DHA was shown to induce release of GABA from nerve terminals in trout brain synaptosomes, while 12,14-dichlorodehydroabietic acid inhibited I_{GABA} in patch-clamped rat cortical neurons. However, modulatory effects on the GABAergic system have been suggested to be secondary to the elevation in cytoplasmic Ca^{2+} induced by these compounds [28,29]. This work constitutes the first report on $GABA_A$ receptor modulatory properties of the abietane diterpene DHA. Pimarane type diterpenoids ,closely related to the abietanes, have been previously identified in our research group as a structural scaffold for $GABA_A$ receptor modulators [30]. However, the potency of DHA on receptors of the subtype $\alpha_1\beta_2\gamma_{2s}$ was higher than that of isopimaric acid (EC_{50} 141.6 μM ± 96.5 μM) and sandaracopimaric acid (EC_{50} 33.3 μM ± 8.7 μM), suggesting that an aromatic ring C is favorable for increasing potency of this scaffold. However, more compounds need to be tested for establishing structure-activity relationships for these diterpenoids. DHA also showed higher potency than the labdane diterpenoids zerumin A (EC_{50} 24.9 μM ± 8.8 μM) and coronarin D (EC_{50} 35.7 μM ± 8.8 μM).[17]. However, the potency of DHA is significantly lower than that of classical BDZs like

triazolam, clotiazepam, and midazolam, which modulate $GABA_A$Rs at nanomolar concentrations [31].

The physicochemical properties of dehydroabietic acid are favorable for oral bioavailability and BBB permeation [32,33]. In fish, the compound has been found to be readily absorbed, and distributed to most organs, including the brain [29]. Although the toxicity observed in fish is a potential liability for DHA [28,34], i*n vitro* and *in vivo* pharmacological and pharmacokinetic studies with the compound should be performed to explore the potential of this scaffold as a starting point for medicinal chemistry.

4. Conclusions

HPLC-based activity profiling of olibanum from *Boswellia thurifera* led to the identification of dehydroabietic acid as a positive allosteric modulator of $GABA_A$Rs of the subtype $\alpha_1\beta_2\gamma_{2s}$ that additionally displays properties of a partial agonist. The EC_{50} of DHA was lower than for other diterpenes (e.g. sandaracopimaric acid), indicating higher affinity to the receptor, even though far from the affinity of BDZs. Further assessment of subunit selectivity and activity *in vivo* are needed.

The terpenoids AKBA and incensole have also been isolated from the active time window of the extract, but were lacking $GABA_A$ receptor modulatory properties. Anxiolytic effects in behavioral models have been reported for incensole acetate, but were attributed to activation of TRPV3 channels in the brain [1]. At this point the potential CNS modulating effects of frankincense are still a matter of speculation.

Acknowledgements

Financial support was provided by the Swiss National Science Foundation through project 205320_126888 (MH). D.C. Rueda thanks the Department of Education of Canton Basel (Erziehungsdepartement des Kantons Basel-Stadt) for a fellowship granted in 2012. This work was supported by the Austrian Science Fund (FWF doctoral program “Molecular drug targets” W1232 to S.H).

References

[1] Moussaieff A, Mechoulam R. *Boswellia* resin: from religious ceremonies to medical uses; a review of in-vitro, in-vivo and clinical trials. J Pharm Pharmacol 2009;61:1281–93.

[2] Mothana RAA, Hasson SS, Schultze W, Mowitz A, Lindequist U. Phytochemical composition and in vitro antimicrobial and antioxidant activities of essential oils of three endemic Soqotraen *Boswellia* species. Food Chem 2011;126:1149–54.

[3] Fu-Shuang L, Dong-Lan Y, Rang-Ru L, Kang-Ping X, Gui-Shan T. Chemical constituents of *Boswellia carterii* (Frankincense). Chin J Nat Med 2010;8:25–7.

[4] Yoshikawa M, Morikawa T, Oominami H, Matsuda H. Absolute stereostructures of olibanumols A, B, C, H, I, and J from olibanum, gum-resin of *Boswellia carterii*, and inhibitors of nitric oxide production in lipopolysaccharide-activated mouse peritoneal macrophages. Chem Pharm Bull (Tokyo) 2009;57:957–64.

[5] Al-Harrasi A, Al-Saidi S. Phytochemical Analysis of the Essential Oil from Botanically Certified Oleogum Resin of *Boswellia sacra* (Omani Luban). Molecules 2008;13:2181–9.

[6] Hamm S, Bleton J, Connan J, Tchapla A. A chemical investigation by headspace SPME and GC–MS of volatile and semi-volatile terpenes in various olibanum samples. Phytochemistry 2005;66:1499–514.

[7] Banno N, Akihisa T, Yasukawa K, Tokuda H, Tabata K, Nakamura Y, et al. Anti-inflammatory activities of the triterpene acids from the resin of *Boswellia carterii*. J Ethnopharmacol 2006;107:249–53.

[8] Chinese Pharmacopoeia Commission. Pharmacopoeia of the People's Republic of China, vol. I. China Medical Science Press, Beijing (English edition); 2010.

[9] European Scientific Cooperative on Phytotherapy. Olibanum indicum. ESCOP Monogr. Second Ed. Suppl. 2009, ESCOP & Thieme; 2009, p. 184–97.

[10] Van Vuuren SF, Kamatou GPP, Viljoen AM. Volatile composition and antimicrobial activity of twenty commercial frankincense essential oil samples. Chem Divers Biol Funct Plant Volatiles 2010;76:686–91.

[11] Tucker A. Frankincense and myrrh. Econ Bot 1986;40:425–33.

[12] Olsen RW, Sieghart W. International Union of Pharmacology. LXX. Subtypes of γ-Aminobutyric Acid A Receptors: Classification on the Basis of Subunit Composition, Pharmacology, and Function. Update. Pharmacol Rev 2008;60:243–60.

[13] Rudolph U, Knoflach F. Beyond classical benzodiazepines: novel therapeutic potential of GABAA receptor subtypes. Nat Rev Drug Discov 2011;10:685–97.

[14] Tan KR, Rudolph U, Lüscher C. Hooked on benzodiazepines: GABAA receptor subtypes and addiction. Trends Neurosci 2011;34:188–97.

[15] Baburin I, Beyl S, Hering S. Automated fast perfusion of *Xenopus* oocytes for drug screening. Pflüg Arch - Eur J Physiol 2006;453:117–23.

[16] Potterat O, Hamburger M. Concepts and technologies for tracking bioactive compounds in natural product extracts: generation of libraries, and hyphenation of analytical processes with bioassays. Nat Prod Rep 2013;30:546.

[17] Schramm A, Ebrahimi SN, Raith M, Zaugg J, Rueda DC, Hering S, et al. Phytochemical profiling of *Curcuma kwangsiensis* rhizome extract, and identification of labdane diterpenoids as positive GABAA receptor modulators. Phytochemistry 2013;96:318–29.

[18] Zaugg J, Eickmeier E, Ebrahimi SN, Baburin I, Hering S, Hamburger M. Positive GABAA Receptor Modulators from *Acorus calamus* and Structural Analysis of (+)-Dioxosarcoguaiacol by 1D and 2D NMR and Molecular Modeling. J Nat Prod 2011;74:1437–43.

[19] Zaugg J, Eickmeier E, Rueda DC, Hering S, Hamburger M. HPLC-based activity profiling of *Angelica pubescens* roots for new positive GABAA receptor modulators in Xenopus oocytes. Fitoterapia 2011;82:434–40.

[20] Zaugg J, Ebrahimi SN, Smiesko M, Baburin I, Hering S, Hamburger M. Identification of GABAA receptor modulators in *Kadsura longipedunculata* and assignment of absolute configurations by quantum-chemical ECD calculations. Phytochemistry 2011;72:2385–95.

[21] Zaugg J, Baburin I, Strommer B, Kim H-J, Hering S, Hamburger M. HPLC-Based Activity Profiling: Discovery of Piperine as a Positive $GABA_A$ Receptor Modulator Targeting a Benzodiazepine-Independent Binding Site. J Nat Prod 2010;73:185–91.

[22] Li Y, Plitzko I, Zaugg J, Hering S, Hamburger M. HPLC-Based Activity Profiling for GABAA Receptor Modulators: A New Dihydroisocoumarin from *Haloxylon scoparium*. J Nat Prod 2010;73:768–70.

[23] Yang X, Baburin I, Plitzko I, Hering S, Hamburger M. HPLC-based activity profiling for GABAA receptor modulators from the traditional Chinese herbal drug Kushen (*Sophora flavescens root*). Mol Divers 2011;15:361–72.

[24] Kim H, Baburin I, Khom S, Hering S, Hamburger M. HPLC-Based Activity Profiling Approach for the Discovery of GABAA Receptor Ligands using an Automated Two Microelectrode Voltage Clamp Assay on *Xenopus* Oocytes. Planta Med 2008;74:521–6.

[25] González MA, Pérez-Guaita D, Correa-Royero J, Zapata B, Agudelo L, Mesa-Arango A, et al. Synthesis and biological evaluation of dehydroabietic acid derivatives. Eur J Med Chem 2010;45:811–6.

[26] Corsano S, Nicoletti R. The structure of incensole. Tetrahedron 1967;23:1977–84.

[27] Belsner K, Büchele B, Werz U, Syrovets T, Simmet T. Structural analysis of pentacyclic triterpenes from the gum resin of *Boswellia serrata* by NMR spectroscopy. Magn Reson Chem 2003;41:115–22.

[28] Lees G, Coyne L, Zheng J, Nicholson RA. Mechanisms for resin acid effects on membrane currents and GABAA receptors in mammalian CNS. Environ Toxicol Pharmacol 2004;15:61–9.

[29] Zheng J, Nicholson RA. Influence of Two Naturally Occurring Abietane Monocarboxylic Acids (Resin Acids) and a Chlorinated Derivative on Release of the Inhibitory Neurotransmitter| γ-Aminobutyric Acid from Trout Brain Synaptosomes. Bull Environ Contam Toxicol 1996;56:114–20.

[30] Zaugg J, Khom S, Eigenmann D, Baburin I, Hamburger M, Hering S. Identification and characterization of GABAA receptor modulatory diterpenes from *Biota orientalis* that decrease locomotor activity in mice. J Nat Prod 2011;74:1764–72.

[31] Khom S, Baburin I, Timin EN, Hohaus A, Sieghart W, Hering S. Pharmacological properties of GABAA receptors containing γ1 subunits. Mol Pharmacol 2006;69:640–9.

[32] Pajouhesh H, Lenz GR. Medicinal chemical properties of successful central nervous system drugs. NeuroRx 2005;2:541–53.

[33] Lipinski CA. Lead- and drug-like compounds: the rule-of-five revolution. Drug Discov Today Technol 2004;1:337–41.

[34] San Feliciano A, Gordaliza M, Salinero M, del Corral J. Abietane Acids: Sources, Biological Activities, and Therapeutic Uses. Planta Med 2007;59:485–90.

Table 1. Potentiation of I_{GABA} in $\alpha_1\beta_2\gamma_{2s}$ receptors by compounds **1-3**, at a test concentration of 100 μM.

Compound	*Maximal potentiation of I_{GABA} (%)*[a]
1	682.3 ± 44.7
2	-13.9 ± 3.2
3	-19.8 ± 4.5
Diazepam (1 μM)[b]	231.3 ± 22.6

(a) Modulation measured in 4 oocytes from 3 different batches.
(b) Positive control.

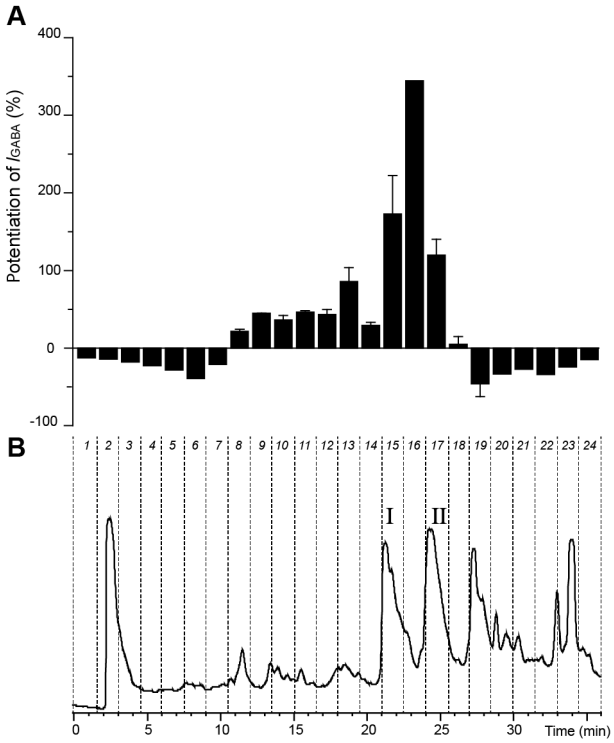

Figure 1. HPLC-based activity profiling of the petroleum ether extract $GABA_A$ receptor modulatory activity. **A.** Potentiation of the I_{GABA} by each microfraction (error bars correspond to S.E.). **B.** HPLC chromatogram (210-700 nm) of a semipreparative separation of 10 mg of extract. The 24 time-based fractions of 90 s each are indicated with dashed lines. Peaks contained in the active time window of the extract are indicated as I and II. After optimization of separation conditions, peak I was resolved into compounds **1** and **2**. Compound **3** was the main constituent of peak II.

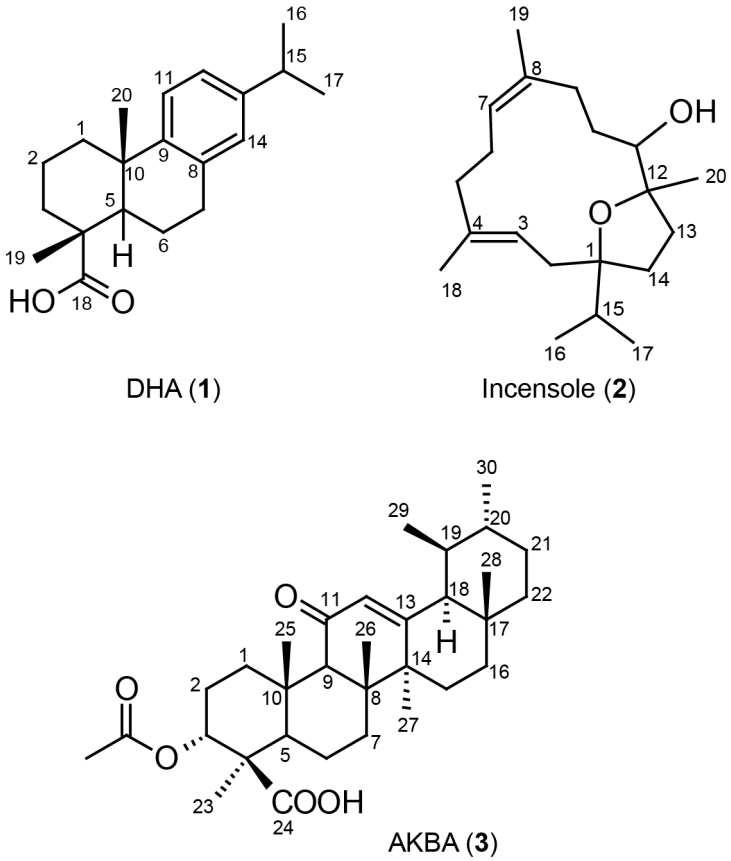

Figure 2. Chemical structures of compounds **1**-**3**.

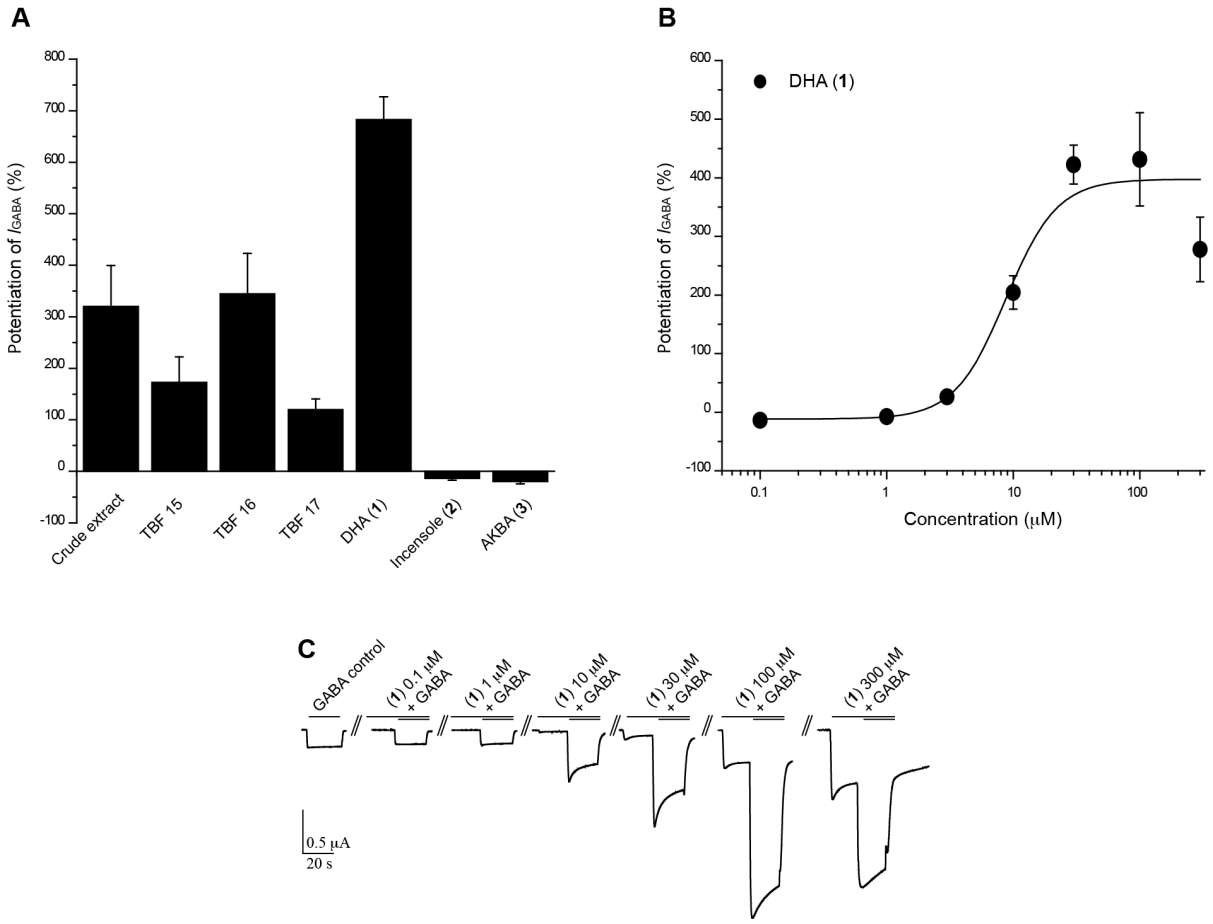

Figure 3. **A.** Potentiation of I_{GABA} by the petroleum ether extract (100 μg/mL), by time-based fractions 15-17, and by compounds **1-3** (100 μM). **B.** Concentration-response curve for compound **1** on $GABA_ARs$ of the subunit composition $\alpha_1\beta_2\gamma_{2S}$. **C.** Typical traces for modulation of I_{GABA} by compound **1**. Please note the pronounced activation of the receptor in the absence of GABA at DHA concentrations > 30 μM. All experiments were carried out using a GABA EC_{5-10}.

Supporting Information

Identification of dehydroabietc acid from *Boswellia thurifera* resin as a positive $GABA_A$ receptor modulator

Diana C. Rueda[a], Melanie Raith[a], Maria De Mieri[a], Angela Schöffmann[b], Steffen Hering[b], and Matthias Hamburger[a,*]

[a] *Division of Pharmaceutical Biology, University of Basel, Klingelbergstrasse 50, CH-4056 Basel, Switzerland*

[b] *Institute of Pharmacology and Toxicology, University of Vienna, Althanstrasse 14, A-1090 Vienna, Austria*

* Corresponding author. Tel.: +41-61-2671425; fax: +41-61-2671474.

E-mail: matthias.hamburger@unibas.ch

S1. Diazepam (1 μM) enhanced I_{GABA} through $\alpha_1\beta_2\gamma_{2S}$ $GABA_A$ receptors and was therefore used as positive control for the assay. Currents in the presence of GABA ($EC_{5\text{-}10}$, single bar, control) and during co-application of GABA and diazepam (1 μM, double bar) are shown. At 1 μM diazepam enhanced I_{GABA} up to 231.3 ± 22.6% (n=3).

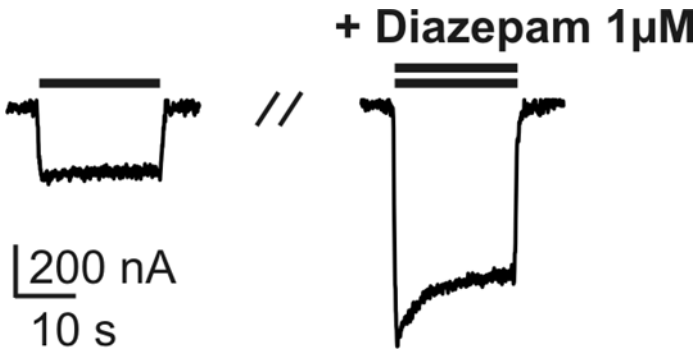

S2. Compounds isolated from *B. thurifera* resin, petroleum ether extract.

	Trivial name	CAS Nr.	MF	Formula weight	Structure
1	Dehydroabietic acid	1740-19-8	$C_{20}H_{28}O_2$	300.44	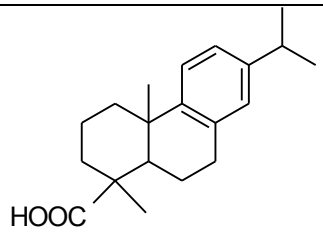
2	Incensole	22419-74-5	$C_{20}H_{34}O_2$	306.48	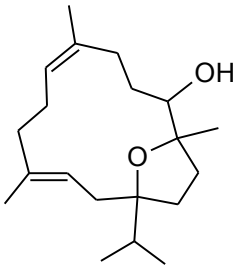
3	AKBA	67416-61-9	$C_{32}H_{48}O_5$	512.72	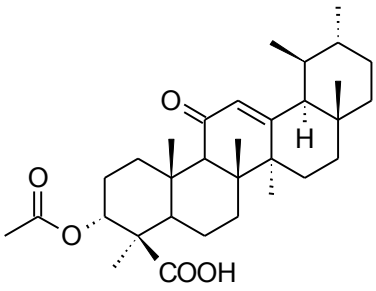

S3. ^{1}H-NMR spectrum (500 MHz in dmso-d_6) of DHA (**1**)

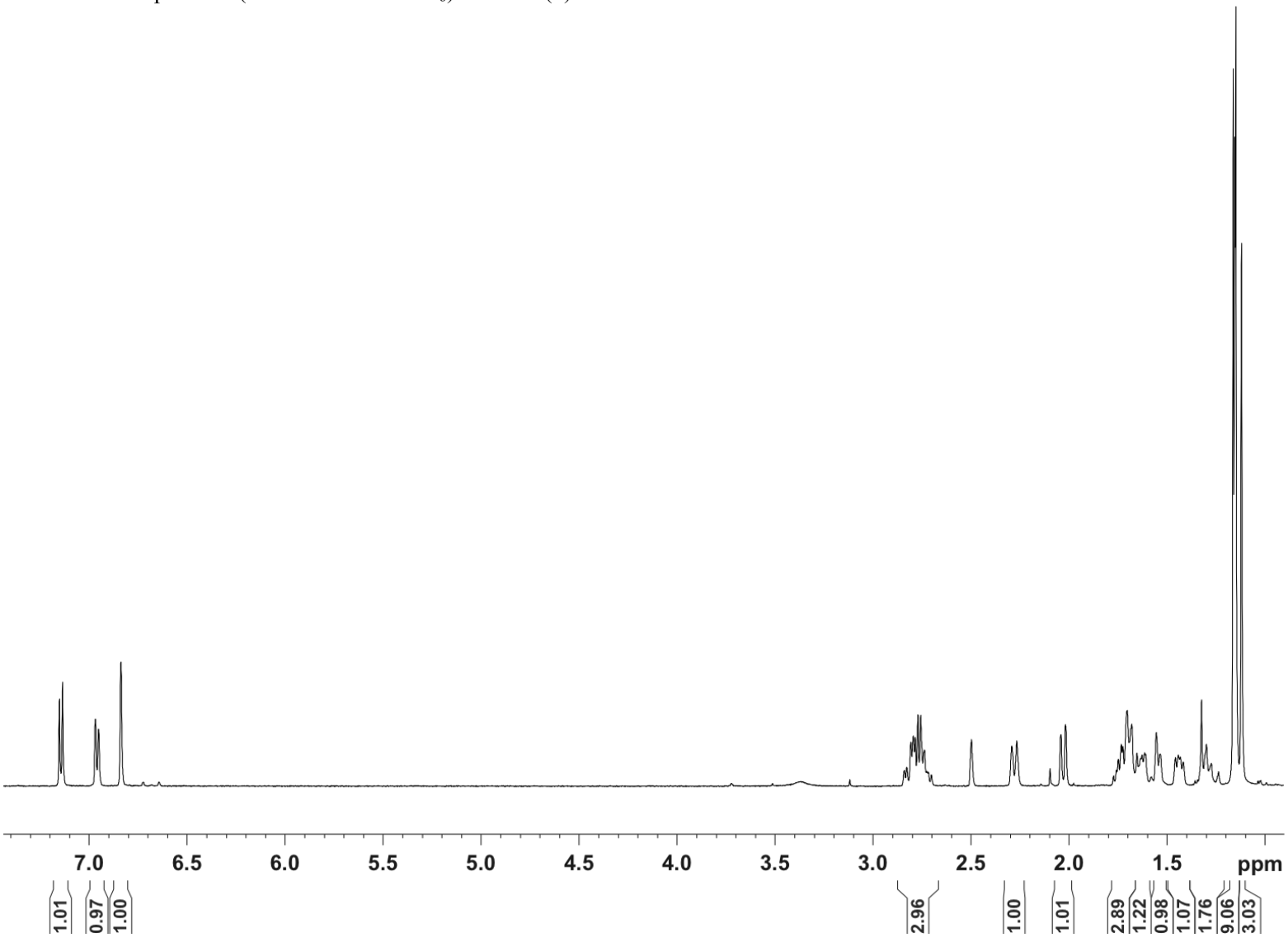

S4. ^{1}H-NMR spectrum (500 MHz in dmso-d_6) of incensole (**2**)

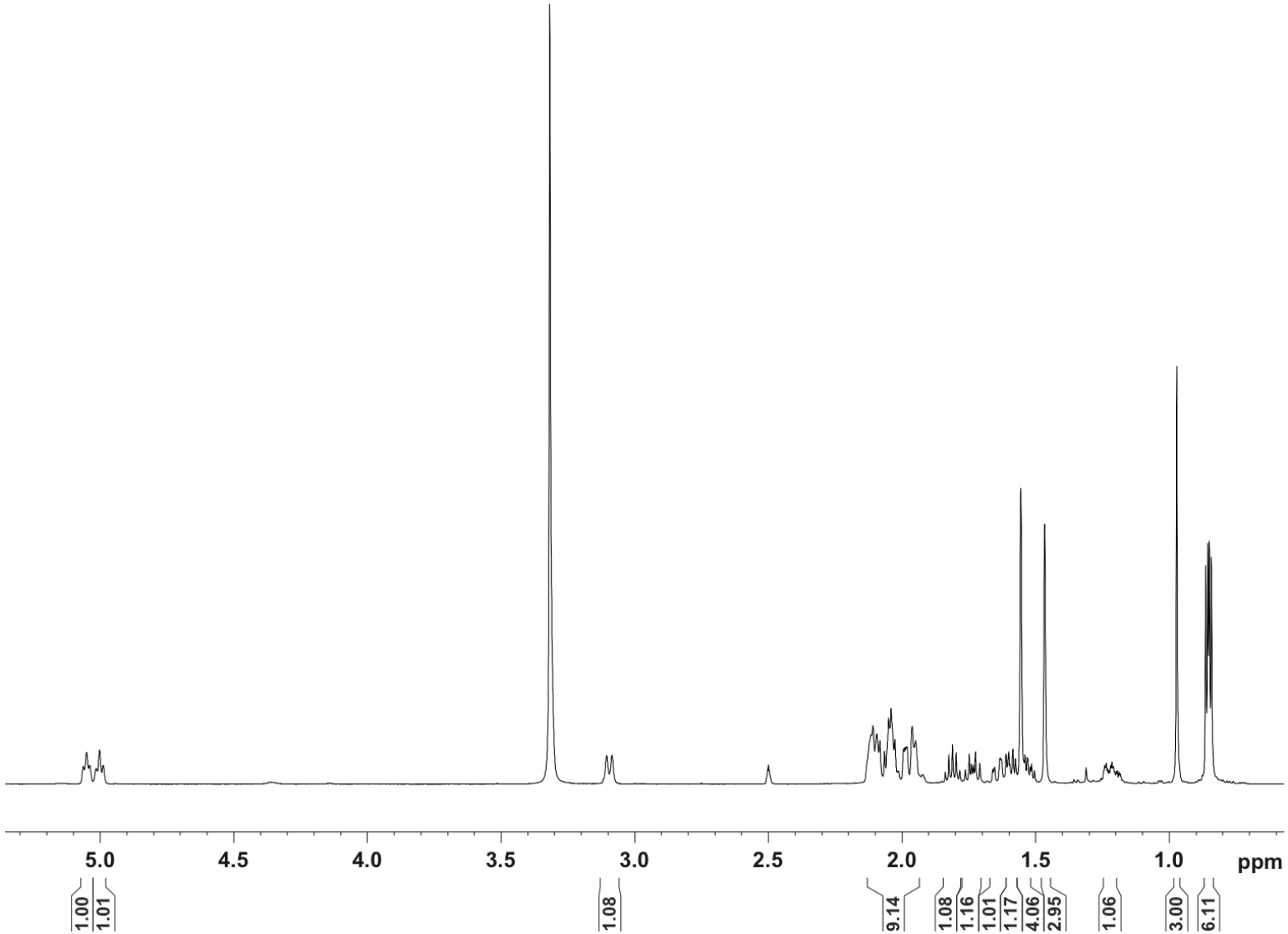

S5. ^{1}H-NMR spectrum (500 MHz in methanol-d_4) of AKBA (**3**)

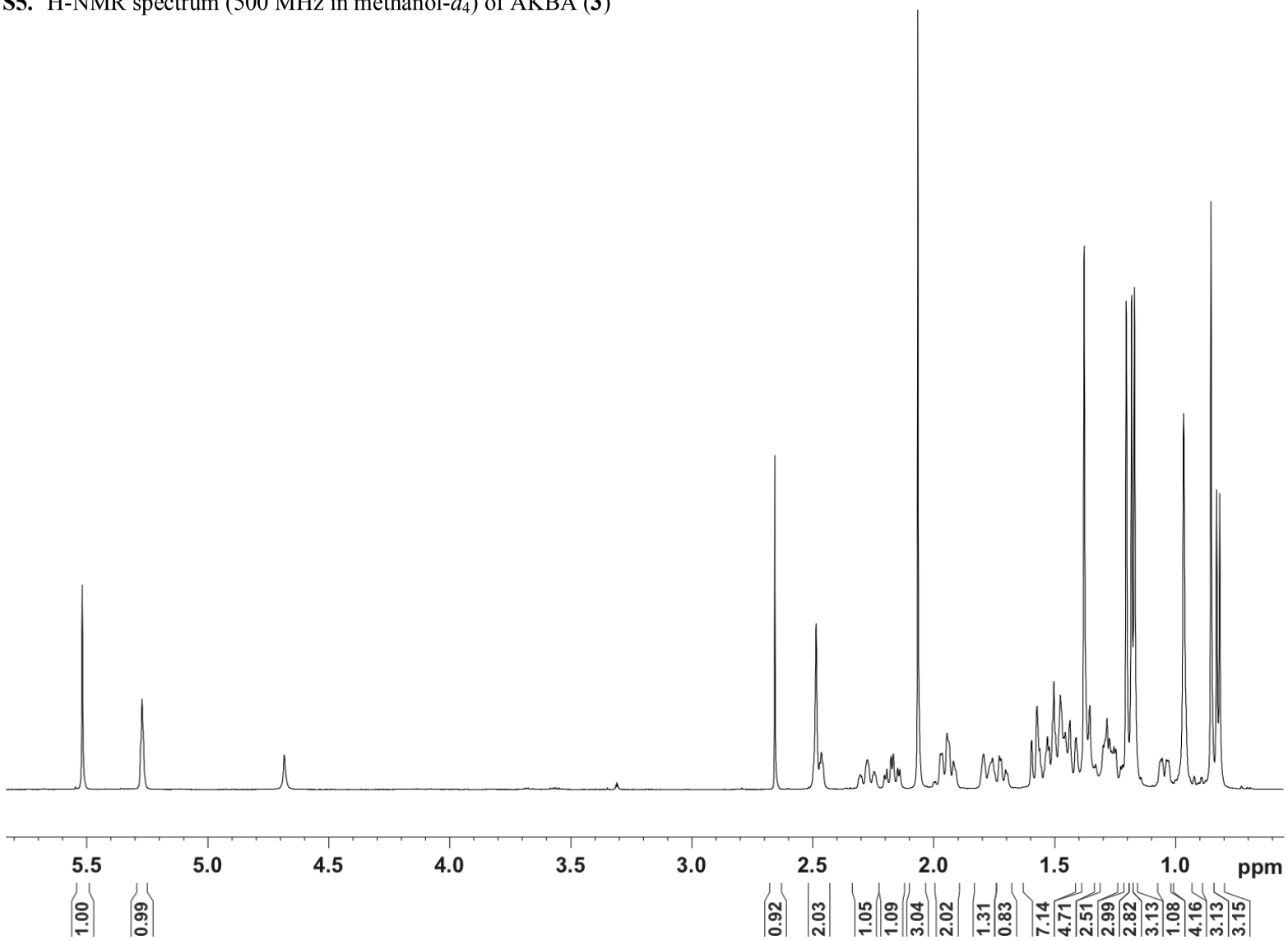

4. CONCLUSIONS AND OUTLOOK

In recent years, HPLC-based activity profiling [1] has been successfully applied in the identification of $GABA_AR$ modulators of natural origin [2–5]. In the present work, this approach was used to trace the $GABA_AR$ modulatory activity in the lipophilic extracts of *Pholidota chinensis* stems and roots, *Adenocarpus cincinnatus* roots and tubers, *Boswellia thurifera* resin, and a commercial sample of *Bupleurum chinense* roots. In every case, at least one NP with GABAergic properties was identified, proving once again the power of HPLC-based activity profiling in the targeted discovery of plant-derived $GABA_AR$ modulators. Furthermore, these results confirmed the value of ethnopharmacology as a refinement tool in NP research.

In the case of *Pholidota chinensis* (**Chapter 3.2**), HPLC-based activity profiling allowed us to identify the dihydrostilbene batatasin III (**1**) as a highly efficient $GABA_AR$ modulator. The lower activity of structurally related compounds in the extract, motivated us to test a series of stilbenes and their semisynthetic dihydro derivatives, in order to assess the role of conformational flexibility in the GABAergic properties of stilbenes. The results of this study enabled us to confirm flexibility as crucial for $GABA_AR$ modulation and to draw some preliminary structure-activity considerations that might be useful for further medicinal chemistry efforts on dihydrostilbenes (Figure 4.1).

HPLC-based activity profiling of *Adenocarpus cincinnatus* (**Chapter 3.3**) allowed us to localize the GABAergic activity in a rather complex extract. Fifteen flavonoid and isoflavonoid derivatives, including eight new natural products, were isolated from the active time window by means of diverse chromatographic techniques. Full structural characterization of all isolates was achieved by HR-TOF-MS, microprobe NMR, CD-spectroscopy, and polarimetry, which were ratified as key analytical tools in NP research during the course of this thesis. Twelve of the isolated compounds (**2**-**13**) (Figure 4.2) showed significant $GABA_AR$ modulation in the oocyte assay, at a concentration of 100 μM. Further concentration-response experiments led us to the identification of pterocarpans and isoflavones with potent $GABA_AR$ modulatory activity. Structural similarities among the diverse flavonoid and isoflavonoid scaffolds provided preliminary insights into some structural features favoring GABAergic properties (Figure 4.2).

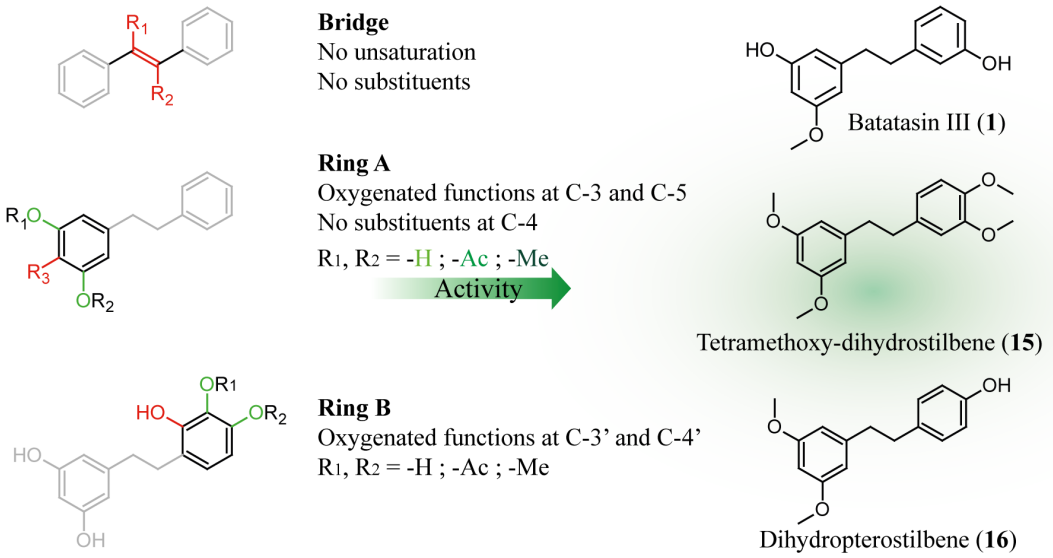

Figure 4.1. Dihydrostilbenes as modulators of $\alpha_1\beta_2\gamma_{2S}$ $GABA_ARs$. Structural features with positive effects on potency and efficiency are highlighted in green. Features with negative influence on $GABA_AR$ modulation are indicated in red. Compound **1** is a natural product, whereas **15** and **16** are the semisynthetic dihydro derivatives of tetramethoxy-piceatannol and pterostilbene, respectively.

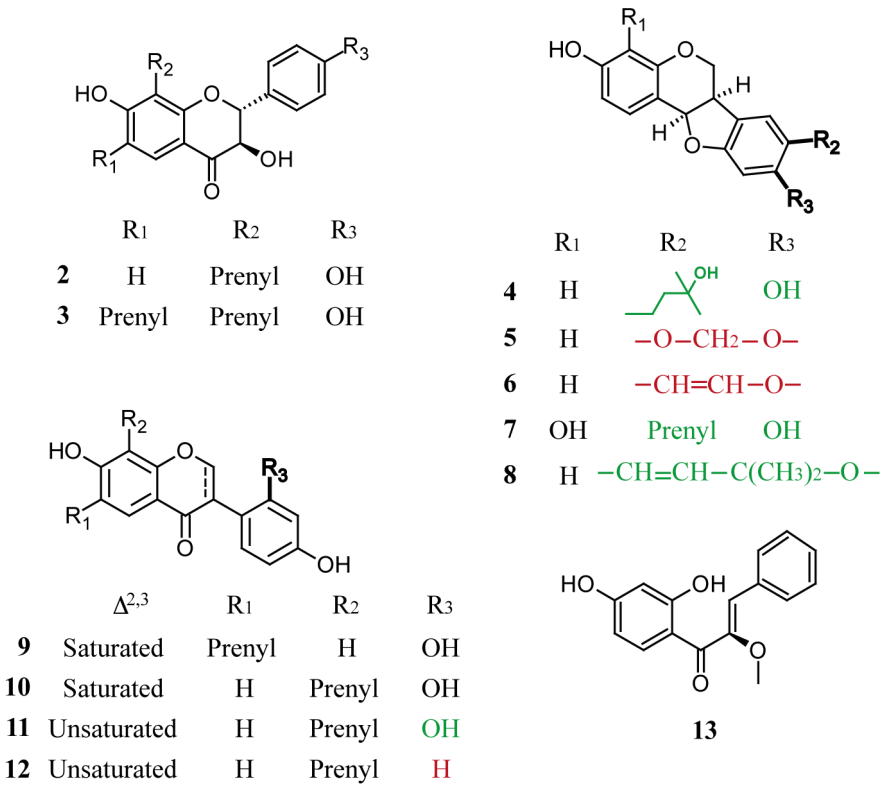

Figure 4.2. $GABA_AR$ modulators with dihydroflavonol (**2**, **3**), pterocarpan (**4**-**8**), isoflavanone (**9**, **10**), isoflavone (**11**, **12**), and chalcone (**13**) scaffolds, isolated from *A. cincinnatus*. Structural features with positive influence on potency and efficiency are indicated in green. Features with negative influence on $GABA_AR$ modulation are highlighted in red.

A $GABA_AR$ modulator bearing the abietane diterpene scaffold, i.e. DHA (**14**), was identified in *Boswellia thurifera* by means of HPLC-based activity profiling (**Chapter 3.4**, Figure 4.3). In the case of the commercial sample of *Bupleurum chinense* (**Chapter 3.1**), not only did HPLC-based activity profiling allow the identification of aristolactone as a mild $GABA_AR$ modulator, but it also led to the detection of a contaminant in the sample, raising concerns about adequate quality control of TCM drugs commercialized in Europe.

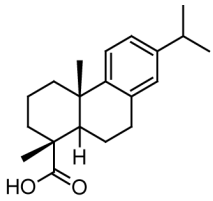

Dehydroabietic acid (14)

Figure 4.3. Dehydroabietic acid, an abietane diterpene with $GABA_AR$ modulatory activity, islated from *Boswellia thurifera*.

Altogether, as a result of this study three main novel scaffolds for $GABA_AR$ modulators were identified, i.e. dihydrostilbenes (**Chapter 3.2**; Figure 4.1), *cis*-pterocarpans (**Chapter 3.3**; Figure 4.2), and abietane diterpenes (**Chapter 3.4**; Figure 4.3). A number of $GABA_AR$ modulators belonging to the known flavonoid and isoflavonoid scaffold families were also isolated (**Chapter 3.3**; Figure 4.2). Most of the active compounds obtained in the course of this thesis meet all the requirements for oral absorption and BBB permeation described in Chapter 2.4 (Table 1), with the only exceptions of lespeflorin B_2 (**3**) and DHA (**14**), which violate Lipinski's RO5 in terms of lipophilicity. However, their cLogP values exceed only slightly the range dictated by the rule and thus, sufficient oral absorption can still be expected. Furthermore, only molecules showing 2 or more violations to the RO5 are predicted to have poor oral absorption (see Chapter 2.4).

Dihydrostilbene **1**, pterocarpans **4**, **7**, and **8**, and abietane diterpene **14** meet the requirements for relevant pharmacological hits for further optimization and development. They possess *i*) novel structural scaffolds for $GABA_AR$ modulators (Figures 4.1-4.3), *ii*) drug-like physicochemical properties for oral absorption and BBB permeation (Table 1), and *iii*) significant potency (EC_{50} value) and efficiency (maximal potentiation of I_{GABA}) at the target (Table 2, Figure 4.4). Isoflavone **11** complies with requirements (*ii*) and (*iii*). Although flavonoid and isoflavonoid derivatives **2**, **3**, **5**, **6**, **9**, **10**, **12**, and **13** do not meet requirement

(*i*), their physicochemical properties make them suitable candidates for further optimization. In this work, they were only tested at a single concentration (100 μM) in the oocyte assay and therefore potency and efficiency of their receptor modulation could not be calculated. However, their performance in single-concentration tests (enhancement of I_{GABA} > 190%), predicts adequate $GABA_AR$ modulation. Furthermore, promising GABAergic activity has been reported for structurally related compounds reported in **Chapter 3.3** and other works [6,7]. Concentration-response experiments will contribute to a better pharmacological characterization of these compounds as $GABA_AR$ modulators.

Table 1. Physicochemical properties of $GABA_AR$ modulators of natural origin isolated in this work.

Compound	H-acceptors	H-donnors	MW	cLogP[(a)]	Rotable bonds	PSA (Å^2)[(a)]
1	3	2	244.3	3.35	4	49.7
2	5	3	340.4	3.41	3	87.0
3	5	3	408.5	5.36	5	87.0
4	5	3	342.4	2.58	3	79.2
5	5	1	284.3	2.88	0	57.2
6	4	1	280.3	3.40	0	47.9
7	5	3	340.4	3.76	2	79.2
8	4	1	322.4	4.41	0	47.9
9,10	5	3	340.4	3.77	3	87.0
11	5	3	338.4	3.07	3	87.0
12	4	2	322.4	4.03	3	66.8
13	4	2	270.3	2.80	4	66.8
14	2	1	300.4	6.09	2	37.3

[(a)] cLogP and polar surface area (PSA) were calculated with ChemBioDraw Ultra 12.0 software (CambridgeSoft).

Table 2. Potency (EC_{50} value) and efficiency (maximal potentiation of I_{GABA}) of drug-like scaffolds isolated in this work, at $GABA_A$ receptors of the subtype $\alpha_1\beta_2\gamma_{2s}$.

Compound	EC_{50} (μM)	E_{max} (%)
1	52.5 ± 17.0	1512.9 ± 176.5
4	8.6 ± 1.6	640.0 ± 53.6
7	18.8 ± 2.3	491.0 ± 22.3
8	40.7 ± 4.08	771.1 ± 4.1
11	2.8 ± 1.4	552.7 ± 84.1
14	8.7 ± 1.3	397.5 ± 34.0

Compared to other receptor modulators of natural origin tested in the same *in vitro* model [3,8–12] (Figure 4.4), batatasin III (**1**) exhibited remarkably higher $GABA_AR$ modulatory efficiency. However, its EC_{50} is still far from the concentration range in which BZD exert their actions. In contrast, pterocarpan **4** and isoflavone **11** showed much higher potencies than average $GABA_AR$ modulators of natural origin (EC_{50} values below 10 µM), indicating higher binding affinity towards the receptor. Although their efficiencies were higher than those of BZDs, they were much lower than that of **1**. Potency of the abietane diterpene **14** was also below 10 µM, but its efficiency was lower than that of compounds **4** and **11**.

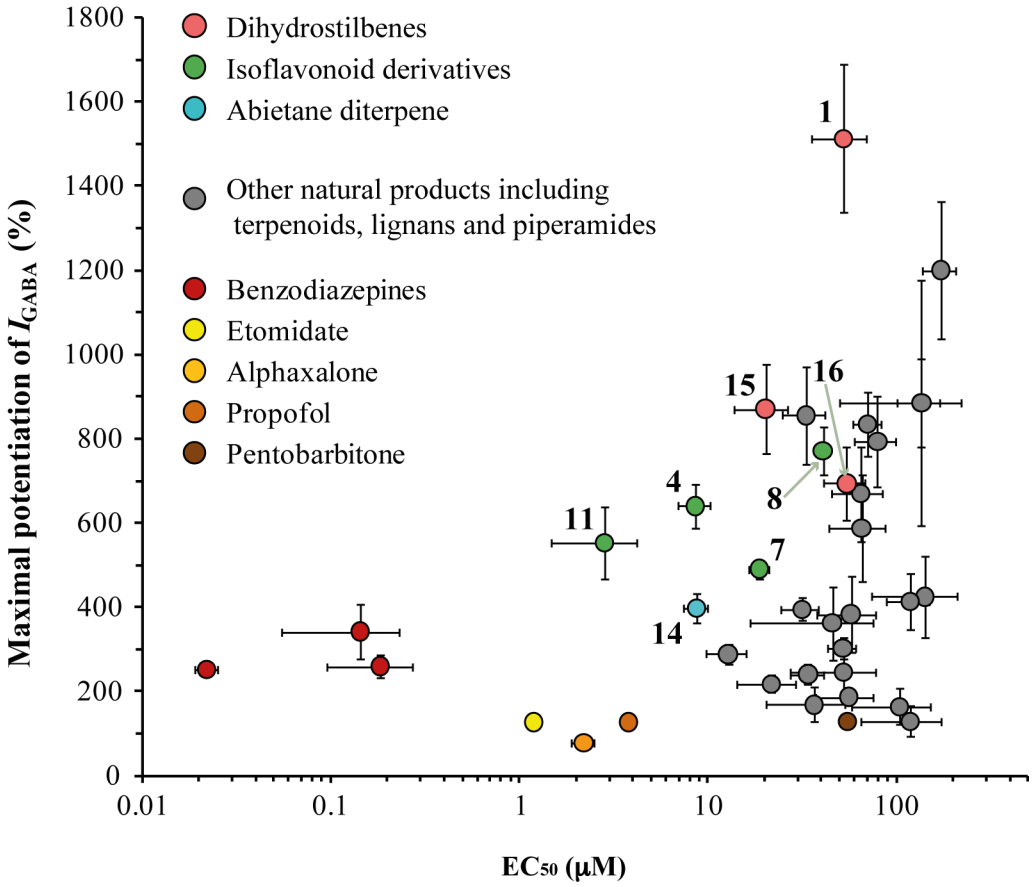

Figure 4.4. Overview of efficiency and potency of $GABA_AR$ modulation exerted by compounds isolated from *Pholidota chinensis* stems and rots, *Adenocarpus cincinnatus* roots and tubers, and *Boswellia thurifera* resin. Compounds are grouped according to their structures. Numbers indicate the compounds as shown in Figures 4.1-4.3. Compounds **15** and **16** are not NPs, but the semisynthetic dihydro derivatives of tetramethoxy-piceatannol and pterostilbene. Flavonoid and isoflavonoid derivatives **2**, **3**, **5**, **6**, **9**, **10**, **12**, and **13** (Figure 4.2) are not depicted, since their potencies and efficiencies were not determined. Potentiation on I_{GABA} was measured in $\alpha_1\beta_2\gamma_{2s}$ receptors, at a GABA $EC_{3\text{-}10}$. Data points in grey correspond to NPs isolated in previous works by Schramm et al. [3] and Zaugg et al. [8–12]. Reference data of benzodiazepines (triazolam, midazolam, clotiazepam) are taken from Khom et al. [13]. Etomidate and alphaxalone values were measured by Pau et al. [14]. Pentobarbitone was investigated by Thompson et al. [15], using a GABA EC_{20}, meaning that its efficiency is underestimated compared to the rest (adapted from Zaugg 2011 [2]).

As a result of this thesis, the dihydrostilbene batatasin III (**1**) was identified as the first representative of this new scaffold for $GABA_AR$ modulators (**Chapter 3.2**). It has been characterized as a positive allosteric modulator in receptors of the subtype $\alpha_1\beta_2\gamma_{2s}$, devoid of significant subtype selectivity. Maximal potentiation of I_{GABA} elicited by **1** was higher than that of any other NP tested up to now, and at least fourfold higher than that of classical BZDs. The semisynthetic dihydro derivatives of tetramethoxy-piceatannol (**15**) and pterostilbene (**16**) were also identified as hits with pharmacological potential as $GABA_AR$ modulators, with efficiencies higher than 700% and potencies between 20 and 50 μM (Figure 4.4). Further medicinal chemistry efforts on compounds **1**, **15**, and **16** should be directed towards enhancement of potency and subunit selectivity. Conformationally restricted derivatives should be synthesized in order to explore in more detail the optimal orientation of the aromatic rings and substituents in the dihydrostilbene scaffold. Animal behavioral studies with these compounds are advisable, in order to assess their $GABA_AR$ modulation *in vivo*. On the other hand, assessment of their ability to cross intestinal and blood-brain barriers should be evaluated by means of *in vitro* and *in vivo* models to confirm our RO5-based predictions. Stilbenes like piceatannol, pterostilbene, and resveratrol are known to undergo rapid metabolic transformations *in vivo*, which severely limits their oral bioavailability and ability to reach CNS upon oral administration [16,17]. *In vitro* and *in vivo* pharmacokinetic studies should then be performed with **1**, **15**, and **16** in order to evaluate their metabolic stability.

The new NPs 3,9-dihydroxy-8-(3-hydroxy-3-methylbutyl)-pterocarpan (**4**) and 3,4,9-trihydroxy-8-(3-methylbut-2-en-yl)-pterocarpan (**7**) represent a novel scaffold for $GABA_AR$ modulators, with favorable efficiencies and high potencies (**Chapter 3.3**, Figure 4.4). The EC_{50} value of **4** positions this compound as one of the most potent NPs tested in receptors of the subtype $\alpha_1\beta_2\gamma_{2s}$. Isoneorautenol (**8**), a known pterocarpan, constitutes an interesting scaffold for $GABA_AR$ modulators too, although its modulatory potency is lower than those of its structural relatives **4** and **7**. The physicochemical properties of these compounds make them attractive candidates for evaluation of $GABA_AR$ subtype selectivity and further optimization of potency and efficiency by medicinal chemistry.

Pterocarpans have attracted the attention of the scientific community in recent years, due to their wide range of biological activities [18]. Although they have been reported to undergo

rapid and extensive oral absorption [19], no CNS effects have been described to date. Behavioral and pharmacokinetic studies in animal models with compounds **4**, **7**, and **8** or their enhanced derivatives, will provide more insights into the potential of pterocarpans as $GABA_AR$ modulators *in vivo*. The behavior of pterocarpans **4**, **7**, and **8** in concentration-response experiments led us to suggest a mechanism of action involving receptor modulation and low affinity channel block. The latter remains to be confirmed through *in vitro* evaluation of the receptor binding properties of these compounds.

The isoflavone scaffold, represented in this work by 7,2',4'-trihydroxy-8-(3-methylbut-2-en-yl)-isoflavone (**11**), provided the most potent $GABA_AR$ modulator identified in this work (**Chapter 3.3**, Figure 4.4). The modulatory potency of **11** in $\alpha_1\beta_2\gamma_{2s}$ $GABA_ARs$ was in fact higher than that of any other NP tested so far in the oocyte assay. Although compound **11** does not constitute a relevant hit regarding scaffold novelty, its high potency and favorable physicochemical properties make it a promising candidate for the further optimization and development. Evaluation of the pharmacologic potential of **11** must be pursued, starting by the *in vitro* assessment of receptor subtype specificity. Medicinal chemistry studies directed to improve potency, efficiency and, if needed, selectivity, can be conducted on the basis of previous SAR studies on $GABA_AR$ modulating isoflavones [6] or structurally related flavonoids [7]. *In vivo* behavioral and pharmacokinetic studies are also advisable for the full pharmacological characterization of **11** as $GABA_AR$ modulator.

The abietane diterpene DHA (**14**) was characterized as potent $GABA_AR$ modulator with "drug-like" physicochemical properties (except for a slightly high cLogP value) and a novel scaffold for the target (**Chapter 3.4**, Figure 4.4). Thus, it constitutes a new candidate to be evaluated for $GABA_AR$ subtype specificity *in vitro*. Compound **14** showed higher affinity towards the receptor than other diterpene scaffolds (i.e. pimarane and labdane diterpenes) acting at the same target [3,8]. Although reported toxicity in fish could be a drawback [20,21], *in vivo* pharmacological and pharmacokinetic experiments should be conducted with **14** in order to assess its potential of this scaffold as a starting point for medicinal chemistry.

Overall, the results of this work confirmed once more the chemical and biological relevance of NPs as a source of attractive hits for drug discovery and development. The compounds isolated and characterized in the course of this thesis contribute to expand the repertory of NPs acting as allosteric $GABA_ARs$ modulators. As a consequence of their significant

modulatory potencies and efficiencies, favorable "drug-like" physicochemical properties and, in almost all cases, scaffold novelty, all compounds shown here constitute interesting pharmacological hits. Furthermore, they can serve as scaffolds for medicinal chemistry approaches intended to the design of derivatives with improved pharmacological profile, including receptor subtype selectivity. In order to explore the potential of these privileged structures as the starting points for the development of drugs with GABAergic properties, further *in vitro* and *in vivo* pharmacological and pharmacokinetic studies must be pursued.

References

[1] Kim H, Baburin I, Khom S, Hering S, Hamburger M. HPLC-Based Activity Profiling Approach for the Discovery of GABAA Receptor Ligands using an Automated Two Microelectrode Voltage Clamp Assay on *Xenopus* Oocytes. Planta Med 2008;74:521–6.

[2] Zaugg J. Discovery of new scaffolds for GABAA receptor modulators from natural origin. Universität Basel, Basel; 2011.

[3] Schramm A, Ebrahimi SN, Raith M, Zaugg J, Rueda DC, Hering S, et al. Phytochemical profiling of Curcuma kwangsiensis rhizome extract, and identification of labdane diterpenoids as positive GABAA receptor modulators. Phytochemistry 2013:318–29.

[4] Kim H, Jung, Baburin I, Zaugg J, Ebrahimi S, Nejad, Hering S, Hamburger M. HPLC-based Activity Profiling – Discovery of Sanggenons as GABAA Receptor Modulators in the Traditional Chinese Drug Sang bai pi (Morus alba Root Bark). Planta Med 2012;78:440–7.

[5] Li Y, Plitzko I, Zaugg J, Hering S, Hamburger M. HPLC-Based Activity Profiling for GABAA Receptor Modulators: A New Dihydroisocoumarin from Haloxylon scoparium. J Nat Prod 2010;73:768–70.

[6] Gavande N, Karim N, Johnston GAR, Hanrahan JR, Chebib M. Identification of Benzopyran-4-one Derivatives (Isoflavones) as Positive Modulators of GABAA Receptors. ChemMedChem 2011;6:1340–6.

[7] Karim N, Gavande N, Wellendorph P, Johnston GAR, Hanrahan JR, Chebib M. 3-Hydroxy-2′-methoxy-6-methylflavone: A potent anxiolytic with a unique selectivity profile at GABAA receptor subtypes. Biochem Pharmacol 2011;82:1971–83.

[8] Zaugg J, Khom S, Eigenmann D, Baburin I, Hamburger M, Hering S. Identification and characterization of GABAA receptor modulatory diterpenes from Biota orientalis that decrease locomotor activity in mice. J Nat Prod 2011;74:1764–72.

[9] Zaugg J, Eickmeier E, Ebrahimi SN, Baburin I, Hering S, Hamburger M. Positive GABAA Receptor Modulators from Acorus calamus and Structural Analysis of (+)-Dioxosarcoguaiacol by 1D and 2D NMR and Molecular Modeling. J Nat Prod 2011;74:1437–43.

[10] Zaugg J, Eickmeier E, Rueda DC, Hering S, Hamburger M. HPLC-based activity profiling of Angelica pubescens roots for new positive GABAA receptor modulators in Xenopus oocytes. Fitoterapia 2011;82:434–40.

[11] Zaugg J, Ebrahimi SN, Smiesko M, Baburin I, Hering S, Hamburger M. Identification of GABAA receptor modulators in Kadsura longipedunculata and assignment of absolute configurations by quantum-chemical ECD calculations. Phytochemistry 2011;72:2385–95.

[12] Zaugg J, Baburin I, Strommer B, Kim H-J, Hering S, Hamburger M. HPLC-Based Activity Profiling: Discovery of Piperine as a Positive GABAA Receptor Modulator Targeting a Benzodiazepine-Independent Binding Site. J Nat Prod 2010;73:185–91.

[13] Khom S, Baburin I, Timin EN, Hohaus A, Sieghart W, Hering S. Pharmacological properties of GABAA receptors containing γ1 subunits. Mol Pharmacol 2006;69:640–9.

[14] Pau D, Belelli D, Callachan H, Peden DR, Dunlop JI, Peters JA, et al. GABAA receptor modulation by the novel intravenous general anaesthetic E-6375. Neuropharmacology 2003;45:1029–40.

[15] Thompson SA, Whiting PJ, Wafford KA. Barbiturate interactions at the human GABAA receptor: dependence on receptor subunit combination. Br J Pharmacol 1996;117:521–7.

[16] McCormack D, McFadden D. Pterostilbene and Cancer: Current Review. J Surg Res 2012;173:e53–e61.

[17] Rimando AM, Suh N. Biological/Chemopreventive Activity of Stilbenes and their Effect on Colon Cancer. Planta Med 2008;74:1635–43.

[18] Goel A, Kumar A, Raghuvanshi A. Synthesis, Stereochemistry, Structural Classification, and Chemical Reactivity of Natural Pterocarpans. Chem Rev 2013;113:1614–40.

[19] Manickavasagam L, Gupta S, Mishra S, Kumar A, Raghuvanshi A, Goel A, et al. Determination of 3-hydroxy pterocarpan, a novel osteogenic compound in rat plasma by liquid chromatography–tandem mass spectrometry: application to pharmacokinetics study. Biomed Chromatogr 2011;25:843–50.
[20] Lees G, Coyne L, Zheng J, Nicholson RA. Mechanisms for resin acid effects on membrane currents and GABAA receptors in mammalian CNS. Environ Toxicol Pharmacol 2004;15:61–9.
[21] San Feliciano A, Gordaliza M, Salinero M, del Corral J. Abietane Acids: Sources, Biological Activities, and Therapeutic Uses. Planta Med 2007;59:485–90.
[22] Zheng J, Nicholson RA. Influence of Two Naturally Occurring Abietane Monocarboxylic Acids (Resin Acids) and a Chlorinated Derivative on Release of the Inhibitory Neurotransmitter| γ-Aminobutyric Acid from Trout Brain Synaptosomes. Bull Environ Contam Toxicol 1996;56:114–20.
[23] Schramm A, Ebrahimi SN, Raith M, Zaugg J, Rueda DC, Hering S, et al. Phytochemical profiling of Curcuma kwangsiensis rhizome extract, and identification of labdane diterpenoids as positive GABAA receptor modulators. Phytochemistry 2013;96:318–29.

ACKNOWLEDGEMENTS

I want to express my deepest gratitude to Prof. Dr. Matthias Hamburger, for giving me the opportunity to pursue my doctoral studies in his research group. Under his careful supervision I have learned to approach science and life from a whole new perspective. Professor Hamburger has been an inspiration during these years, a constant example of discipline and passion for knowledge. I am truly honored to have had the chance to be one of his PhD students. I am also thankful to Prof. Dr. Steffen Hering, who hosted me in his institute in Vienna several times during the course of my doctoral studies. I felt welcome every time and was offered the best possible working conditions, which made every stay in his lab an enjoyable and fruitful experience. I also want to thank Prof. Dr. Anna Rita Bilia, who very kindly agreed to evaluate my thesis and come to Basel as co-referee for my PhD defense. In addition, I'm very thankful to Prof. Dr. Angelo Vedani, chair of my PhD examination.

I'd like to express my gratitude to the Swiss Federal Commission for Scholarships for foreign students (FCS), and the Basler Commission for Scholarships for young professionals from developing countries, for the financial support during the periods September 2009 - June 2011 and January 2012 - December 2012, respectively. Special thanks to Mrs. Andrea Delpho (Mobility Office, UniBasel), for her invaluable help during my first months in Basel.

A separate paragraph must be dedicated to Dr. Inken Plitzko and Dr. Chee Seng Hee, who proofread my whole thesis with great patience and dedication. Thank you guys for your always helpful input, corrections, advises, and encouragement. Concerning my thesis document, I am also grateful to Dr. Olivier Potterat, who carefully checked the Zusammenfassung (translated by Inken Plitzko), and to Daniela Eigenmann, one of our BBB girls, who kindly offered her help to read and comment on chapter 2.4.

Each and every member of the Division of Pharmaceutical Biology deserves a special place here. I'm grateful to you all, for your constant support and the great working environment you create. I feel privileged for having had the opportunity to share and learn from each of you in every aspect of life. Yoshie, Anja, Samad, Christian, and Tasquiah, it was a pleasure to share the ride with you. I wish you all the best and hope our paths will some day cross again. Janine, your patience and caring guidance helped me through the first stages of my PhD. I couldn't have had a better guide. Thanks a lot for your friendship. Inken, Melanie, and Maria, I owe you girls my current NMR knowledge and skills. You were

always ready to answer every question with the greatest pleasure and patience. Thanks for sharing your experience and for your friendship, which I really value. Orlando, thanks for keeping everything going well in the lab, for your help in all technical aspects, for your great diligence to help in everything you could. Manuela, thank you for all your help since the very beginning. You're the coolest secretary one can ever have. Alen, Carmela, Daniela, Eliane, Elisabetta, Evelyn, Fahimeh, Justine, Karin, Maria, Mouhssin, Niels, Olga, Patrick, Petra, Sofi, Teresa, thanks for the moments we shared, however short. It was always fun to be around you. Last but not least, special thanks to Dr. Olivier Potterat, who was always ready to answer every question and share his wide experience. He always found the time to help every time I needed.

From the lab in Vienna I'm especially grateful to Angela Schöffmann. Not only was she a great support in academic issues, she has been such a good friend. I owe my gratitude to Neda Panic and Amela Resic, for their caring support during my first research stay in Vienna. Schwarzwälder kirschtorte in Aida will never be as good as it was back then. I'm also thankful to Dr. Igor Baburin and Dr. Sophia Khom, for their technical help.

I cannot stress enough, how thankful I am to my good friends Yoshie Hata and Inken Plitzko. My dear girls, this experience would have been very different without you. Every single day, 24/7, you took care of me, listened, comforted, helped, advised, scolded, surprised, cheered. Thanks a lot for your valuable friendship, love and trust. Last but not least, my very dear Chee Seng, I am constantly amazed by your capacity to give, your kindness, your big heart. Your devoted support kept me going until the very end of this process and made it much easier. I owe you the happiness of having someone to share this with. My deepest gratitude to you, for your love and patience.

Dice un proverbio chino que el viaje de mil millas comienza con el primer paso. El paso inicial en esta cadena de eventos que ahora termina, se lo debo al Profesor Roberto Pinzón (Universidad Nacional de Colombia) y por ello le agradezco inmensamente. A mi familia amigos en Colombia les estoy profundamente agradecida por el permanente apoyo que, aun desde la distancia, me mantuvo en pie durante estos años. Mami, Papi, Lina Ospina, MaFe Zuluaga, Gina Bernal, Laura Pineda, Angelica Sandoval, Angela Zambrano, Nadia Vergel, Yasmin Cabieles, David Becerra, Miguel Dussan, Juan Carlos Galeano, Julian Serna, Francisco Romero, los quiero. Sepan perdonarme aquellos a quienes aquí no menciono. Son muchas las personas que han jugado un papel decisivo en el curso de mi vida. Tiempo y espacio escasean, pero en mi memoria los llevo a todos con especial cariño.